Designing strategies to improve the T cell mediated immunotherapy of mouse tumours.

Haley Ataera

Malaghan Institute of Medical Research

A thesis submitted for the degree of

Doctor of Philosophy

at the Victoria University of Wellington,

New Zealand

November 2009

Abstract

The adoptive transfer of activated dendritic cells (DC) loaded with tumour antigen or tumour specific T cells improves weak anti-tumour responses, however, without treatments to relieve suppression, these therapies will continue to fall short of their full potential. The aim of this thesis was to understand the role of hypoxia-induced increases in adenosine and of $CD4^+$ $CD25^+$ $Foxp3^+$ regulatory T cells (Treg) in the suppression of anti-tumour immune responses and to design strategies to abrogate these mechanisms. These aims were investigated using the B16.OVA murine melanoma model because the OVA specific $CD4^+$ (OTII) and $CD8^+$ (OTI) T cell transgenic mice allowed detailed investigation of Ag specific T cell responses.

Recent studies have shown that the inhibition of adenosine signalling in activated $CD8^+$ T cells can improve the anti-tumour activity of these cells. To investigate these findings using the B16.OVA model, tumour-bearing mice were given activated OTI T cells and the adenosine receptor inhibitor caffeine. Caffeine treatment did not improve the anti-tumour response, possibly because this response was suppressed due to the increased frequency of myeloid derived suppressor cells observed in mice that received T cells.

To determine whether the defective function of tumour infiltrating DC (TIDC) in tumours is due to suppression by Treg, mice were treated with the anti-CD25 monoclonal antibody PC61 to deplete Treg and challenged with tumours. PC61 treatment caused a delay in tumour growth but did not affect DC frequency, or expression of the DC activation markers CD40, CD86 and MHC II in tumours or lymph nodes. DC function was tested using *in vitro* and *in vivo* T cell proliferation assays and was found to be unaffected by PC61 treatment. Studies in RAG1-/- mice, which lack Treg, also showed no improvement

in DC activation status or function. These results show that Treg do not suppress TIDC in the B16.OVA model.

It is well known, however, that Treg suppress T cell responses and it has been suggested that Treg may mediate some of this suppression by using the perforin-granzyme pathway to cause T cell death. To investigate this possibility, naïve, perforin sufficient OTI T cells were transferred into normal and perforin knockout (PKO) mice, with or without PC61 treatment. To stimulate an OTI T cell response, mice also received OVA-loaded DC. Depletion of both normal and PKO Treg resulted in decreased death and increased proliferation of the transferred cells, increased expression of IFN-γ and TNF-α, and improved *in vivo* target cell killing by the transferred cells. These findings indicate that perforin expression by Treg is not required to suppress T cell responses or cause T cell death.

In conclusion, the results of this thesis were consistent with the observation that there are multiple suppressive mechanisms in tumours and that there is substantial redundancy of these mechanisms. Depletion of Treg was found to improve the anti-tumour response, however, suppression of the DC was still evident, demonstrating that the neutralisation of a single suppressive mechanism may not be sufficient to treat aggressive, late stage cancers such as melanoma.

Acknowledgements

I would like to express my heart felt thanks and appreciation to my supervisor Prof. Franca Ronchese, for her endless patience, the helpful discussion and debate and for her understanding and much needed guidance. I wish to thank my second supervisor Dr. Ian Hermans for showing an interest and providing feedback and my third supervisor Dr. Anne La Flamme for being encouraging and supportive every time I saw her.

I am grateful to Dr. Rachel Perret for her perseverance in showing me how to handle mice and to Jianping (Mark) Yang for so diligently answering all of my questions regarding protocols and the location of various things. Evelyn Spittle, you saved me from a number of obnoxiously long experimental days, which I appreciate immensely. Thank you also to my student intern Markus Hoffman for the hours spent counting fluorescently labelled cells. I would like to thank the cancer immunotherapy group (past and present) for their support and feedback though out my thesis, especially Dr. Patrizia Stoitzner who was a wonderful mentor and an inspiration to me. To my fellow PhD students (again past and present) at the Malaghan Institute, I will never forget your unending support, advice and friendship. Thank you to the wonderful staff that keep the animal facility running, you do a fantastic job.

I gratefully acknowledge Prof. Alexander Rudensky and Dr. Joanna Kirman for allowing me to use the Foxp3-GFP and RAG1-/- mice respectively.

I wish to give special recognition to Te Roopu Awhina Putaiao and in particular Liz Richardson who is responsible for luring me back to Victoria University, through the Malaghan Institute to pursue a PhD. I will also be forever grateful to the Malaghan Institute for providing such a wonderful, challenging, interesting, stimulating and most of all supportive environment in which to study.

Thank you to the Health Research Council of NZ for providing the funding for my PhD. I also wish to express my appreciation to the Wellington division of the cancer society and ASI for awarding me travel grants and to Victoria University for awarding me a PhD submission scholarship, which allowed me to finish writing my thesis.

Thank you seems completely inadequate when it comes to my friends and family. Liz Forbes, you gave me a place to stay when I needed one and with the aid of your wonderful fiancé Jay helped me move residences numerous times. You have supported and encouraged me and I only hope one day that I can return the favour. I also want to acknowledge Helen Mearns for her endless support and encouragement. I will treasure all the fun times I've had with both of you, you certainly helped keep me sane and hopefully taught me not to take myself too seriously. And finally, I will always be grateful to my mother, Lyn, for her unfailing love, encouragement and support.

Thank you to all of you for helping me to achieve my goals and dreams.

Table of contents

List of Figures

List of Tables

List of abbreviations

2-ME	**2-Mercaptoethanol**
^{3}H-thymidine	**Tritiated thymidine**
3LL	**Lewis lung carinoma**
6132A-PRO	**Murine tumour cell line**
ACT	**Ammonium Chloride Tris**
Ag	**Antigen**
AIDS	**Acquired immune deficiency syndrome**
APC	**Antigen presenting cell**
ADA	**Adenosine deaminase**
ADO	**Adenosine**
ADP	**Adenosine diphosphate**
AK	**Adenosine kinase**
AMP	**Adenosine monophosphate**
ATP	**Adenosine triphosphate**
BM	**Bone marrow**
BMDC	**Bone marrow-derived dendritic cell**
CIIV	**MHC II vesicle**
C57	**C57BL/6 mice**
cAMP	**Cyclic adenosine monophosphate**
CCR	**Chemokine (C-C motif) receptor**
CD	**Cluster of differentiation**
CFSE	**Carboxyfluorescein diacetate succinimidyl ester**
CLIP	**Class II-associated invariant-chain peptide**
CMV	**Cytomegalovirus**

CPM	**Counts per minute**
CREB	**cAMP response element binding**
CTL	**Cytotoxic T lymphocyte**
CTLA-4	**Cytotoxic T lymphocyte associated antigen 4**
CTO	**CellTracker Orange**
CXCR	**Chemokine (C-X-C motif) receptor**
Cyt c	**Cytochrome c**
D3tx	**Day 3 thymectomised mice**
DAMPs	**Damage associated molecular pattern molecules**
DC	**Dendritic cell**
DMSO	**Dimethyl Sulfoxide**
DNA	**Deoxyribonucleic acid**
dsRNA	**Double stranded ribonucleic acid**
DTR	**Diptheria Toxin Receptor**
EDTA	**Ehylenediaminetetraacetic acid**
ER	**Endoplasmic reticulum**
EtOH	**Ethanol**
FACS	**Fluorescence Activated Cell Sorting**
FBS	**Foetal Bovine Serum**
FCA	**Flow cytometry analysis**
FDA	**Food and Drug Administration (America)**
FITC	**Fluorescein Isothiocyanate**
Flt3L	**Fms-like thyrosine kinase 3 Ligand – a dendritic cell growth factor**
Foxp3	**Forkhead box P3**
FSC	**Forward Scatter**

GFP	**Green Fluorescent Protein**
GITR	**Glucocorticoid-induced TNF superfamily related receptor**
GM-CSF	**Granulocyte macrophage colony stimulating factor**
Gzm	**Granzyme**
HIF	**Hypoxia inducible factor family of transcription factors**
HLA	**Human Leukocyte Antigen**
HSV	**Herpes Simplex virus**
IDO	**Indoleamine 2,3-dioxygenase**
i.p.	**Intraperitoneal**
i.v.	**Intravenous**
ICAM-1	**Intracellular adhesion molecule 1**
IFN	**Interferon**
IL	**Interleukin**
IPEX	**Immune dysregulation, polyendocronopathy, enteropathy and X-linked inheritance**
IMDM	**Isove's Modified Dulbecco's Medium**
KLRG-1	**Killer cell lectin-like receptor G 1**
KO	**Knockout**
L	**Ligand**
Lamp	**Lysosomal-associated membrane protein**
LCMV	**Lymphocytic choriomeningitis virus**
Li	**Invariant chain**
LL-LCMV	**$LCMV_{33-41}$ transfected Lewis lung carcinoma cell line**
LPS	**Lipopolysaccharides**
MIIC	**MHC II loading compartment**
mAb	**Monoclonal antibody**

MACS	**Magnetic Cell Sorting**
MAGE	**Melanoma antigen-encoding gene**
MART	**Melanoma Antigen Recognised by T cells**
MCA	**3-Methylcholanthrene**
MDSC	**Myeloid derived suppressor cells**
Melan-a	**Melanocyte lineage antigen a (also known as MART-1)**
MFI	**Mean fluorescence intensity**
MHC	**Major Histocompatibility Complex**
MPR	**Mannose-6-phosphate receptor**
mRNA	**Messenger ribonucleic acid**
NK	**Natural killer cell**
NKT	**Natural killer T cell**
OVA	**Ovalbumin**
PBS	**Phosphate Buffered Saline**
PCR	**Polymerase Chain Reaction**
PD-1	**Programmed death receptor-1**
PE	**Phycoerythrin**
PerCP	**Peridinin Chlorophyll Protein**
PI	**Propidium Iodide**
PKA	**Protein Kinase A**
PKO	**Perforin knockout**
R	**Receptor**
RAG	**Recombination Activating Gene**
RISC	**Ribonucleic acid induced silencing complex**
s.c	**Subcutaneous**
SA	**Streptavidin**

SCID	**Severe Combined Immunodeficiency**
SD	**Standard deviation**
SEM	**Standard error of the mean**
siRNA	**Small interfering ribonucleic acid**
SSC	**Side Scatter**
TAA	**Tumour Associated Antigen**
TAE	**Tris-acetate-ethylenediaminetetraacetic acid**
TAP	**Transporter associated with antigen processing**
TCR	**T cell receptor**
Teff	**Effector T cell**
TGF-β	**Transforming growth factor β**
T_C1	**Cytotoxic $CD8^+$ T cell secreting T_H1-like cytokines**
T_C2	**Cytotoxic $CD8^+$ T cell secreting T_H2-like cytokines**
T_H1	**T helper type 1**
T_H2	**T helper type 2**
T_H17	**T helper type 17**
TIDC	**Tumour infiltrating dendritic cell**
TLR	**Toll-like receptor**
TNF	**Tumour necrosis factor**
Tr1	**T regulatory cells 1**
Treg	**Regulatory T cell**
Ts	**$CD8^+$ suppressor T cells**
TSA	**Tumour Specific Antigen**
TSDR	**Treg specific demethlated region**
V	**Volts**
Vα	**Variable α region of the T cell receptor**

Vβ	**Variable β region of the T cell receptor**
VEGF	**Vascular endothelial growth factor**

CHAPTER ONE

GENERAL INTRODUCTION

1.1 General Introduction

It is recognised that the immune system functions as one of the body's defences against pathogens, parasites and cancers. Over the last few decades, much has been learned about the individual components of the immune system and how they interact. This knowledge has been successfully applied to the treatment of various cancers in murine models where the tumour antigens (Ag) are well characterised and T cell receptor (TCR) transgenic mice that produce high numbers of tumour specific T cells are available. In contrast, human cancers vary amongst individuals and generating Ag specific T cells is difficult and costly. It is possible to generate tumour specific T cell responses in humans, both spontaneously and in response to immunotherapy but despite this, cancer immunotherapy has had limited success. The discovery of a number of immunosuppressive mechanisms invoked by the tumour has helped to explain why this occurs. The challenge ahead lies in understanding these mechanisms and thereafter finding ways to overcome them.

1.2 The adaptive immune response

1.2.1 Dendritic cells

Dendritic cells (DC) are a specialised form of professional antigen presenting cells (APC), which are part of both the innate and adaptive immune responses. DC are classed as professional APC because in contrast to non-professional APC such as various epithelial and mesenchymal cells, they constitutively express low levels of the class II Major Histocompatibility Complex (MHC II) and accessory molecules (1). B cells and macrophages are also professional APC, however, most DC subsets are superior to these cells in their ability to stimulate naïve T cell responses (2, 3).

1.2.2 DC subtypes

Murine DC can be divided into a number of subpopulations based on their tissue distribution, phenotype and function (4, 5). The subpopulations have been defined using markers such as CD11c, MHC II, CD11b, CD4, CD8, DEC205 and F4/80. Further characterisation is possible using the activation markers CD40, CD80 and CD86. There is no definitive marker for DC and it is technically difficult to use such a large range of markers to define the DC subpopulation, therefore, the DC subpopulations have been summarised below using expression of CD11c, CD4, CD8, DEC205 and CD11b, which are the markers most commonly used in publications on DC.

Langerhans cells ($CD11c^{+}$, $CD4^{-}$, $CD8^{low}$, $DEC205^{high}$, $CD11b^{+}$) are a subtype of DC found mainly as immature cells in the skin, or as mature cells in the skin draining lymph nodes (4, 6-8). Langerhans cells acquire Ag in the periphery and traffic from the skin, to skin draining lymph nodes (6) where it was originally thought these cells were able to upregulate $CD8^{+}$ expression (4, 9, 10) and present Ag to $CD8^{+}$ T cells. More recent studies have shown that the Ag is passed from the Langerhans cells to the resident $CD8^{+}$ DC subpopulation (11-13) for presentation to $CD8^{+}$ T cells. Aside from Langerhans cells, skin-draining lymph nodes also contain significant populations of resident and skin emigrant $CD11c^{+}$, $CD4^{-}$, $CD8^{-}$, $DEC205^{+/-}$, $CD11b^{+}$ DC and a $CD11c^{+}$, $CD4^{-}$, $CD8^{high}$, $DEC205^{high}$, $CD11b^{-}$ DC subpopulation (4, 6-8). The $CD8^{-}$ DC subpopulation has been shown to present Ag to $CD4^{+}$ T cells, whereas the $CD8^{+}$ DC subpopulation has been shown to be superior at cross-presenting Ag to $CD8^{+}$ T cells in comparison to other DC subpopulations (14, 15). Mesenteric lymph nodes contain DC subpopulations similar to the skin-draining lymph nodes, however, they do not contain a population of Langerhans cells. In contrast to the skin and lymph nodes, splenic DC mostly consist of a $CD11c^{+}$, $CD4^{+}$, $CD8^{-}$, $DEC205^{-}$,

$CD11b^+$ subpopulation with some $CD11c^+$, $CD4^-$, $CD8^-$, $DEC205^-$, $CD11b^+$ DC and $CD11c^+$, $CD4^-$, $CD8^{high}$, $DEC205^{high}$, $CD11b^-$ DC (4, 6-8) with cross presenting capabilities.

Tissue derived DC primarily exist in an immature state characterised by low expression of markers such as CD40, CD80, CD86 and MHC II (1). These immature DC are highly efficient at sampling the environment and also express the chemokine receptors CCR1, CCR2, CCR5 and CXCR1 that allow them to home to sources of inflammation (16).

1.2.3 DC, maturation and tolerance

In the absence of an inflammatory stimulus (the steady state), immature DC can spontaneously upregulate the maturation markers MHC II and CD40 and the co-stimulatory molecules CD80 and CD86 to become phenotypically mature (17, 18). These DC migrate to the lymph nodes where they present Ag to naïve $CD4^+$ and $CD8^+$ T cells, but because these DC have not been exposed to an inflammatory stimulus, they are unable to release immuno-stimulatory cytokines such as interleukin (IL)-12 and are known as quiescent or tolerising DC (19) (Figure 1.1). T cells activated by tolerising DC are able to proliferate, however, these T cells fail to produce cytokines and acquire cytotoxic function (20, 21). This phenomenon is called T cell anergy because of the cells' inability to mount an appropriate response against the source of Ag and most of these anergic T cells will die (21, 22) (Figure 1.1). In this way, peripheral tolerance towards the source of Ag (usually self tissue) is maintained.

1.2.4 DC activation

In response to "danger signals" or CD40L (23, 24), immature DC acquire an activated, mature phenotype by up regulating the maturation markers MHC II and CD40 and the co-stimulatory molecules CD80 and CD86 (23). These danger signals include inflammatory stimuli such as microbial or viral pathogens (25), which signal through Toll-like receptors (TLR) (26, 27) and other microbial patterns, which are recognised by pattern recognition receptors. The tumour microenvironment provides danger signals in the form of the inflammatory cytokines IL-1 and tumour necrosis factor-α (TNF-α) (28, 29) and by producing damage associated molecular pattern molecules (DAMPs). Examples of DAMPs that occur in tumours include extracellular DNA fragments, which can be produced when cells undergo necrosis (30), and heat shock proteins, which are a cell survival factor (31) and are often over-expressed in tumours (32). During maturation or activation, the chemokine receptors CCR7, CCR4 and CXCR4 are also upregulated (16), and expression of CCR7 allows the DC to migrate to the lymph node. In contrast to mature DC, activated DC are able to release IL-12 (23, 24), which promotes the production of the cytokines Interferon-γ (IFN-γ), tumour necrosis factor-α and IL-2 from T cells. Production of these cytokines is known as a T_H1 ($CD4^+$ T helper type 1) or T_C1 (cytotoxic $CD8^+$ T cell secreting T_H1-like cytokines) response (33, 34). Activated DC are also known to produce a large range of cytokines including IL-18 (35), IL-23, IL-27 (36) and IL-6 as well as IFN-α, IFN-β (37) TNF-α (38) and IL-10 (39) and can stimulate T_H2, T_H17 and regulatory T cell (Treg) responses depending on the stimulus and quality of signalling (40).

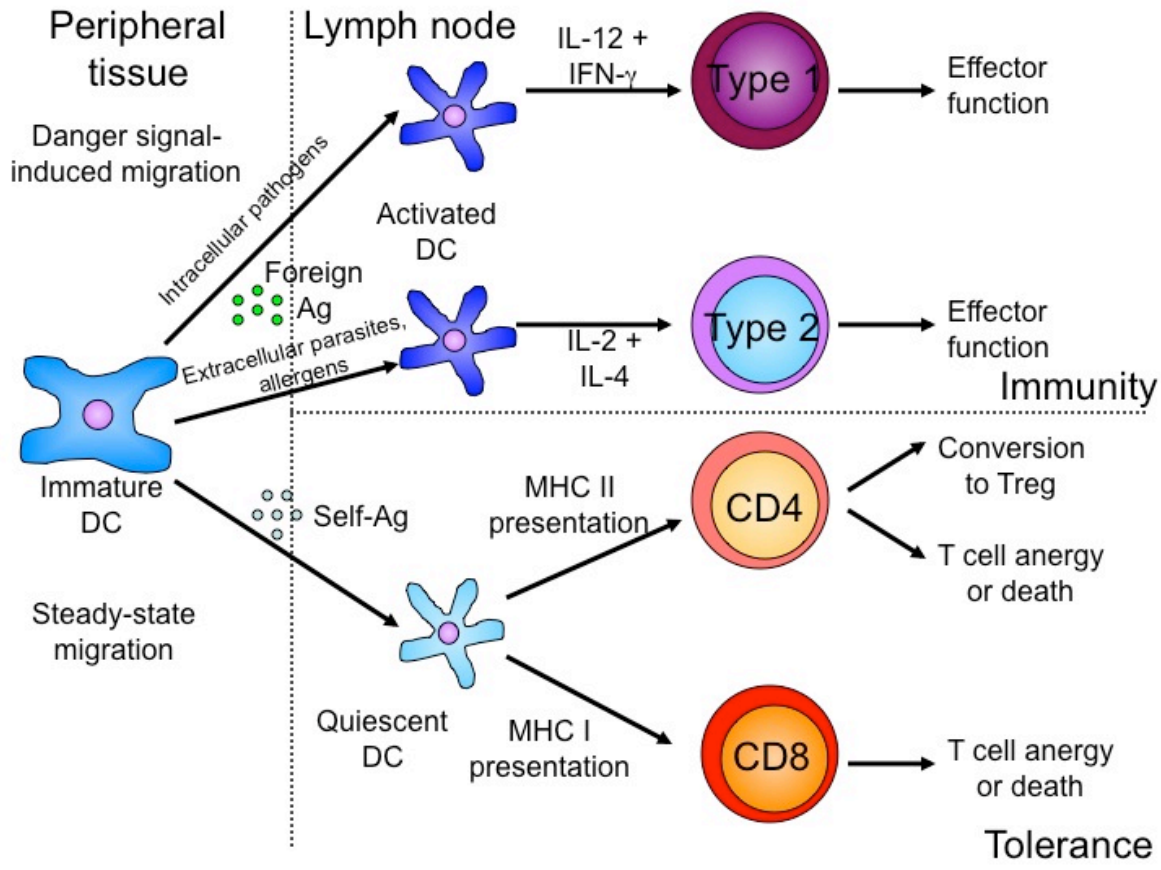

Figure 1.1: T cell responses differ depending on the context in which DC come into contact with Ag.

In the absence of inflammatory stimuli, peripheral DC spontaneously partially mature and migrate to the lymph nodes at a low rate. These quiescent DC present self-Ag to $CD4^+$ and $CD8^+$ T cells and promote tolerance by stimulating the formation of Treg and the anergy or deletion of self-reactive T cells. Microbial infection, inflammation and tissue damage are so called "danger signals" that mature and activate DC and increase the rate of migration to the lymph node. These highly activated DC are able to produce a number of cytokines to produce strong type 1 or type 2 CD4 and CD8 T cell responses depending on the type of signals the DC have received (41, 42).

1.2.5 Classical Antigen presentation

DC process Ag via two distinct pathways and present MHC I-bound Ag to $CD8^+$ T cells and MHC II-bound Ag to $CD4^+$ cells. These pathways are discussed in detail below.

1.2.5.1 MHC I presentation

In jawed vertebrates, MHC I molecules are expressed to varying degrees on the surface of all nucleated cells. Intracellularly synthesized Ag such as those of viral (43, 44) or self-origin are processed into peptides by the proteasome and transported into the Endoplasmic Reticulum (ER) via the heterodimeric Transporters of Antigen-Processing (TAP)-1 and 2 molecules (45) (Figure 1.2). The class I MHC molecules (MHC I) are assembled (45) and loaded with peptide Ag in the ER (46), exported to the plasma membrane via the Golgi body and presented to $CD8^+$ T cells (43, 44) (Figure 1.2).

1.2.5.2 MHC II presentation

MHC II molecules are expressed only on APC such as DC, B cells and macrophages. MHC II molecules are also assembled in the ER (47, 48) and are associated with an invariant chain (Ii) to prevent the MHC II molecule from binding to endogenous proteins. The MHC II-Ii complexes are transported via the Golgi body to the MHC II loading compartment (MIIC, also known as the MHC II vesicles (CIIV)) where the invariant chain is degraded leaving a class II-associated invariant-chain peptide (CLIP) (Figure 1.2). Extracellular Ag are taken up via receptor-mediated endocytosis into lysosomes and late endosomes (49) where the Ag is processed into peptides. The peptides are then transferred to the MIIC/CIIV compartment where they displace the CLIP on the MHC II molecule (25). Peptide-MHC II complexes are then exported to the plasma membrane and presented to $CD4^+$ T cells (50) (Figure 1.2).

1.2.6 Cross presentation

It was first suggested in the late 1980's that an exogenous pathway for processing peptide to be presented by MHC I molecules must exist in order to control pathogens that do not infect DC or which compromise the function of the DC they infect (51). This was demonstrated by showing that self Ag (22) and tumour Ag (52) can be presented to $CD8^+$ cells by bone marrow derived antigen presenting cells. This process has come to be known as cross presentation, resulting in the cross priming of $CD8^+$ T cells and is known to require large amounts of Ag (53) in comparison to the Ag requirements of classical presentation. There are a number of proposed mechanisms to explain how cross presentation occurs. The original model of cross presentation, referred to as the vacuolar route, showed that phagocytosed Ag was processed into peptide-Ag within the phagosome and loaded onto MHC I molecules that had been recycled from the plasma membrane during phagocytosis (54). The most well known model, called the cytosolic route, postulated that phagocytosed Ag was diverted from the phagosome to the cytosol where it was treated similar to intracellularly synthesised Ag and could enter the class I Ag processing, loading and presentation pathway (55-57) (Figure 1.2). A later model, known as the phagosome-ER fusion route, describes a mechanism where the ER membrane is able to fuse to the membrane of the phagocytic cup during phagocytosis, thereby introducing ER proteins such as MHC I and TAP molecules and the TAP-associated glycoprotein tapasin into the phagosome. Ag is diverted into the cytosol, processed by the proteasome and then diverted back into the phagosome where it is loaded onto the MHC I molecule (58-60).

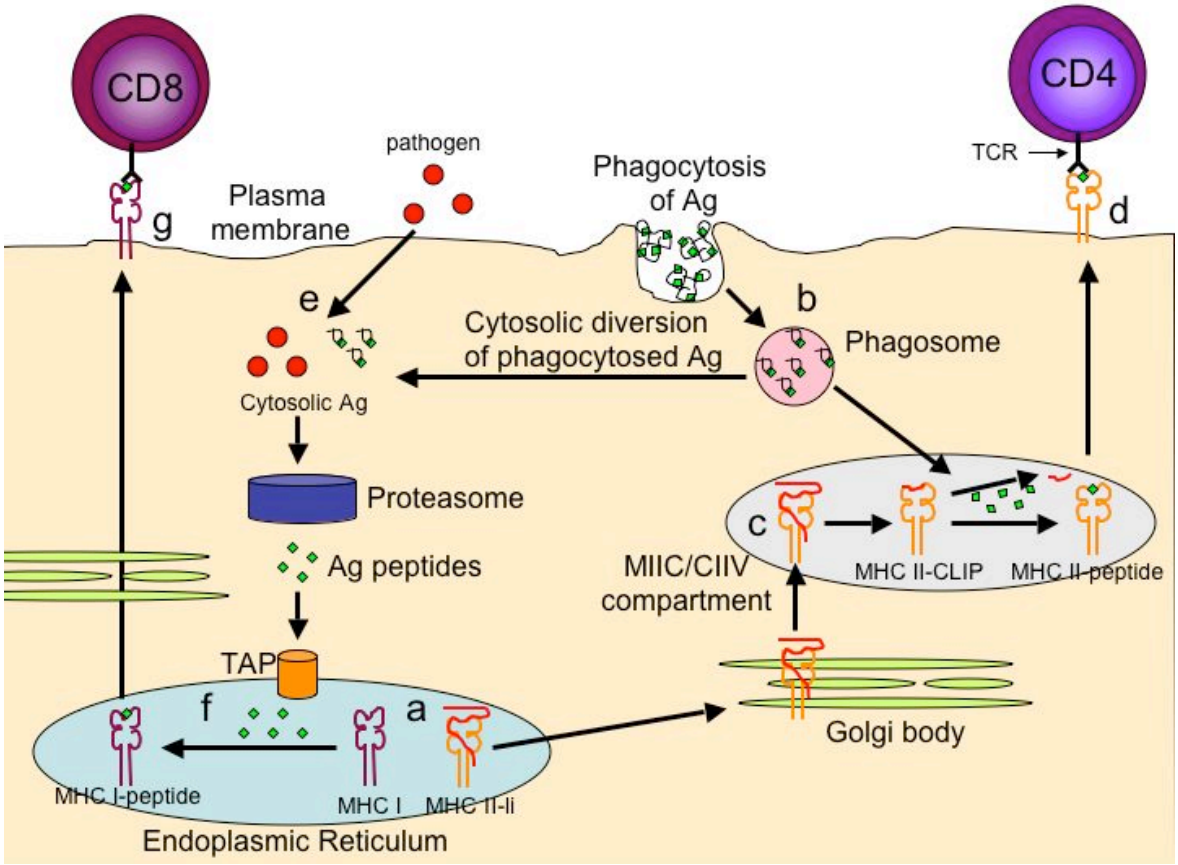

Figure 1.2: Ag presentation pathways.

MHC II molecules associated with the invariant chain (MHC II-li) and MHC I molecules are assembled in the Endoplasmic Reticulum (ER). MHC II-li molecules are exported to the MIIC (MHC II loading compartment)/CIIV (MHC II vesicle) compartment via the Golgi body. B) Extracellular Ag are taken up into endosomes and processed into peptides. Peptides can then either be transferred to the MHC II loading compartment (MIIC, also known as MHC II vesicles (CIIV)) or diverted to the cytosol. C) The invariant chain (li) of the MHC II-li complex is degraded to a class II-associated invariant-chain peptide (CLIP), which is then exchanged for peptide. D) The peptide-MHC II complex is then exported to the plasma membrane where it is recognised by the T cell receptor (TCR) and presented to $CD4^+$ T cells. E) Pathogens that infect the DC are processed into peptides by the proteasome. These Ag peptides then enter the ER via the Transporters of Antigen-Processing (TAP) molecules where they are loaded onto MHC I molecules and exported to the plasma membrane via the Golgi body to be presented to $CD8^+$ T cells. Cross presentation occurs when Ag is diverted from the endosome into the cytosol where it can enter the class I presentation pathway beginning with being processed into peptides by the proteasome.

DC take up Ag by phagocytosis (61), macropinocytosis and receptor-mediated endocytosis (50, 62, 63) and the method by which the Ag is endocytosed has been proposed to be an important factor in determining whether an Ag can be cross presented (50). Burgdorf *et al* showed that pinocytosed Ag was presented to $CD4^+$ T cells whereas Ag endocytosed by the Mannose-6-Phosphate receptor (MPR) in DC or by Scavenger receptors in macrophages was cross-presented to $CD8^+$ T cells. Molecules taken up by MPR mediated endocytosis were directed into early endosomes rather than lysosomes and could therefore be loaded onto MHC I molecules rather than the expected MHC II molecules (50).

1.2.7 $CD8^+$ T cell activation and differentiation

T cells recognise peptide/MHC complexes on the surface of DC via their TCR. $CD8^+$ T cells require 3 signals, namely Ag, co-stimulation in the form of CD80 and CD86 and the presence of IL-12 to become fully activated effector T cells (cytotoxic T lymphocytes, CTL) with effector function or memory T cells (64, 65). Upon activation, the effector CTLs show increased expression of activation markers such as CD69 (66), CD25 (67) and CD44 (68) and down regulation of the lymph node homing molecule CD62L (69). In addition, effector CTL downregulate expression of the homeostatic cytokine receptor subunit IL-7Rα (CD127) (70), meaning they cannot receive long-term survival signals and will, therefore, only persist as long as Ag is available. Terminally differentiated, exhausted effector T cells are also known to express high levels of the Killer Cell Lectin like Receptor G1 molecule (KLRG1) (71). The co-stimulatory molecules Glucocorticoid-Induced TNF receptor (GITR) and OX40 and the negative regulator of T cell function Cytotoxic T lymphocyte-associated Antigen 4 (CTLA-4), are also upregulated on CTL (72). CTL undergo extensive proliferation, secrete effector cytokines such as TNF-α, IFN–γ (23), IL-2, IL-4 and IL-10 (73), depending on the stimulus, and exhibit cytotoxic

function resulting in lysis and death of target cells (74). Expansion of the activated $CD8^+$ T cell population is followed by a contraction phase, after which, a subset of Ag experienced T cells remains as the memory $CD8^+$ T cell population. These cells are able to persist for the lifespan of the host and are able to expand and/or acquire effector function much quicker than naïve $CD8^+$ T cells when exposed to the same Ag (75). Memory $CD8^+$ T cells are characteristically $CD44^+$ (68) and a subpopulation is $CD62L^+$ (76), however, in contrast to effector T cells, the memory T cell population is IL-7Rα^+ and IL-2/IL-15Rβ $(CD122)^+$ (70), meaning they are capable of receiving long term survival signals.

1.2.8 $CD8^+$ T cell effector function

The main role of CTL is to identify and kill infected or malignant cells. CTL express the effector cytokines TNF-α and IFN-γ as well as the death-receptor ligands FASL and TNF-related apoptosis-inducing ligand (TRAIL) and contain cytotoxic granules, all of which contribute to the effector function of the cells (77, 78).

IFN-γ has been shown to be involved in host protection against transplanted, spontaneous and primary, chemically induced tumours (79-82) and a number of mechanisms have been proposed to explain these findings. The presence of IFN-γ in tumours can trigger the production of additional inflammatory cytokines and chemokines, which leads to the activation and recruitment of other effector cells such as NK cells, macrophages and granulocytes (83). One study has shown that IFN-γ may cause the tumour stroma to become vulnerable to attack by the immune system (84), thereby weakening the tumour. IFN-γ has also been shown to inhibit tumour angiogenesis (85), which is likely to limit the growth of tumours or even cause some regression. Both TNF-α and IFN-γ are known to aid in the lysis of target cells (86-88). $CD8^+$ T cells increase levels both of plasma

membrane-bound and secreted TNF-α after activation through their TCR. The secreted form of TNF-α was found to have no role in lysis of the target cell, even in the absence of the perforin-granzyme pathway, however, the membrane-bound form has been shown to induce a slow (18 hour) lysis reaction (86). These examples demonstrate the importance of the production of TNF-α and IFN-γ to the function of CTL and the anti-tumour response.

There are two main contact-dependent cytolytic pathways used by T cells to cause target cell lysis and death. The FAS-FASL pathway involves the binding of the death receptor FAS (CD95) on the target cell to the FASL on the T cell resulting in caspase activation and cell death by apoptosis. Previous studies have shown that the FAS-FASL pathway can be further improved by, and may be dependent on the presence of IFN-γ (87, 89). This pathway is largely thought to function in maintenance of lymphocyte homeostasis (90).

The granule exocytosis pathway is required for the control of most viruses and cancers (91-93) and is used by CTL, natural killer (NK) and NKT cells to lyse target cells recognised by their specific receptors. Recognition of MHC-peptide complexes on target cells by the TCR on the CTL or NKT cell causes the CTL or NKT cell to release cytotoxic granules. These granules contain perforin, granzymes and various lysosomal proteins such as cathepsins B and D, β-hexosaminidase and the lysosome-associated membrane proteins Lamp-1 (CD107a), Lamp-2 (CD107b) and Lamp-3 (CD63) (94). The lytic activity of cytotoxic granules is associated with perforin and the granzyme family (95, 96).

Perforin is so named for its pore forming abilities and is believed to have a pivotal role in the lysis of target cells by CTL because in the absence of perforin, lysis of target cells is severely impaired (95, 96). Perforin is also believed to have a critical role in the regulation of $CD8^+$ T cell responses. Evidence for this theory came from the observation that perforin

deficient mice show increased or prolonged $CD8^+$ T cell expansion after immunization with Staphylococcal Enterotoxin B or viral infections such as Lymphocytic Choriomeningitis virus and Cytomegalovirus (97, 98).

The granzymes are a family of serine proteases that include granzymes A, B, K and M in mice and humans (99). Humans also have a granzyme H, which corresponds to granzyme C in mice and in addition, mice also have granzymes D, E, F, G, L and N, although little is known about the role of these molecules (99). Granzyme B is thought to be the most efficient proapoptotic granzyme (100).

The cytotoxic granule contents are taken up by the target cell, in a mechanism that has been the subject of much debate (Figure 1.3). Originally it was thought that the role of perforin was to create a pore in the plasma membrane (101-103), which allowed the cytotoxic granules to enter the cell and trigger apoptosis. It has since been determined that the pores formed by perforin are unlikely to be large enough to allow the entry of the contents of cytotoxic granules into target cells (95). Instead, the contents of cytotoxic granules have been shown to be able to enter cells in the absence of perforin through receptor-mediated endocytosis (96, 104). An MPR and clathrin/dynamin independent mechanism of granule entry has also been demonstrated (99) (Figure 1.3).

The exact role of perforin is still unclear, however the current understanding is that perforin facilitates the exit of granzyme B (GzmB) from the endocytosed vesicles, into the cytoplasm of the target cell (95, 96). Once in the cytoplasm, GzmB mimics caspases by cleaving and activating caspase substrates (105) such as Bid, which is a propaptotic member of the Bcl-2 family (Figure 1.3). Truncated Bid (tBid) signals through Bax molecules on the mitochondrial surface (106-108) resulting in the release of Cytochrome c

(Cyt c) from the mitochondrion. Cyt c participates in the cleavage of pro-caspase 9 to its active caspase 9 form, which in turn, cleaves pro-caspase 3 to its active caspase 3 form. Caspase 3 is translocated to the nucleus where it causes DNA fragmentation and cell death (109, 110). GzmB is also able to directly activate the pro-caspases 3 and 8 (111, 112). Caspase 8, similar to GzmB, is able to induce cell apoptosis by the activation of Bid (111) (Figure 1.3).

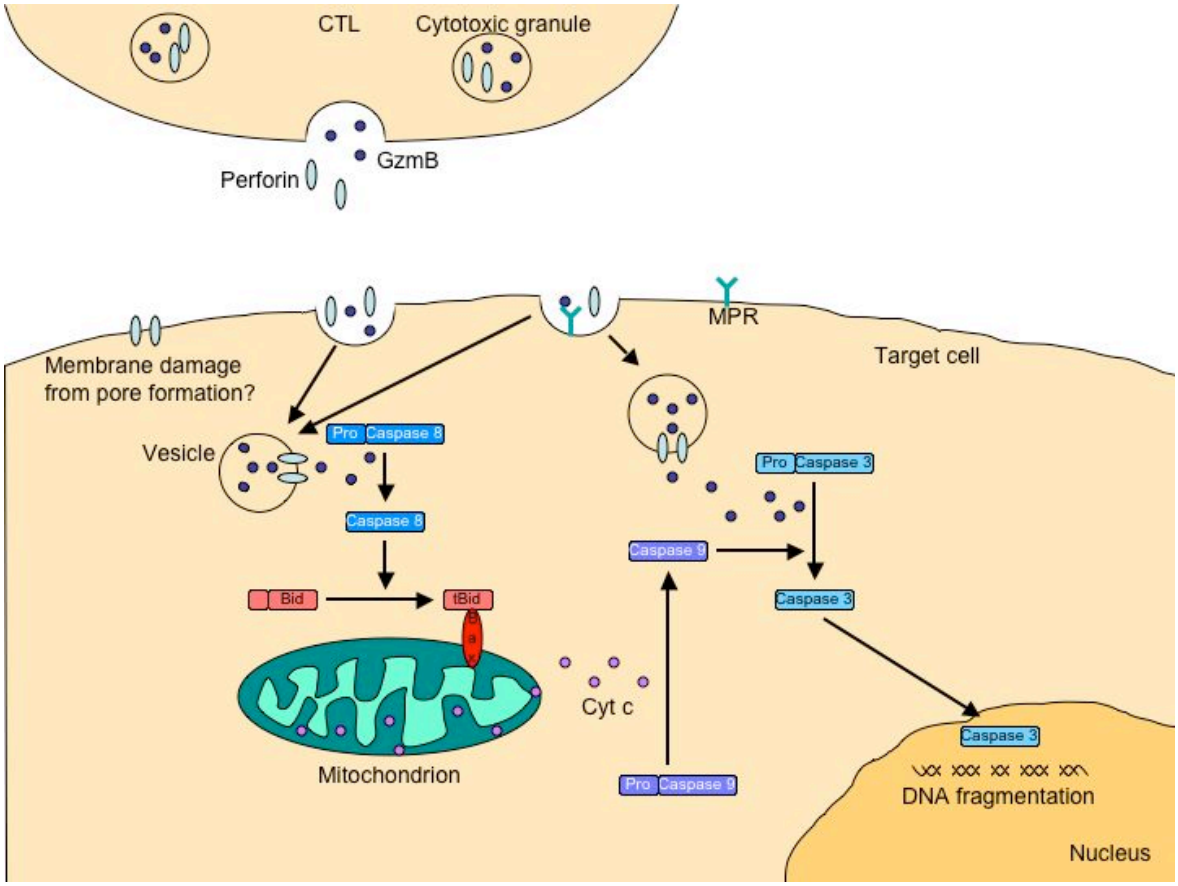

Figure 1.3: Schematic diagram of the perforin-granzyme pathway of target cell apoptosis.

Cytotoxic granules are released into the extracellular space between the CTL and the target cell. The granule contents are then endocytosed by receptor dependent and independent mechanisms, a process that forms vesicles within the target cell. Perforin disrupts the membrane potential of the vesicle, allowing granzyme B (GzmB) and other molecules to enter the cytoplasm where GzmB cleaves the pro-caspase 8 to its active caspase 8 form. Caspase 8 can then activate Bid by cleavage to form truncated tBid molecules, which interact with Bax molecules in the mitochondrial membrane causing the loss of membrane integrity and the release of cytochrome c (Cyt c). Cytoplasmic Cyt c cleaves pro-caspase 9 to its active caspase 9 form, which in turn cleaves pro-caspase 3 to its active caspase 3 form. Caspase 3 is then translocated to the nucleus where it causes DNA fragmentation, which results in apoptosis of the cell. Receptor mediated endocytosis largely occurs via the mannose-6-phosphate receptor (MPR).

1.3 Tumour Immunology

While it has been observed for at least a hundred years that tumours could spontaneously regress, presumably because of an immune response, it wasn't until the late 1800s that an immune-based method of cancer therapy was actually established (113). Dr. William Coley found that treating resected or non-operable cancer patients with a mixture of killed bacteria caused the tumour to regress in some patients. In many cases the cancer never returned. Coley's toxins, as the treatment became known, was used to treat various cancers in the United States up until 1963 when it became classed as a "new drug" by the Food and Drug Administration (FDA) because it had not undergone adequate safety testing. Since then a number of small clinical trials have been conducted to try and prove the efficacy of the treatment with mixed results.

1.3.1 Cancer immune surveillance and immunoediting

Understanding how the immune system interacts with malignant cells is important for the successful development of anti-cancer immunotherapies in the future. It was first suggested by Paul Ehrlich in 1909 that one of the roles of the immune system was to protect the host against cancer in a process called cancer immune surveillance (114). This theory was modified by Burnet in the late 1950's, who proposed that the immune system could survey the host for precancerous or cancerous cells and eliminate them (115, 116). This process was termed cancer immunoediting and was further defined by Dunn *et al* (117) as consisting of three stages: elimination, equilibrium and escape.

1.3.2 Cancer elimination

The first phase of the cancer immunoediting model involves the elimination of nascent tumour cells by the innate and adaptive immune systems. Evidence to support this theory came in the 1990's when a number of studies in which mice were deficient for IFN-γ (79-82) or perforin function (81, 82, 93, 118, 119) or completely devoid of functional T and B cells (Recombination Activation Gene 2, RAG2-/- mice) (120), showed that immunodeficient mice were more susceptible to spontaneous tumour development. Observational studies of transplant recipients (121-123) and AIDS (124) sufferers have also shown an increased incidence of cancer in immunosuppressed individuals, providing evidence that immunoediting also occurs in humans.

Recognition and destruction of cancerous cells by the immune system implies that tumours must express proteins that allow these cells to be distinguished from normal cells. A number of such Ag have so far been identified, further supporting the immunoediting argument. For example, a range of tumours, including melanomas, are known to express Ag such as the melanoma antigen (MAGE) family of melanoma differentiation proteins (125) and the NY-ESO-1 family (126). Melanomas in particular have been shown to express proteins such as gp100/Pmel-17 (127) and Melan-a/MART-1 (128). These Ag are known as tumour associated Ag (TAA) because they are expressed by subsets of normal cells as well. For example, the NY-ESO-1 and MAGE family of Ag are cancer/testis Ag, which means they are expressed in immune privileged sites and are ectopically expressed in a range of tumours. In comparison, gp100 is a melanocyte differentiation Ag, which is expressed in both melanocytes and melanomas. Several novel tumour Ag have also been identified and are referred to as tumour specific Ag (TSA) or mutated Ag because they are only expressed on tumour cells. Examples of TSA include a mutated form of MART-2

(129) and the BCR-ABL fusion protein, which is found in a range of leukaemias (130). $CD4^+$ and/or $CD8^+$ T cell responses can be generated against these Ag, demonstrating their usefulness in the targeting of tumours using immunotherapy (125-129). The identification of TAA and TSA presents new possibilities for the development of effective therapeutic cancer vaccines.

1.3.3 Cancer equilibrium

The term cancer equilibrium refers to the period of time when cancer is present and the immune system is able to prevent the expansion of these cells but not eliminate them. Evidence for the existence of an equilibrium phase was originally inferred from studies involving organ transplant. The transplant of organs from donors who had previously undergone treatment for cancer and were thought to be cancer-free into recipients resulted in the development of tumours in the recipient that were of donor origin (131, 132). These findings suggest that although the donor no longer had a detectable tumour, cancerous cells still remained in the body, unable to re-establish a solid tumour but also unable to be cleared completely by the immune system. It was thought that these transferred cells were able to proliferate and become established tumours because the hosts were taking immunosuppressive medication to prevent organ rejection and also because the host immune system had not encountered these cancerous cells before and no Ag experienced cells existed. Direct experimental evidence of the equilibrium phase was provided by Koebel *et al* who showed that mice that originally failed to develop tumours after treatment with a low dose of a chemical carcinogen, could develop tumours after treatment with mAb designed to compromise the immune system (133).

It has been proposed that the equilibrium phase occurs because of a phenomenon called immune sculpting. Malignant cells are constantly mutating and it is thought that the immune system sculpts the development of the tumour by eliminating the cells that are most immunogenic, leaving behind malignant cells of low immunogenicity. This theory was demonstrated using 3-methylcholanthrene (MCA) induced sarcomas obtained from either wild type (wt) or RAG2-/- mice (120). When tumours from either wt or RAG2-/- mice were transplanted into RAG2-/- mice, they grew with similar kinetics, indicating that tumours grown in the presence or absence of an intact immune system exhibit no inherent growth differences (120). All tumours transplanted from wt mice into wt mice became established, in contrast 40% of tumours transplanted from RAG2-/- mice into wt mice were rejected (120). The results of this study (120), and other similar studies (82, 118, 134, 135), indicate that tumours formed in the absence of a competent immune system are more immunogenic than those formed in immunodeficient hosts. Through the process of immune "sculpting", tumours are able to reach the equilibrium stage of cancer immunoediting.

1.3.4 Cancer escape

Given that more than 7 million people die every year from various forms of cancer, it is obvious that tumours are often able to evade the immune system and continue to grow. This is the final stage of immunoediting, known as the escape phase and involves the use of multiple mechanisms by malignant cells to evade the immune response and become an established tumour. Strategies used by tumours to evade the immune response include the activation of immunosuppressive mechanisms (as discussed below in 1.4), the induction of T cell tolerance and mutations that render cancerous cells less sensitive to immune effector molecules (136, 137).

1.3.5 Treatment of cancer using immunotherapy

A number of prophylactic anti-cancer immunotherapeutic vaccines have shown that it is possible to prevent or delay tumour growth in mice (138-141) and this information has been a valuable tool for researchers. The relevant setting for cancer treatment in humans, however, is the therapeutic treatment of tumours. A number of different vaccination strategies have been used to successfully treat various murine cancers by immunotherapy. These strategies include the adoptive transfer of DC or T cells or treatment of subjects with various factors designed to either directly improve the activity of DC and T cells, or to block immune suppressive factors present in tumour bearing individuals.

The adoptive transfer of activated, Ag loaded DC to mice has been shown to result in an increase in activated T cells and can cause the regression of tumours. For example, Mayordomo *et al* showed that mice treated with DC that had been loaded with defined TAA developed an Ag specific $CD8^+$ T cell response. Furthermore, the Authors showed that the treatment of mice given otherwise lethal doses of C3 sarcoma or 3LL lung carcinoma with these DC resulted in tumour regression and survival in up to 80% of mice (142). In addition, Zitvogel *et al* showed that the adoptive transfer of DC loaded with undefined acid-eluted peptides from autologous tumour to mice bearing established C3 (H-2b) tumours resulted in the complete eradication of tumours and 100% survival of the mice in comparison to the controls, none of which survived (143). In another study, Fields *et al* showed that the treatment of MCA-207 sarcoma or MT-901 breast carcinoma bearing mice with DC that had been loaded with whole MCA-207 or MT-901 tumour lysates, respectively, resulted in a ~90% reduction in the number of established pulmonary metastases in comparison to the controls (144). Regression of the metastases was found to be primarily the result of a $CD8^+$ T cell response with some $CD4^+$ T cell help (144). In

contrast to the above studies, which involve the adoptive transfer of *in vitro* activated DC into tumour bearing mice, Merad *et al* showed that it is possible to achieve an effective anti-tumour response by activated DC *in vivo* (145). Merad *et al* found that the treatment of mice with the DC growth factor Fms-like tyrosine kinase 3 Ligand (Flt3L) caused an increase in the number of lymph node DC. Treatment of these mice with the TLR ligand CpG resulted in a further increase in the number of DC and upregulation of MHC II and CD86, indicating that the DC were activated. CpG treatment was also found to increase the survival of Flt3L expanded DC and to improve the size and quality of the $CD8^+$ T cell response. Finally, the Authors showed that adding the defined tumour Ag OVA to the Flt3L and CpG treatment of tumour bearing mice resulted in the regression of established B16.OVA tumours and a 60% survival rate in treated mice in comparison to the controls none of which, survived (145). DC vaccines hold much hope for the future of cancer immunotherapy because they prime an appropriate T cell response *in vivo* and the quality of this T cell response may differ from those stimulated *in vitro*. Furthermore, these DC are able to prime T cells of more than one specificity, can prime both a $CD4^+$ and a $CD8^+$ T cell response (144) and can protect mice against subsequent tumour challenges (146) indicating that a memory cell population has been formed.

The treatment of tumour bearing mice with adoptively transferred T cells has shown promise in the field of cancer immunotherapy. Peng *et al* showed that mice bearing otherwise lethal doses of EL-4 and MCA tumours showed 100% survival after the adoptive transfer of 2 $x10^7$ $CD8^+$ T cells that had been isolated from the draining lymph node of tumour bearing mice and then activated *in vitro* (147). Similar results were obtained after the transfer of OVA specific OTI T cells that had been activated using anti-CD3 and anti-CD28 mAb to mice bearing the acute myeloid leukaemia C1498 that had been modified to express the model antigen OVA (148). Interestingly, even the transfer of

10^7 naïve $CD8^+$ OTI T cells can clear established E.G7-OVA but not EL4 thymomas (149). CD4 T cells have also been shown to have a role in the elimination of tumour cells. Mumberg *et al* showed that the adoptive transfer of $CD4^+$ T cells into 6132A-PRO tumour bearing SCID mice, which themselves have no T cells, was sufficient to eliminate the tumours (150). The Authors showed using a neutralizing mAb specific for IFN-γ that production of IFN-γ by the transferred $CD4^+$ T cells was responsible for tumour cell death (150). The adoptive transfer of T cells is attractive as a cancer immunotherapy because patients can be treated with a large number of highly activated tumour-specific T cells, which have been activated in the absence of the suppressive factors present *in vivo*.

Other immunotherapies use mAb to target the tumours or modulate immune responses. Treatment of individuals with mAb designed to block receptors required for survival can slow tumour growth or cause tumour regression. For example Herceptin is a mAb that targets the HER2 receptor expressed on malignant human mammary tissue and significantly inhibits tumour growth (151). In contrast, tumours can also be directly targeted for destruction by the immune system using mAb such as anti-CD20, which targets B cell lymphomas in humans (152) and mice (153). In this case, the effector mechanism involved is thought to be Antibody-Dependent Cell-Mediated Cytotoxicity (ADCC), which involves the lysing of Ab bound targets by NK cells.

The anti-tumour immune response can be improved by the *in vivo* administration of mAb designed to inhibit or deplete immunosuppressive cells such as Treg. For example, the anti-CD25 mAb PC61 has been shown to deplete Treg, resulting in an improved T cell response and tumour regression in mice bearing 6 out of 8 different leukaemias, myelomas or sarcomas (154). The anti-tumour immune response can also be improved by treating tumour-bearing mice with a mAb that directly improves cell function. Llopiz *et al* found

that treating mice bearing an otherwise lethal dose of E.G7-OVA with an agonistic anti-CD40 mAb, the TLR Ligand adjuvant poly I:C, and tumour Ag resulted in an improvement in the Ag presenting function of DC and complete tumour regression in 100% of mice (155). Some mAb treatments are believed to have a dual role in improving the anti-tumour response by directly inhibiting the function of suppressor cells and directly improving the effector function of T cells. Intratumoral injection of the mAb OX86, which targets OX40 expressed on both Treg and activated T cells has been shown to block the suppressive function of Treg while also directly stimulating $CD8^+$ T cells resulting in the rejection of 80% of otherwise lethal CT26 tumours in mice (156). Similar results were seen when B16-BL6 melanoma bearing mice were treated with CTLA-4 (also known as CD152) specific antibodies to inactivate Treg and directly stimulate the effector function of activated $CD8^+$ T cells. These mice were also treated with the leukocyte growth factor Granulocyte-macrophage colony-stimulating factor (GM-CSF), and tumour regression was found to be dependent on $CD8^+$ T cells (157).

In contrast to the murine models discussed above, cancer immunotherapy appears to be successful only in a minority of humans. Expanded $CD8^+$ and $CD4^+$ T cell populations specific for tumour associated Ags have been found in individuals treated with DC vaccines (158-163), however, these responses rarely result in a clinical objective response (160-164). A study of 86 clinical trials for the treatment of various tumours including melanoma, prostate cancer and colorectal cancer found that only 3.3% of the 1306 patients showed an objective clinical response (165). In fact, despite the huge amount of resources dedicated to developing modern cancer immunotherapies, a retrospective study found that patients receiving these therapies fared no better than those that had received Coley's toxins (166). One of the proposed reasons for the lack of objective clinical responses to cancer immunotherapies in humans is the immunosuppressive mechanisms used by

tumours to evade the immune response. This demonstrates the importance of further understanding these mechanisms to the development of successful cancer immunotherapies.

1.4 The suppressive tumour environment

It is believed that the T cell dependent elimination of tumours requires the activation of tumour specific $CD8^+$ T cells in the lymph node followed by trafficking of these CTL into and throughout the tumour. The CTL must then be able to survive and maintain effector function long enough to eradicate the tumour. As discussed below, evidence exists that tumours are able to suppress each of these stages.

Tumours over-express growth factors such as the vascular endothelial growth factor (VEGF) family of molecules, which leads to abnormal vasculature within the tumour (167, 168) and hypoxia (169). Poor vasculature also means that cells and anti-cancer treatments are likely to have reduced access to the tumour tissue. Despite this, tumour specific $CD8^+$ T cells have been found in the tumour tissue with (170) and without (171, 172) adoptive T cell transfer. Studies have shown, however, that both CD4 (173, 174) and CD8 (173, 175, 176) T cell responses are impaired in tumour bearing mice. Tumour infiltrating T cells are thought to have sub-optimal effector function due to the expression of inhibitory ligands such as the non-classical HLA-E (177) and HLA-G (178) MHC molecules in human primary tumours and to a lesser extent in metastases. These molecules signal through inhibitory receptors on the surface of activated T cells and suppress the cytotoxic function of these cells (177).

Indoleamine 2,3-dioxygenase (IDO) is an intracellular enzyme that catalyses the rate limiting step of the tryptophan degradation pathway. Over-expression of IDO has been observed in a number of murine and human tumours and is thought to inhibit T cell activation, proliferation and survival by starving cells of tryptophan (179). Soluble inhibitory factors such as TGF-β and IL-10 are produced by many cell types, including malignant cells (180-182). Adenosine is produced during normal cellular responses, however, the extracellular levels of adenosine are elevated in tumours in response to hypoxia (183). As discussed in detail below in 1.4.4, adenosine has a number of anti-inflammatory properties (184-187).

Evidence exists to support the theory that the tumour environment decreases the survival of tumour specific CTL. Dong *et al* showed that a range of human tumours and the murine P815 tumour promoted apoptosis of activated tumour specific T cells *in vitro* (188). Apoptosis of the T cells was linked to the ectopic expression of B7-H1 molecules by the tumours and was found to be the result of signalling via the programmed death receptor-1 (PD-1) and other receptors, which are expressed on activated T cells (188). Similar results have been observed in other studies (189, 190).

Tumours are known to have elevated levels of a number of cell types with immunosuppressive function including Treg (191), MDSC (192, 193) and tumour associated macrophages (194), all of which are associated with a poor disease outcome. The role of hypoxia induced increases in intratumoral adenosine levels, and the presence of Treg in tumours is discussed in more detail below.

1.4.1 Hypoxia

Clinicians and physiologists define tissue hypoxia as a state of compromised biological function in response to oxygen availability or partial pressures that have fallen below a critical threshold. This threshold is poorly defined since different biological functions have differing requirements for oxygen however it is clear that hypoxia plays a very big part in tumour biology and treatment. Despite the fact that tumours have their own blood supply, most tumours are also hypoxic because the vasculature is abnormal (167, 169, 195). Hypoxia has been linked with driving proteomic and genomic changes in tumour cells for example through the hypoxia inducible factor family of transcription factors (HIF) resulting in increased survival and malignancy (196). Tumour hypoxia has been shown to reduce the efficacy of radiotherapy and some cytotoxic drugs either because of the requirement for oxygen by these therapies or because of the limited access of these drugs to hypoxic regions of tumour tissue (196). Tumour hypoxia further results in increased levels of adenosine, which has anti-inflammatory properties (197).

1.4.2 Hypoxia induced increases in adenosine levels

Intracellular adenosine triphosphate (ATP) is sequentially dephosphorylated by nucleoside triphosphate diphosphohydrolases to adenosine diphosphate (ADP) and adenosine monophosphate (AMP), which is then dephosphorylated to adenosine by 5' nucleotidases (Figure 1.4). Under normoxic (adequate oxygen supply) conditions, most of the adenosine is rephosphorylated to form AMP again by adenosine kinase (AK). The remaining adenosine is then either broken down by adenosine deaminase (ADA) to form inosine, or released from the cell via bi-directional nucleoside transporters (198-200) (Figure 1.4). Tumours contain immunosuppressive levels of adenosine (183) because hypoxia causes a

decrease in AK activity such that it can no longer process the adenosine fast enough causing an intracellular build up of adenosine (200), which is then released into the tumour microenvironment (Figure 1.4).

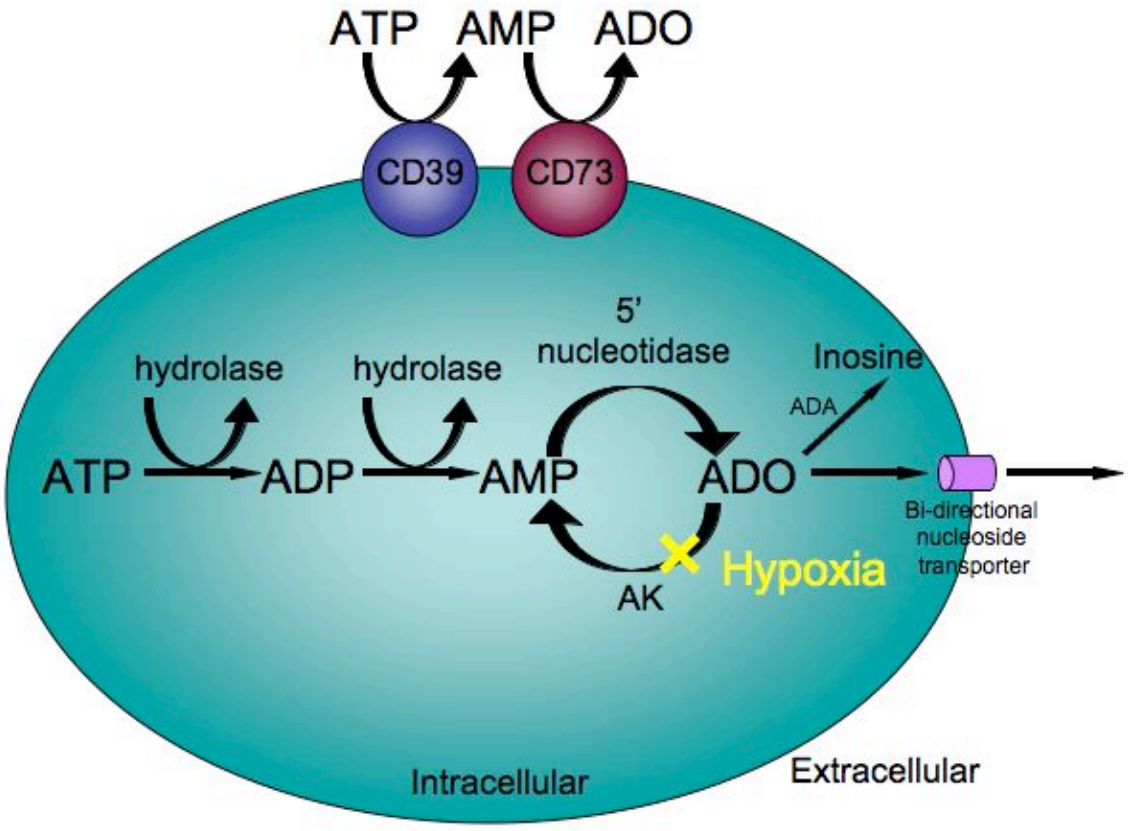

Figure 1.4: Adenosine metabolism and the effect of hypoxia.

ATP is sequentially dephosphorylated to AMP by a variety of hydrolases, and AMP is then converted to adenosine (ADO) by 5' nucleotidases. Under normoxic conditions, most ADO is rephosphorylated to AMP by adenosine kinase (AK). The remaining ADO is broken down into inosine by adenosine deaminase (ADA) or released from the cell via bi-directional nucleoside transporters. Under hypoxic conditions, AK activity is inhibited causing a build up of ADO, which cannot be completely compensated for by ADA activity leading to increased intracellular and extracellular levels of ADO. A similar pathway also occurs on the cell surface where ATP is sequentially dephosphorylated to AMP by the hydrolase CD39 and then converted to ADO by the 5' nucleotidase CD73.

1.4.3 The adenosine receptors

Adenosine mediates its effects through a family of four (A1, A2a, A2b and A3) G protein coupled seven transmembrane domain adenosine receptors. These receptors have non-redundant functions based on their differing cellular and tissue distribution as well as the type of G protein coupled to the cytoplasmic tail of the receptor. The G protein is made up of three subunits (α, β and γ) and following ligation of the adenosine molecule to the receptor, the α subunit dissociates from the receptor and causes changes in cAMP levels through its effects on Adenylyl cyclase, the enzyme which converts ATP to cAMP. If the α subunit is stimulatory (α_s), cAMP levels will increase, and in contrast, if the α subunit is inhibitory (α_i) cAMP levels will decrease (Figure 1.5).

The A1 and A3 receptors are negative regulators of cAMP levels and are mostly found in the brain and testis respectively. A1 receptors help control conditions such as bradycardia (abnormally low heart rate) and ischemic preconditioning (resistance to subsequent damage caused by oxygen deprivation). A3 receptor signalling is thought to enhance mediator release from mast cells. The A2b receptor is a positive regulator of cAMP levels, and is mainly found in the caecum, colon and bladder. This receptor has a role in relaxation of smooth muscle in vasculature and inhibition of monocyte and macrophage function. The A2a receptor is also a positive regulator of cAMP levels and is found in high levels in the spleen, thymus and on leukocytes and blood platelets (201). Triggering of the A2a receptors on blood platelets can lead to vasodilation via the release of ADP and ATP that stimulate the release of endothelium-derived NO (EDNO) (201).

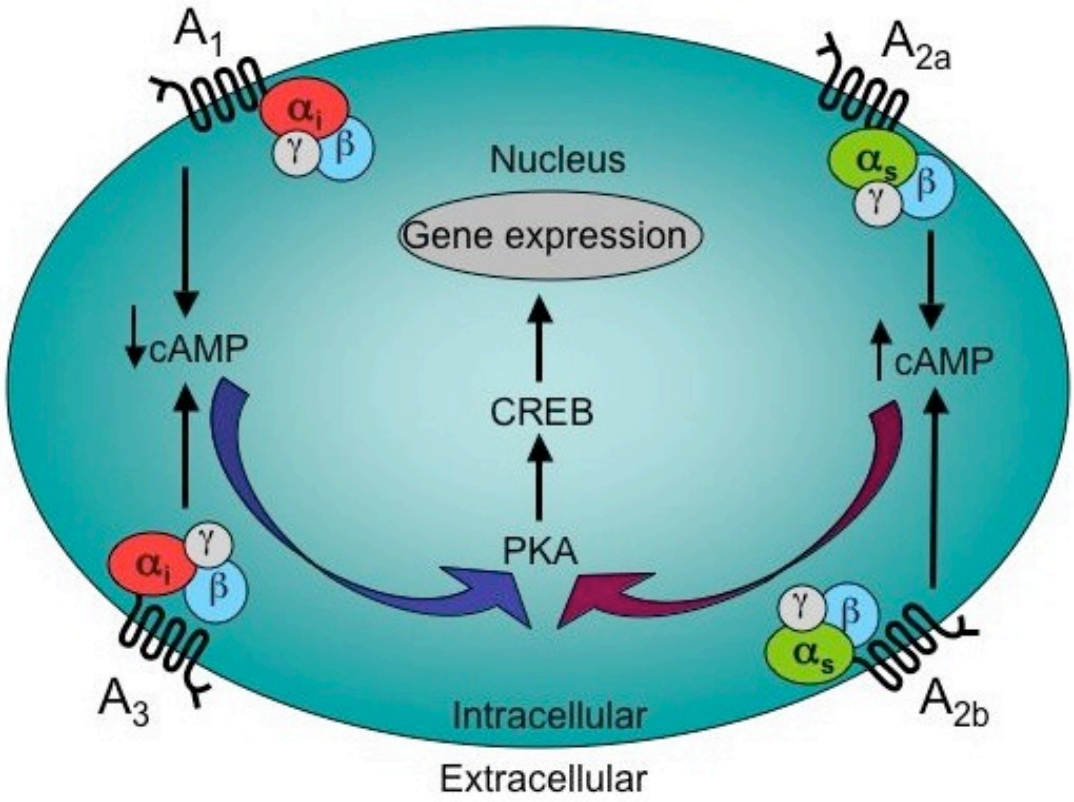

Figure 1.5: The tissue distribution and signalling pathways of the adenosine receptor family.

The cytoplasmic tail of each of the 7 transmembrane domain adenosine receptor family is coupled to a Gs protein consisting of an α, β and γ subunit. The α Gs subunit coupled to the A1 and A3 receptors is inhibitory (α_i) and results in decreased cAMP levels whereas the α Gs subunit coupled to the A2a and A2b receptors is stimulatory (α_s) and results in increases in cAMP levels. Changes in cAMP levels affect Protein Kinase A (PKA) and leads to changes in the cAMP Response Element Binding (CREB) family of transcription factors and results in altered gene expression.

1.4.4 Anti-inflammatory properties of adenosine

At high levels, adenosine has anti-inflammatory properties, which are mostly mediated via the A2a receptor due to its high expression on leukocytes. The use of A2a receptor knock out mice and selective A2a agonists and antagonists have shown that adenosine inhibits

TCR induced activation of thymocytes (184) and T cells (185, 186). T cells exhibited decreased proliferation, cytokine production and cytotoxic function in response to A2a receptor signalling (185-187). These direct effects of adenosine signalling on T cells are further exacerbated by the effect of adenosine signalling in DC. DC matured in the presence of adenosine show decreased CD86 and MHC II in mouse models (202) but increased levels in human cells (203) via A2b and A2a receptors respectively. However in both models, the overall effect of adenosine signalling was reduced TNF-α and IL-12 production, and increased IL-10 production (202-205). In mice these DC were associated with an increase in tumour growth (204). Natural Killer T cells show impaired release of cytotoxic granules (206), platelet activation is inhibited (207, 208) and TNF-α and IL-12 production by monocytes (209) and macrophages (210, 211) is also decreased in response to A2a signalling. Studies have further shown adenosine inhibits the oxidative burst in neutrophils via A2a (212, 213) and A3 (214) signalling.

Studies using selective A2a receptor agonists and antagonists on human tumour specific $CD4^+$ and $CD8^+$ T cells have shown that these cells have decreased cytokine production (215). The results of these studies demonstrate that the presence of adenosine is likely to contribute significantly to the immunosuppressive environment of solid tumours and emphasise that methods of abrogating adenosine signalling *in vivo* are a viable goal for cancer immunotherapy.

1.4.5 Treg

The existence of a regulatory T cell subset that prevents autoimmunity by suppressing self-reactive T cell responses was first proposed in the 1970s. Through a lack of supporting

evidence, this theory was largely disregarded until in 1995 Sakaguchi *et al* showed that $CD4^+$ $CD25^+$ T cells could prevent autoimmunity and graft rejection (216).

1.4.6 Treg phenotype

The term "regulatory T cells" refers to a range of cells of which $CD4^+$ $CD25^+$ $Foxp3^+$ Treg are only one example (Table 1.1). Some of these populations are summarised in table 1.1.

Commonly Known as:	Phenotype	Cytokines produced	References
Th3	$CD4^+$	TGF-β^{high}, IL-10^{low}, IL-4^{low}	(217)
Tr1	$CD4^+$ $CD25^{+/-}$	IL-10^{high}, IL-4^{low}	(218)
Treg	$CD4^+$ $CD25^+$ $Foxp3^+$	TGF-β, IL-10, IL-35	(219)
Ts	$CD8^+$ $CD28^-$	IL-10	(220)

Table 1.1: Regulatory T cell populations.

Originally Treg were classified as $CD4^+$ $CD25^+$ T cells (216) however naïve $CD4^+$ T cells will also express CD25 upon activation. The markers CTLA-4 (221-223), GITR (72, 222-224) and OX40 (CD134) (225) are also constitutively expressed on Treg, however, as with CD25, naïve T cells will also up-regulate these markers after activation. CD39 and CD73 can be individually expressed on many cell types, but they are only co-expressed to a high degree on Treg (226, 227). These markers are all thought to contribute to Treg function as outlined below. Activated Treg are further characterised as $CD103^+$ (222-224), $CD69^{high}$, $CD62L^{high}$ (223) and $CD127^{low}$ (228). Expression of the above markers varies from ~15 to ~90 % of the Treg population depending on their activation status and animal model and

expression of these markers also overlaps with other cell subsets. Obviously it is not practical to use all of these markers simultaneously to define the Treg population highlighting the need for a definitive Treg marker.

The discovery of the forkhead box (Fox) transcription factor Foxp3, which is expressed exclusively by Treg in mice (219), allowed Treg to be distinguished from newly activated $CD4^+$ effector T cells. In humans however it has been proposed that Foxp3 is also transiently expressed on newly activated $CD4^+$ T cells (229). The genome wide analysis of murine $CD4^+$ $CD25^+$ $Foxp3^+$ Treg identified ~700 genes and an intergenically encoded microRNA that had Foxp3 binding regions (230). Foxp3 was found to act as a transcriptional activator for some genes and as a transcriptional repressor for other genes. The target genes of Foxp3 in thymic and peripheral Treg were mostly plasma membrane proteins as well as cell signalling proteins. How the genes controlled by $CD4^+$ $CD25^+$ $Foxp3^+$ Treg interact together and contribute to the suppressive function of Treg is complicated and poorly understood.

1.4.7 The link between CD25 and Treg

The IL-2R is a heterodimer consisting of an α chain (CD25), a β chain (CD122) and a γ chain (70). CD25 itself has a low affinity for IL-2, however, when complexed with the β and γ chains, it becomes a high affinity receptor for the T cell survival cytokine IL-2 (231). Studies using IL-2-/- or IL-2Rα-/- mice have shown that while IL-2 is not required for initial $CD8^+$ T cell activation and proliferation, it is critical for optimal expansion and long-term proliferation of these cells (67). However the observation that these same mice develop a lymphoproliferative autoimmune syndrome (232, 233) proves that the cytokine also has a role in limiting T cell responses. Originally it was thought that this was because

the *de novo* expression of Foxp3 in the thymus was regulated by TCR engagement and IL-2 and TGF-β signalling (234) and in the periphery it was also thought to require CD28 signalling (235). Surprisingly, IL-2-/- and IL-2Rα-/- mice are still capable of producing normal levels of functional $Foxp3^+$ Treg, suggesting some redundancy in the role of IL-2 in Treg induction (223). TGF−β deficient mice were also found to produce normal levels of functional $Foxp3^+$ Treg but only in the presence of IL-2 signalling (234). These findings suggest that the critical role of IL-2, and therefore CD25, in limiting $CD8^+$ T cell responses is to maintain the Treg population rather than to induce Foxp3 expression or to facilitate the suppressive function of Treg (236).

1.4.8 Generation of Treg

Natural Treg are produced in the thymus (237) in a TGF-β and IL-2 dependent manner (234). Murine $Foxp3^-$ $CD4^+$ T cells can be induced to express Foxp3 *in vitro* using TGF−β (224, 238, 239), or can convert to the $Foxp3^+$ phenotype *in vivo* in the periphery (240). These cells subsequently acquire the suppressive function of Treg and are referred to as adaptive Treg. In most of these cells, however, Foxp3 expression and subsequently suppressive function is lost when cells are restimulated with antigen in the absence of exogenous TGF-β (241). This indicates an inherent instability of these adaptive Treg since suppressive function is dependent on continuous expression of Foxp3 (241).

1.4.9 Distinguishing a true $CD4^+$ $CD25^+$ $Foxp3^+$ Treg population with suppressive function in humans

The correlation between Treg and Foxp3 remains controversial in humans. Studies using *in vitro* expansion of $CD4^+$ $CD25^-$ $Foxp3^-$ cells have shown Foxp3 expression correlates

precisely with suppressive function (242). Other studies, in contrast, including one by Wang *et al* used retroviral vectors to over-express Foxp3 in $CD4^+$ $CD25^-$ $Foxp3^-$ T cells and found that Foxp3 expression does not result in a suppressive phenotype in all cases (229, 243, 244), however, this is likely because the cells were not expressing enough Foxp3 (245). In addition, the study by Wang *et al* involved the *in vitro* expansion and activation of $CD4^+$ $CD25^-$ T cell populations using anti-CD3, anti-CD28 and IL-2 (229), conditions that have been shown to cause significant proliferation of human $CD4^+$ $CD25^+$ $Foxp3^+$ Treg (246). This makes it difficult to draw firm conclusions from the study by Wang *et al*. It is possible that the expression of Foxp3 on newly activated $CD4^+$ T cells appeared transient because a contaminating Foxp3 regulatory T cell population had preferentially expanded, or because a large proportion of the Foxp3 expressing cells later died off leaving mostly $Foxp3^-$ cells (229). Furthermore, only high expression levels of Foxp3 were found to result in suppressive function. (244) The level of Foxp3 which is transiently expressed by newly activated $CD4^+$ T cells appears to be equivalent to that expressed by unactivated Treg and this is 4 fold lower than the level of Foxp3 expression seen in activated Treg with full suppressive function (245). This indicates that activated Treg can still be distinguished from newly activated $CD4^+$ T cells in humans using Foxp3 expression as a marker.

1.4.10 Treg function

In the steady state, Treg act as a protective mechanism against over active immune responses to self-Ag caused by self-reactive T cells that have escaped negative selection in the thymus. This was demonstrated by using both scurfy mice (219) and mice thymectomised at postnatal day 3 (d3tx) (237). Scurfy mice carry a defect in the Foxp3 gene, which produces a non-functional Foxp3 protein and these mice fail to properly

control $CD4^+CD8^-$ T cell responses (219). D3tx mice spontaneously develop autoimmunity, which can be rescued by the transfer of Treg (237, 247). It was originally proposed that this occurred because d3tx mice were able to develop $CD4^+$ and $CD8^+$ T cells but not $CD4^+$ $CD25^+$ Treg, which were thought to develop after post-natal day 3. Recent studies, however, have shown that d3tx mice actually have higher numbers of $CD4^+$ $Foxp3^+$ Treg than normal mice (247, 248). Treg from d3tx mice were shown to be capable of suppressing the inflammatory conditions autoimmune ovarian disease and dacryoadenitis when transferred into d3tx hosts, demonstrating that these Treg are capable of *in vivo* suppression and able to control autoimmunity (247). The authors suggest that in mice that have not received adoptively transferred Treg, the fully functional Treg in d3tx mice are unable to control autoimmunity because these mice also exhibit enhanced effector T cell (Teff) function (247). It is presumed that Treg from d3tx mice are able to control autoimmunity when transferred into d3tx hosts because the balance of Treg and Teff cells in these mice has been tipped in favour of the Treg.

Using diphtheria toxin to deplete Treg from adult Foxp3-*DTR* mice which have the diphtheria toxin receptor inserted downstream of the Foxp3 promoter, has further demonstrated the role of Treg in protection against autoimmunity (249). In humans, mutations in the Foxp3 gene result in absent or dysfunctional Treg and this is known to cause a syndrome of systemic autoimmunity known as immune dysregulation, polyendocronopathy, enteropathy and X-linked inheritance (IPEX) (250). IPEX syndrome is a rare recessive disorder that only affects male infants and is characterised by autoimmune enteropathy, diabetes, thyroiditis, food allergies and severe skin disease. Most sufferers of IPEX syndrome have a significantly shortened life expectancy (251). Treg are also thought to help control hyper-inflammation caused by infectious agents such as *Helicobacter hepaticus* (252), *Pneumocystis carinii (253)*, and ocular Herpes Simplex

virus (HSV-1) (254), which would otherwise cause severe tissue damage, and can help prevent graft rejection (255, 256).

It has also become apparent that the presence of Treg in certain conditions such as parasite, bacterial, fungal and viral infections (257) and cancers (154, 258, 259) is negatively correlated with disease outcome. In most cases, the frequency of Treg increases in response to these diseases suggesting they prevent efficient immune responses to these pathogens and allow them to persist in the individual.

1.4.11 Suppressive capabilities of Treg

It is generally accepted that *in vitro* Treg require activation via TCR stimulation to acquire their suppressive function (260-263). Once activated, however, Treg can suppress bystander cells in an antigen non-specific manner (262, 263). One study has even suggested that the suppression of fresh T cells by activated Treg does not require restimulation of the Treg via the TCR and is not MHC restricted implying the Treg may not need to be in contact with the APC during suppression of the target cell (263).

Conflicting reports have emerged over whether Treg mediated suppression is cell-cell contact dependent (260, 264, 265) or independent (266). This confusion may partially arise over the failure of some studies to distinguish between natural and adaptive Treg, or differences between *in vitro* versus *in vivo* function. This issue has further been complicated by work showing that transwell cultures, the method typically used to distinguish contact dependent versus independent reactions, may be misleading in this instance. This study concluded that the reason transwell cultures fail to show suppression is not because the cells require physical contact but because the system separates the cells

so much that the suppressive molecules are unable to come into contact with the target cell (264). Recent work has shown that natural and adaptive Treg can be distinguished from each other by using a PCR to determine the methylation state of the Treg specific demethylated region (TSDR) (267). *Ex vivo* isolated $CD4^+$ $CD25^+$ $Foxp3^+$ Treg were found to be completely demethylated and had stable Foxp3 expression. In contrast, TGF-β induced Treg showed only a partial demethylation of the TSDR region and both Foxp3 expression and suppressive activity were lost when these Treg were restimulated in the absence of TGF-β. These results show that stable Foxp3 expression requires epigenetic modification to produce a stable, suppressive, Treg (267).

Treg exhibit multiple layers of suppression as evidenced by their ability to suppress a range of cells, including T cells, macrophages, neutrophils, B cells, NK cells and DC (268-272). The suppressive effect of Treg on DC and T cells is discussed in detail below.

1.4.12 Mechanisms of Treg suppression

Strong evidence exists to suggest that Treg can suppress a number of aspects of DC function. Treg have been shown to inhibit the expression of the DC activation markers CD40, CD80, CD86 and MHC II, both in *in vitro* models (273, 274) and in an *in vivo* NOD mouse model (272). Two photon intra-vital microscopy experiments using the mouse EAE model have shown that Treg can decrease the interaction time between effector cells and DC in the lymph node (275). This is likely to result in ineffective priming of $CD4^+$ T cells, because these cells require contact with the APC throughout the expansion phase (which lasts days), to achieve optimal expansion (276, 277) and differentiation (278). Optimal $CD8^+$ T cell responses require a relatively short exposure (2-24 hours) to antigen (279, 280) combined with $CD4^+$ T cell help (281, 282). Reducing the interaction time

between DC and T cells may represent an indirect method of suppressing the T cell response. *In vivo* studies have also shown that Treg may indirectly suppress the homeostatic proliferation of DC in the peripheral lymphoid organs (249, 283, 284) by suppressing the production of Flt3L from an as yet unknown source (283).

There are 3 main stages at which Treg are thought to suppress the T cell response: suppression of T cell proliferation, suppression of T cell cytotoxicity and elimination of the T cells.

Studies have shown that Treg can produce a number of immunosuppressive molecules such as adenosine (226, 285), TGF-β (265), IL-10 (238, 286) and IL-35 (266) all of which can inhibit T cell proliferation. It has been suggested that Treg produce pericellular adenosine due to the co-expression of CD39 and CD73 on the surface of Treg (Figure 1.4), however, it is difficult to speculate on the importance of this mechanism because extracellular adenosine levels increase in tumours in response to hypoxia as discussed above.

Treg are also thought to mediate suppression of T cell proliferation through their control of known T cell growth factors such as IL-2. Originally it was thought that Treg inhibited the production of IL-2 by Teff (260). An alternative mechanism known as the "IL-2 sink" model was proposed where Treg were thought to inhibit the overall expansion of the Teff population by consuming vast quantities of cytokines such as IL-2 (287), which caused the Teff cells to apoptose due to cytokine deprivation (288). The relevance of the IL-2 sink theory is questionable *in vivo* because there are far less Treg than T cells present in the body and the chance of Treg encountering and utilizing the majority of the IL-2 molecules is therefore unlikely. A further study by Oberle *et al* using human Treg showed that Treg

rapidly prevent the transcription of IL-2 by activated $CD4^+$ T cells (289) and confirmed that the most likely explanation of how Treg control IL-2 levels is by inhibiting the production of IL-2 by activated T cells.

CTLA-4 is a CD28 homologue expressed constitutively on Treg (222) and is upregulated on various other cell types including T cells after activation (290). CTLA-4-/- mice die prematurely from lymphoproliferative disease (291) indicating that CTLA-4 negatively regulates T cell responses. There is both a direct and indirect explanation for this observation. Engagement of the CTLA-4 molecule on the Treg with the B7 family of receptors (CD80 and CD86 respectively) on T cells blocks CD28 mediated co-stimulation and suppresses T cell expansion (292) and possibly cytotoxic function (293). CTLA-4 expressing Treg can also engage the B7 family of receptors on DC causing down regulation of CD80 and 86 resulting in a decreased ability of these DC to stimulate T cell responses (222). Furthermore, CTLA-4 expressed on activated T cells inhibits the effector function of these T cells (294). Therefore anti-CTLA-4 mAb therapy boosts immune responses by increasing the activity of effector T cells directly and by decreasing the level of Treg mediated suppression on both the effector T cells and the DC (222, 292-294). Aside from its role in Treg function, CTLA-4 may also play a role, along with TGF−β, in Treg development (295).

GITR belongs to the tumour necrosis factor receptor (TNFR) family and like CTLA-4 is constitutively expressed on Treg (72) and various activated cell types including T cells (296, 297). Although GITR-/- mice can still generate a reduced number of functional Treg (298, 299), studies using mAb to block GITR signalling on Treg have shown greatly impaired suppressive function of these cells indicating they also have a role in Treg mediated suppression of T cell proliferation (72, 300).

OX40 is also a member of the TNFR family expressed constitutively on Treg and upregulated on activated T cells (300). Treg have been shown to have greatly impaired suppressive function in the presence of anti-OX40 mAb suggesting that OX40 has a role in Treg function similar to that observed for GITR (156, 300). In contrast to GITR-/- mice, OX40-/- mice are able to generate normal numbers of peripheral Treg. Fewer OX40-/- $CD4^+$ $Foxp3^-$ cells can be converted *in vitro* to $CD4^+$ $Foxp3^+$ Treg, however, which suggests that OX40 exerts some control over the expression of the Foxp3 gene (301, 302).

Treg have been shown to suppress T cell cytotoxicity by inhibiting the release of IFN-γ (262, 289) and cytotoxic granules (175, 303). The exact mechanism of this suppression is unclear but it is thought to be TGF-β dependent (176, 304).

As previously discussed, Treg may cause target cell death indirectly by cytokine deprivation induced apoptosis (288). It has also been proposed that Treg may directly kill target cells using GzmB (305, 306) and perforin (305-307). *In vitro* studies have shown that in addition to the reduced proliferation of $CD4^+$ T cells seen in the presence of Treg, the rate of $CD4^+$ T cell but not Treg apoptosis was increased in both murine (306) and human models (307, 308). In addition, Cao *et al* showed that wild type but not perforin deficient Treg promoted tumour growth and correlated with an increase in the rate of apoptosis in the $CD8^+$ T cell and NK cell compartments of the tumour (305).

It is obvious that Treg suppress immune responses in a vast and eclectic manner, and multiple mechanisms are likely used at any one time. Therefore finding ways that either completely inactivate or deplete these cells exclusively is likely to be a key step towards successfully treating many diseases including cancer.

1.4.13 Abrogating Treg function *in vivo*

Finding a treatment that selectively and effectively eliminates or inactivates Treg has been complicated by the fact that the most definitive marker of Treg is Foxp3, which is a transcription factor and therefore only found intracellularly.

In mice, anti-CD25 mAb treatment is routinely used to abrogate Treg mediated suppression *in vivo*, however, the exact mechanism of this treatment has been the subject of some debate. The anti-CD25 mAb 7D4 has been shown to functionally inactivate >90% of the $CD4^+$ $CD25^+$ $Foxp3^+$ population without depleting the cells (309). In contrast, the anti-CD25 mAb PC61 has been shown to deplete 45-75% of the $CD4^+$ $CD25^+$ $Foxp3^+$ population in the spleen (138) and 30-65% in the lymph node (156, 310, 311) and inactivate the remaining $CD4^+$ $CD25^+$ $Foxp3^+$ Treg (311). The degree to which the Treg are depleted or inactivated using PC61 is likely dependent on the amount of mAb administered or encountered by the individual T cells. In mice, cyclophosphamide and denileukin diftitox (recombinant human IL-2 protein fused to fragments of the diphtheria toxin and also known as ONTAK) have also been used with some success however only PC61 appears to be able to reduce Treg numbers without affecting $CD8^+$ T cell numbers (138). PC61 treatment has been shown to improve anti-tumour effector (154, 259) and memory (312) responses, especially when used in conjunction with other treatments involving the use of anti-CD40 mAb (313) and immunisation with tumour Ag (314) for example. The effect of PC61 on Treg typically lasts only a matter of weeks (138) and repeat treatment is not advisable because activated T cells may also be affected which would cancel out any anticipated benefit of further depleting Treg. PC61 has therefore been a useful tool in demonstrating that depleting Treg is a viable treatment for boosting

immune responses. It is evident, however, that more selective and effective treatments are still required.

Recent studies have also used mAb specific for the folate receptor 4 (FR4) to deplete Treg *in vivo*. Doses as low as 1 μg of anti-FR4 mAb have been shown to reduce the frequency of $CD4^+$ $CD25^+$ Treg in the blood by up to 80%, however, the $CD4^+$ $CD25^-$ T cell population was also depleted by 30% (315).

CTLA-4, GITR and OX40 have all been shown to have some control over Treg function as discussed above. A number of studies have investigated the use of antibodies against these molecules to deplete Treg and boost immune responses. Tumour regression was observed in mice treated with anti-CTLA-4 mAb (316). Treatment of tumour bearing mice with anti-GITR mAb also resulted in the regression of tumours in an IFN–γ dependent manner. Co-treatment with anti-CTLA-4 further increased the anti-tumour response and caused the regression of larger tumours. Administration of anti-OX40 mAb has also been shown to cause tumour regression (317). The adoptive transfer of wild type or OX40-/- Treg into tumour bearing mice has shown that part of the increased immune response is due to inhibition of the Treg. This led to increased numbers of DC migrating to the lymph node to stimulate a T cell response which was further boosted by the direct stimulatory action of OX40 on the T cells (156). PC61 treatment, however, actually decreased the efficacy of anti-GITR and anti-OX40 mAb therapies (156, 318). Anti-GITR and anti-CTLA-4 mAb also have a stimulatory effect on T cells (299) making it difficult at this stage to determine how much of the increased immune response observed after treatment with these mAb was due to Treg suppression versus T cell stimulation.

While the use of mAb to block CTLA-4, GITR and OX40 have shown great promise as anti tumour therapies, these markers are expressed only on a subset of Treg indicating there is still room for improvement. It is difficult to study the role of CTLA-4, GITR and OX40 therapy in suppressing Treg function because of the role these molecules also have in stimulating T cell function. Therefore, in order to study the effects of Treg, PC61 treatment remains the simplest model.

1.5 Hypothesis and Aims

The success of cancer immunotherapies designed to improve the function of DC and/or T cells *in vivo* has so far been limited, largely because of the immunosuppressive methods employed by the tumour to evade the immune response. Studies combining immune boosting therapies with methods to abrogate the immunosuppressive environment have shown some success, however, objective clinical responses to these cancer immunotherapies still only occur in a minority of patients. Understanding which immunosuppressive mechanisms tumours use and how they mediate immunosuppression is likely to lead to the design of combination treatments with improved efficacy.

The hypothesis of this thesis was that in the B16.OVA murine melanoma model, tumour specific $CD8^+$ T cell function is suppressed by intratumoral adenosine. It was further hypothesised that Treg also inhibit DC and T cell function using a perforin-dependent mechanism.

To test these hypotheses, the following aims were investigated:

1) To determine if the anti-tumour activity of transferred tumour specific $CD8^+$ T cells could be improved by inhibiting adenosine signalling.

2) To investigate whether the DC presenting tumour Ag show an improved capacity to stimulate an anti-tumour T cell response in Treg deficient mice.

3) To evaluate whether Treg mediated suppression of $CD8^+$ T cell activation is perforin-dependent.

CHAPTER TWO

MATERIALS AND METHODS

2.1 Materials

2.1.1 Labware

Product	**Supplier/Distributor**
ABI Prism® optical tubes (8 tubes/strip) & optical caps (8 caps/strip)	Applied Biosystems, Foster City, CA, USA
Acrodisc® 32 mm syringe filters with a 0.2μm Supor® membrane	PALL LifeSciences, Cornwall,U.K
Axygen Micro Tubes 0.6 & 1.7ml	Axygen Scientific Inc., Union city, CA, USA
Cuvettes: Disposable electroporation chambers Gap electroporation cuvettes	 Life Technologies, Gaithersburg, Maryland, USA. BioRad, Hercules, California, USA
BD 1 mL Tuberculin syringes & BD 10 mL syringes	BD BioSciences, Bedford, MA, USA
BD PrecisionGlide™ Needles: 18, 20, 25 & 27.5 gauge	
BD Ultra-Fine™ needle Insulin syringes (29 gauge): 0.3, 0.5 & 1 mL	
Falcon® Polystyrene sterile conical tubes: Blue Max 50mL & Blue Max Jr 15 mL	
Falcon® Polystyrene sterile multiwell tissue culture plates: 6 well & Microtest™ U-bottom 96 well	

plates	
Falcon® Polystyrene sterile tissue culture flasks: 200mL & 600mL	
Falcon® Polystyrene sterile serological pipettes	
Nylon cell strainers (40 & 70 μm)	
No. 1 22x22 cover slips	Biolab Ltd., Auckland, NZ
Nylon Gauze (70mm)	NZ Filter Specialists Ltd., Auckland, NZ
Superfrost® Plus microscope slides	Biolab Ltd., Auckland, NZ
TitreTubes® Micro Tubes	BioRad, Hercules, CA, USA

2.1.2 Reagents and Buffers

2 Mercaptoethanol (2 ME)

2 ME was purchased as a 55 mM solution in PBS from Sigma (St. Louis, Missouri, USA) and stored at 4^{o}C.

α-Galactosylceramide (α-Gal)

α-Gal was kindly provided by Gavin Painter (IRL, Lower Hutt, NZ) and was manufactured as described in Lee *et al* (319). The lyophilised powder was reconstituted to a stock concentration of 10 mg/mL using a 10:10:3 ratio of methanol, chloroform and injection grade dH_2O respectively and stored at 4^{o}C until used. The stock concentration was diluted using PBS containing 5% Tween (original concentration of 70%) to a working solution of 200 μg/mL and stored at 4^{o}C until used.

Acetone

Acetone was purchased from Merck (Darmstadt, Germany) and stored at room temperature until used.

Ambion DNAfree kit

The DNA*free* kit was purchased from Ambion Inc, (Austin, Texas USA) and stored at -20^{o}C. The kit contains 10x DNAse buffer, 2 U/μL DNAse and 10x DNAse Inactivation reagent.

Ammonium Chloride Tris (ACT) Lysis Buffer

0.16 M NH_4Cl, pH 7.4 (Sigma, St. Louis, Missouri, USA) and 0.17 M Tris-HCl pH 7.65 (Merck, Darmstadt, Germany respectively) were mixed in a 9 to 1 ratio to give final concentrations of 0.144 M NH_4Cl and 0.017 M HCl. Buffer was stored at 4^{o}C until used.

Alsever's Solution

20.5 mg/mL Dextrose, 4.2 mg/mL NaCl and 8 mg/mL sodium citrate,$2H_2O$ (all from BDH Laboratory Supplies, Poole, England), were dissolved in distilled H_2O (MilliQ) and the pH was adjusted to 6.1 with 1 M citric acid (BDH Laboratory Supplies, Poole, England). Alsever's solution was stored at room temperature until used.

5-(and-6)-carboxyfluorescein diacetate, succinimidyl ester (CFSE)

CFSE was purchased in powder form from Molecular Probes (Eugene, Oregon, USA), resuspended as a 10 mM solution in DMSO (Sigma, St. Louis, Missouri, USA) and stored in 10 μL single use aliquots at -20^{o}C.

CellTracker Orange (5-(and-6)-(((4-chloromethyl)benzoyl)amino)tetramethylrhodamine) (CTO)

CTO was purchased in powder form from Molecular Probes (Eugene, Oregon, USA), resuspended as a 10 mM solution in DMSO (Sigma, St. Louis, Missouri, USA) and stored in 10 μL aliquots at -20^{o}C. Aliquots were freeze-thawed not more than 3 times.

Chloroform

Chloroform was purchased from Merck (Darmstadt, Germany) and stored at room temperature until used.

DNase I

DNase I was purchased as a lyophilised powder from Roche, (Mannheim, Germany), dissolved in IMDM to a concentration of 10 mg/mL and stored at -20^{o}C.

Ethanol (EtOH)

Molecular grade 100% EtOH was purchased from Carlo Erba Reagents (Milan, Italy) and stored at room temperature until used.

Ethylenediaminetetraacetic Acid (EDTA)

EDTA (Sigma, St. Louis, Missouri, USA) was purchased in powder form and dissolved in dH_2O to give a stock concentration of 0.5 M and stored at room temperature until used.

Flow Cytometry Analysis (FCA) Buffer

0.5 M EDTA, 5% NaN_3 (Sigma, St. Louis, Missouri, USA) and FBS (GIBCO, Invitrogen, Auckland, NZ), were added to PBS along with FBS to give final concentrations of 10 mM EDTA, 0.01% NaN_3 and 2% FBS. Buffer was stored at 4^{o}C until used.

Fluorescence Activated Cell Sorting (FACS) Buffer

0.5 M EDTA (Sigma) and FBS (GIBCO) were added to RPMI medium 1640 containing L-glutamine but not phenol red (GIBCO, Invitrogen, Auckland, NZ), to give final concentrations of 10 mM and 2 % respectively. Buffer was stored at 4^{o}C for up to 1 week.

Foetal Bovine Serum (FBS)

FBS was purchased from GIBCO (Invitrogen, Auckland, NZ) and stored in 25 mL aliquots at -20^{o}C. After thawing, aliquots were stored at 4^{o}C for a maximum of 2 weeks. The endotoxin levels of the FBS was determined before purchase and found to be 27 EU/mL. FBS was also screened for Mycoplasma and virus before purchase.

Geneticin® (G418)

The selective antibiotic Geneticin® (G418, GIBCO, Invitrogen, Auckland, NZ) was made into aliquots and stored at -20 °C. In use aliquots were stored at 4^{o}C.

Intracellular cytokine detection kits

The BD Cytofix/Cytoperm kit containing 1x Cytofix/Cytoperm buffer and 10x Perm/Wash buffer was purchased from BD Pharmingen (San Diego, Calilfornia, USA) and stored at 4^{o}C until used. The Foxp3 flow kit containing 4x Fix/Perm buffer and 10x Perm buffer was purchased from eBioscience (Bedford, Maryland, USA) and stored at 4^{o}C until used.

Iscove's Modified Dulbecco's Medium (IMDM)

IMDM supplemented with GlutaMAX^{TM}, 25 mM HEPES buffer and 3.024 mg/L $NaHCO_3$ was purchased from GIBCO (Invitrogen, Auckland, NZ) and stored at 4^{o}C until used.

Complete Iscove's Modified Dulbecco's Medium (cIMDM)

IMDM was supplemented with 100 U/mL Penicillin-Streptomycin (GIBCO, Invitrogen, Auckland, NZ), 55 μM 2 ME and 5% FBS. Media was stored at 4°C for a maximum of 2 weeks.

Isopropanol

Analytical grade Isopropanol was purchased from Scharlau Chemie, (Barcelona, Spain) and stored at room temperature until used.

Liberase CI

Liberase CI was purchased as a lyophilised powder from Roche (Mannheim, Germany), dissolved in injection grade dH_2O to a concentration of 16.7 mg/mL and stored in single use aliquots of 125 μL at -20°C.

Lipopolysaccharides (LPS)

LPS from *Escherichia coli*, serotype 0111:B4, was purchased as a lyophilised powder from Sigma (St. Louis, MO, USA), dissolved in IMDM to a stock concentration of 1 mg/mL and stored at 4°C. The stock concentration was further diluted 100x in IMDM to a working solution of 10 μg/mL, which was used immediately.

Magnetic Separation (MACS) Beads

Anti-CD8α, anti-CD4, anti-CD11c and anti-biotyn MACS Microbeads were purchased from Miltenyi Biotec (Germany) and stored at 4°C until used.

Methanol

Analytical grade methanol was purchased from Scharlau Chemie (Barcelona, Spain) and stored at room temperature until used.

Polymerase Chain Reaction (PCR) reagents

10 mM dNTP mix (containing 10 mM ATP, GTP, CTP and TTP), 0.2 U/μL Platinum® Taq DNA polymerase, 10x PCR buffer (-$MgCl_2$) and 50 mM $MgCl_2$ were purchased from (Invitrogen, Auckland, NZ) and stored at -20^{o}C.

Primer sequences

Primers were obtained from Sigma GenoSys (Sigma Aldrich, Auckland, NZ)

Gene target	Name of primer set	Annealing Temperature	Expected size of product (bp)	Sequence of primers 5'-3' Forward primer listed first
A2a adenosine receptor	For1/Rev1	56^{o}C	374	CTCACGCAGAGTTCCATCCT TCCATCTGCTTCAGCTGTCT
	For2/Rev2	61^{o}C	316	CGTTGTCAACCCCTTCATCT CTGGTGCTCCTGGGTAAGAA
18S rRNA		56 or 61^{o}C	150	GTAACCCGTTGAACCCCATT CCATCCAATCGGTAGTAGCG
GAPDH		61^{o}C	222	AACTTTGGCATTGTGGAAGG ACACATTGGGGGTAGGAACA

Penicillin-Streptomycin

Penicillin-Streptomycin was purchased in liquid form from GIBCO (Invitrogen, Auckland, NZ) and stored as single use aliquots at -20^{o}C until used.

Phosphate Buffered Saline (PBS)

$CaCl_2$ and $MgCl_2$ free PBS was purchased from GIBCO (Invitrogen, Auckland, NZ) and stored at 4^{o}C after opening.

Reverse Transcription Reagents

50 μM Random Hexamer primer, 10 mM dNTP mix, 100 mM DTT, 40 U/μLRNAse OUT, 200 U/μL Superscript III RT and 2 U/μL RNase H were purchased from Invitrogen (Auckland, NZ) and stored at -20^{o}C until used.

Small Interfering RNA (siRNA) sequences

The A2a adenosine receptor siRNA sequence was obtained from Chen et al (320) and was purchased from Sigma-Proligo (Sigma Aldrich, Auckland, NZ).

Sense strand: 5'-AAGUGGCACUUGGCUAUUUCU

Anti-sense strand: 5'-AAAUAGCCAAGUGCCACUUCU

Glyceraldehyde 3-phosphate dehydrogenase (GAPDH) siRNA was purchased as part of a positive control kit from Ambion Inc (Austin, TX USA).

Sodium Azide (NaN_3)

NaN_3 (Sigma, St. Louis, Missouri, USA) was purchased in powder form and dissolved in dH_2O to give a stock concentration of 5%. The solution was stored at room temperature until used.

Sodium Chloride (NaCl)

NaCl was purchased in powder form from Sigma (St. Louis, MO, USA), dissolved in dH_2O to a final concentration of 1.8% and stored at room temperature.

Tris-acetate-EDTA (TAE) buffer

TAE buffer containing 2 M Tris Acetate and 50 mM EDTA was purchased as a 50x concentrated stock from GIBCO (Invitrogen, Auckland, NZ) and diluted to a 1x working solution using dH_2O.

Tris Buffered Saline (TBS)

TBS buffer was made by adding 2.5 mL 20% Triton X and 25 mL FBS to 500 mL PBS to give a final concentration of 0.1% Triton X and 5% FBS. The buffer was stored at 4^oC until used.

Tritiated Thymidine

6-Methyl-3H thymidine (5 mCi), with a specific activity of 5 Ci/mmol, was purchased from Amersham Biosciences (Little Chalfont, UK). The stock was diluted in IMDM to a working solution of 20 μCi/mL and stored at 4^oC.

Triton® X405 (Triton X)

Triton X was purchased as a 70% solution from Sigma (St. Louis, Missouri, USA) and stored at room temperature until used. A 20% working solution was made by adding 10 mL Triton X to 15 mL PBS and was stored at room temperature until used.

Trypsin/EDTA

Trypsin/EDTA solution containing 0.25% Trypsin and 1 mM EDTA in Hanks' Balanced Salt Solution, was purchased from GIBCO (Invitrogen, Auckland, NZ), and aliquots were stored at -20^{o}C. In use aliquots were stored at 4^{o}C.

Tween® 20 (Tween)

Tween was purchased from Sigma (St. Louis, Missouri, USA) and stored at room temperature until used.

Vectashield

Vectashield was purchased from Vector Laboratories, Inc (Burlingam, California, USA) and stored at 4^{o}C until used.

Wuerzburger Buffer

0.5 M EDTA, 10 mg/mL DNAse I and FBS was added to sterile PBS to give a final concentration of 5 mM EDTA, 20 μg/mL DNase and 1 % FBS. Buffer was stored at 4^{o}C until used.

2.1.3 Cytokines

Granulocyte-macrophage colony stimulating factor (GM-CSF)

Recombinant murine GM-CSF was produced using stationary phase cultures of the murine X63 cell line, modified to secrete the full-length murine GM-CSF protein. The modified murine X63 cell line was kindly provided by Dr Antonius Rolink (Basel Institute for Immunology, Basel, Switzerland).

IL-4

Recombinant murine IL-4 was produced using stationary phase cultures of a Chinese Hamster Ovary cell line (CHO), modified to secrete the full length murine IL-4 protein (321). The IL-4 producing CHO cell line was kindly provided by Dr Antonius Rolink (Basel Institute for Immunology, Basel, Switzerland).

IL-2

Recombinant human IL-2 was produced using stationary phase cultures of the IL2L6 cell line, generated by modifying the murine J558 parental line to secrete the full-length human IL-2 protein (322).

Cytokines were collected by growing adherent cells in cIMDM, harvesting the culture supernatants and filtering through a 0.2 μm serum filter. The cytokines were titrated using BMDC cultures (GM-CSF and IL-4) or IL-2 dependent T cell clones (IL-2) to determine the optimal amount to be used and were stored as aliquots at -80^{o}C. In use aliquots were stored at 4^{o}C for up to 2 weeks.

2.1.4 Antibodies and fluorophores

4′,6-diamidino-2-phenylindole, dihydrochloride (DAPI)

DAPI was purchased as a lyophilised powder from Invitrogen (Auckland, NZ) and dissolved in dH_2O to a stock concentration of 5 mg/mL. The solution was then further diluted to a working solution of 200 mg/mL in FCA buffer and stored in aliquots at 4^{o}C until used.

Streptavidin (SA) Alexa Fluor 555

SA-Alexa Fluor 555 was purchased from Invitrogen (Auckland, NZ) and stored in aliquots at -20^{o}C. In use aliquots were stored at 4^{o}C.

The following antibodies were purified from B cell hybridoma cell lines using protein G-Sepharose (Pharmacia Biotech, Uppsala, Sweden):

Specificity	**Clone**
FcγRII/III (CD32/CD16)	2.4G2
CD3	2C11
CD4	GK1.5
CD8α	2.43
CD11c	N418
CD25/IL-2Ra	PC61
CD86/B7-2	GL1
F4/80	BM8
MHC II (I-A)^{b}	3JP

The following antibodies were purchased from eBioscience (San Diego, CA, USA):

Specificity	**Clone**	**Isotype**
Foxp3	FJK-16s	Rag IgG2aκ
KLRG-1	2F1	Golden Hamster IgG
TNF-α	MP6-XT22	EBRG1

The following antibodies and fluorophores were purchased from BD Pharmingen (San Diego, CA, USA):

Specificity	**Clone**	**Isotype**
CD8α	53-6.7 & Ly-2	
CD11b	M1/70	
CD11c	HL3	
CD25/IL-2Rα	7D4 & PC61	Rat $IgG1_{\lambda}$ Rat IgM_{κ}
CD40	3/23	
CD45	30-F11	
CD45.1	A20	
CD122/IL-15Rβ	TM-β1	G155-178
IFN-γ	XMG1.2	
Vα2	B20.1	
Vβ5.1,5.2	MR9-4	
Propidium Iodide (PI)		
SA – FITC, PE, PerCP, APC		

2.1.5 Proteins and peptides

Ovalbumin protein from chicken egg white (OVA) was purchased from Sigma-Aldrich NZ Ltd, Auckland, NZ. The ovalbumin peptides SIINFEKL ($OVA_{257-264}$) and ISQAVHAAHAEINEAGR ($OVA_{323-339}$) were purchased from Mimotopes Pty Ltd (Clayton, VA, Australia).

2.1.6 Tumour cell lines

The B16.OVA melanoma tumour cell line was generated by Drs. Edith Lord and John G. Frelinger, University of Rochester, Rochester, NY (323) and kindly provided by Drs. Roslyn Kemp and Dick Dutton, Trudeau Institute, NY, USA. The B16.F1 melanoma tumour cell line was purchased from American Type Culture Collection (ATCC, Manassas, VA, USA) and used as a control because the growth kinetics was similar to B16.OVA.

2.1.7 Mice

2.1.7.1 Maintenance and ethical approvals

All mice were bred and maintained in the Biomedical Research Unit of the Malaghan Institute of Medical Research. The experimental procedures performed on these mice were approved by the Victoria University Animal Ethics Committee and carried out in accordance with the guidelines of Victoria University of Wellington.

2.1.7.2 Mouse strains

C57BL/6 (C57) breeding pairs were obtained from the Jackson Laboratories (Bar Harbour, ME, USA).

B6.SJL-Ptprc^{a}Pep3^{b}/BoyJArc (B6 congenic) mice were created by backcrossing the inbred strain SJL, expressing the Ptprc^{a} gene (CD45.1), onto the C57BL/6 (CD45.2) background (324). C57BL/6 and B6 congenic cells can therefore be differentiated on the basis of

CD45.1 and CD45.2 expression respectively. Breeding pairs were obtained from the Animal Resources Centre (Canning Vale, WA, Australia).

Foxp3GFP mice (325) were created by the in-frame insertion of the eGFP gene into the first coding exon of the Foxp3 gene located on the X chromosome. These mice produce a fully functional Foxp3 protein fused to the eGFP protein. Breeding pairs were obtained from Prof. Alexander Y Rudensky, University of Washington (Seattle, Washington, USA).

OTI and OTII mice (326, 327) express transgenic TCR specific for K^b+ $OVA_{257-264}$ and I-A^b + $OVA_{323-339}$, respectively, and were obtained from Dr. Sarah Hook, School of Pharmacy, Dunedin, NZ, with the permission of Prof. Frank Carbone, Melbourne University, Australia.

OTI congenic mice were created in-house, by crossing OTI mice ($CD45.2^+$) with B6 congenic mice ($CD45.1^+$).

Perforin deficient (PKO) breeding pairs (92) were obtained from Jackson Laboratories (Bar Harbour, ME, USA).

V(D)J Recombination Activation Gene RAG-1 deficient mice (RAG1-/-) are defective in their ability to recombine the T cell receptor (TCR) and B cell receptor (BCR) and as a consequence have no mature T or B cells (328). RAG1-/- breeding pairs were purchased from the Waler and Eliza Hall Institute (Melbourne, Australia).

Mouse strains were maintained by mating between brothers and sisters. For all experiments mice were sex matched and 6-8 weeks old when the experiments commenced.

2.2 Methods

2.2.1 General cell culture

All cells were cultured in cIMDM at 37°C with 5 % CO_2 and 95 % humidity. Tumour cell cultures also contained 0.5 mg/mL G418 (GIBCO, Auckland, NZ). Adherent cells were incubated for 1 minute at 37°C in 3 mL Trypsin/EDTA to detach them from the flask. Proteolysis was stopped by the addition of an equal volume of FBS and cells were washed twice in IMDM before injecting into mice.

2.2.2 Dendritic cells (DC)

2.2.2.1 Generation of Bone marrow derived DC

C57BL/6 mice were euthanised and the hind legs were detached at the hip and collected into IMDM. All soft tissue was removed and the knee joints and ends of the femur and tibia were cut off to allow access to the bone marrow (BM). Bone marrow was then flushed from the bones by inserting a 25-gauge needle attached to a 10 mL syringe into one end of the bone and then pushing the IMDM through the bone and into a 50 mL Falcon tube. Cell clumps were disrupted by vigorous repeat pipetting followed by passing the suspension through a 70 μm nylon filter. Live cells were identified by trypan blue (GIBCO, Invitrogen, Auckland, NZ) exclusion and counted using a haemocytometer. Cells were pelleted by centrifugation at 320 xg for 4 minutes and resuspended at 4 x 10^5 cells/mL. Cells were plated out into 6 well plates at 2 x 10^6 cells/well containing 10 ng/mL GM-CSF and 20 ng/mL IL-4 (329). Cells were incubated at 37°C and supplemented with

nutrients on days 2, 4 and 6 by replacing 2 mL from each well with 2 mL of cIMDM containing 10 ng/mL GM-CSF and 20 ng/mL IL-4.

2.2.2.2 Activation of DC

During the final ~16 hours of the 7 day DC culture, DC were activated by the addition of 50 μL of 10 μg/mL LPS to the cultures to give a final concentration of 100 ng/mL LPS. Adherent cells were harvested on day 7 by gently rinsing the plates with the supernatant 2-3 times before collecting the supernatant a final time.

2.2.2.3 Loading of DC with α-Gal

During the final ~24 hours of the 7 day DC culture, α-Gal was added to the culture at a final concentration of 100 ng/mL. Adherent cells were harvested on day 7 by gently rinsing the plates with the supernatant 2-3 times before collecting the supernatant a final time.

2.2.2.4 Loading of DC with OVA protein

OVA protein was added to DC cultures at a final concentration of 1 mg/mL, 24 hours before harvesting and 8 hours before LPS treatment. Cells were washed twice in sterile PBS and resuspended in sterile PBS at the appropriate concentration for i.v. injection of 200 μL/mouse.

2.2.3 In vitro T cell activation

LPS-treated DC were plated out into 6 well plates at 4 x 10^5 cells/well in a 2.5 mL volume of cIMDM. SIINFEKL was added to the DC culture to give a final concentration of 2 μM. Four hours after the addition of SIINFEKL, lymph nodes from euthanised, OTI mice were collected into IMDM and processed into single cell suspensions by using the plunger from a 1 mL syringe to press the cells through a 70 μm nylon filter. Live cells were counted and added to each well such that each well contained 4 x 10^5 DC and 2 x 10^6 lymph node cells (1:5 ratio) per well in a 5 mL volume. Plates were incubated for 4 days at 37^{o}C after which the T cells were harvested by repeat pipetting. To expand the T cell population, cells were washed twice in IMDM and cultured in tissue culture flasks containing 100 U/mL IL-2 at 5 x 10^5 cells/mL and media was changed every 2 days.

2.2.4 Electroporation of siRNA into activated T cells and analysis of the effectiveness of RNA silencing

2.2.4.1 Electroporation of siRNA into activated T cells

In vitro activated T cells were harvested from culture and centrifuged at 320 g. Cells were washed and resuspended in IMDM at concentrations from 18.75-37.5 x 10^6 cells/mL, and 400 μL of the cell suspension was transferred into each cuvette. A2a adenosine receptor or GAPDH siRNA was added to the cuvettes at a range of concentrations from 0.625-1500 μM and mixed by repeat pipetting. The cuvettes were chilled on ice for 5 minutes and electroporated using a range of conditions as detailed in the results section. Immediately after electroporation, the cuvettes were incubated on ice for 10 minutes. Cells were placed in cIMDM containing 100 U/mL IL-2 and cultured for 2 days before assessing the cell yield by exclusion of the cell viability dye trypan blue. The success of the RNA silencing

was also assessed using a $CD8^+$ T cell proliferation assay, established in Figure 3.2 or by reverse transcription-PCR as described below.

Samples were contained in disposable electroporation chambers chamber (Life Technologies, Gaithersburg, Maryland, USA) and electroporated using a Cell-Porator™ (Life Technologies). For later experiments, as indicated in the results section, samples were instead contained in gap electroporation cuvettes (BioRad, Hercules, CA, USA) and were electroporated with the Gene Pulser (BioRad).

2.2.4.2 Isolation of total RNA from cells

Naïve, activated or activated and siRNA treated OTI T cells (10^5 – 10^6) were collected into 1.7 mL microtubes, centrifuged for 2 minutes at 320 g and resuspended in 1 mL TRIzol® (Invitrogen) per 5 x 10^6 cells. Cells were incubated at room temperature for 5 minutes to allow dissociation of nucleoproteins after which 200 μL chloroform (Merck) was added for every 1 mL of TRIzol® used. Tubes were shaken vigorously for 15 seconds, incubated at room temperature for 3 minutes and centrifuged at 13700 g for 15 minutes at 4°C. The colourless aqueous phase was transferred to a new tube containing 500 μL isopropanol (Scharlau Chemie), mixed and incubated at room temperature for 10 minutes to precipitate the RNA. Samples were centrifuged for 10 minutes at 4°C and the supernatant was discarded. The pellet was washed in 1 mL 75 % EtOH (Carlo Erba Reagents) by vortexing to resuspend the pellet followed by centrifugation for 5 minutes at 5350 g and 4°C. The EtOH was carefully removed and the pellet was air dried and resuspended in 20 μL RNase free dH_2O. The RNA was then DNase treated using the Ambion DNA*free* kit (Ambion Inc, Austin, Texas, USA) to remove any contaminating DNA. The 20 μL RNA solution was mixed gently with 2 μL 10x DNase buffer and 1 μL (2 U) DNase I and incubated at 37°C

for 25 minutes. The reaction was stopped by the addition of 2.3 μL 10x DNase Inactivation reagent. The reaction was incubated for 2 minutes at room temperature, centrifuged for 1 minute at 9520 g and the supernatant containing the DNase-free RNA was removed to a fresh 0.6 mL microtube.

2.2.4.3 Reverse transcription of RNA into cDNA

Primer annealing: Total RNA (up to 5 μg RNA in 8 μL) was mixed with 1 μL 50 μM random hexamer primer and 1 μL 10 mM dexoynucleotide triphosphates (dNTP) mix. The 10 μL annealing mix containing a final concentration of 5 μM primer and 1 mM dNTP was incubated for 5 minutes at 65^{o}C and left on ice for 1 minute.

cDNA synthesis: A cDNA synthesis cocktail was prepared from 4 μL Reaction buffer, 1 μL 100 mM DTT, 1 μL RNAse OUT and 1 μL Superscript III RT and was made up to a total volume of 10 μL with RNAse/DNAse free dH_2O. The final solution contained 2x Reaction buffer, 10 mM DTT, 40 U RNAse OUT and 200 U Superscript III RT. The cDNA synthesis cocktail and the annealing mix were mixed gently and spun briefly to collect the reagents. The sample was then incubated for 50 minutes at 50^{o}C and the reaction was stopped by incubating a further 5 minutes at 85^{o}C. The sample was chilled on ice. To remove residual RNA the sample was mixed with 0.5 μL (1U) RNase H and incubated for 20 minutes at 37^{o}C. The reaction was stopped by incubation at 65^{o}C for 20 minutes. Samples were stored at -20^{o}C for up to 2 months. All reagents used were purchased from Invitrogen (Auckland, New Zealand).

2.2.4.4 PCR amplification of cDNA

A 25 μL PCR mix was prepared using 0.5 μL 10 mM dNTP mix, 1 μL 10 μM forward primer, 1 μL 10 μM reverse primer, 0.2 μL 0.2 U/ μL Platinum® Taq DNA polymerase, 2.5 μL 10x PCR buffer (-Mg) and 0.75 μL 50 mM $MgCl_2$. cDNA (up to 2 ng in a maximum volume of 19.05 μL) and dH_2O were added to the PCR mix containing final concentrations of 0.2 mM dNTP mix, 0.4 μM forward primer, 0.4 μM reverse primers, 0.04 U Platinum® Taq DNA polymerase, 1x PCR buffer (-Mg) and 1.5 mM $MgCl_2$. cDNA sequences were PCR amplified using the iCycler PCR system (BioRad, Hercules, CA, USA). The thermal cycling conditions used were as follows: DNA templates were initially denatured for 2 minutes at 94^{o}C followed by 32 cycles of denaturing for 30 seconds at 94^{o}C, annealing the primers to the template for 30 seconds at 61^{o}C and a 30 second extension step at 72^{o}C. After the final cycle, reactions were incubated a further 5 minutes at 72^{o}C and then stored at 4 ^{o}C.

2.2.4.4 Gel electrophoresis

PCR products were mixed with a loading dye at a 5:1 ratio and loaded into a 1 % agarose gel containing a final concentration of 1x SYBR® Safe DNA gel stain. A 1kb+ DNA ladder was also loaded onto the gels for a size comparison. Gels were submerged in 1x TAE buffer (GIBCO™) which also contained a final concentration of 1x SYBR® Safe DNA gel stain. All reagents except those specified were purchased from Invitrogen, (Auckland, New Zealand).

2.2.5 Fluorescent labelling of cells and flow cytometry

2.2.5.1 Preparation of leukocyte suspensions

Blood

Blood was collected either from the tail vein (live mice) or the heart (of mice euthanased by CO_2 asphyxiation) into 1.7 mL micro tubes containing at least an equal volume of Alsever's Solution. The samples were centrifuged at 600 g for 2 minutes and the supernatant was removed. Pellets were resuspended in 1 mL ACT buffer and incubated at 37^{o}C for 10 minutes to lyse the red blood cells. Large blood samples underwent a second round of red blood cell lysis where the cells were resuspended and incubated in 0.5 mL dH_2O at room temperature for 30 seconds followed by the addition of 0.5 mL 1.8% NaCl. Cells were washed twice and resuspended in FCA buffer and stored on ice in preparation for fluorescent labelling on the same day.

Lymph node and spleen

Lymph nodes and spleens were disrupted by using the plunger from a 1 mL syringe to press the tissue through a 70 μM cell strainer. Splenocytes were incubated in 5 mL ACT buffer for 5 minutes at 37^{o}C to lyse red blood cells and washed in IMDM. Cells were washed and resuspended in the appropriate buffer and stored on ice in preparation for tissue digestion on the same day.

Tissue digestion to release DC

Lymph nodes and tumours were digested in a total volume of 1 mL and 5 mL of IMDM respectively. Tissues were broken into small pieces using tweezers. DNase and Liberase CI

were added to the suspensions at a final concentration of 100 μg/mL and 0.4 mg/mL respectively. The digestions were incubated at 37°C and mixed regularly throughout the 30 minute incubation. The reaction was stopped by adding EDTA at a final concentration of 10 mM and incubating for a further 5 minutes at 37°C. The digests were then pressed through a 70 μM cell strainer to achieve a single cell suspension, washed twice and resuspended in IMDM and stored on ice in preparation for fluorescent labelling on the same day.

2.2.4.5 Detection of surface marker expression

Single cell suspensions were counted, washed once in FCA buffer and transferred to 96 well plates such that each well contained up to 2 x 10^6 cells. Plates were centrifuged for 2 minutes at 320 g and the supernatants were removed by tipping the plate upside down and flicking once. Pellets were resuspended by gentle vortexing. Fc receptors were blocked by incubating in FCA buffer containing 10 μg/mL 2.4G2 for 10 minutes on ice. Fluorescently conjugated antibodies against cell surface markers of interest were added to the 2.4G2 containing cell suspensions at the appropriate dilutions and incubated a further 10 minutes on ice. Cells were washed once with FCA buffer and then incubated with the appropriate streptavidin-conjugated fluorochrome for 10 minutes on ice, where required. Cells were washed a further two times, resuspended in 150 μL FCA buffer and 150 μL of a 1 to 1000 dilution of the 200 μg/mL DAPI stock solution was added directly before analysis by flow cytometry. The final concentration of the cell viability dye DAPI in the sample was 0.1 μg/mL. Alternatively, the cells were resuspended in 300 μL FCA buffer and 1 μL 75 μg/mL PI was added directly before analysis by flow cytometry. The final concentration of the cell viability dye PI in the sample was 0.25 μg/mL.

2.2.4.6 *In vitro* restimulation

Prior to intracellular labelling of IFN-γ and TNF-α, splenocytes were resuspended at 10^6 cells/mL in cIMDM and 6 mL of each suspension was transferred into a single well of a 6 well plate. Cells were restimulated by incubating for 5 hours at 37°C with a final concentration of 1 μM SIINFEKL peptide. 6 μL 1 mg/ml GolgiStop (Pharmingen, BD Biosciences, San Diego, CA, USA) was also added to give a final concentration of 1 μg/ml and was present to prevent the export of proteins from the Golgi bodies. Cells were then harvested, washed in IMDM, resuspended in FCA buffer and stored on ice in preparation for labelling of intracellular markers.

2.2.4.7 Detection of intracellular molecules

TNF-α and IFN-γ production was detected using the Cytofix/Cytoperm kit from BD Pharmingen and Foxp3 signal was detected using the Foxp3 flow kit from ebioscience. Peptide restimulated cells were fixed and permeabilised by resuspension in 200 μL Fix/Perm buffer per well. Cells were incubated for 30 minutes at 4°C, washed twice and incubated a further 15 minutes in 80 μL 1x Perm/Wash solution at 4°C. Cells were incubated a further 30 minutes at 4°C with 1 μL of the anti-IFNγ or anti-TNFα specific antibodies , or 0.5 μL anti-Foxp3 specific antibody, or the respective isotype matched controls. Cells were washed twice and incubated a further 25 minutes with 1x Perm/Wash buffer to reduce the level of background staining. Cells were then washed and resuspended in 300 μL FCA buffer and stored on ice until acquisition.

2.2.4.8 Acquisition and analysis

Data was acquired using a FACSort, a FACScalibur or an LSRII SORP flow cytometer (Beckton-Dickinson, San Jose, CA, USA) and analysed using FlowJo software (Tree Star, San Carlos, CA, USA). Live cells, or whole-fixed cells, were identified on the basis of Forward Scatter (FSC) and Side Scatter (SSC) properties. In some experiments, live cells were also identified on the basis of their ability to exclude PI or DAPI. To calibrate the acquisition voltages and compensate for spectral overlap between the fluorophores used, unstained samples and samples labelled with a single fluorophore for each of the fluorophores used in each experiment were included. Where available, appropriately matched isotype control antibodies were used to control for background fluorescence caused by non-specific antibody binding. In some instances, fluorescence minus one controls were also included to help identify shifts in the level of background staining.

2.2.5 Cell purification/Sorting

2.2.5.1 Magnetic Cell Separation (MACS)

OTI lymph node suspensions were enriched for $CD8^+$ T cells by incubating 10^7 cells in 90 μL Wuerzburger buffer and 10 μL anti-CD8α MACS Microbeads (Miltenyi Biotec, Germany) for 20 minutes at 4^oC. Cells were mixed a number of times during incubation. Unbound beads were removed by adding a ten-fold excess of Wuerzburger buffer to the suspension and centrifuging the cells at 320 g for 4 minutes. Pelleted cells were resuspended at 10^8 cells/mL in Wuerzburger buffer for positive selection on the AutoMACS machine (Miltenyi Biotec).

OTII lymph node suspensions were first depleted of $CD25^+$ cells by Fc receptor blocking followed by cell surface labelling with anti-CD25-PE. Ten million cells were then incubated in 90 μL Wuerzburger buffer and 10 μL anti-PE MACS Microbeads (Miltenyi Biotec) for 20 minutes at 4^oC. Cells were resuspended at 10^8 cells/mL in Wuerzburger buffer and the CD25 negative population was collected using the AutoMACS machine (Miltenyi Biotec). Cells were then enriched for $CD4^+$ T cells using the same method as $CD8^+$ T cell enrichment except anti-CD4 MACS Microbeads were used (Miltenyi Biotec).

2.2.5.2 Fluorescence Activated Cell Sorting (FACS)

To purify $CD4^+$ $Foxp3^+$ Treg from tumours, tumour cell suspensions from Foxp3GFP mice were enriched for $CD4^+$ T cells by Automacs separation using anti-CD4 MACS Microbeads (Miltenyi Biotec). Enriched cells were washed twice and resuspended in FACS buffer at 1.5×10^7 cells/mL. Cell suspensions were sorted for GFP positive cells using a FACSDiVa (Becton Dickinson, San Diego, California, USA). The resulting population consisted of >98 % GFP^+, and therefore $CD4^+$ $Foxp3^+$, cells.

To purify $CD45^+$ $CD11c^+$ DC from tumours, tumour cell suspensions were enriched for $CD45^+$ cells by Fc receptor blocking, using the mAb 24G2, followed by Automacs separation using anti-CD11c MACS Microbeads (Miltenyi Biotec). Enriched cells were washed with Wuerzburger buffer, Fc receptor blocked and labelled for 10 minutes on ice with anti-CD11c-APC. Cells were washed twice and resuspended in FACS Sort Buffer at 1.5×10^7 cells/mL. Cell suspensions were sorted for $CD45^+$, $CD11c^+$ cells using a FACSDiVa (Becton Dickinson, San Diego, CA, USA). The resulting population consisted of >96 % $CD45^+$, $CD11c^+$ cells.

2.2.6 Assays of cell function

2.2.6.1 In vitro proliferation assays

In vitro activated $CD8^+$ T cells (10^5 cells per well) were incubated in cIMDM containing IL-2 (10 or 100U). Adenosine or the stable adenosine analogue 5'-N-Ethylcarboxamidoadenosine (NECA) was titrated into the T cell cultures. To maintain high levels of adenosine throughout the experiment, the adenosine metabolic inhibitor erythro-9-(2-hydroxy-3-nonyl)adenine (EHNA 30μM) was also added to half of the cultures containing adenosine. As a measure of proliferation, 1μCi ^{3}H-thymidine (Amersham Biosciences, Little Chalfont, UK) was added to wells during the final 6 hours of the 2-day culture period. Cells were harvested using an automated cell harvester (Tomtec Inc., Orange, CT, USA) on to Wallac Filters (Turku, Finland). Filters were dried and sealed in sample bags (Wallac) with 5 mL BetaScint scintillation fluid (Wallac). ^{3}H-thymidine incorporation was measured using a Betacounter (Wallac).

2.2.6.2 In vitro suppression assay

A population of highly pure (<96%) $CD4^+$ $Foxp3^+$ Treg were isolated from tumour cell suspensions by positive magnetic sorting followed by electronic sorting.

Treg were titrated in duplicate into 96 well U bottom plates containing 2.4 x 10^3 DC and 4 x 10^4 $CD4^+$, $CD25^-$ effector T cells per well and stimulated with 1μg/ml anti-CD3 for 3 days. Proliferation was measured similar to the *in vitro* proliferation assay with the exception that the cells were cultured for 3 days.

2.2.6.3 Ex vivo proliferation assay

A population of highly pure (<96%) $CD45^+$ $CD11c^+$ TIDC were isolated from tumour cell suspensions by positive magnetic sorting followed by electronic sorting.

TIDC were titrated in duplicate into 96 well U bottom plates containing 2 x 10^5 purified OTI or OTII T cells in a total volume of 200μL. As a positive control, specific peptide (1 μM SIINFEKL or ISQAVHAAHAEINEAGR) was loaded onto 3 x10^3 DC by incubating at 37^{o}C for 1 hour before these DC were also added to the appropriate T cell cultures. Balb/c T cells were used as a positive allogeneic control for proliferation. Proliferation was measured in a manner identical to that used for the *in vitro* proliferation assay with the exception that the cells were cultured for 3 days.

2.2.6.4 In vivo proliferation assays

In vivo proliferation in response to tumours

$CD45.1^+$ B6 congenic mice were treated with PC61 or left untreated and inoculated with B16.OVA tumours. Approximately 14 days later 1.5 x 10^6 OT-I and 1.5 x 10^6 OT-II T cells labelled with CFSE were adoptively transferred into the mice by i.v. injection. Tumour draining and non-draining lymph nodes were removed 3 days after T cell transfer and analysed by flow cytometry for T cell proliferation. As controls, tumour bearing and non-tumour bearing mice were given 2 x10^5 DC +/- 1uM SIINFEKL peptide by s.c injection to the forearm one day prior to the T cell transfer.

In vivo proliferation in response to DC

C57BL/6 and PKO mice received a single i.p. injection containing 100 μg PC61 or were left untreated. Two days after PC61 treatment, all mice received 75 $x10^3$ naïve OTI congenic lymphocytes. Lymphocytes were prepared by removing the lymph nodes from a naïve OTI congenic mouse and using the plunger from a 1 mL syringe to press the lymph nodes through a 70 μM cell strainer. The resulting single cell suspension was washed twice in PBS and resuspended at 375 $x10^3$ cells/mL. One day after the adoptive transfer of T cells, mice received 5 $x10^5$ OVA loaded, LPS matured DC by i.v. injection. As a control, a second group of PC61 untreated mice received 5 $x10^5$ untreated DC by i.v. injection. Blood samples were taken on days 4, 7 and 15 after the transfer of DC and analysed by flow cytometry to determine the extent of the expansion of the transferred T cell population in response to treatment.

2.2.6.5 *In vivo* VITAL assay for cytotoxicity function

The VITAL assay is an established method of assessing the cytotoxic function of cells by analysing the rate of elimination of fluorescently-labeled, antigen-loaded target cells in comparison to a control population of non-antigen carrying cells (330).

2.2.6.5.1 Peptide loading of splenic targets

Single cell suspensions containing 2 $x10^7$ cells/mL in cIMDM, were prepared from the spleens of C57BL/6 mice, and divided into 3 tubes of equal volumes. SIINFEKL peptide was added to each of the 3 groups at a final concentration of 0, 10 and 100 nM respectively. The cells were incubated for 2 hours at 37^{o}C and mixed regularly by

inverting the tubes. Cells were washed once with IMDM and re-pelleted by centrifuging at 320 g for 4 minutes.

2.2.6.5.2 Labelling of cells with VITAL dyes

Non-antigen loaded cells were resuspended at 5 x 10^6 cells/mL in pre-warmed cIMDM containing CTO dye at a final concentration of 10 μM. Cells were incubated at 37°C for 15 minutes, washed and resuspended in at least 10 mL pre-warmed cIMDM. After a further 20-minute incubation at 37°C the cells were washed twice and resuspended at 36-52 x10^6 cells/mL in PBS.

Ag loaded cells were resuspended at 5 x 10^6 cells/mL in cold PBS. Cells that were treated with 10 nM SIINFEKL received CFSE at a final concentration of 0.02 μM and cells treated with 100 nM SIINFEKL were labelled with 0.2 μM CFSE. Tubes were vortexed and incubated for 10 minutes at 37°C. To stop the labelling reaction, 5 volumes of cold PBS were added to each tube. Cells were then washed twice and resuspended at 36-52 x10^6 cells/mL in PBS.

The 3 groups of cells were pooled together at equal ratios to give a final concentration of 36-52 x10^6 cells/mL. Mice each received a 200 μL i.v. injection of the suspension, which contained 4-6 x10^6 of each of the 3 groups of cells.

2.2.6.5.3 Analysis of cell killing

Blood was collected 6 hours after the administration of targets, red blood cells were lysed and the samples were analysed by flow cytometry. The % killing that occurred in each mouse was calculated as follows:

$$\% \text{ killing} = 100 - 100 \times \frac{\#\ CFSE^{+} \text{ cells (10 nM or 100 nM SIINFEKL treated)}}{\#\ CTO^{+} \text{ cells}}$$

The % killing was averaged for each treatment group and a significant increase in % killing over the negative control was recognised as specific killing.

2.2.6.6 Tumour growth

Tumour cells were inoculated into the left flank by s.c injection and tumour growth was monitored regularly over time by measuring the bisecting diameters using Mitutoyo callipers. To account for the thickness of the skin, 1 mm was subtracted from each diameter measurement. Mice were euthanised when tumour size reached 150-200 mm^2.

PC61 treatment

Mice received either a single i.p. injection of 75-125 μg PC61 3 days before tumour inoculation or 2 i.p. injections of 100 μg PC61 given 1 and 4 days before tumour inoculation, as described in the appropriate figure legends.

Adoptive transfer of T cells

In vitro activated OTI T cells (2 x10^6 to 10^7 as indicated in the results section) were resuspended in sterile PBS and adoptively transferred into mice by iv injection once tumours became palpable (10-14 days after tumour inoculation).

Caffeine treatment

Once tumours became palpable, mice received *in vitro* activated T cells. On the same day as the T cell transfer, mice also began daily i.p. injections of caffeine (0.4-0.6 mg/dose) for 4-6 days and drinking water was supplemented with 0.1% caffeine for the remainder of the experiment.

2.2.7 Imaging of tumour sections

2.2.7.1 Preparation of tumour sections

Euthanased mice were cardiac perfused with room temperature PBS for 5 minutes followed by 4% paraformaldehyde in PBS (0.15 M, Ph 7.4) at 4^{o}C for 15 minutes. Tumours were removed and post-fixed in 4% paraformaldehyde for 2-4 hours at 4^{o}C. The tumours were then transferred to PBS containing 30% sucrose at 4^{o}C and left overnight. Tumours were mounted in Cryo-M-Bed freezing compound (Bright Instrument Company Ltd, Huntingdon, UK) and 20 μM sections were cut using an HM 500 OM series cryostat microtome (Microm International GmbH, Walldorf, Germany). Sections were mounted directly onto microscope slides (Biolab) and stored at -20^{o}C until used.

2.2.7.2 Immunohistochemical staining of tumour sections

After frozen sections were post-fixed by incubating in acetone (Merck) for 10 minutes, the sections were air-dried and nail polish was used to create a "frame" around the section. Sections were re-hydrated in TBS for 20 minutes, after which, the excess TBS was tipped off. The primary antibody was added onto the section within the frame and the slide was transferred to a moist chamber consisting of a lidded box containing a moist paper towel. The chamber was then incubated at 37^{o}C, in the dark, for 30 minutes. Excess antibody was tipped off and the section was gently washed 3 times with TBS using a pipette and incubated a further 5 minutes in TBS. The secondary antibody was added to the section and the slide was treated similarly to the initial antibody binding protocol. Excess TBS was first tipped off and then removed by blotting. Except where indicated, all incubations where at room temperature. To mount the section for microscopy, the non-fade permount Vectashield (Vector Laboratories) was added, the section was covered with a coverslip (Biolab) and a thin layer of nail polish was applied around the perimeter of the coverslip to form a seal. The sections were imaged directly after IHC staining using an Olympus BX51 immunofluorescence microscope (Olympus, Auckland, New Zealand) attached to an Olympus DP70 camera and using the Olympus analysis LS Research software.

2.2.8 Statistical calculations

Statistical calculations were performed using the Graphpad Prism® Version 4 statistical package (Graphpad Software Inc., San Diego, CA, USA). The type of statistical test used is described in the appropriate figure legends.

CHAPTER THREE

TARGETING ADENOSINE RECEPTORS FOR CANCER IMMUNOTHERAPY

3.1 Introduction

The tumour microenvironment is known to be high in immunosuppressive factors such as TGF-β, IL10 (180-182) and adenosine (183). While it is possible that tumour infiltrating Treg may produce some of this adenosine (226, 285), the main source of adenosine is thought to be the malignant cells and is the result of the hypoxic tumour conditions (200). As described in detail in the general introduction, hypoxia inhibits the activity of the adenosine metabolising enzyme adenosine kinase. This results in a build up of intracellular adenosine, which is released from the cell via bi-directional nucleoside transporters, leading to increased extracellular levels of adenosine.

Adenosine mediates a variety of responses depending on which of the four adenosine receptor subtypes (A1, A2a, A2b and A3) it engages. The A2a receptor is the predominant subtype found on leukocytes although low levels of the A2b subtype can also be found (201). A number of studies using both A2a knockout mice and selective A2a receptor agonists and antagonists have shown that adenosine signalling through the A2a receptor results in decreased proliferation, cytokine production and cytotoxic function of T cells (185-187). Based on these findings, it was proposed that the prevention of adenosine signalling in T cells might improve the anti-tumour activity of these cells.

There are a number of ways in which adenosine signalling can be abrogated. RNA silencing is a method of preventing gene expression by introducing small interfering RNA molecules (siRNA), which match part of the target sequence, into the target cell. These double stranded RNA molecules (dsRNA) are then incorporated into the RNA induced silencing complex (RISC), which separates the strands of the dsRNA and binds only the anti-sense strand (331). This complex binds to the complementary mRNA strand within

the cell and causes the target RNA molecule to be degraded by endo- and ecto-nucleases contained within the RISC complex (332) (Figure 3.1).

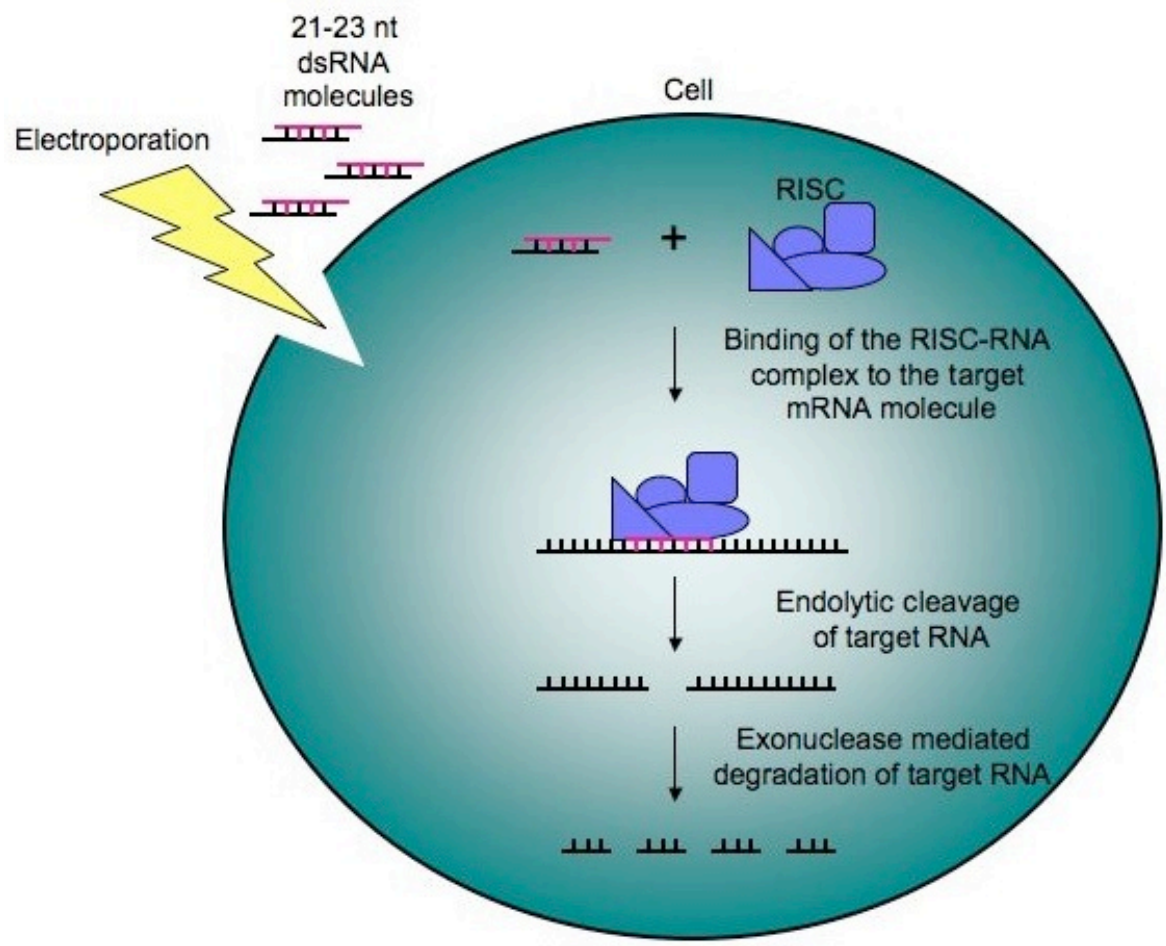

Figure 3.1: Mechanism of RNA silencing.

dsRNA molecules measuring 21-23 nucleotide (nt) long and with 2-3 nt overhanging ends are introduced to the cell by electroporation. These molecules are incorporated into the RNA induced silencing complex (RISC), which includes helicase, RecA and endo- and exonucleases. The dsRNA molecule is unwound and separated by the helicase, leaving only the anti-sense strand bound to the RISC molecule. The RISC-anti-sense RNA strand (RISC-RNA) complex then binds to the complementary mRNA molecule and degrades the molecule by using the endonuclease to cleave the molecule in two followed by exonuclease-mediated degradation from the exposed ends (333, 334). If the target molecule is not present, the unstable RISC-RNA complex dissociates and the anti-sense RNA molecule is degraded (335).

RNA silencing techniques have been used successfully on primary, activated, murine T cells to decrease cell surface expression of CD4 and CD8 (336). Therefore, it is possible that RNA silencing may be used to decrease the level of A2a receptors on the surface of *in vitro* activated, tumour specific $CD8^+$ (OTI) T cells. OTI T cell transgenic mice were used because they yield a high number of OVA Ag specific $CD8^+$ T cells, which are also specific for B16.OVA tumour cells. The effect of gene silencing is specific to the cells that have been treated.

In addition to its effects on T cells, adenosine is also known to inhibit DC function. Both murine and human DC matured in the presence of adenosine produce less TNF-α and IL-12 and more IL-10 resulting in impaired allostimulatory activity of the DC (202-205). Administering an A2a receptor antagonist, *in vivo*, may improve the function of DC and T cells thereby providing a further improvement in the anti-tumour response in comparison to using siRNA to silence the A2a receptor in activated tumour specific T cells alone.

Caffeine is a non-selective adenosine receptor antagonist, which means it will block adenosine signalling through all 4 receptor subtypes. Since the A2a receptor is the predominant subtype found on leukocytes, the effect of caffeine on T cells and DC will be primarily by blocking this receptor but with some contribution from the A2b receptor. Caffeine is cheap, it is widely available, it can be administered repeatedly and easily and it will target more than one cell type. These factors may make caffeine treatment advantageous over siRNA treatment, which is costly and technically challenging, despite the short half-life of caffeine *in vivo* (52 minutes in mice as measured in the plasma after i.p. administration of 20 mg/kg caffeine) (337).

3.2 Aims

The purpose of the experiments described in this chapter was to establish a reliable and effective method of preventing adenosine signalling in activated OTI T cells. The hypothesis was that the prevention of adenosine signalling in activated OTI T cells would improve the anti-tumour immune response by making these cells refractory to extracellular adenosine.

The specific aims were:

- To assess whether A2a receptor silencing of *in vitro* activated OTI T cells affects the anti-tumour activity of these T cells
- To determine if *in vivo* caffeine treatment can enhance the anti-tumour activity of adoptively transferred, activated OTI T cells
- To determine the effect of *in vivo* caffeine treatment on the frequency of tumour infiltrating cells

3.3 Results

3.3.1 Electroporation of the appropriate siRNA molecules fails to silence expression of either the A2a adenosine receptor or the control Glyceraldehyde 3-phosphate dehydrogenase genes

A reliable assay was required to determine if the treatment of activated OTI T cells with A2a receptor specific siRNA resulted in significant changes in cell function. It was decided that an *in vitro* proliferation assay would be used to determine the functional effect of A2a mRNA silencing on activated OTI T cells because cells that have been inhibited by adenosine would show a reduced capacity to proliferate and reduced effector function (185-187). Therefore, restoring proliferative and cytotoxic capabilities to the activated OTI T cells by silencing the A2a receptors is also likely to improve the anti-tumour activity of these cells.

Activated OTI T cells were cultured in complete media containing either 10 U or 100 U IL-2 to allow the T cells to survive and proliferate. Increasing amounts of adenosine or the stable adenosine analogue 5'-N-Ethylcarboxamidoadenosine NECA were also added to the cultures. To maintain high levels of adenosine throughout the culture, the adenosine deaminase inhibitor EHNA was also added to the cultures containing adenosine. Concentrations of NECA and EHNA were chosen based on studies that have shown that adenosine suppresses T cell proliferation (185, 338). The effect of high levels of adenosine or NECA on T cell proliferation was assessed after 2 days of culture by tritiated thymidine incorporation. T cell proliferation was unaffected by adenosine treatment alone because adenosine is metabolised quickly. T cell proliferation was found to decrease as the amount of NECA or adenosine (in the presence of EHNA) increased (Figure 3.2, blue and red lines, respectively). A similar trend was seen when using 10 U or 100 U IL-2 (Figure 3.2 A

and B, respectively). Further experiments were performed using 10 U IL-2 because the assay was more sensitive.

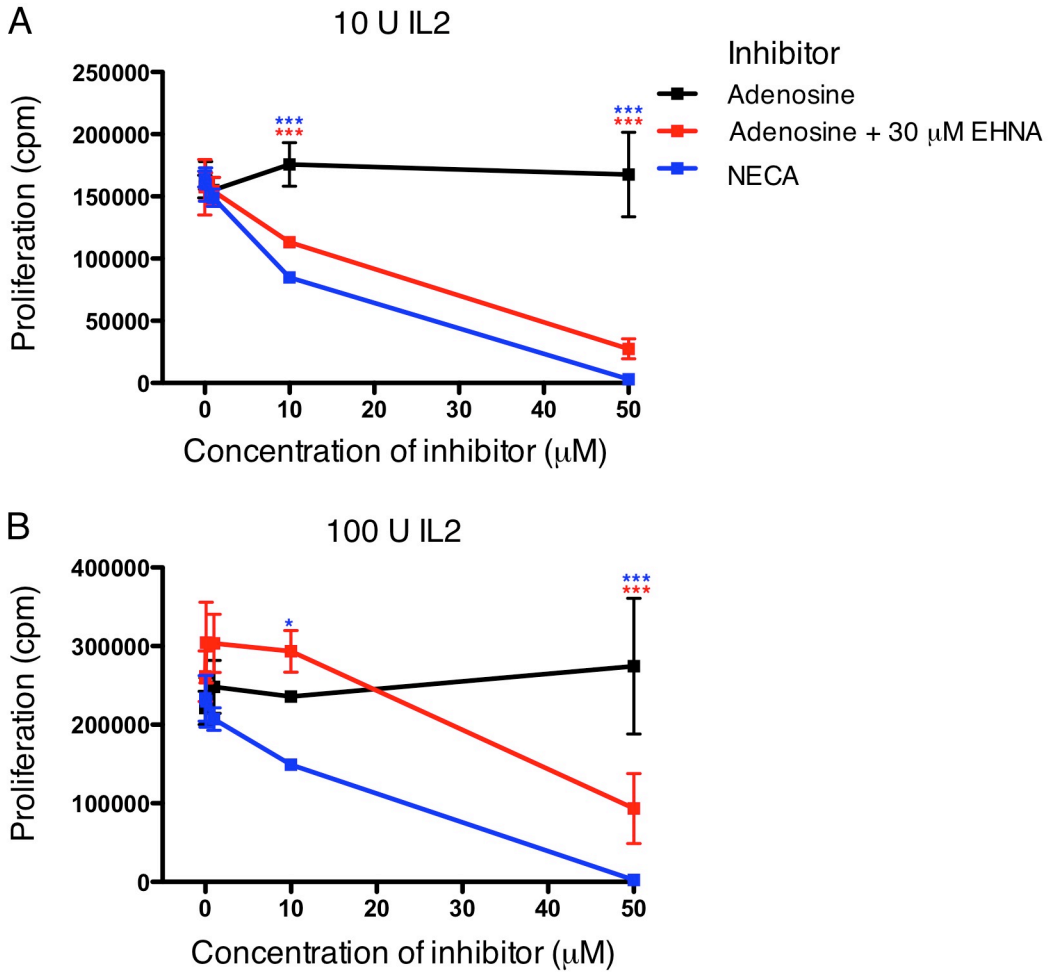

Figure 3.2: *In vitro* CD8$^+$ T cell proliferation is inhibited by adenosine.

Activated OTI T cells (10^5 cells per well) were incubated in cIMDM containing 10 U (A) or 100 U IL-2 (B) and increasing amounts of adenosine (black and red lines) or the stable adenosine analogue NECA (blue line). The adenosine metabolic inhibitor EHNA (30 μM) was also added to sustain high levels of adenosine in the culture (red line). After ~18 hours of culture, 1 μCi ^{3}H-thymidine was added to each well and the cells were cultured a further 6-7 hours. The assay was performed once with triplicate samples for each concentration. Graphs show the mean ± SD. Values of *p* represent statistical differences (*=<0.05 and ***=<0.001) between the adenosine only group and the group indicated by the colour of the asterix and were calculated using an unmatched two-way ANOVA test with a Bonferroni post-test.

It was important to establish if adenosine signalling could also suppress proliferation of the tumour cells themselves in order to fully understand the effect of high adenosine levels in the tumour microenvironment. Therefore B16.OVA tumour cells were also cultured *in vitro* in the presence of adenosine or NECA (Figure 3.3). NECA caused a decrease in tumour cell proliferation in a dose dependent manner (Figure 3.3) similar to its effects on activated T cells (Figure 3.2)

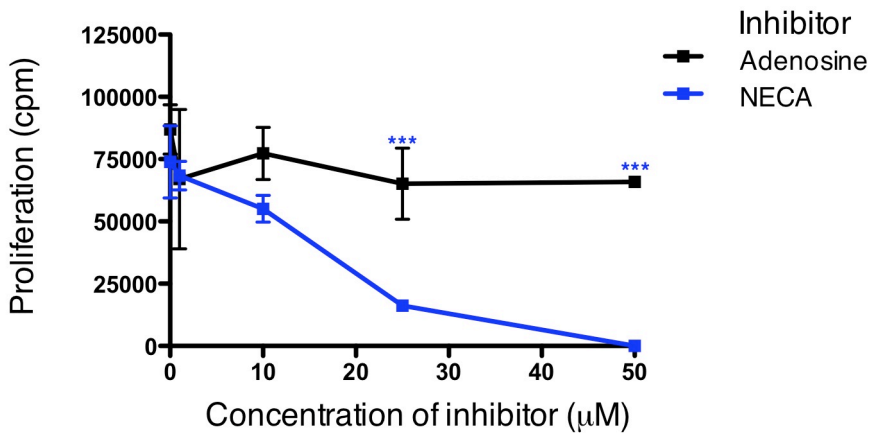

Figure 3.3: Adenosine inhibits *in vitro* proliferation of B16.OVA tumour cells.
B16.OVA tumour cells (2.5 x10^4 cells per well) were incubated in cIMDM with increasing amounts of adenosine (black line) or the stable adenosine analogue NECA (blue line). ^{3}H-thymidine (1μCi per well) was added after ~24 hours of culture and the cells were incubated a further ~12 hours before ^{3}H-thymidine incorporation was measured. The assay was performed once with triplicate samples for each concentration. Graphs show the mean ± SD. Values of *p* (***=<0.001) were calculated using an unmatched two-way ANOVA test with a Bonferroni post-test.

To optimise the electroporation conditions used in future experiments, the cell viability of activated $CD8^+$ T cells was assessed in response to electroporation using a range of voltages (Figure 3.4A) and after using two different initial numbers of activated T cells (Figure 3.4B). Electroporation transiently compromises the membrane integrity of viable

cells, which makes them unable to be reliably distinguished from dead or dying cells directly afterwards. For this reason, cell viability was also assessed 48 hours after electroporation and was found to be similar when samples were electroporated, using voltages between 300 and the maximum achievable voltage of 400 V (Figure 3.4A). These electroporation conditions were chosen based on the findings of other Authors (336, 339). Similar cell viability was also observed when either 7.5 or 12.4 x 10^6 activated $CD8^+$ T cells were electroporated at 400 V. Based on these results and the findings of other Authors (336, 339), 15 x10^6 activated $CD8^+$ T cells and the optimal 400 V electroporation conditions were used for further experiments.

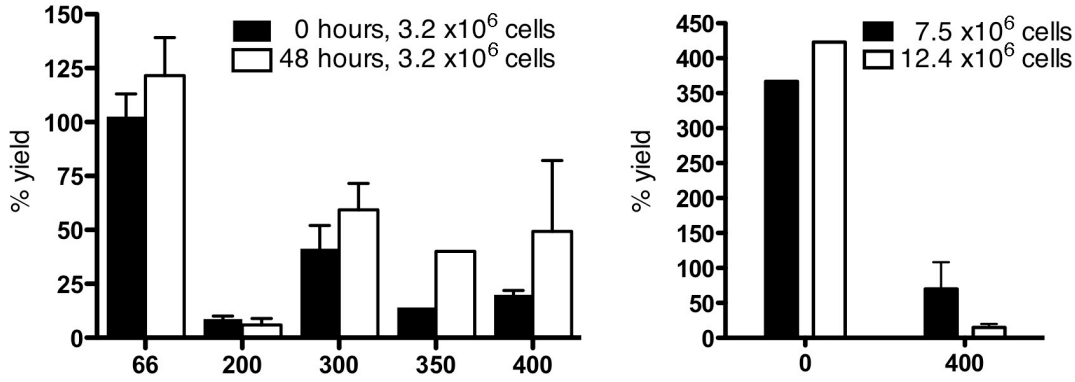

Figure 3.4: Optimisation of siRNA electroporation conditions.

Activated $CD8^+$ T cells were electroporated at the indicated voltages in the absence of siRNA and the cell yield relative to the pre-electroporation cell number was assessed by trypan blue dye exclusion. A) Activated T cells (3.2 x10^6) were electroporated and cell viability was assessed directly afterwards (0 hours). The remaining cells were rested for 48 hours in the presence of IL-2, at which time cell viability was again assessed. B) Two different numbers of activated T cells were electroporated at the indicated voltages, cells were rested in the presence of IL-2 for 48 hours and rested cells were assessed for viability.

To determine the overall effectiveness of A2a receptor mRNA silencing, the proliferation of siRNA treated cells in the presence of adenosine was assessed. To silence the A2a

adenosine receptors, 0-5 μM A2a siRNA was electroporated into activated T cells at 400V using the Cell-Porator™ (Figure 3.5). After the siRNA treatment, cells were rested for two days to allow time for the A2a receptor gene to be silenced. Rested cells were then assayed for function using the *in vitro* proliferation method established in Figure 3.2. T cells treated with siRNA showed decreased proliferation in response to EHNA and adenosine in a dose dependent manner similar to that of cells that did not receive the siRNA (Figure 3.5). This indicates that the A2a receptor gene had not been silenced sufficiently in these cells to show a difference in function.

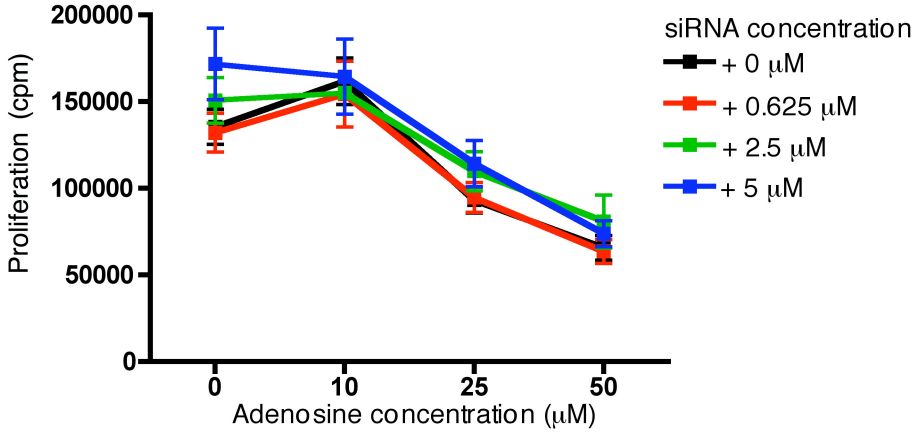

Figure 3.5: The electroporation of siRNA specific for the A2a receptor into activated CD8$^+$ T cells fails to restore T cell proliferation in the presence of adenosine.

Increasing amounts of A2a siRNA were electroporated into 15 x10^6 SIINFEKL activated T cells. The T cells were incubated at 37^{o}C in cIMDM supplemented with 10 U/ml IL-2 for 48 hours to recover from electroporation. The sensitivity of electroporated cells to adenosine was then evaluated using the EHNA + adenosine proliferation assay established in Figure 3.2. The assay was performed once with triplicate samples for each concentration. Graphs show the mean ± SD.

There are several reasons why the T cell proliferation assay may have failed to show an improvement in T cell function in response to A2a mRNA silencing. First of all, the siRNA may not have entered the cell, secondly, the siRNA molecules may not have

silenced the mRNA and thirdly, silencing of the A2a receptor gene may not be sufficient to restore proliferation of the T cells when cultured in the presence of adenosine. To address these issues, a vast excess (1.5 mM) of the control Glyceraldehyde 3-phosphate dehydrogenase (GAPDH) siRNA was electroporated into activated T cells using a Gene Pulser (Figure 3.6). Cells were rested in culture for two days before RNA extraction, reverse transcription and PCR amplification of the GAPDH cDNA. Serial dilutions of the PCR products were run side by side on an electrophoresis gel so that any subtle differences in yield could be visualised. No differences in the band intensities were seen at any of the dilutions compared indicating that no silencing of the gene had occurred (Figure 3.6). This is a control siRNA, which has been shown by Ambion to be capable of successfully silencing the GAPDH gene. These results indicate that the most likely reason attempts to silence the adenosine receptor were unsuccessful because the electroporation conditions were not sufficient to allow entry of the siRNA molecules into the cell.

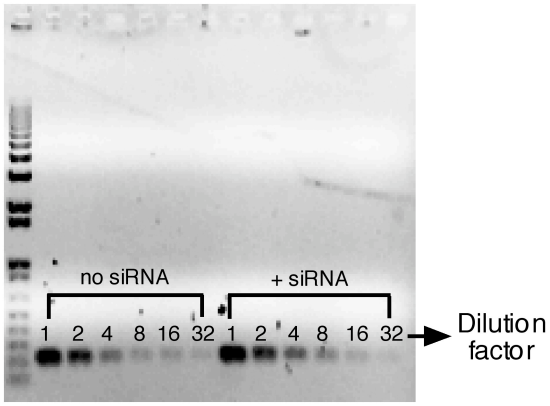

Figure 3.6: The electroporation of siRNA against GAPDH into activated CD8$^+$ T cells fails to silence GAPDH at the mRNA level.

SIINFEKL activated T cells (7.5 x 10^6 cells) were electroporated with 1.5 mM GAPDH siRNA at 450 V for 1.5 milliseconds using the BioRad Gene Pulser. Total RNA was isolated from 10^6 cells, reverse transcribed and PCR amplified using GAPDH primers. Serial dilutions of the PCR products were run on a 1% gel for 60 minutes at 90 volts. The results shown are from 1 of 3 electroporations with similar results.

3.3.2 Caffeine treatment does not improve the anti-tumour response of adoptively transferred, activated OTI T cells

Attempts to silence the A2a adenosine receptor on activated T cells using siRNA were unsuccessful. Instead, the question of whether the anti-tumour activity of activated OTI T cells could be improved by inhibition of the A2a adenosine receptor was investigated using the *in vivo* administration of caffeine. Mice with palpable B16.OVA tumours were given activated OTI T cells and caffeine treatment commenced on the same day. Caffeine treatment consisted of daily i.p. injections of caffeine, as indicated in the figure legends, and supplementation of the drinking water for the remainder of the experiment. Tumour size was monitored throughout the experiments. Where required, tumours were excised 6 days after the adoptive transfer of T cells and analysed by flow cytometry (Figure 3.7).

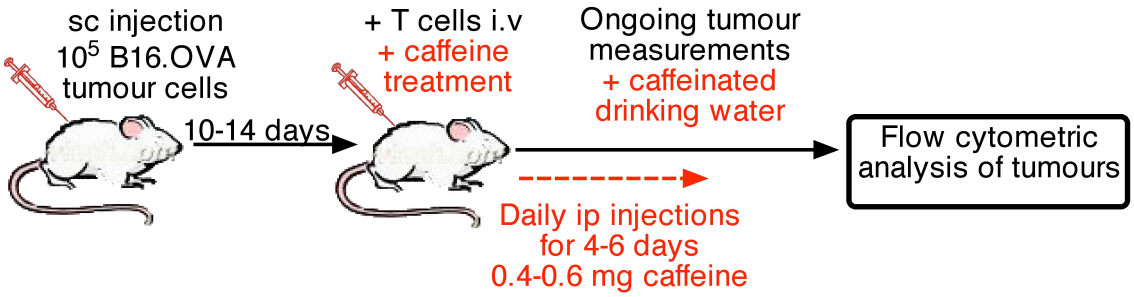

Figure 3.7: Model used to investigate the effect of A2a receptor blocking using *in vivo* administration of caffeine.

C57 mice were inoculated with 10^5 B16.OVA tumour cells by s.c injection to the left flank. Once tumours became palpable, activated OTI T cells were administered by i.v. injection and caffeine treatment was initiated. Caffeine was administered as daily i.p. injections of 0.4-0.6 mg (as indicated in each figure legend) caffeine for 4-6 days (as indicated in each figure legend) and in the drinking water (0.1 % w/v) for the duration of the experiment. For tumour infiltration experiments, tumours were removed and analysed 6 days after the adoptive transfer of the activated OTI T cells.

To determine if caffeine improved the ability of the adoptively transferred T cells to reject tumours, tumour-bearing mice received adoptively transferred, activated OTI T cells with or without caffeine treatment (see Figure 3.7 for model) and tumour growth was monitored over time. Initial experiments where mice received treatment when tumours were barely palpable (4-9 mm^2) gave inconsistent and contradictory results (Figure 3.8A and B). Delaying treatment until the tumours were larger and the levels of hypoxia were likely to be higher failed to show even a subtle improvement of tumour rejection with caffeine treatment (Figure 3.8C).

It is possible that no improvement was seen after caffeine treatment because the T cells were already achieving the maximum response and no further improvement could therefore be elicited. To address this possibility, the number of transferred T cells was titrated. The minimum number of T cells required to elicit a noticeable effect on tumour growth was determined to be 4 $x10^6$ (Figure 3.9A). The number of B16.OVA tumour cells was also titrated to determine if a lower number of cells could be inoculated and still reliably cause tumour growth in all animals (Figure 3.9B). Tumour growth was seen in 100% of mice that received 2 $x10^4$ B16.OVA cells but 5 $x10^4$ B16.OVA cells were used in further experiments to avoid problems with experimental variation. A final experiment using the optimised number of T and B16.OVA cells and using the highest dose of caffeine tested, showed no improvement in the anti-tumour activity of the transferred T cells in response to the caffeine treatment (Figure 3.9C). It is possible that despite previous experiments to optimise all aspects of the model, the transferred T cell treatment alone was still too effective to allow any improvement in the anti-tumour activity of these T cells to be determined.

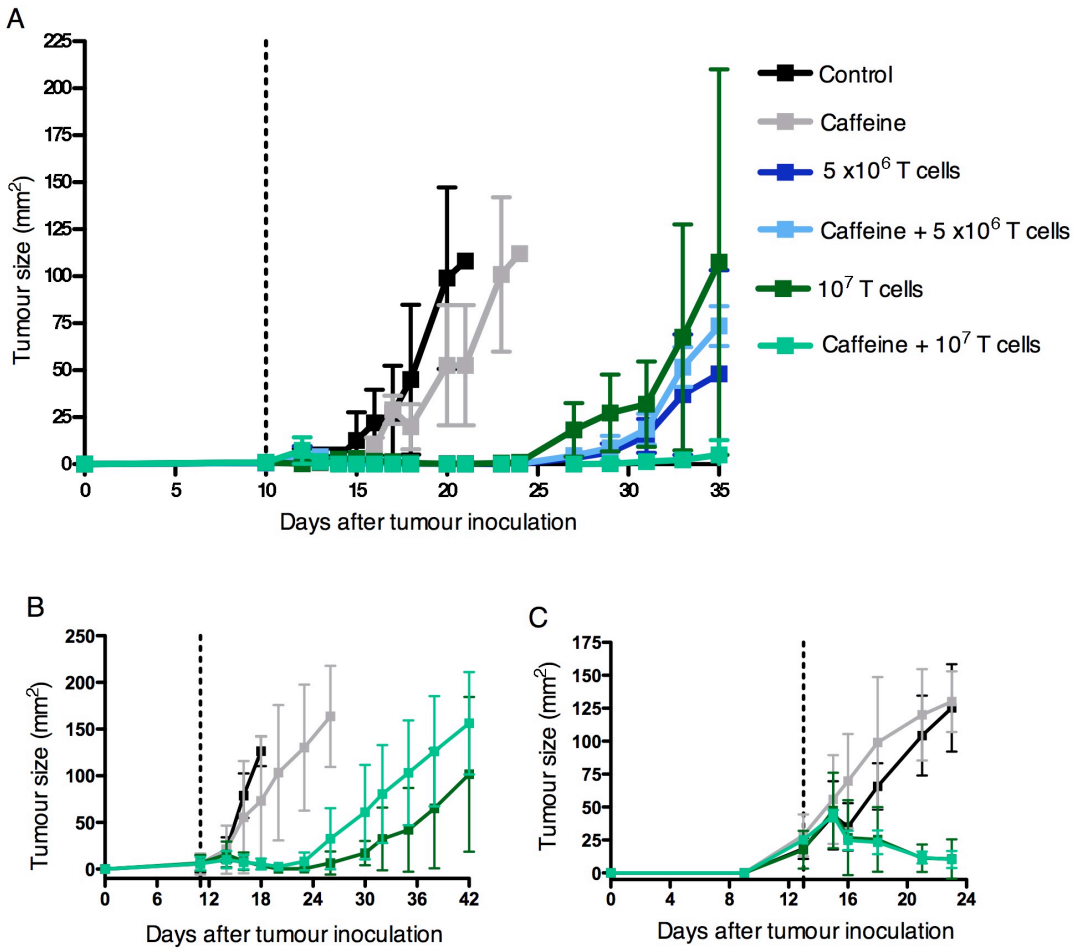

Figure 3.8: Caffeine treatment does not improve the ability of activated OTI T cells to reject tumours.

Mice were treated as in Figure 3.7 and tumour size was monitored throughout the duration of the experiment. Each panel shows the results of one experiment. A) Treatment was compared when different numbers of T cells were transferred followed by 6 days of 0.4 mg caffeine injections. Treatment was initiated when all tumours measured 4-9 mm^2. Groups consisted of 3 mice. B) Treatment was compared when 10^7 T cells were transferred followed by 4 days of 0.4 mg caffeine injections. Treatment was initiated when all tumours measured 4-9 mm^2 and tumour growth was monitored over time. Groups consisted of 10 mice. C) Treatment was compared when 10^7 T cells were transferred followed by 4 days of 0.4 mg caffeine injections. Treatment was initiated when all tumours measured 16-25mm^2 and tumour growth was monitored over time. Groups consisted of 5 mice per group. The broken line indicates the day on which mice received the T cell and/or caffeine treatment started. Graphs show mean ± SD.

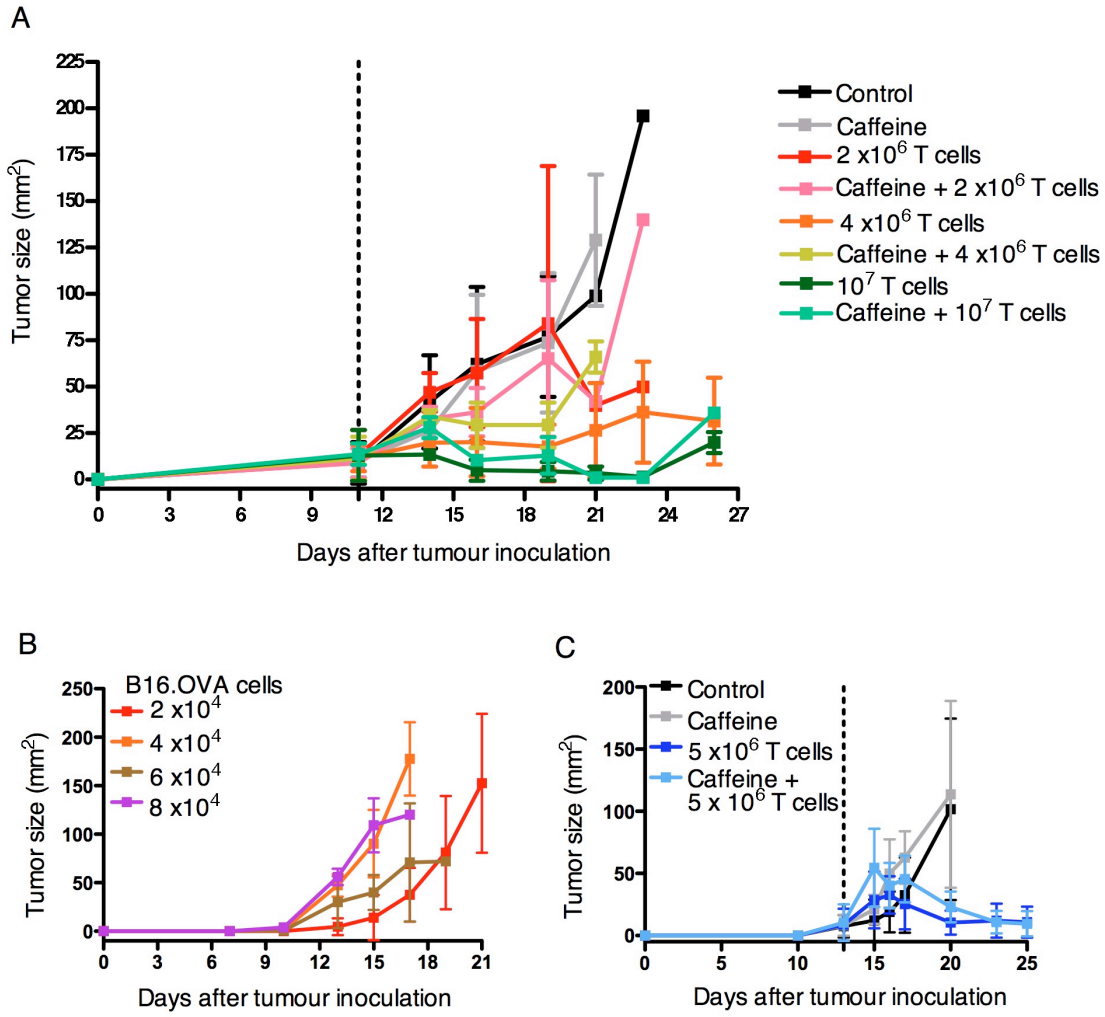

Figure 3.9: Optimising the number of T cells and tumour cells used fails to reveal an effect of caffeine on the ability of activated OTI cells to reject tumours.

A) Mice were treated as in figure 3.7 and tumour size was monitored throughout the duration of the experiment. Mice were inoculated with 10^5 B16.OVA cells. The number of T cells was titrated down from 10^7 to 2 x 10^6 while mice received 0.6mg caffeine injections for 4 days. Groups consisted of 5 mice. B) B16.OVA tumour cells were titrated down from 8 x 10^4 to 2 x 10^4 cells. Mice were monitored for tumour growth. Groups consisted of 4-5 mice. C) Mice were treated as in figure 3.6 and tumour size was monitored throughout the duration of the experiment. Mice received 5 x 10^4 B16.OVA tumour cells followed by 5 x 10^6 T cells and 0.6mg caffeine injections for 4 days. Groups consisted of 5 mice. The broken line indicates the day on which mice received the T cell and/or caffeine treatment. Each panel represents a separate experiment. Graphs show mean ± SD.

3.3.3 The adoptive transfer of activated OTI T cells is associated with an increase in a subset of tumour infiltrating CD11b$^+$ cells

It is possible that caffeine treatment failed to improve the anti-tumour activity of the OTI T cells because of an effect on the ability of the cells to infiltrate the tumour. To address this possibility, tumours were removed from mice 6 days after the adoptive transfer of T cells, processed into single cell suspensions and analysed by flow cytometry. Tumours from mice that received the adoptively transferred T cells showed a slight trend towards an increase in the frequency of infiltrating CD8$^+$ but not CD4$^+$ T cells (Figure 3.10). Caffeine treatment did not appear to significantly affect the frequency of infiltrating cells.

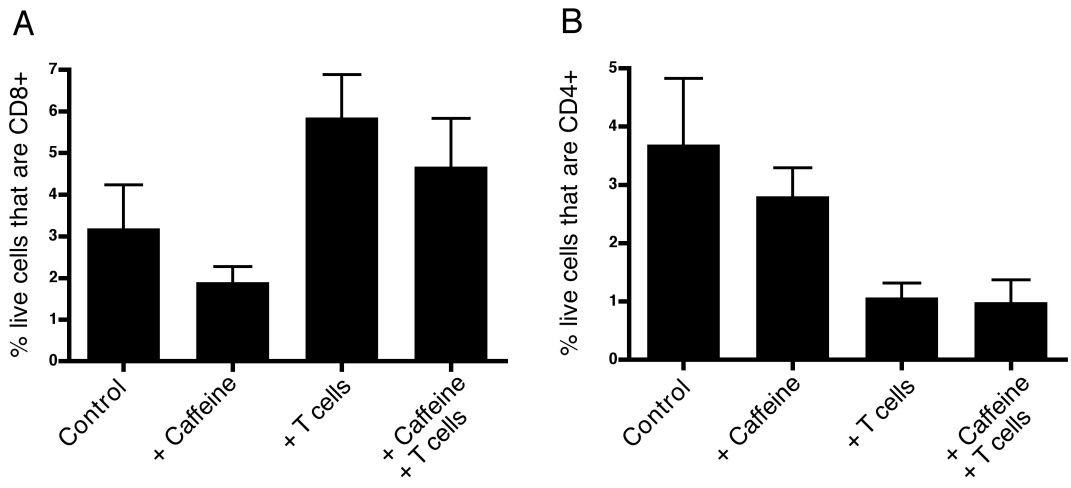

Figure 3.10: Flow cytometric analysis of B16.OVA tumours shows adoptively transferred, *in vitro* activated CD8$^+$ T cells are able to infiltrate the tumours.

Mice were treated as in figure 3.7. Tumour cell suspensions were examined 6 days after caffeine treatment commenced to analyse the infiltration of (A) CD8$^+$ and (B) CD4$^+$ cells, expressed as a percentage of live cells. Experiments consisted of 5 mice per group and data shown is from 1 of 2 experiments which each showed similar results. Bars show the mean + SD. Values of *p* were calculated using a one-way ANOVA test with a Tukey's multiple comparisons post-test.

Tumours from mice that received adoptively transferred T cells showed a significant increase in the frequency of CD45$^+$ cells expressed as a percentage of live cells (Figure

3.11A). However when the $CD45^+$ population was analysed, there appeared to be no change in the frequency of infiltrating $CD8^+$ cells while the frequency of $CD4^+$ T cells decreased (Figure 3.11B and C). This implies that in response to the transfer of activated OTI T cells, there is also an increase in other $CD45^+$, non-T cells. The ability of $CD45^+$ cells to infiltrate tumours was again found to be unaffected by caffeine.

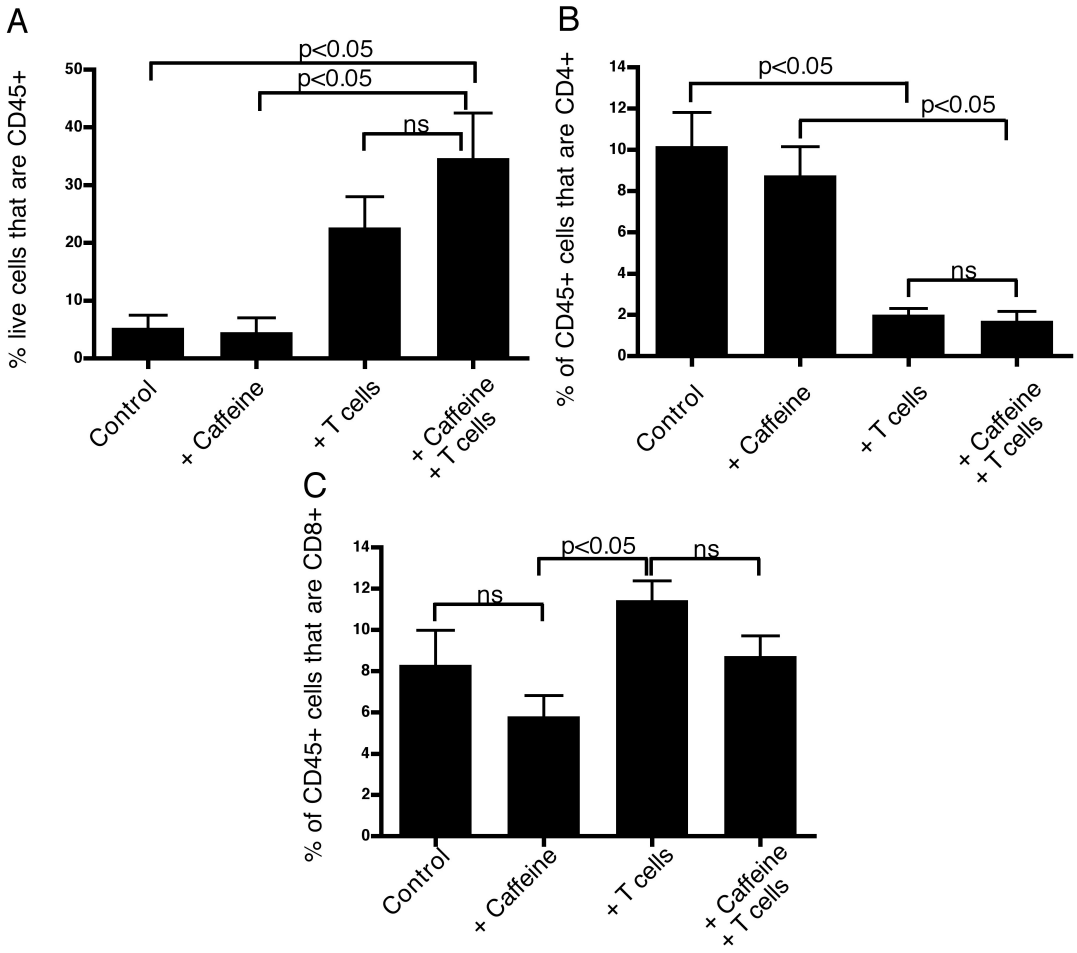

Figure 3.11: The adoptive transfer of *in vitro* activated $CD8^+$ T cells causes an increase in the frequency of $CD45^+$ non-T cells in B16.OVA tumours.

Mice were treated as in Figure 3.7. Tumour cell suspensions were examined for the frequency of live, $CD45^+$ cells (A). The live, $CD45^+$ population was further analysed to determine the frequency of (B) $CD4^+$ and (C) $CD8^+$ T cells. Experiments used 5 mice per group, the data shown is from 1 of 2 experiments which each showed similar results. Bars show the mean + SD. Values of *p* were calculated using a one-way ANOVA test with a Tukey's multiple comparisons post-test.

The tumour infiltrating $CD45^+$ population was further analysed to determine which non-T cell populations showed increased infiltration after the adoptive T cell treatment. No increase in the frequency of NK or NKT cells was observed after adoptive T cell treatment, irrespective of caffeine treatment (Figure 3.12A-B).

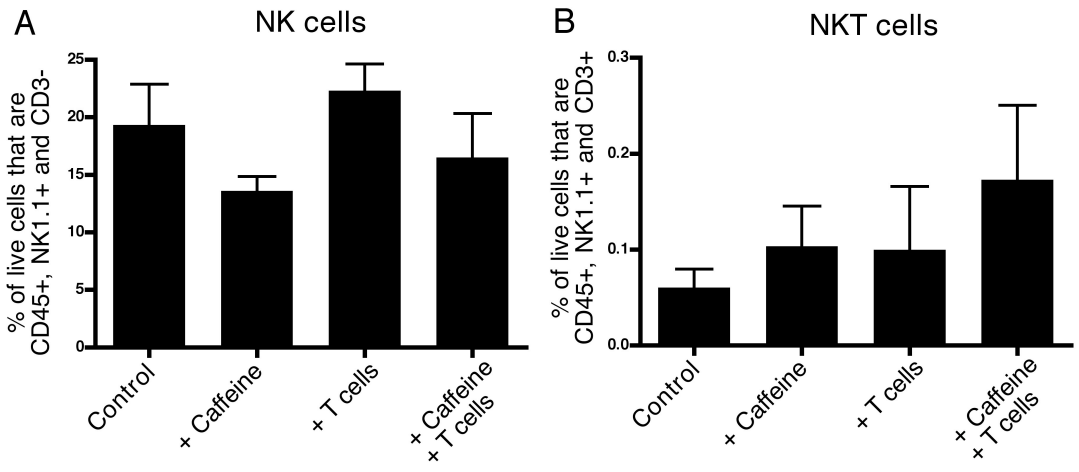

Figure 3.12: The adoptive transfer of *in vitro* activated $CD8^+$ T cells does not affect the frequency of $NK1.1^+$ cells in tumours.

Mice were treated as in Figure 3.7. Tumour cell suspensions were examined for the infiltration of (A) NK cells and (B) NK T cells expressed as a percentage of live cells. Experiments used 5 mice per group and data shown is from 1 of 2 experiments which each showed similar results. Graphs show the mean + SD. No statistical differences were found using a one-way ANOVA test.

The $CD45^+$ non-T cell population that was increased in tumours in response to adoptive T cell treatment (Figure 3.11) was identified as being $CD11b^+$ (Figure 3.13A). No difference was found in the frequency of $CD45^+$, $CD11b^+$, $F4/80^{high}$ cells, which may include macrophages, monocytes, eosinophils and some DC (Figure 3.13B). A significant increase was observed, instead, in the $CD45^+$, $CD11b^+$ $Gr1^+$ population (Figure 3.13C), which may include neutrophils and myeloid derived suppressor cells (MDSC). Caffeine treatment did not affect the ability of any cell population tested to infiltrate tumours. These data show

that while caffeine treatment does not affect the ability of cells to infiltrate the tumour, the transfer of activated OTI T cells allows increased infiltration of other, non-T cells, into the tumour.

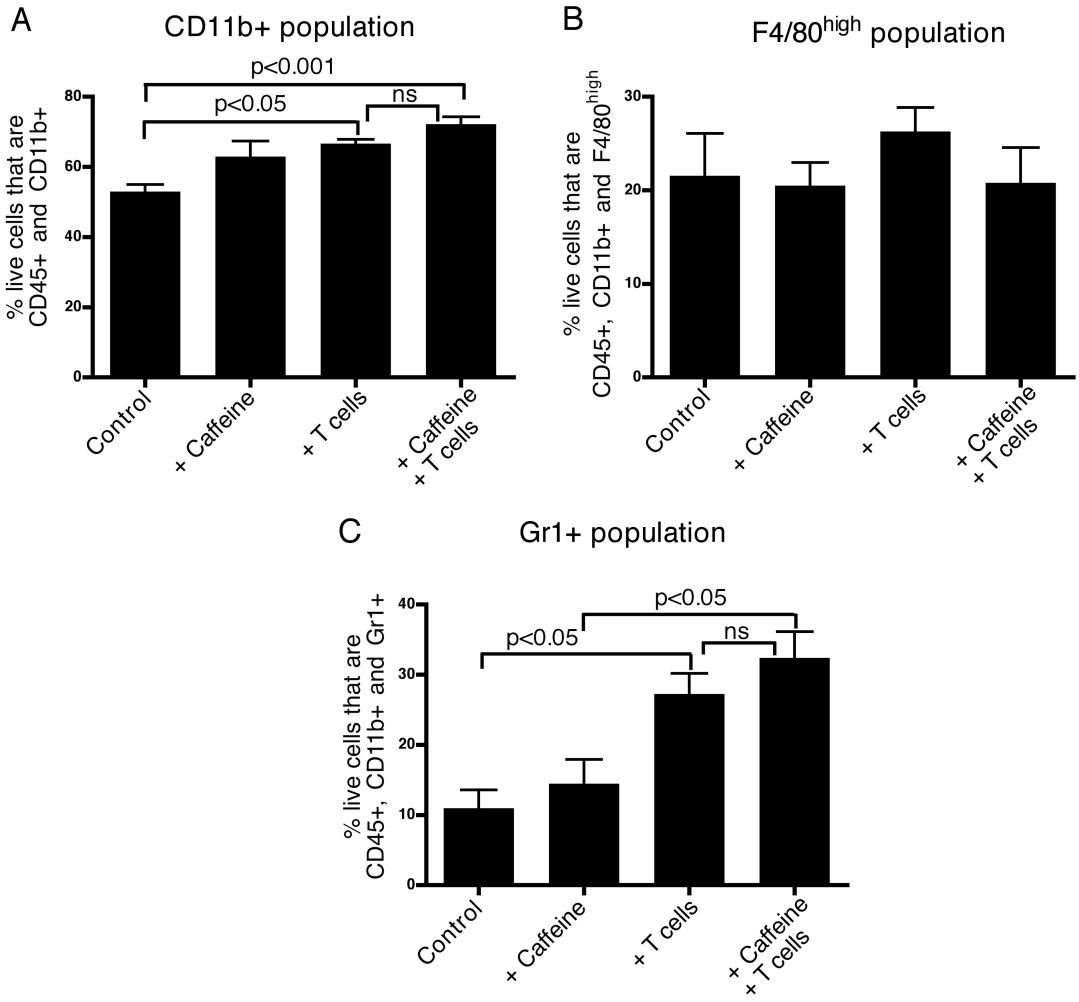

Figure 3.13: The adoptive transfer of *in vitro* activated CD8$^+$ T cells increases the frequency of CD11b$^+$ subpopulations in tumours.

Mice were treated as in figure 3.7. Tumour cell suspensions were examined for the infiltration of populations that were CD45$^+$ and (A) CD11b$^+$ (B) CD11b$^+$ and F4/80^{high} or (C) CD11b$^+$ and Gr1$^+$. All graphs are from one experiment containing 5 mice per group. Values of *p* were calculated using a one-way ANOVA test with a Tukey's multiple comparison post-test. Graphs show the mean + SD.

3.4 Discussion

The aim of this chapter was to establish whether it was possible to increase the ability of activated OTI T cells to reject tumours by inhibiting adenosine signalling.

The proliferation assay established in Figure 3.2 showed that electroporation of A2a receptor specific siRNA did not reverse the inhibitory effects of adenosine. Further analysis using a PCR assay to evaluate changes at the mRNA level in response to electroporation of the predesigned positive control GAPDH siRNA showed no decrease in the GAPDH mRNA levels in response to siRNA treatment. Both the A2a siRNA sequence and the electroporation conditions were obtained from studies that had performed RNA silencing successfully (320, 336). The most likely reason the activated OTI T cells did not show improved proliferation after siRNA treatment, therefore, is that the conditions achievable by the electroporators used were not sufficient to deliver the siRNA molecules into the cells.

Adenosine is known to inhibit T cell proliferation (185), however, Figure 3.3 unexpectedly revealed that the proliferation of tumour cells is also inhibited by adenosine. Studies have shown that in a range of mouse and human tumours, including B16.F10, the parental strain of the B16.OVA tumour cell line used in this thesis, express various adenosine receptors (340-343). This is in contrast to murine T cells, which predominantly express the A2a receptor with some expression of the A2b receptor. It is therefore possible that the suppressive effect of adenosine on tumour cells may be mediated through more than one of these adenosine receptors. This presents the possibility that adenosine mediated suppression of proliferation may have a slightly different mechanism in tumour cells in comparison to T cells.

After experiments in this thesis on A2a gene silencing had commenced, work was published showing that silencing both the A2a and A2b receptors in anti-tumour T cells improved the adoptive immunotherapy of murine CMS4 sarcomas and RMA T lymphomas (337). Mice that received *in vitro* activated, A2a and A2b receptor silenced tumour specific T cells showed a reduced tumour burden or increased survival in comparison to those that received the non-silenced T cells. This work elegantly demonstrated that RNA silencing techniques could be utilised to silence A2 receptors and that silencing these receptors on activated T cells improves their anti-tumour activity *in vivo*. It is presumed that most of this effect is due to adenosine signalling via the A2a receptors because they are the most abundant adenosine receptor subtype found on T cells. In fact, the authors used a variety of tumour models, adenosine receptor knock out mice and adenosine receptor inhibitors including caffeine to further support their finding that it is predominantly the A2a receptor which prevents the T cells from mounting an efficient anti-tumour response. However one study has shown that the number of A2b receptors on T cells is increased in response to hypoxia (344). In order to design effective therapeutic cancer vaccines, it is vital to understand the relative contributions of the two adenosine receptors to T cell inhibition.

It was not possible to assess whether the anti-tumour activity of activated OTI T cells could be improved by using the siRNA technology available for this study, so it was decided to pursue this investigation further using the adenosine receptor antagonist caffeine. Caffeine has been shown to improve CTL mediated tumour rejection, using tumour models different to that used in this thesis (337). To expand these findings, the ability of caffeine to improve the CTL cell mediated rejection of B16.OVA melanomas and the infiltration of various cell types in response to T cell and caffeine treatment was investigated.

The effects of caffeine on tumour growth were found to be inconsistent in the B16.OVA tumour model. Varying the number of T cells transferred, the number of tumour cells inoculated and the concentration of caffeine did not result in a clear improvement in the anti-tumour effect of transferred T cells. This is in contrast to the LL-LCMV solid tumour and CMS4 liver tumour models that have shown an improved anti-tumour response when caffeine is administered in conjunction with the transfer of activated anti-tumour T cells (337). In fact the CL-8 melanoma tumour model shows an improved anti-tumour response after caffeine treatment alone (337). It is possible that the LL-LCMV, CMS4 and CL-8 tumour models all show an improved anti-tumour response in the presence of caffeine but the B16.OVA model used in this thesis does not because the tumour models have varying degrees of dysregulated vasculature and hypoxia. Tumours with higher levels of hypoxia may be more sensitive to treatments that prevent adenosine signalling in activated T cells.

Tumour tissue becomes hypoxic once it is more than 120-130 μm from a blood vessel (345), therefore tumours, which have dysregulated vasculature, usually become hypoxic at a very early stage of growth. While the level of intratumoral adenosine may vary between tumour models, the level of adenosine is likely to be elevated in all models and cannot explain the differences seen in tumour responses to caffeine treatment. Instead, differences in tumour responses to caffeine treatment are likely to be the result of differential expression of the adenosine receptors between the B16.OVA model and the LL-LCMV, CMS4 and CL-8 tumour models. Figures 3.2 and 3.3 showed that the proliferation of activated T cells and tumour cells can be inhibited by adenosine. Based on these findings, tumours expressing high levels of adenosine receptors, may be expected to show increased growth in response to caffeine treatment because the inhibitory effects of adenosine would be abrogated. Blocking the adenosine receptors on activated T cells using the *in vivo* administration of caffeine may restore the anti-tumour activity of these T cells however it

may also restore the proliferative capabilities of the tumour cells and the two responses would negate each other. If this possibility were true, one would also expect to see that the caffeine treated group (without the T cell treatment) has larger tumours than the tumour only group, however this was not observed.

Caffeine is also a known psychoactive stimulant and diuretic, that has further effects such as vasodilation, tachycardia and increased blood pressure (346-348), none of which are anticipated to have a negative impact on the anti-tumour response. In fact, vasodilation is likely to decrease hypoxia slightly although it is not likely to relieve the hypoxia enough to result in decreased adenosine levels. Instead, in the caffeine treated group, increased tumour growth may be offset by improved function of existing activated anti-tumour cells or decreased angiogenesis limiting the blood supply to the tumour cells. Angiogenesis is primarily mediated via the A2b receptors (349, 350), which are suggested to be upregulated in response to hypoxia (344). Caffeine can also block the A2b adenosine receptors, which may be enough to decrease angiogenesis (337). This illustrates the importance of using methods such as the siRNA therapy, which enables the silencing of one or more specific genes in target cells.

To try to further understand why, in contrast to other tumour models (337), caffeine treatment did not improve the anti-tumour response in mice that also received activated OTI T cells, the tumour cell infiltrate was analysed. The frequency of tumour infiltrating cells that were $CD8^+$ showed a trend towards being increased in mice that received the activated OTI T cells. This difference was not found to be statistically significant but was sufficient to result in decreased tumour size. Caffeine was not found to affect the ability of these activated OTI T cells to infiltrate the tumours.

Interestingly, mice that received activated OTI T cells also showed increased infiltration of a $CD45^+$, $CD11b^+$, $Gr1^+$ population of cells. Based on the literature, this population probably consists of neutrophils and myeloid derived suppressor cells (MDSC) (351-354). There are a number of possible explanations for this observation. The increased infiltration of non-T cells could be because the tumours are physically smaller due to the anti-tumour activity of the T cells making the tissue more accessible, or simply increasing the ratio of infiltrating cells to tumour cells. For either of these explanations to be correct, there would need to be an increase of all cell types analysed and not just the $CD45^+$, $CD11b^+$, $Gr1^+$ population so this possibility alone is unlikely. Solid tumours elicit an inflammatory immune response (355) characterised by the early and persistent infiltration of eosinophils (356) and MDSC (192, 193). Factors secreted by T cells such as IFN-γ (357) and GM-CSF (357) have been suggested to cause conversion of myeloid cells to MDSC (358-361), which then suppress T cell responses (351, 359, 362). Mice that received the T cell treatment would obviously have more circulating and possibly tumour infiltrating T cells that may lead to increased conversion of myeloid cells to MDSC. These observations would lead suggest that the increase in $CD45^+$, $CD11b^+$, $Gr1^+$ cells found in the groups that received the T cell treatment are therefore mostly MDSC.

The increased tumour infiltration of $CD45^+$, $CD11b^+$, $Gr1^+$ cells may explain why caffeine treatment did not improve the anti-tumour response. MDSC are known to be capable of directly suppressing T cell responses (351, 362) but they have also been shown to induce Treg (363) and to mediate at least some of their suppressive function via Treg activity (363, 364). Increased T cell function in response to caffeine treatment may then be counteracted by the increased activity of MDSC and Treg in response to the T cell treatment.

3.5 Conclusions

Electroporation of siRNA specific for the A2a receptor or GAPDH genes was found to be insufficient to silence these genes. The *in vivo* administration of caffeine also did not improve the anti-tumour response of the transferred activated OTI T cells. The increased frequency of $CD45^+$, $CD11b^+$, $Gr1^+$ cells observed in response to T cell treatment, most of which are believed to be MDSC, and their link to Treg may explain why no improvement in the anti-tumour response was observed in mice that received the caffeine treatment. This suggests that caffeine and T cell therapy may also complement Treg therapies to produce safe and effective cancer vaccines in the future.

CHAPTER FOUR

TREG IN MURINE MELANOMAS ARE SUPPRESSIVE AND LOCALISE IN CLOSE PROXIMITY TO DC

4.1 Introduction

Studies using injected tumours have shown that spontaneous anti-tumour responses are generally poor, as evidenced by the establishment and continued growth of the tumour (365, 366). Studies have shown that tumour infiltrating DC (TIDC) fail to elicit an effective immune response *in vivo* (365, 366) unless the TIDC are first exposed to tumour Ag *ex vivo* (367). This implies that mechanisms acting within the tumour may be suppressing the ability of the DC to stimulate an efficient anti-tumour immune response.

Treg and DC are both found in tumours (154, 258, 259, 365-367). Treg are known to suppress anti-tumour responses because the presence of Treg is negatively correlated with the disease outcome of tumour bearing individuals (154, 258, 259). This is supported by numerous studies that have shown that immune responses in tumour bearing individuals can be enhanced by the depletion of Treg using PC61 in mice (138, 139, 154, 259) or ONTAK in humans (158, 314). The possibility that Treg may mediate some of their tumour immunosuppression by interacting with DC was investigated in this chapter.

4.2 Aims

The purpose of the experiments described in this chapter was to determine whether it is possible for Treg and TIDC to interact in B16.OVA tumours. The murine B16.OVA melanoma model was used because previous studies showing TIDC function is inefficient also used this model. It was hypothesised that Treg would be able to interact with DC in the tumour.

4.3 Results

4.3.1 Characterisation of TIDC and Treg populations by flow cytometry

Flow cytometry provides the most comprehensive method of phenotyping cell populations because of the multiple parameters that can be simultaneously analysed. Large tumours were removed from mice ~17 days after inoculation and were processed into single cell suspensions. Live tumour cells were identified using FSC and SSC, rather than a viability dye, because the flow cytometers used for most of the experiments in this thesis were only capable of detecting four fluorochromes at a time. TIDC were defined as $CD45^+$ and $CD11c^{high}$. These DC were further divided into $CD11b^+$ and $CD11b^-$ subpopulations (Figure 4.1). The $CD11b^+$ and $CD11b^-$ DC subpopulations were analysed separately in further experiments. Tumour infiltrating Treg were defined as $CD45^+$, $CD4^+$ $Foxp3^{high}$ cells (Figure 4.1).

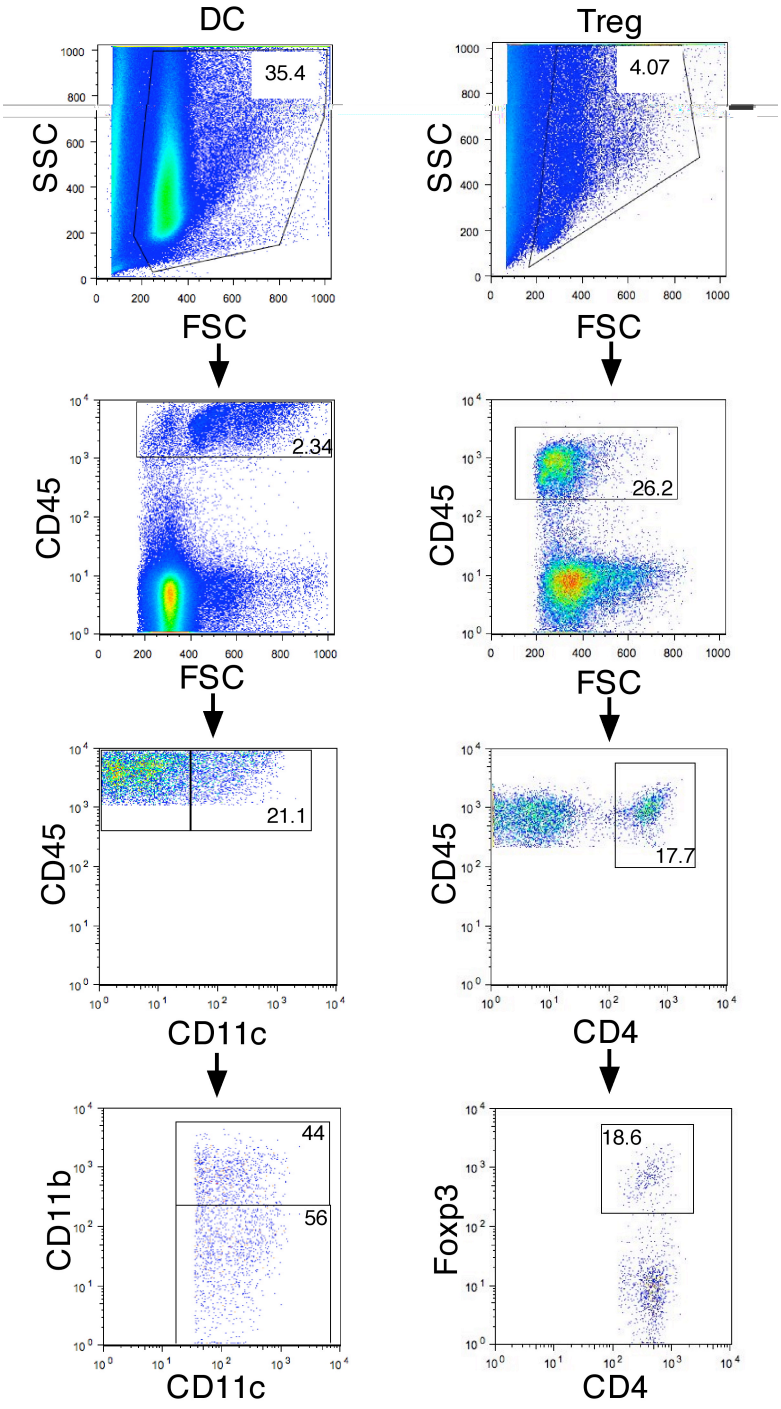

Figure 4.1: Identification of TIDC and Treg by flow cytometry

B16.OVA tumours were excised from mice ~17 days after inoculation and analysed by flow cytometry. Live cells were selected based on FSC and SSC properties. DC were defined as $CD45^{+}$, $CD11c^{high}$ cells that contained both a $CD11b^{+}$ and $11b^{-}$ subpopulation. In a separate experiment, Treg were defined as $CD45^{+}$, $CD4^{+}$ and $Foxp3^{+}$. Numbers shown in graphs represent the percent of the population within the gate.

It has been shown that various murine and human tumours and tumour cell lines can express the Treg marker Foxp3 (368-370), which has the potential to complicate the analysis of Treg within tumours. It was therefore important to determine whether the murine B16.OVA melanoma cell line also expressed the Treg markers Foxp3 and CD25 at levels that could be detected by flow cytometry.

Reliable tumour specific antibodies that could distinguish tumour cells from endogenous cells when analysing tumours grown *in vivo* were not available. Instead, in order to examine markers expressed by tumour cells, *in vitro* cultured B16.OVA tumour cells were used. Live cells were selected using forward and side scatter properties, consistent with previous experiments. B16.OVA tumour cells were found to express neither Foxp3 nor CD25 *in vitro*, as assessed by comparison to the appropriate isotype controls (Figure 4.2). This indicates that the use of Foxp3 and CD25 to identify Treg and their subpopulations is appropriate in this tumour model.

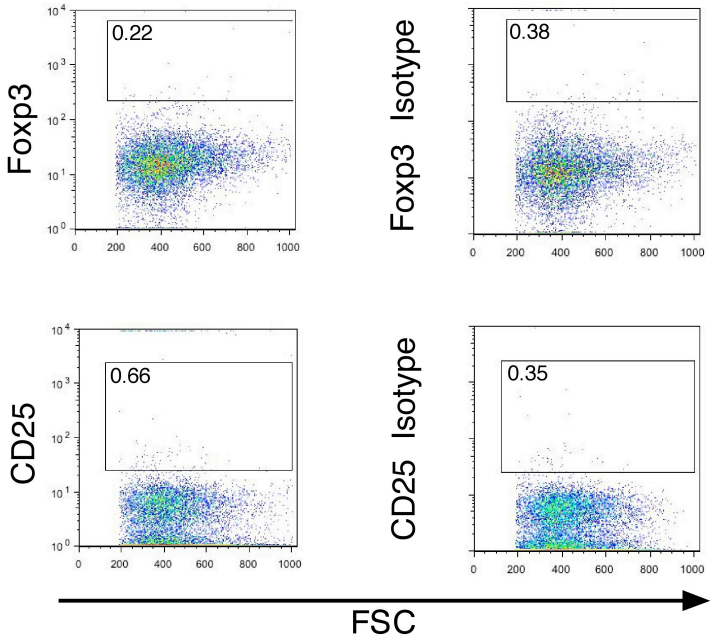

Figure 4.2: B16.OVA tumour cells do not express typical Treg markers.
Live *in vitro* cultured B16.OVA tumour cells were identified using FSC and SSC properties. Expression of the markers Foxp3 and CD25 were compared to the appropriate isotype controls. Numbers shown in graphs represent the percent of the population within the gate.

4.3.2 Flow cytometric quantification of DC frequency in tumours and lymph nodes

The failure of tumour bearing mice to raise an efficient anti-tumour immune response may be due to problems within multiple stages of the response. One of the earliest events during an adaptive immune response is the accumulation and migration of DC.

To determine whether DC recruitment to the tumour or lymph nodes was impaired, tumours along with the tumour draining and non-draining lymph nodes were removed from mice ~17 days after inoculation and processed into single cell suspensions. Flow cytometric analysis of B16.OVA tumours showed that the tumour draining and non-

draining lymph nodes contained similar frequencies of DC (Figure 4.3). Tumours also contained DC although at a lower frequency than the lymph nodes (Figure 4.3).

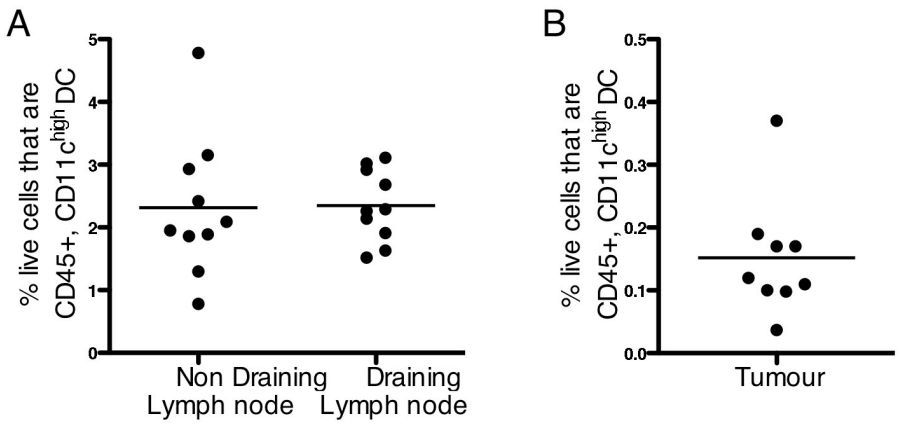

Figure 4.3: Flow cytometric analysis of lymph node and tumour tissue reveals the presence of CD45^{+}, CD11c^{high} DC.

A) B16.OVA tumours and B) draining and non-draining lymph nodes were excised from mice ~17 days after tumour inoculation and analysed by flow cytometry. The frequency of CD11c^{high} DC in the live population of each tissue was compared. Each dot represents a single mouse. Lymph node data is compiled from 2 experiments with 5 mice per group and tumour data is compiled from 2 experiments with 4-5 mice per group. Data was analysed using a non-parametric, one-way ANOVA test.

4.3.3 Flow cytometric analysis of various sized tumours shows Treg accumulate in tumours from an early stage

Most studies show that Treg numbers negatively correlate with the survival outcome of tumour bearing individuals (371-373). It was therefore important to investigate the frequency of Treg in the B16.OVA tumour model used in this thesis.

Mice were inoculated with B16.OVA 10-17 days before tumours of different sizes were removed and analysed by flow cytometry on the same day. This allowed the direct

comparison of the cell populations within the different sized tumours. The frequency of Treg in small tumours (<25mm^2) was found to be twice the frequency of Treg found in blood (as shown below in Figure 4.8B). The high frequency of tumour infiltrating Treg occurs even at very early stages in tumour development and continues to increase as the tumour increases in size (Figure 4.4).

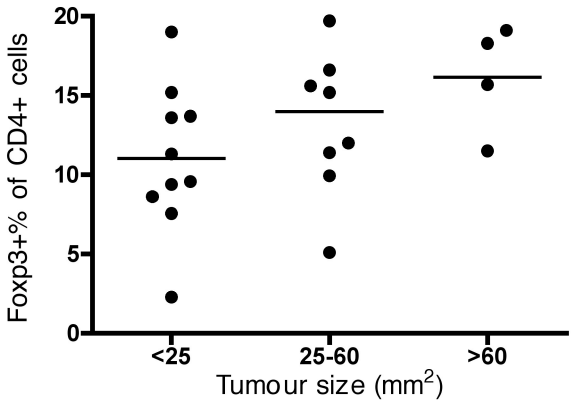

Figure 4.4: A comparison of the frequency of CD4$^+$ Foxp3$^+$ Treg in tumours of various sizes shows the frequency of Treg increases as tumours increase in size.

Different sized tumours were generated by the inoculation of mice with B16.OVA 14-17 days before analysis. Tumours were excised and analysed on the same day. Data is from one experiment with 22 mice, which were stratified according to tumour size. Each dot represents a single mouse. Data was analysed using a non-parametric, one-way ANOVA test.

4.3.4 Tumour infiltrating Treg are capable of suppressing T cell proliferation in vitro

The ability to suppress the proliferation of T cells is a characteristic of functional Treg. Since newly activated $CD4^+$ T cells have also been shown to transiently express Foxp3 in humans (229, 242, 245), an *in vitro* suppression assay was used to determine whether the population defined in previous experiments is in fact a Treg population capable of suppressive function.

To generate tumours from which $Foxp3^+$ Treg could be isolated based on the expression of GFP, B16.OVA tumours were inoculated into Foxp3-GFP mice (325). Tumours were excised ~17 days after inoculation and processed into single cell suspensions which were enriched for the $CD45^+$ population using positive magnetic sorting. Tumour-infiltrating Treg were then sorted by FACS from the CD45 enriched population to a purity of 98% based on their expression of CD4 and GFP (as an indicator of Foxp3 expression). $CD4^+$ T cells were incubated with increasing numbers of Treg along with DC and anti-CD3 to activate the Treg and stimulate $CD4^+$ T cell proliferation in a non-antigen specific manner. T cell proliferation decreased with the increasing number of Treg (Figure 4.5), indicating that the tumour infiltrating $Foxp3^+$ population represents a functional Treg population.

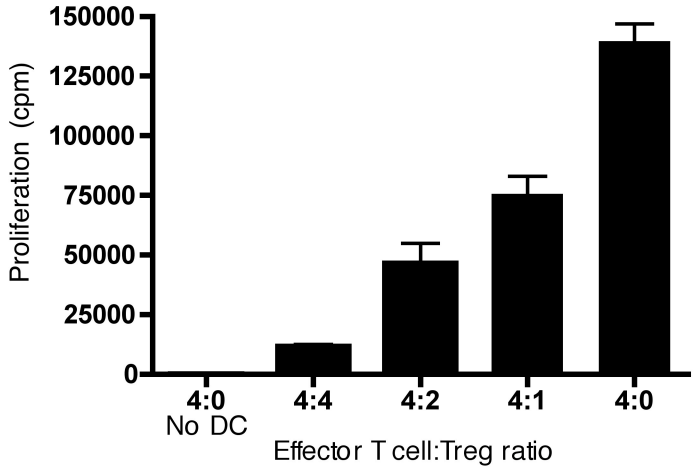

Figure 4.5: Tumour infiltrating Treg are capable of suppressing T cell proliferation *in vitro.*

B16.OVA tumours were excised from Foxp3-GFP mice ~17days after tumour inoculation and samples were enriched for $CD4^+$ cells by positive automacs separation. GFP^+ cells were then sorted by FACS and the resulting $CD4^+$ $Foxp3^+$ Treg population (>98% pure) was titrated into wells containing 4 $x10^4$ purified $CD4^+CD25^-$ effector T cells, 3 $x10^3$ DC, and 1 μg/ml anti-CD3. Cultures were incubated at 37°C for 3 days with ^3H thymidine added in the last ~18 hours of culture. Proliferation was determined as the counts (of ^3H thymidine) per minute (cpm). Bars represent average ± range for duplicate samples from a single experiment.

4.3.5 Titrating the amount of PC61 administered shows two 100 μg doses of PC61 give the optimal depletion of Treg and cause a significant delay in tumour growth

PC61 is typically administered in relatively large quantities (200-500 μg/mouse) to cause a decrease in the frequency of $CD25^+$ Treg in the blood and organs of mice (310, 311, 374). It was of interest to determine if optimal depletion of the Treg population could be achieved using lower or repeated doses of PC61.

Mice were given a single i.p. injection of 75, 100 or 125 μg of PC61 and then tail bled over subsequent days so that the effect of PC61 on the frequency of Treg in the blood

could be examined by flow cytometry over time (Figure 4.6A). By day 6 after PC61 treatment, all of the groups exhibited approximately 85% depletion of the $CD25^+$ $CD4^+$ Treg population. The frequency of this population slowly increased over time until it returned to basal levels by day 44 in the mice that received 75 μg, and day 53 for the groups that received 100 μg and 125 μg. Because the rate of recovery of the Treg population was similar in mice that received 100 μg or 125 μg PC61, 100 μg of PC61 was chosen as the optimal amount to be delivered in a single dose. Representative dot plots from mice 3 days after they were given a single i.p. injection of 100 μg of PC61 are shown (Figure 4.6B).

Figure 4.6: A single 100 μg dose of PC61 is sufficient to reduce the frequency of both $CD25^+$ and $Foxp3^+$ cells in the blood for a prolonged period of time.

Mice were given a single dose of PC61 by i.p. injection, or were left untreated as a control, and were tail bled regularly. Blood samples were analysed by flow cytometry using forward and side scatter properties to select the live leukocyte population. A) The frequency of $CD25^+$ cells as a percentage of $CD4^+$ cells was monitored as an indication of the frequency of Treg in the blood. Data represents a single experiment with 3 mice per group. Average frequencies ± SD are shown. Statistics were calculated using a two-way repeated measures ANOVA test with a Bonferroni post-test. Values of *p* represent statistical differences between the control group and the group indicated by the colour of the asterix and the values are: *=<0.05, **=<0.01 and ***=<0.001. B) Flow cytometric data from a separate experiment is shown. Blood samples were analysed in more detail by including a Foxp3 antibody to show a reduction in the frequency of $Foxp3^+$ cells as well as a reduction in the frequency of $Foxp3^+$ $CD25^+$ cells. Numbers shown in graphs represent the percent of the population within the gate.

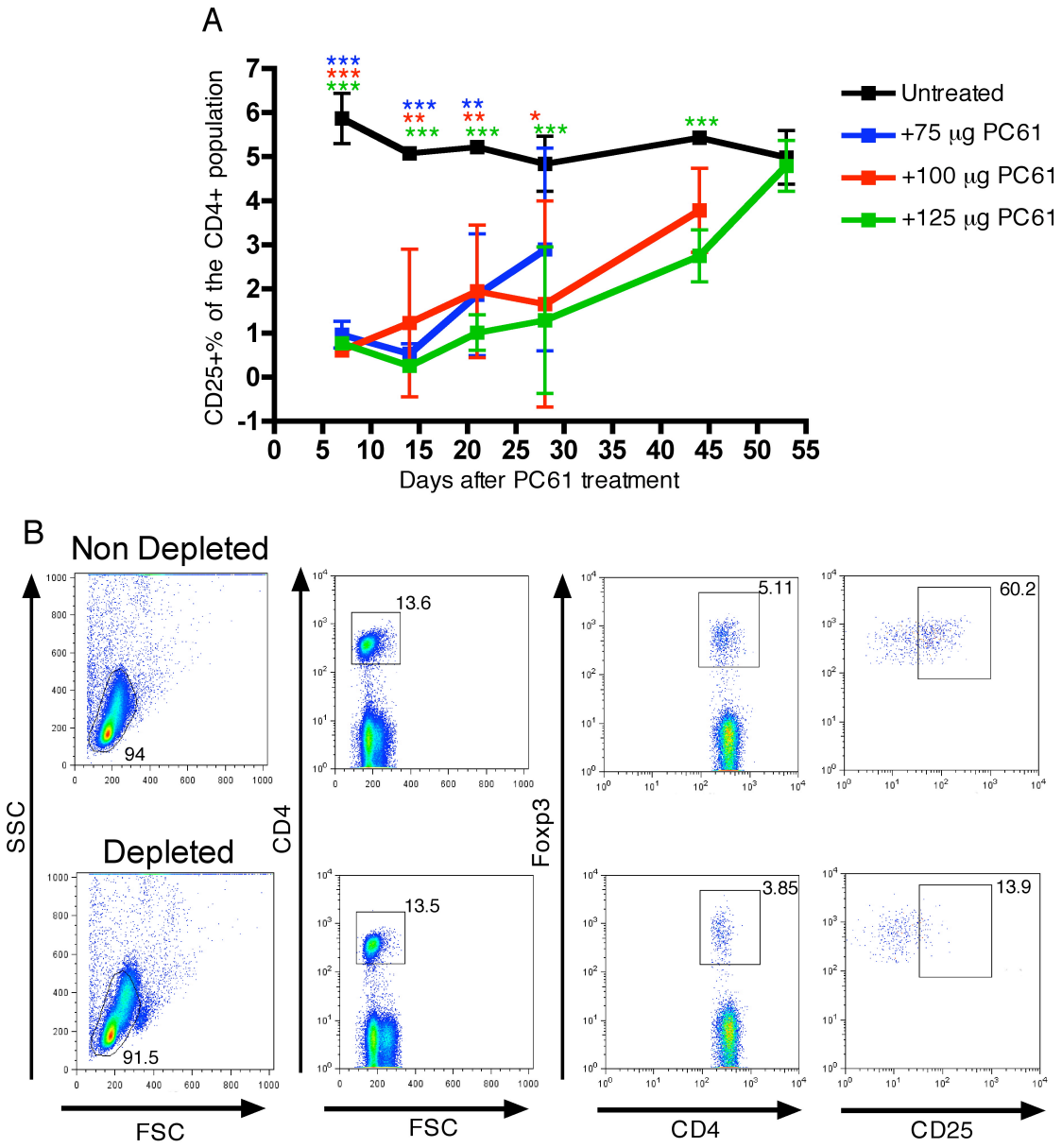
A
CD25+% of the CD4+ population
Days after PC61 treatment
Untreated
+75 μg PC61
+100 μg PC61
+125 μg PC61
B
Non Depleted
Depleted
SSC
FSC
CD4
Foxp3
CD25
94
91.5
13.6
13.5
5.11
3.85
60.2
13.9

Depletion of Treg using PC61 is known to improve the anti-tumour immune response as evidenced by a delay in or even complete regression of a range of tumours such as various leukaemias and fibrosarcomas (154). To establish the effect of Treg on tumour growth in the B16.OVA model, tumour size was monitored over time in mice that had or had not received either one or two 100 μg i.p. injections of PC61 prior to tumour inoculation. Experiments reached their endpoint when the first mouse required euthanasia due to the tumour reaching the largest size permitted by ethics (150-200 mm^2). This typically occurred no earlier than day 17 after tumour inoculation but natural variation between experiments means that some experiments ran for a longer time.

Tumours showed a trend towards delayed growth after treatment with a single 100 μg dose of PC61 (Figure 4.7A), but the delay in growth only became significant after treatment with two 100 μg doses of PC61 prior to tumour inoculation (Figure 4.7B). The experiment in Figure 4.6A showed that there was little benefit in administering more than 100 μg of PC61 in a single dose. However, administering two doses probably results in a significant delay in tumour growth simply because the treatment gives more reproducible depletions. Mice, therefore, received two 100 μg doses of PC61 prior to B16.OVA injection in all subsequent tumour experiments unless stated. At the experimental endpoint, tumours and tumour draining and non-draining lymph nodes were removed and processed into single cell suspensions. The frequency of Treg was found to be significantly lower in the lymph nodes and tumours of PC61 treated mice (Figure 4.7C). No difference in Treg frequency was found when comparing the draining and non-draining lymph nodes of the same mouse.

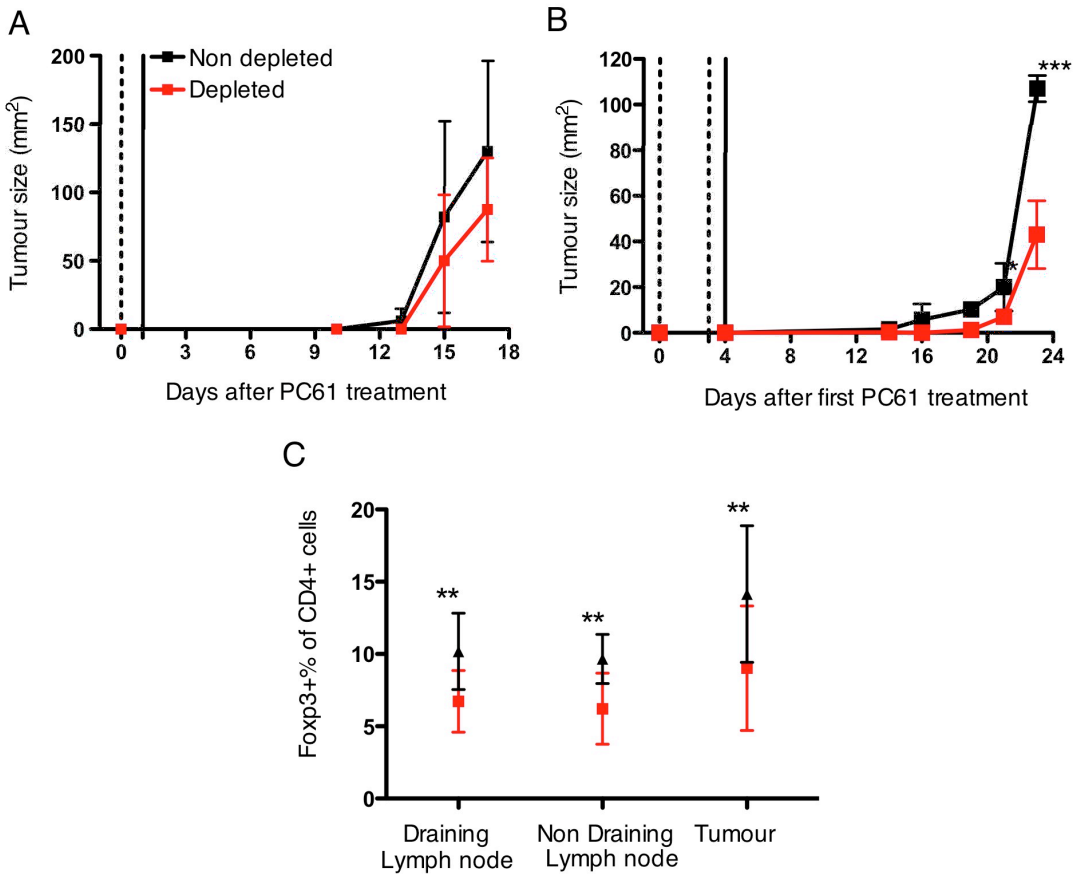

Figure 4.7: PC61 treatment delays tumour growth.

C57BL/6 mice were treated with (A) a single 100 μg dose of PC61 (dotted line) or (B) two 100 μg doses of PC61 (dotted line) or left untreated, and inoculated with tumour one day after PC61 treatment (solid line). Tumour growth was measured over time. Average tumour sizes ± SD are shown. Results are from 1 of 3 repeat experiments containing 4-5 mice per group that gave similar results. Statistics were calculated using a two-way repeated measures ANOVA test with a Bonferroni post-test where * = $p<0.05$ and *** = $p<0.001$. C) Lymph nodes and tumours were analysed 17 days after tumour inoculation by flow cytometry and Treg levels were compared. Data represents a compilation of 2 experiments containing 5 mice per group per experiment. Average frequencies ± SD are shown. Statistics were calculated using a two-way ANOVA test with a Bonferroni post-test where ** = $p<0.01$.

4.3.6 The presence of tumour does not affect the kinetics of Treg depletion and recovery after PC61 treatment

Studies have shown that tumours are able to actively recruit Treg based on the production of CCL22 by NK cells and macrophages within the tumour (372, 375). This suggested the possibility that peripheral reconstitution of the Treg population may be altered in tumour bearing individuals.

Mice were given two 100 μg i.p. injections of PC61, 3 days apart, before tumour inoculation, and the circulating Treg levels were again followed over time in the blood. The frequency of $Foxp3^+$ Treg was reduced by a moderate amount (40-50%) by day 6 in both the non-tumour bearing and tumour bearing mice. This reduction in the number of Treg was maintained throughout the experiment, which ended when the tumour bearing mice were euthanased for ethical reasons (Figure 4.8A). The frequency of Treg in the blood of non tumour bearing mice at day 3 was similar in Treg depleted and non depleted groups, however, this is probably because the cells can survive for a few days without IL-2 after engagement of CD25 on the T cell by PC61. This is supported by the finding that at day 3, PC61 treatment reduced the frequency of the $CD25^+$ population of $Foxp3^+$ cells from 60% to 0%. CD25 expression by the $Foxp3^+$ Treg returned to pre-treatment levels by day 22 in both the non-tumour bearing and tumour bearing mice (Figure 4.8B). This indicates that the expression of CD25 by Treg in tumour bearing and non-tumour bearing mice was affected similarly by PC61 treatment.

These data show that the $Foxp3^+$ population was expressing CD25 by the end of the experiment but the frequency of the $Foxp3^+$ Treg population was still reduced in PC61 treated mice, and the presence of tumour did not alter these trends.

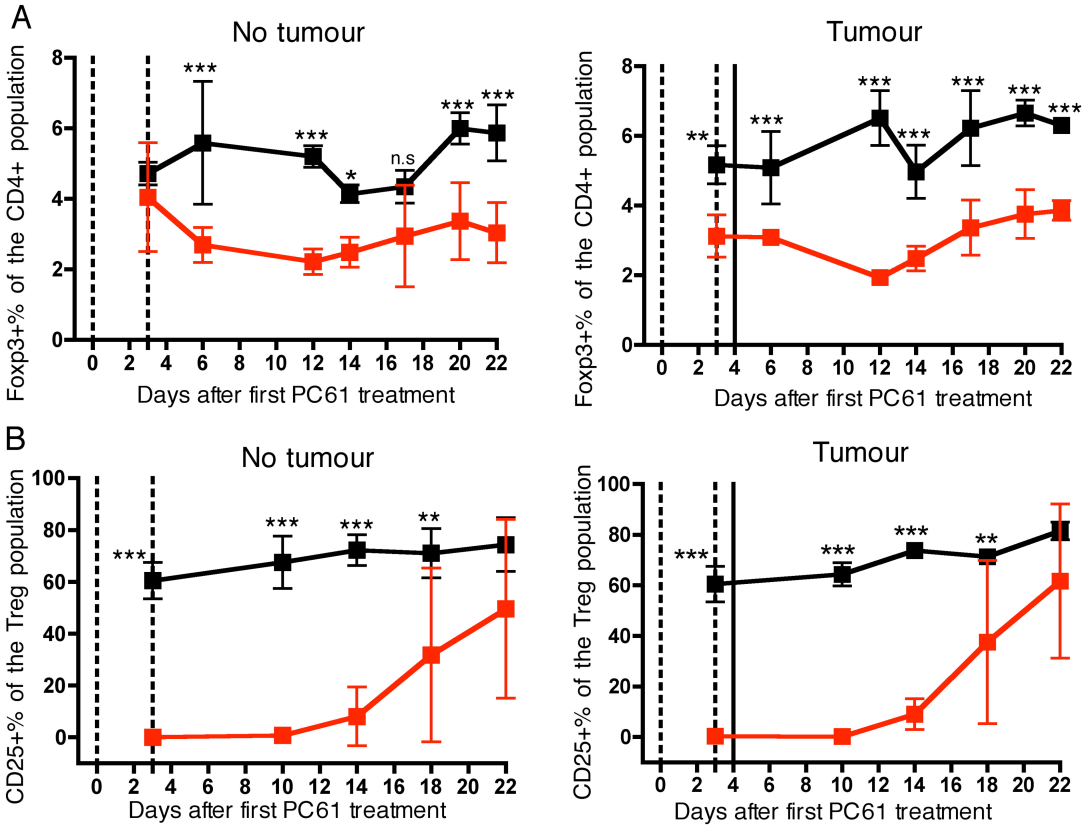

Figure 4.8: The presence of tumour does not affect the kinetics of peripheral Treg depletion and recovery after PC61 treatment.

Foxp3-GFP mice were depleted of Treg using two 100 μg doses of PC61 (solid red squares) or left non depleted (solid black squares) as a control and tail bled regularly. The dotted and solid lines indicate when mice received the PC61 treatment and B16.OVA tumour inoculation, respectively. (A) The frequency of $Foxp3^+$ Treg within the $CD4^+$ population was monitored. (B) The expression of CD25 by $CD4^+$ $Foxp3^+$ Treg was monitored. Data is from 1 of 2 experiments with each experiment containing 5 mice per group. Average frequency ± SD are shown. Statistics were calculated using a two-way repeated measures ANOVA test with a Bonferroni post-test where * = $p<0.05$, ** = $p<0.01$ and *** = $p<0.001$.

4.3.7 IHC staining of tumour sections shows Treg and DC co-localise within tumours

Figures 4.1 to 4.8 show that both Treg and DC are present in tumours and that in the absence of Treg, tumours grow more slowly. It was of interest to investigate the possibility that Treg interact with DC within tumours and, therefore, have the opportunity to directly suppress DC. To examine this possibility, immunohistochemical (IHC) staining of sections using fluorescently labelled mAb was performed.

The fluorescence microscope used to identify cells by IHC staining was capable of distinguishing two fluorophores. Unfortunately, there is no single marker that can be used to definitively identify DC and cell types other than DC also express CD11c, however, DC express the highest level of CD11c (376). To assess the specificity of the CD11c antibody, a tumour section labelled using the appropriately matched FITC conjugated CD11c isotype control mAb (Figure 4.9A) was compared to a consecutive tumour slice that had been labelled with CD11c-FITC (Figure 4.9B). This was further confirmed by comparing the labelling of CD11b-bio-Str Alexa Fluor 555 and CD11c-FITC on the same tumour section (Figure 4.9C). A range of cells expresses CD11b, including granulocytes, immature myeloblasts and some DC subsets (354, 376). Overlaying the CD11c and CD11b stains showed some co-expression of the two markers as expected (Figure 4.9D). Cells that were positive for CD11c or CD11b alone did not co-localise indicating that these cells are unlikely to interact with each other (Figure 4.9D). It was decided that CD11c would be sufficient to define TIDC in this context because only the highest antibody expressing cells were easily discernible from background in these IHC stains, and a reasonable proportion of these cells appeared to co-express CD11b (Figure 4.9D).

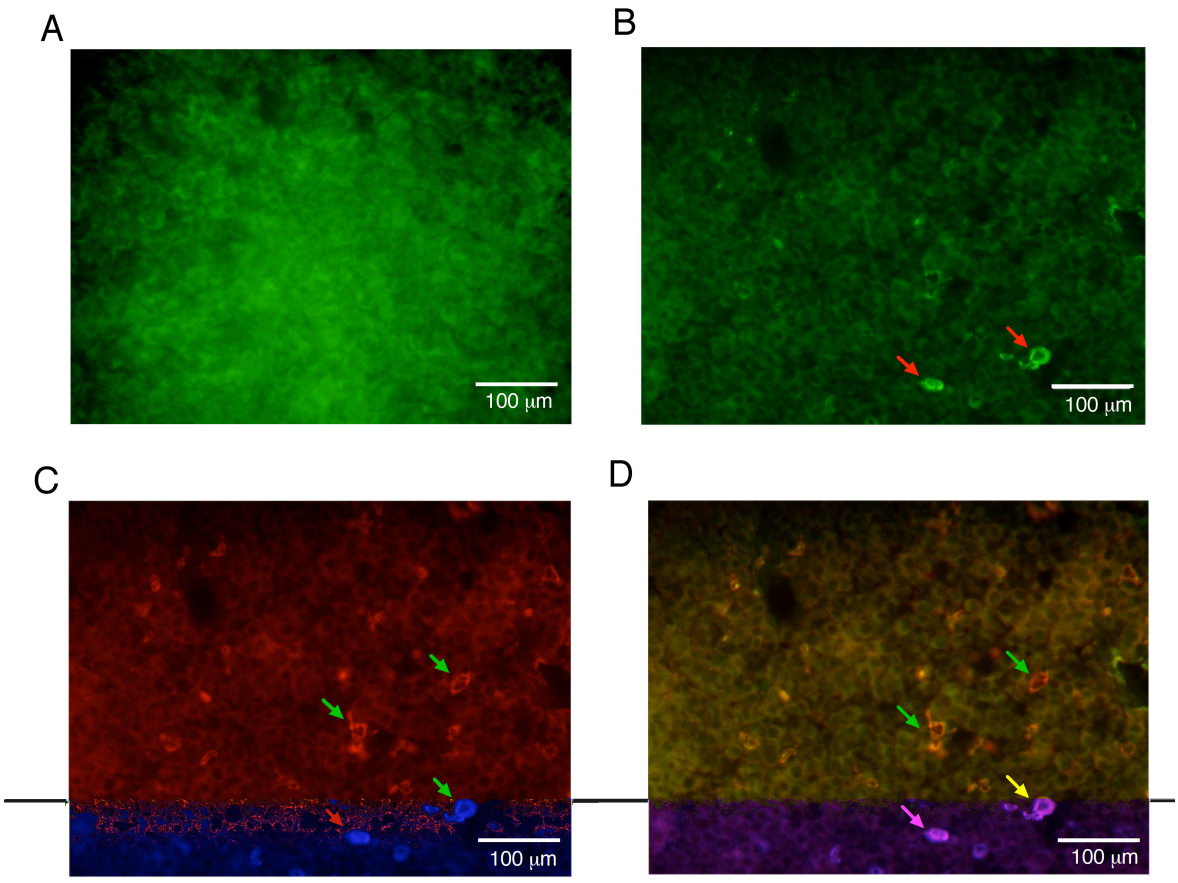

Figure 4.9: Fluorescent IHC analysis of B16.OVA tumour sections reveals the presence of DC.

B16.OVA tumours were excised from mice 14 days after inoculation, sliced into 20 μM thick sections and mounted in preparation for IHC staining. Consecutive sections were stained using mAb for either A) the appropriately matched FITC conjugated CD11c isotype control or B) CD11c-FITC (red arrows) and C) CD11b-bio-Str Alexa Fluor 555 (green arrows). D) Images of the CD11c-FITC and CD11b-bio-Str Alexa Fluor 555 mAb staining of the same section were overlayed to show co-localisation of the two markers (yellow arrows). Some CD11b-Alexa Fluor 555 single positive cells (green arrows) are also present.

Tumours are characterised by abnormal vasculature (167, 168) and necrotic areas, particularly in the centre of the tumour, leading to poor penetration of immune cells (167, 377). To determine if this leads to an uneven distribution of DC throughout the tumour section, whole tumour sections were examined by IHC staining.

The outermost layer of brightly stained cells (white circle Figure 4.10) was determined to consist of tumour stromal cells because they consistently showed a high proportion of mAb labelling, regardless of the mAb used (data not shown). Furthermore, under brightfield microscopy, these cells did not appear to be the characteristic black colour of the melanoma cells (data not shown). TIDC (CD11c-Alexa Fluor 555^{+} cells) were found just inside the stromal layer (white arrows) and exhibited lower levels of mAb labelling in comparison to the stromal layer, although they were still easily distinguishable from background. The tumours used in this experiment contained some DC deep within the tumour interior although most were found to reside around the tumour perimeter (Figure 4.10).

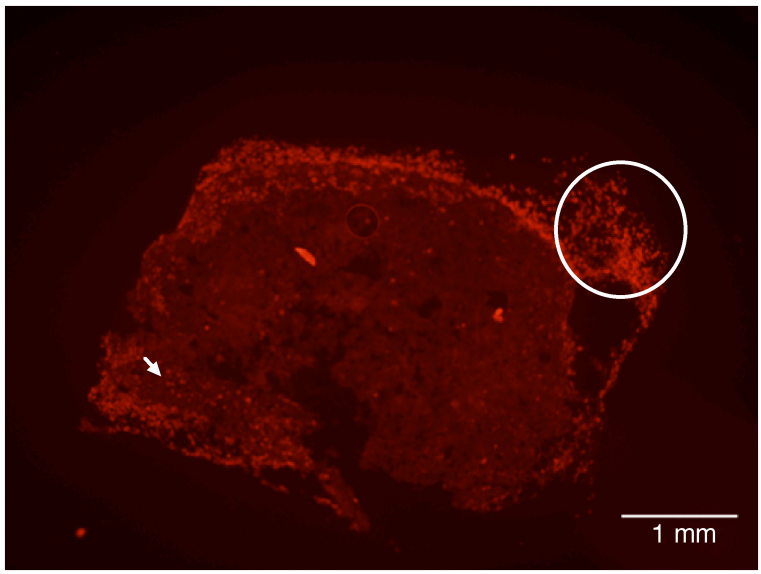

Figure 4.10: TIDC are found at the tumour perimeter.

Sections were prepared as in Figure 4.1 and stained using a CD11c-bio-Str Alexa Fluor 555 mAb. The white arrow indicated $CD11c^{+}$ DC. The white circle highlights non-specific binding of the mAb by the tumour stromal cells.

Foxp3 is accepted as the most definitive marker currently known for Treg (219). The presence of Treg within tumour tissue was therefore examined by labelling consecutive tumour sections with mAb for the appropriately matched FITC conjugated Foxp3 isotype

control (Figure 4.11A) and Foxp3-FITC (Figure 4.11B). Positive staining was only observed in the presence of the Foxp3-FITC antibody (Figure 4.11B). The specificity of the Foxp3 antibody was further confirmed by co-labelling the Foxp3-FITC labelled section with a CD4-bio-Str Alexa Fluor 555 mAb (Figure 4.11C). Foxp3 is a nuclear protein, while CD4 is mostly found at the cell surface so $CD4^+$ $Foxp3^+$ cells appear as a green nucleus surrounded by a red sphere and are found mostly around the tumour perimeter (Figure 4.11D).

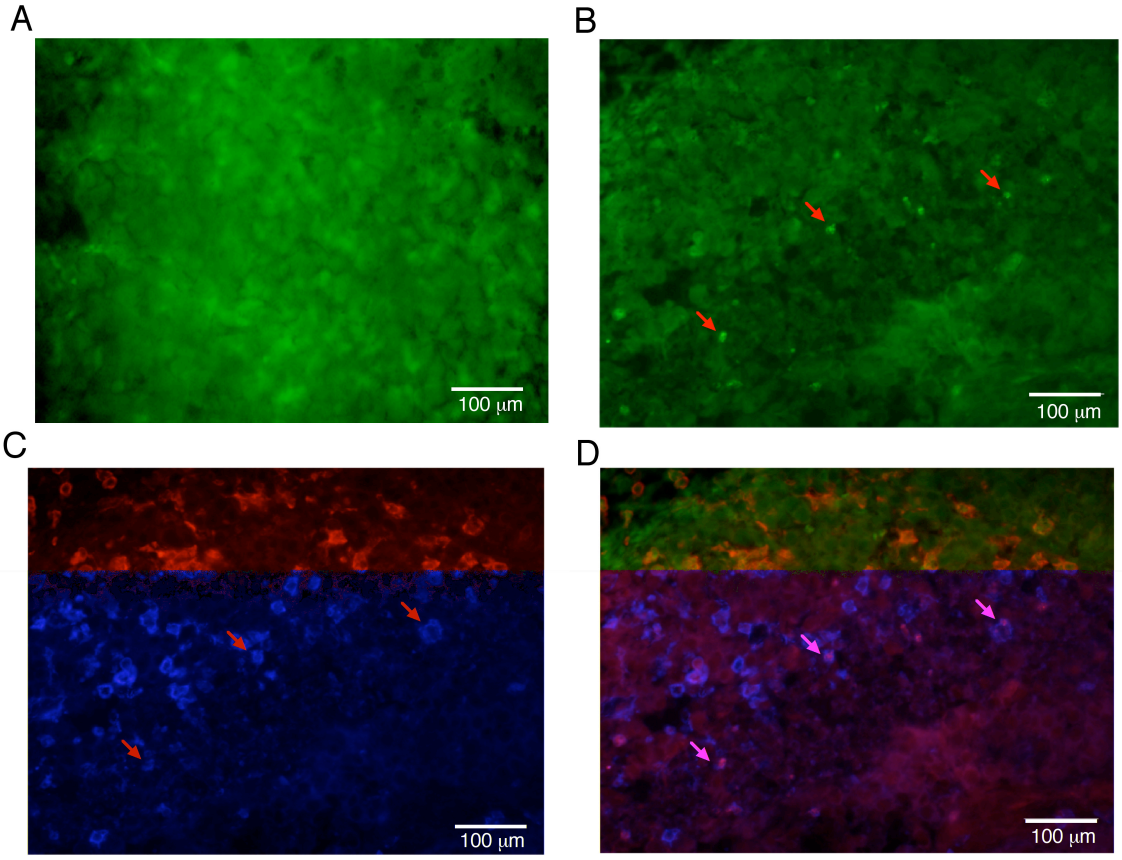

Figure 4.11: Fluorescent IHC analysis of B16.OVA tumour sections reveals the presence of Treg.

Consecutive tumour sections were prepared as in Figure 4.1 and stained using either A) the appropriately matched FITC conjugated Foxp3 isotype control or B) Foxp3-FITC (red arrows) and C) CD4-bio-Str Alexa Fluor 555 (green arrows). D) Images of the Foxp3-FITC and CD4-bio-Str Alexa Fluor 555 mAb staining of the same section were overlayed to show co-localisation of the two markers (yellow arrows).

The experiments shown in Figures 4.9 to 4.11 have validated that the CD11c and Foxp3 antibodies are specific and sufficient to define TIDC and Treg, respectively, in IHC labelling of sections. If Treg are responsible for suppressing TIDC, these cells must interact or at least come into close contact within the tumour (260, 264-266). The possibility of co-localisation of Treg and DC within tumours was therefore investigated using a combination of flow cytometry and IHC staining of tumour sections.

Large tumours were removed from mice ~17 days after inoculation and processed into single cell suspensions. Flow cytometric analysis of the suspensions showed that tumour resident Treg and DC occur at very low frequencies (Figure 4.12A). Despite this, analysis of tumour sections by IHC staining showed that an average of 13% of the Treg could be found co-localising with DC within the tumour (Figure 4.12B and D). This was far higher than the ~2.25% of total $CD4^+$ T cells found co-localising with DC (Figure 4.12C). To determine the percentage of the $CD4^+$ T cells found co-localising with DC that were actually Treg, the following calculations were performed:

W = proportion of Treg found co-localising with DC in tumours = 0.13 (Figure 4.12D)

X = proportion of $CD4^+$ cells that are Treg in tumours = 0.15 (Figure 4.7A)

Y = proportion of $CD4^+$ cells found co-localising with DC in tumours = 0.0225 (Figure 4.12C)

Z = percentage of $CD4^+$ T cells found co-localising with DC that were Treg

$$= \frac{W.X}{Y} \times 100 = \frac{0.13 \times 0.15}{0.0225} \times 100 = 87\%$$

Treg constitute ~15% of the $CD4^+$ population within tumours, however according to the above calculations, Treg constitute 87% of the $CD4^+$ cells that were found co-localising with DC in tumours. This is far higher than one could expect if this were chance alone.

Figure 4.12: Fluorescent IHC analysis of B16.OVA tumour sections shows the co-localisation of DC and Treg.

B16.OVA tumours were excised from mice ~17 days after inoculation. A) Tumour samples were analysed by flow cytometry for the frequency of $CD4^+$, $Foxp3^+$ Treg and $CD45^+$, $CD11c^{hi}$ DC within the live cell population. B) Sections were prepared as in Figure 4.1 and stained for Foxp3-FITC (B, red arrow) and CD11c-bio-Str Alexa Fluor 555 (B, green arrow). Images of the two antibodies from the same section within the white boxes were enlarged and overlayed to show co-localisation of the $CD11c^+$ DC and the $Foxp3^+$ Treg (B-white arrow). C) An overlay of a tumour section prepared as in Figure 4.1 and stained for CD4-FITC (orange arrow) and CD11c-bio-Str Alexa Fluor 555 (green arrow). The white circle indicates a $CD4^+$ T cell and a TIDC that are co-localising together. D) The frequency of $CD4^+$ T cell and $Foxp3^+$ Treg found co-localising with $CD11c^+$ DC was determined by scoring the numbers of cells occurring individually or co-localising with the DC. Data is an average of the frequencies obtained from IHC analysis of 2 tumour sections, from each of 2 different tumours or 4 sections in total.

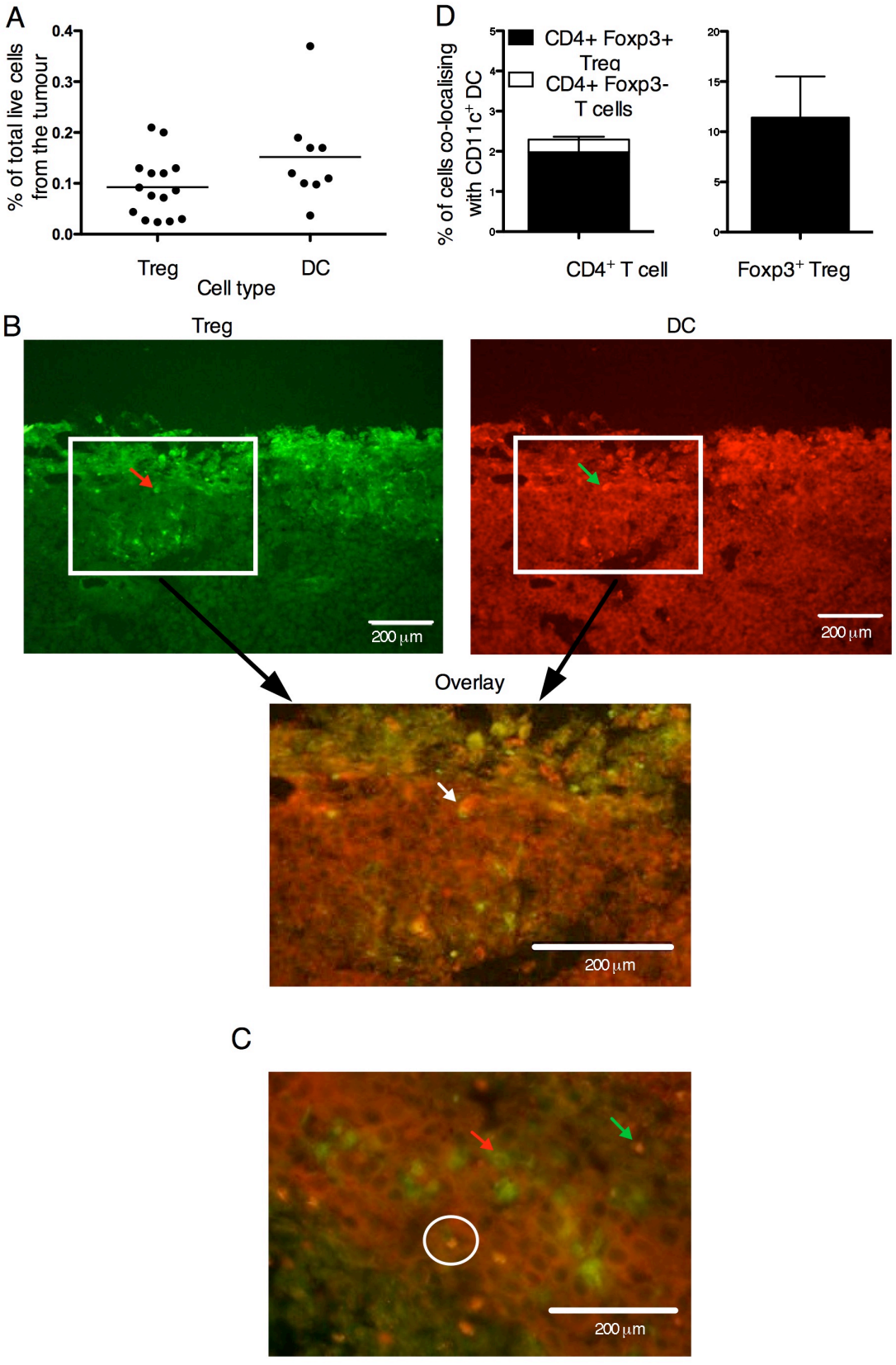
A
% of total live cells from the tumour
0.4
0.3
0.2
0.1
0.0
Treg
DC
Cell type
D
% of cells co-localising with CD11c+ DC
CD4+ Foxp3+ Treg
CD4+ Foxp3- T cells
5
4
3
2
1
0
CD4+ T cell
20
15
10
5
0
Foxp3+ Treg
B
Treg
DC
200 µm
200 µm
Overlay
200 µm
C
200 µm

4.4 Discussion

The purpose of the experiments described in this chapter was to investigate the possibility that Treg interact with DC within murine B16.OVA melanomas.

In order for an efficient immune response to be mounted, Ag bearing DC must migrate to the draining lymph node (156). It is possible that the inability of mice to control B16.OVA growth may be explained by results described in this thesis showing that there is no increase in the frequency of DC in the tumour draining lymph node. This data, combined with the large frequency of DC observed in the tumour and the similar sizes of the draining and non draining lymph nodes may suggest that the DC are migrating inefficiently to the draining lymph node. This possibility is supported by studies that show that treatments that improve DC maturation status and migration to the lymph node are effective anti-tumour immunotherapies (156, 378).

Previous studies have further suggested that Treg may interfere with DC migration to the draining lymph node in both a tumour (156) and an inflammation (379) model. To examine this possibility, the effect of Treg on DC frequency, phenotype and function in tumours and lymph nodes was assessed. Treg were found in high frequencies even in very small tumours (as small as $8mm^2$) and the frequency continued to increase as the tumours increased in size. These Treg were assumed to be fully functional based on their expression of CD25 and on their ability to suppress CD4 T cell proliferation *in vitro*. The accumulation of Treg from a very early time point in tumour growth would indicate that immunosuppression by Treg has an important early role in the B16.OVA tumour evading the immune response and becoming established. Studies in which Treg frequency showed a neutral (380) or positive (381) correlation with clinical outcome may have been subject

to various confounding issues. These studies were conducted in humans where Foxp3 staining can be ambiguous and may even be the result of confusion due to the transient expression of Foxp3 by newly activated $CD4^+$ T effector cells (245), which would account for the positive correlation with Treg. Individuals with fast growing tumours may not have sufficient time to mount an anti-tumour response, regardless of the presence or absence of Treg resulting in a neutral correlation with Treg.

There are a number of possibilities that could influence the accumulation of Treg in tumours: trafficking of Treg out of other tissues and into the tumour, conversion of $CD4^+$ $Foxp3^-$ T cells to $CD4^+$ $Foxp3^+$ Treg, or thymic production of Treg. It is unlikely that large numbers of Treg traffic from other tissues to the tumour since no increase in peripheral Treg levels were seen in tumour bearing mice. It is possible that some Treg are converted from $CD4^+$ $Foxp3^-$ T cells because the tumour environment is known to have high levels of TGF-β, which can be produced in small amounts by the tumour cells themselves or in larger amounts by Treg (382) and immature myeloid DC (383). TGF-β and IL-2 are known to drive the conversion of $Foxp3^-$, $CD4^+$ T cells to $Foxp3^+$ Treg *in vivo* (235, 384, 385), while TGF-β alone can stimulate proliferation of $CD4^+$ $Foxp3^+$ Treg.

It is most likely, however, that the Treg that accumulate in the tumour come from the natural pool of thymically produced Treg and are not the result of conversion from $CD4^+$ $Foxp3^-$ T cells. This possibility is supported by work showing that the majority of Treg that accumulate in tumours are the result of proliferation of natural Treg and not the conversion of $CD4^+$ $Foxp3^-$ cells to Treg (383, 386). The authors showed this by adoptively transferring a 10 to 1 ratio of Thy1.1 $CD4^+$, $CD25^-$ T cells and $Thy1.2^+$ $CD4^+$ $CD25^+$ Treg together into Balb/c SCID mice, which have no T or B cells of their own. After challenging the mice with the fibrosarcoma CMS-5, $CD4^+$ $CD25^+$ Treg were found to

constitute 30-50% of the tumour infiltrating lymphocytes in the developing tumours indicating the Treg population had expanded. However, 80% of the Treg were found to express the Thy1.2 marker. The Authors suggest this data indicates that the majority of the Treg present were the result of proliferation of the transferred Treg rather than conversion of the Thy1.1$^+$ CD4$^+$ CD25$^-$ T cells into Treg (386), however, proliferation of the Treg was not directly assayed. It is, therefore, possible that the high level of Thy1.2$^+$ CD4$^+$ CD25$^+$ Treg found in the tumour were the result of differential tissue homing of the Thy1.1$^+$ CD4$^+$ CD25$^-$ T cells and the Thy1.2$^+$ CD4$^+$ CD25$^+$ Treg. A further study using the B16.F10 melanoma model in C57BL/6 mice showed that CD4$^+$ CD25$^+$ Treg can incorporate BrdU while in the tumour in response to TGF-β produced by immature myeloid DC (383). This shows that Treg are actively proliferating in the tumour, and that the local proliferation of thymically produced Treg is the main method of Treg accumulation in the tumour. In contrast to those studies, one study using the CT26 tumour model in Balb/c mice has shown that reconstituted Treg are mainly the result of tumour driven conversion of Thy1.1$^+$ CD4$^+$ CD25$^-$ T cells into CD4$^+$ CD25$^+$ Treg and does not require CD4$^+$ CD25$^+$ Treg to be produced by the thymus (240). However, this study only transferred CD4$^+$ CD25$^-$ T cells and so it cannot compare this rate of Treg reconstitution to that seen as the result of proliferation of existing Treg.

In order to be able to study aspects of the immune response in the absence of Treg, mice were treated with the anti-CD25 mAb PC61. Little benefit to the level or duration of Treg depletion was found in administering more than 100 μg PC61 in a single injection. However, two 100 μg doses of PC61 were required to show a significant delay in tumour growth. For this reason, in all further experiments mice were given two 100 μg doses of PC61 three days apart before tumour inoculation to achieve maximal Treg depletion and delayed tumour growth. Using this treatment regime, it was determined that the Treg

population remained significantly depleted even when the tumours reached the maximum size. A similar time course of Treg reconstitution was also observed in non-tumour bearing mice. These results indicate that the presence of tumours did not accelerate the reconstitution of the peripheral Treg population despite the fact that tumours have been reported to produce TGF-β (180, 182), which promotes the conversion of $CD4^+$ $Foxp3^-$ T cells to Treg.

The $Foxp3^+$ Treg population that persisted after PC61 treatment lacked CD25 expression. While Treg isolated from IL-2-/- or IL-2Rα-/- mice still show suppressive function *in vitro* (223, 387), it has been shown that the down regulation of CD25 expression by Treg results in a loss of suppressive function by these cells *in vivo* (311). These cells were able to recover to normal levels of CD25 expression by the end of the experiments performed in this thesis, however, these cells represented only 30-50% of the Treg population. At the endpoint of the experiments conducted in this thesis, therefore, a significant reduction in tumour size and the frequency of Treg in the blood, lymph nodes and tumours of PC61 treated mice was still evident.

Two-photon intravital microscopy has been used to show that Treg and DC interact within lymph nodes resulting in a decreased interaction time between DC and $CD4^+$ T cells (275). Using IHC staining of tumour sections, experiments within this thesis showed that a high proportion of Treg and DC could be found co-localising within the tumour periphery. IHC methods cannot definitively show that the cells are interacting within the tumour tissue. However, the high frequency of Treg and DC found co-localising within the tumour indicates that the cells have ample opportunities to interact with one another.

It is possible that the co-localisation of TIDC and Treg would allow the Treg to suppress the TIDC. It has also been suggested, using an allograft model, that activation of the Treg

by tissue resident DC is necessary for the Treg to become functional, migrate to the lymph node and suppress the immune response (388). The activation of Treg might therefore explain the co-localisation of TIDC and Treg observed in this chapter. Both of these possibilities would result in a suppressed anti-tumour immune response.

4.5 Conclusions

The experiments performed in this chapter clearly show that B16.OVA melanomas grow faster in the absence of Treg. Treg and DC were found to co-localise within tumours at a rate far higher than could be expected by random chance alone suggesting that these cells may in fact, interact within the tumour tissue.

CHAPTER FIVE

TREG DO NOT AFFECT DC FREQUENCY, PHENOTYPE OR FUNCTION IN A MURINE MELANOMA MODEL

5.1 Introduction

The experiments described in Chapter 4 showed that Treg are present in murine B16.OVA melanomas and that they are functional as demonstrated by their ability to suppress $CD4^+$ T cell proliferation *in vitro* and by the decreased rate of tumour growth in mice that were treated with PC61 to deplete Treg. Treg and DC were also found to co-localise in the tumour periphery suggesting that these cells interact.

Two possibilities exist to explain why Treg and DC interact in the tumour. A recent study using an allograft model has suggested that Treg are activated by DC in the tissue and then traffic to the draining lymph node where they suppress the T cell response to the allograft (388). Alternatively, the Treg could be inhibiting the activation of the DC and impairing the ability of the DC to stimulate a T cell response in the draining lymph node. As discussed in detail in the general introduction, *in vitro* studies (273, 274) and an *in vivo* NOD mouse model (272) have shown that the expression of DC activation markers CD40, CD80, CD86 and MHC II is reduced in the presence of Treg. To date, no studies have shown whether Treg play a significant role in suppressing DC in the tumour micro-environment where other suppressive factors such as IL-10, TGF-β (180) and myeloid derived suppressor cells (389) are also present .

5.2 Aims

The purpose of the experiments described in this chapter was to investigate the effects of Treg on DC frequency, phenotype and function. The murine B16.OVA melanoma model was used because previous studies from our laboratory showing TIDC function is inefficient also used this model. In addition, tumour specific T cell responses could be analysed because of the existence of OVA specific TCR transgenic mice. It was hypothesised that in the absence of Treg, host DC would be more effective at mounting an effective anti-tumour immune response.

The specific aims were:

- To investigate the effects of Treg on DC frequency and phenotype in tumours and lymph nodes
- To determine if Treg affect the ability of DC to elicit an anti-tumour T cell response either *ex vivo* or *in vivo*

5.3 Results

5.3.1 Flow cytometric analysis shows that Treg do not affect DC frequency in tumours or lymph nodes

Figure 4.11 showed that PC61 treatment delayed tumour growth, presumably because of an improved anti-tumour immune response. The following experiments were designed to investigate if the improved anti-tumour response observed in PC61 treated mice was the result of an increase in the migration of DC from the tumour to the tumour draining lymph node. To address this possibility, the frequency of DC in the tumour and lymph nodes was assessed.

Tumours were excised from PC61 treated and untreated mice 17 days after tumour inoculation, processed into single cell suspensions, and the number of DC was determined by flow cytometry. The number of DC per mg of tumour tissue was found to be similar in PC61 treated (depleted) and untreated (non-depleted) mice (Figure 5.1A). It was shown in Figure 4.7, however, that PC61 treated mice have smaller tumours at the later stages of growth. To investigate whether differences in tumour size between Treg depleted and non-depleted groups affected the frequency of DC per mg of tumour tissue, the frequency of TIDC was compared using size matched tumours from PC61 treated and untreated mice. Mice were inoculated with tumour 1-7 days apart so that tumours of a range of sizes could be compared by flow cytometry on the same day. When the number of TIDC per mg of tumour tissue was analysed according to tumour size, no difference was found between the PC61 treated and untreated mice (Figure 5.1B). For further experiments it was meaningful to compare DC at day 17-19 because at this time, the difference in tumour sizes between PC61 treated and untreated mice was most apparent (Figure 4.7) and there was still a significant reduction in the blood, lymph node and intratumoral Treg frequency (Figure

4.7). No difference in the frequency of DC within the $CD45^+$ population (Figure 5.1C) was observed in tumours or tumour draining and non-draining lymph nodes regardless of PC61 treatment. Furthermore, no difference in the frequency of DC was observed between the draining and non-draining lymph nodes of the same animal. Total cell numbers of the lymph nodes was not assessed, however, the draining lymph node did not appear to be bigger than the non-draining lymph node. This suggests that the frequency of DC in the draining lymph node was not significantly increased because there was no increase in the migration of DC to the draining lymph node in response to the presence of tumour.

The similar DC frequency found in the draining and non-draining lymph nodes (Figure 5.1) suggests that there is no significant migration of DC to the tumour draining lymph node irrespective of pre-treatment with PC61. To further investigate this possibility, the expression of CCR7 by tumour infiltrating and lymph node DC was investigated. CCR7 is an important lymph node homing chemokine receptor (390, 391) expressed at low levels on circulating T cells and DC and must be upregulated for cells to home to the lymph node. Treg mediated suppression of DC migration may therefore be reflected in changes in CCR7 expression by DC.

Expression of CCR7 by tumour infiltrating and lymph node DC was examined in PC61 treated and untreated mice ~17 days after tumour inoculation. CCR7 was expressed by very few TIDC (Figure 5.2A and B) and at very low levels (Figure 5.2C). No difference in CCR7 expression by TIDC was observed between PC61 treated and untreated mice. In the lymph node, however, a moderate number of DC expressed a low amount of CCR7 (Figure 5.2D-F). PC61 treatment appeared to slightly decrease CCR7 expression by lymph node DC. These results further show that the delay in tumour growth caused by PC61 treatment

is unlikely to be the result of an increase in DC migrating to the lymph node, and the consequent immune response.

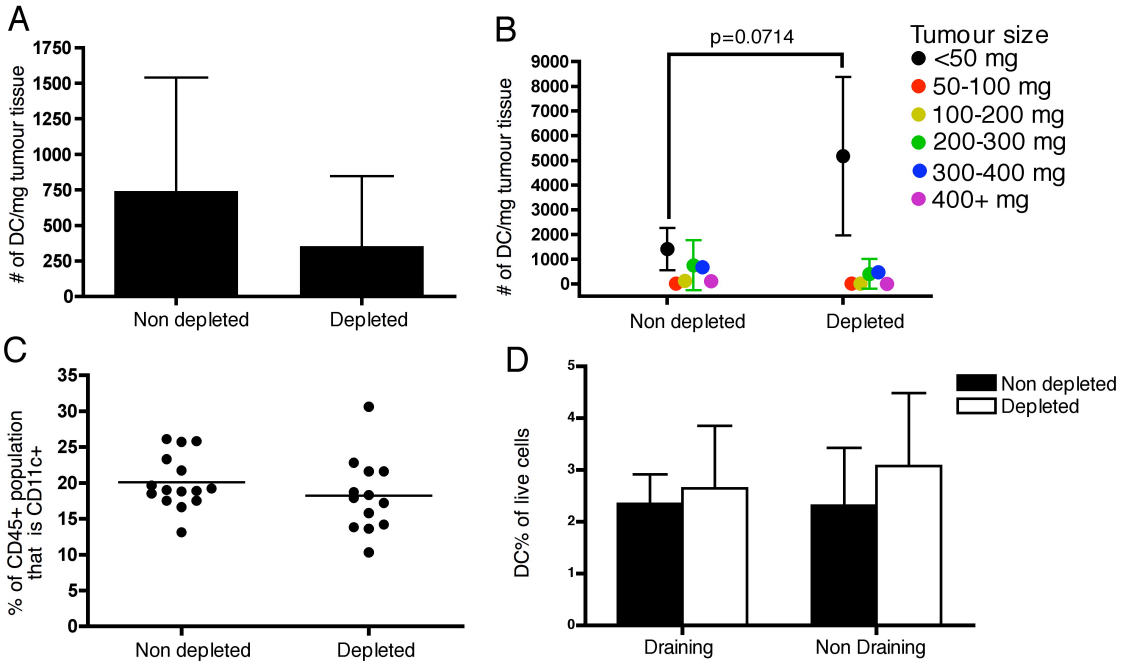

Figure 5.1: Treg do not affect DC frequency in tumours or lymph nodes.

C57BL/6 mice were depleted of Treg using two 100ug doses of PC61 or left non-depleted, as shown in Figure 4.7B, and inoculated with 10^5 B16.OVA cells. Tumours were excised from mice 10-17 days after tumour inoculation and analysed by flow cytometry. A) The number of DC per mg of tumour tissue at day 17 after tumour inoculation was compared. Bars show the average number of DC + SD for pooled data from 2 experiments each with 3-4 mice per group. B) Mice were inoculated with tumour 1-7 days apart to generate tumours of various sizes on the same day. Tumours were excised 10-17 days after tumour inoculation, divided into groups according to size and analysed for DC number per mg of tumour tissue. Bars show the average number of DC $\pm$ SD for pooled data from 2 experiments each with 3-4 mice per group. C) The frequency of TIDC within the $CD45^+$ population was compared in PC61 treated and untreated mice 17 days after tumour inoculation. The graph is a compilation of data from 3 experiments, each with 4-5 mice per group. Each dot represents one mouse. D) Lymph nodes were also excised at day 17 after tumour inoculation and analysed for the frequency of DC within the live population. Bars show the mean + SD. Data is a compilation of 3 experiments each with 5 mice per group.

Figure 5.2: PC61 treatment may decrease the expression of CCR7 by DC in the lymph node but not the tumour.

C57BL/6 mice were depleted of Treg using two 100ug doses of PC61 or left non-depleted, as shown in Figure 4.7B, and inoculated with 10^5 B16.OVA cells. Tumours and lymph nodes were excised from mice ~17 days after tumour inoculation and analysed by flow cytometry for the expression of CCR7 by all $CD11c^{high}$ DC. A) A representative histogram showing the percent of TIDC expressing CCR7 (solid black line) in comparison to the appropriately matched isotype control (grey filled histogram). The percentage of $CD11c^{high}$ TIDC expressing CCR7 (B) and the MFI of $CD11c^{high}$ TIDC expressing CCR7 (C) was compared in PC61 treated and untreated mice. D) A representative histogram showing the percent of lymph node DC expressing CCR7 (solid black line) in comparison to the appropriately matched isotype control (grey filled histogram). The percentage of $CD11c^{high}$ lymph node DC expressing CCR7 (E) and the MFI of $CD11c^{high}$ lymph node DC expressing CCR7 (F) was compared in PC61 treated and untreated mice. Results are from one experiment with 5 mice per group. Bars show the mean +SD and values of *p* were calculated using an unmatched two-way ANOVA test with a Bonferroni post-test.

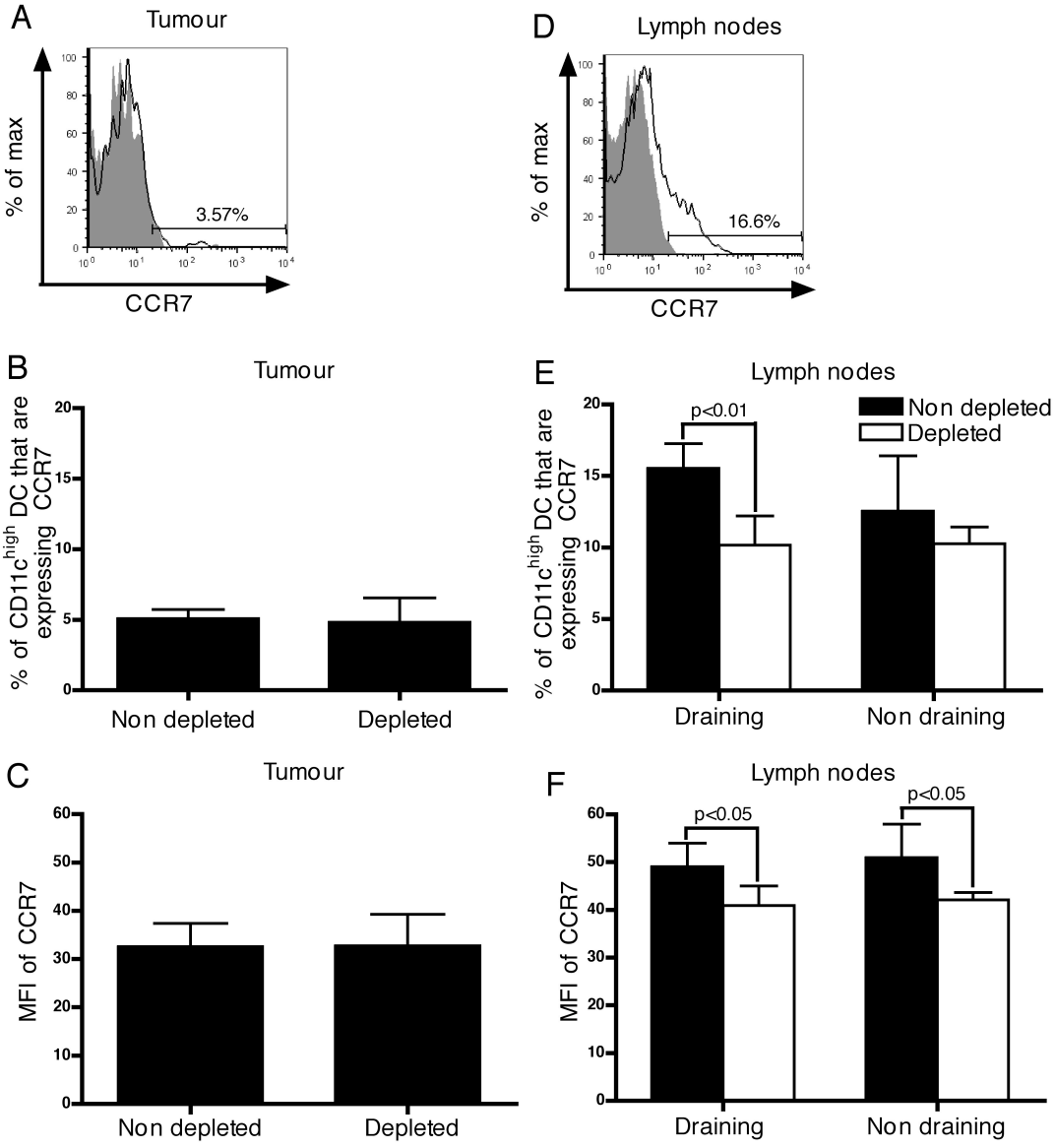
A
Tumour
% of max
3.57%
CCR7
D
Lymph nodes
% of max
16.6%
CCR7
B
Tumour
% of CD11c^high DC that are expressing CCR7
Non depleted
Depleted
E
Lymph nodes
p<0.01
Non depleted
Depleted
% of CD11c^high DC that are expressing CCR7
Draining
Non draining
C
Tumour
MFI of CCR7
Non depleted
Depleted
F
Lymph nodes
p<0.05
p<0.05
MFI of CCR7
Draining
Non draining

5.3.2 Flow cytometry analysis shows Treg do not affect DC phenotype in tumours or lymph nodes

The cell surface molecules CD40, CD86 and MHCII are maturation markers of DC and were found, by other Authors, to be altered in *in vitro* cultures of DC (272-274) in the presence or absence of Treg. It was therefore relevant to investigate the maturation status of DC in the B16.OVA model and the effects of Treg thereon.

Expression of CD40, CD86 and MHC II on TIDC was examined by flow cytometry in comparison to isotype or fluorescence minus one (FMO) controls. The results showed that while most of the DC were mature, the $CD11b^+$ subpopulation (Figure 5.3A) appeared to be more mature than the $CD11b^-$ subpopulation (Figure 5.3B) and the $CD11b^+$ subpopulation might, therefore, be expected to migrate to the lymph node. Based on these findings, the following experiments show only the results for the $CD11b^+$ DC subset and were designed to investigate the effect of Treg depletion on the phenotype of intratumoral and lymph node DC *in vivo*.

Expression of the maturation markers CD40, CD86 and MHCII by TIDC was examined in PC61 treated and untreated mice ~17 days after tumour inoculation. All markers were expressed on a similar number of cells (Figure 5.4A) and in similar amounts (MFI) on TIDC from both PC61 treated and non-treated mice (Figure 5.4B). This indicates the phenotype of TIDC is unaffected by Treg in the murine B16.OVA melanoma model.

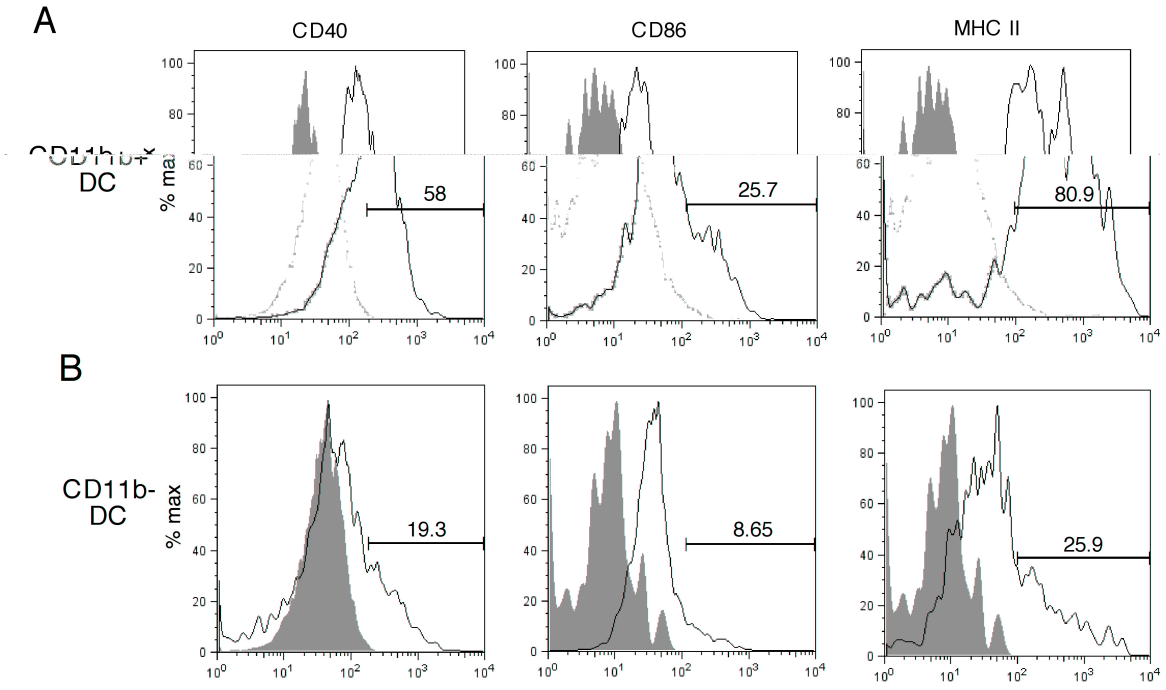

Figure 5.3: Analysis of the phenotype of TIDC by flow cytometry.

Tumours were excised from C57BL/6 mice ~17 days after tumour inoculation and analysed by flow cytometry. $CD45^{+}$, $CD11c^{high}$ DC were segregated into $CD11b^{+}$ (A) and $CD11b^{-}$ (B) subpopulations that were then analysed for CD40, CD86 and MHC II expression. Fluorescence-minus-one controls (CD40) and appropriately matched isotype controls (CD86 and MHC II) are shown as grey filled histograms, while empty histograms show the level of expression of the various markers. Numbers on the graphs represent the percentage of cells expressing the relevant markers.

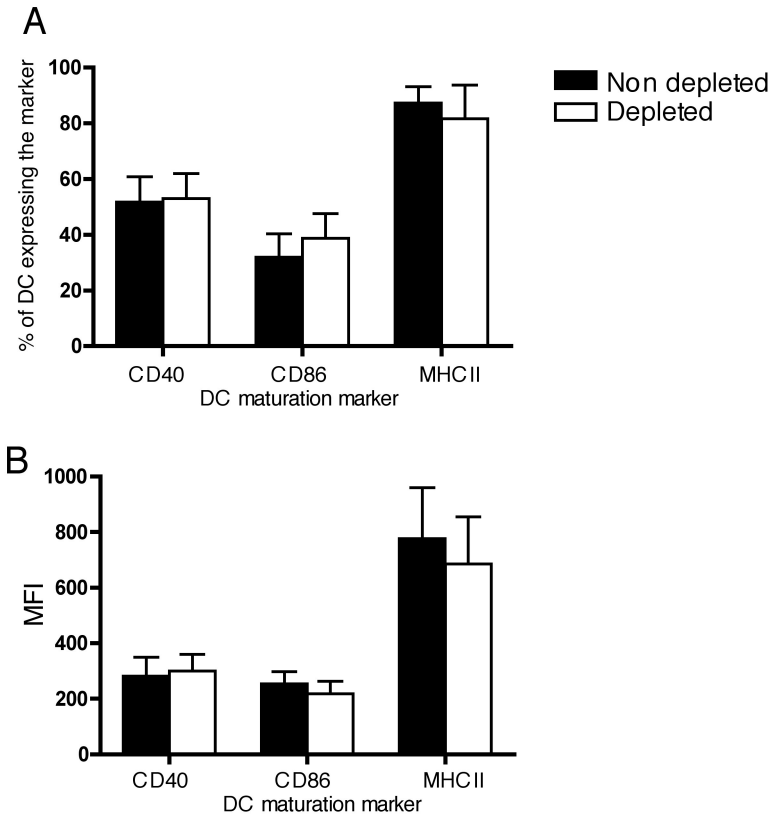

Figure 5.4: Treg do not affect the expression of activation markers by TIDC.

C57BL/6 mice were depleted of Treg using two 100ug doses of PC61 or left non-depleted, as shown in Figure 4.7B, and inoculated with 10^5 B16.OVA cells. Tumours were excised from mice ~17 days after tumour inoculation and analysed by flow cytometry. The percentage (A) and MFI (B) of TIDC expressing the indicated maturation markers was compared between Treg depleted and non-depleted mice. The MFI values were calculated only for the cells that showed positive staining for the relevant marker as defined in A. Bars show the average + SD of a compilation of 3 independent experiments with 5 mice per group.

The activation status of the DC found in the lymph node was also examined because DC prime T cells in the lymph node. DC from the lymph nodes of the mice described in Figure 5.4 were examined for expression of the DC maturation markers CD40, CD86 and MHC II. An increased frequency of DC expressing CD86 was observed in both the PC61 treated and untreated tumour bearing mice in comparison to the naïve control (Figure 5.5B). The DC of PC61 treated and untreated mice were also found to be expressing more CD86 and MHC II as indicated by an increase in MFI values (Figure 5.5B and C). No change in CD40 expression, or the percentage of DC expressing MHCII was observed (Figure 5.5A and C). These data indicate that the lymph node DC from tumour bearing mice are only moderately mature but that the maturation status of these DC is unaffected by Treg.

Figure 5.5: Treg do not affect the expression of activation markers by CD45^{+} CD11c^{high} DC in lymph nodes.

C57BL/6 mice were depleted of Treg using two 100ug doses of PC61 or left non-depleted, as shown in Figure 4.7B, and inoculated with 10^5 B16.OVA cells. Lymph nodes were excised from mice ~17 days after tumour inoculation and analysed by flow cytometry. The percentage and MFI of DC expressing CD40 (A), CD86 (B) and MHCII (C) were compared in the tumour draining and non-draining lymph nodes from Treg depleted and non-depleted mice. The MFI values were calculated only for the cells that showed positive staining for the relevant marker. Values for lymph nodes from non-tumour bearing mice were included as controls. Bars show the average + SD of a compilation of 3 independent experiments with 5 mice per group per experiment. Values of *p* were calculated using a non-parametric one-way ANOVA test with a Dunn's multiple comparison post-test.

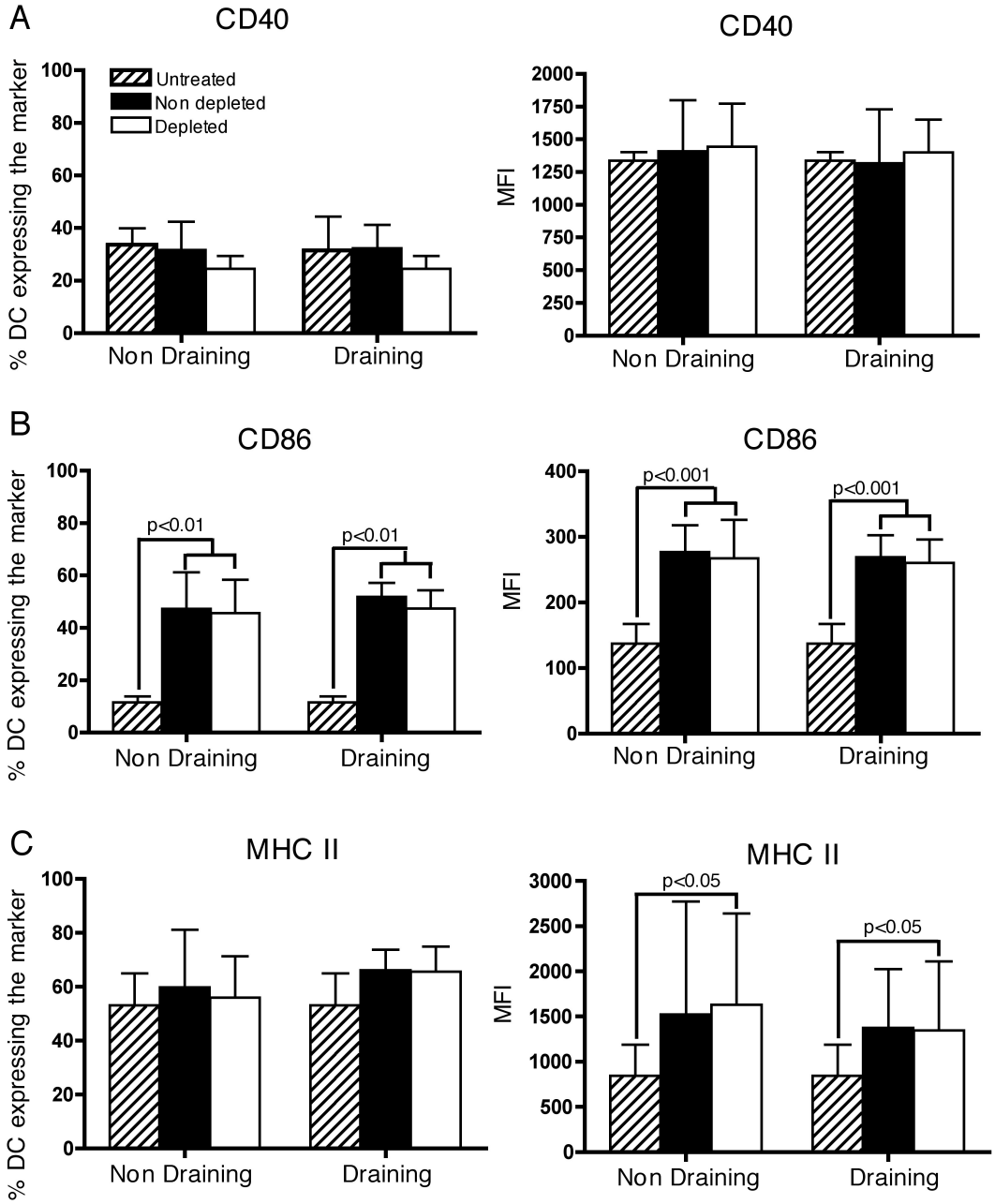
A
CD40
% DC expressing the marker
Untreated
Non depleted
Depleted
Non Draining
Draining
CD40
MFI
Non Draining
Draining
B
CD86
% DC expressing the marker
p<0.01
p<0.01
Non Draining
Draining
CD86
MFI
p<0.001
p<0.001
Non Draining
Draining
C
MHC II
% DC expressing the marker
Non Draining
Draining
MHC II
MFI
p<0.05
p<0.05
Non Draining
Draining

5.3.3 Treatment with PC61 does not affect the ability of TIDC to stimulate T cell proliferation ex vivo

Figures 5.1 to 5.5 have shown that Treg do not affect DC frequency or phenotype, however, it is still possible that Treg may affect DC function. To evaluate the function of TIDC, B16.OVA tumour samples were enriched for $CD45^+$ cells by positive automacs separation and sorted by FACS to isolate a highly pure (>96%) $CD45^+$ $CD11c^+$ TIDC population. These TIDC were used to stimulate the proliferation of OVA specific $CD4^+$ (OTII) and $CD8^+$ (OTI) T cells *in vitro*. To test the presentation of tumour Ag taken up by DC within the tumour, no further Ag was added to the assay except in the positive controls.

In the absence of added Ag, sorted DC were unable to stimulate proliferation of OVA specific OTII T cells (Figure 5.6A) and induced only minimal proliferation of OVA specific OTI T cells (Figure 5.6B). The low proliferation of OTI T cells was not Ag specific, as it has been observed even when DC were prepared from B16 tumours not expressing OVA (366). When TIDC were prepared from the tumours of Treg-depleted mice, no increase in the proliferation of OTI or OTII T cells could be observed (Figure 5.6A and B). In fact OTI T cell proliferation was significantly decreased when stimulated with DC from the tumours of Treg-depleted mice (Figure 5.6B). This is unlikely to be due to a direct adverse effect of PC61 on DC function because although CD25 is expressed on 20-30% of DC, it is only expressed at low levels (392). Furthermore, since the proliferation of OTI T cells is not thought to be Ag specific (366), the difference observed between DC from PC61 treated and untreated tumour bearing mice was not considered to be of consequence. Although TIDC were unable to present OVA Ag taken up within the tumour context, they appeared functional because they were able to stimulate T cell proliferation in the presence of specific peptide (Figure 5.6A and B). As a further test of

DC function, TIDC were used to stimulate the proliferation of allogeneic BALB/c T cells *in vitro*. TIDC from the tumours of Treg-depleted or non-depleted mice were both able to induce T cell proliferation, and Treg depletion did not improve this response (Figure 5.6C). The unpulsed TIDC control was not able to be included in these experiments due to the poor yield, however, this is not expected to influence the conclusion that the T cell proliferation observed was not Ag specific. These results suggest that while the TIDC may be able to present a range of Ag, presentation of tumour specific Ag is poor and is not improved by the depletion of Treg.

5.3.4 Treg do not irreversibly impair the ability of TIDC to take up, process or present tumour protein

To examine if the impaired *in vitro* T cell expansion seen in Figure 5.6 was due to an inability of the TIDC to take up and process proteins, TIDC were sorted by FACS from the day 17 tumours of PC61 treated and untreated mice. These TIDC were incubated with OVA specific peptide or OVA protein, washed to remove excess Ag, and used to stimulate OTII (Figure 5.7A) and OTI (Figure 5.7B) T cell proliferation *in vitro*. TIDC incubated with peptide were able to stimulate a high level of Ag specific T cell proliferation (Figures 5.6 and 5.7) indicating they were functional. When incubated with OVA protein, TIDC were also able to stimulate Ag specific OTII and OTI T cell proliferation indicating that these TIDC have not lost the ability to take up, process and present protein. The level of T cell proliferation was much lower in response to protein compared to peptide, however, this may be due at least in part to the short incubation time with the protein. No difference in T cell proliferation was observed between TIDC from PC61 treated or non-treated mice (Figure 5.7). These results show that prior exposure to Treg does not impair the ability of TIDC to take up, process and present Ag to $CD4^+$ or $CD8^+$ T cells.

Figure 5.6: Treg depletion does not affect the ability of TIDC to stimulate T cell proliferation *ex vivo*.

C57BL/6 mice were depleted of Treg using two 100ug doses of PC61 or left non-depleted, as shown in Figure 4.7B, and inoculated with 10^5 B16.OVA cells. Tumours were excised ~17 days later and processed into single cell suspensions. $CD45^+$ $CD11c^{high}$ TIDC were sorted and titrated into cultures containing 2 $x10^5$ T cells, and specific Ag where indicated. ^3H thymidine was added to the samples for the final 18 hours of the 3-day culture. Proliferation was determined as the counts (of ^3H thymidine) per minute (cpm). (**A**) OTII T cell proliferation; specific peptide was used as a positive control and loaded on 10^3 TIDC/well before co-culture with T cells. (**B**) OTI T cell proliferation; specific peptide was used as a positive control and loaded on 10^3 TIDC/well before co-culture with T cells. (**C**) Allogeneic T cell proliferation. Each graph is from one of 3 independent experiments containing 2-3 samples per group that gave similar results. Average ± range is shown and *p* was calculated using a two-way ANOVA test (excluding the +Ag groups) with a Bonferroni post-test.

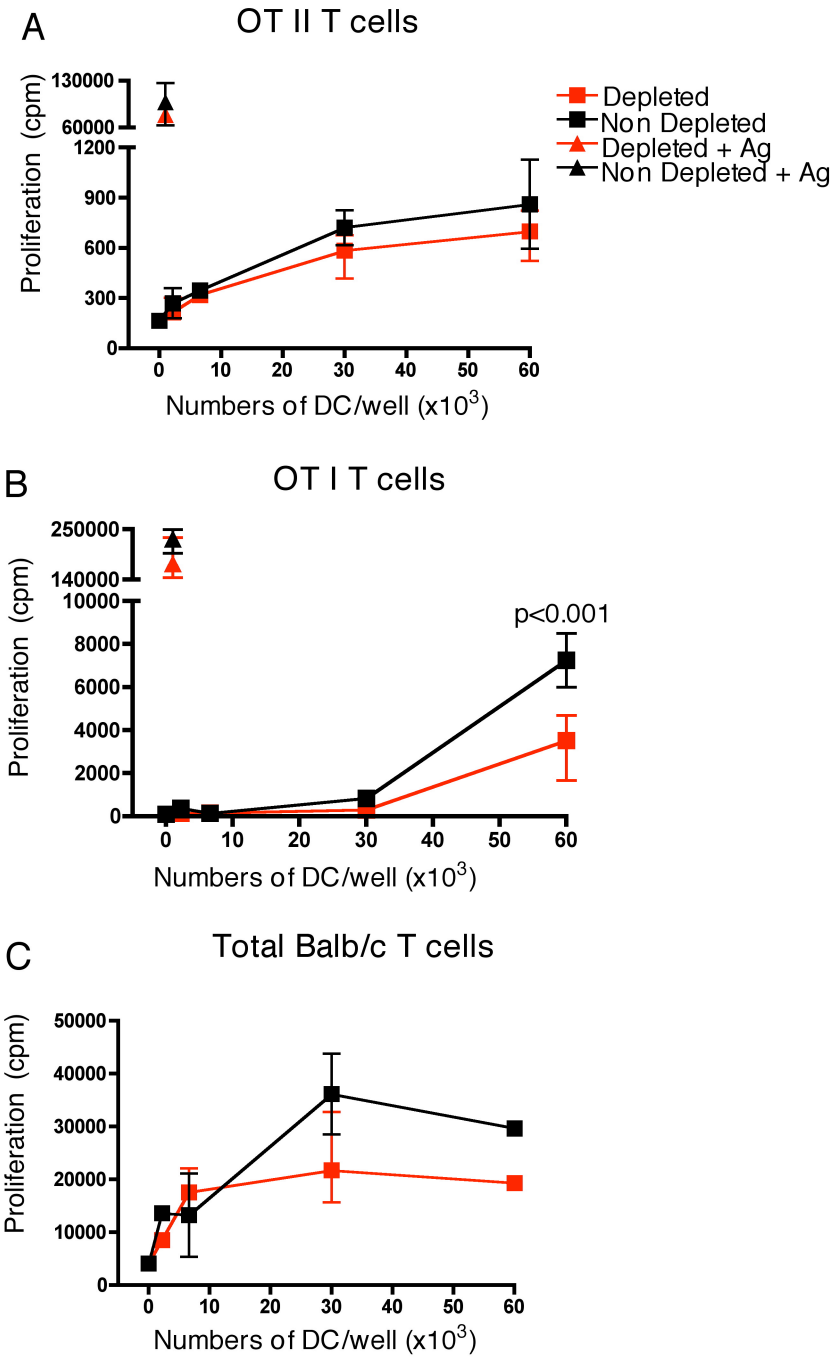
A
OT II T cells
Proliferation (cpm)
130000
60000
1200
900
600
300
0
0 10 20 30 40 50 60
Numbers of DC/well (x10^3)
Depleted
Non Depleted
Depleted + Ag
Non Depleted + Ag
B
OT I T cells
Proliferation (cpm)
250000
140000
10000
8000
6000
4000
2000
0
p<0.001
0 10 20 30 40 50 60
Numbers of DC/well (x10^3)
C
Total Balb/c T cells
Proliferation (cpm)
50000
40000
30000
20000
10000
0
0 10 20 30 40 50 60
Numbers of DC/well (x10^3)

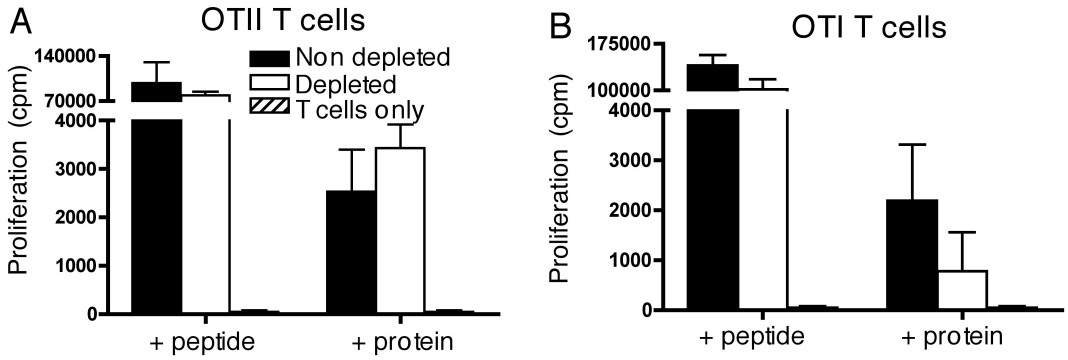

Figure 5.7: TIDC are capable of taking up, processing and presenting Ag.
C57BL/6 mice were depleted of Treg using two 100ug doses of PC61 or left non-depleted, as shown in Figure 4.7B, and inoculated with 10^5 B16.OVA cells. Tumours were excised from mice ~17 days after tumour inoculation and processed into single cell suspensions. $CD45^+$ $CD11c^{high}$ TIDC were sorted and incubated with 1 μg/ml specific peptide (1 hour) or 1 mg/ml OVA protein (2 hours) where indicated. The DC (3 $x10^3$/well) were then washed and incubated with 2 $x10^5$ Ag specific T cells for 3 days. ^3H thymidine was added to the samples for the final 18 hours of culture. Proliferation was determined as the counts (of ^3H thymidine) per minute (cpm). Bars show the average + SD of a single experiment with 3-5 samples per group.

5.3.5 The absence of Treg does not improve the proliferation of transferred naïve Ag specific T cells in response to tumour Ag in vivo

Several studies have shown that Treg mediated suppression is cell contact dependent (260, 265, 266). It is possible that for effective inhibition, Treg must remain in contact with the target cell, which is not the case in the *ex vivo* assay used in the previous experiments of this project. It was therefore necessary to examine the function of TIDC using an *in vivo* assay.

Lymph node cells from naive OTI and OTII mice were CFSE labelled and transferred into Treg-depleted or non-depleted mice approximately 2 weeks after tumour inoculation.

Proliferation of the transferred cells was examined in the tumour draining lymph nodes 3 days later. A significant number of the transferred OTI T cells could be observed proliferating in some mice, however, no obvious proliferation of the transferred OTII T cells occurred (Figure 5.8A). Furthermore, OTI T cell proliferation was observed in only some mice that received the transferred T cells (Figure 5.8B) possibly due to the tumours being slightly too small at the time of T cell transfer. Depleting host mice of Treg did not significantly increase the number of mice that showed proliferation of the transferred T cells (Figure 5.8B). Despite this, all mice within each group were included in further analysis to avoid unintentionally biasing results.

When the level of OTI T cell proliferation in the lymph node was compared, as shown in Figure 5.8B, some of the non-depleted mice showed proliferation, however, overall these mice did not show a significant increase in proliferation over the negative control (Figure 5.8C). Depletion of Treg did not improve the level of OTI T cell proliferation over either the negative control or the non-depleted mice (Figure 5.8C). The high level of proliferation observed in the positive control groups indicated that the transferred T cells were functional. These data show that depleting mice of Treg does not improve the proliferation of tumour specific T cells *in vivo*.

5.3.6 Using a RAG1-/- mouse model confirms that Treg do not affect DC phenotype or function

RAG1-/- mice are completely devoid of all mature T cells (and B cells), including Treg (328). The experiments conducted in Figures 5.1 to 5.8 showed there was no effect of Treg on DC frequency, phenotype or function, however, at the time point examined, Treg depleted mice still had low levels of Treg in the blood, tumour and lymph nodes (Figure

4.7). Comparing anti-tumour responses in RAG1-/- and C57BL/6 mice, therefore, provides a model in which DC function can be studied in the complete absence of Treg.

To assess whether the ability to recruit similar numbers of mature DC to the tumour after inoculation is similar in C57BL/6 and RAG1-/- mice, tumours were removed ~17 days after tumour inoculation and analysed by flow cytometry. Tumours from both mouse strains were found to have a similar frequency of DC (Figure 5.9A). RAG1-/- mice were found to have slightly fewer DC expressing the activation markers CD40, CD86 and MHC II (Figure 5.9B), however, when expressed, these markers were expressed at similar levels on the TIDC (Figure 5.9C).

Figure 5.8: Treg depletion failed to improve the *in vivo* proliferation of transferred T cells.

C57BL/6 mice were depleted of Treg using two 100ug doses of PC61 or left non-depleted, as shown in Figure 4.7B, and inoculated with 10^5 B16.OVA cells. After 13-16 days each mouse was injected with 1.5 x 10^6 naïve, CFSE-labelled OTI T cells and 1.5 x 10^6 naïve, CFSE-labelled CD25 depleted OTII T cells. Lymph nodes were removed 3 days later and OTI and OTII T cell proliferation was determined by flow cytometry. A) Representative dot plots of transferred OTII and OTI T cells in the tumour draining lymph node. Numbers on the graph refer to the percent divided cells. B) The frequency of mice that showed either OTII (top) or OTI (bottom) T cell proliferation was determined using data compiled from 4 experiments. Population size (*n*) is shown on the graphs above the relevant bars. C) Percent divided OTI T cells in the tumour draining or injection site draining lymph nodes of mice receiving untreated DC, DC loaded with SIINFEKL Ag +/- tumour and +/- PC61, or tumour bearing mice +/- PC61, calculated as shown in panel A. Bars show the average percentage of divided cells. The graph shows data from 1 of 4 independent experiments that gave similar results. Experiments were performed with 5-10 mice per group and *p* was calculated using a non-parametric one-way ANOVA test.

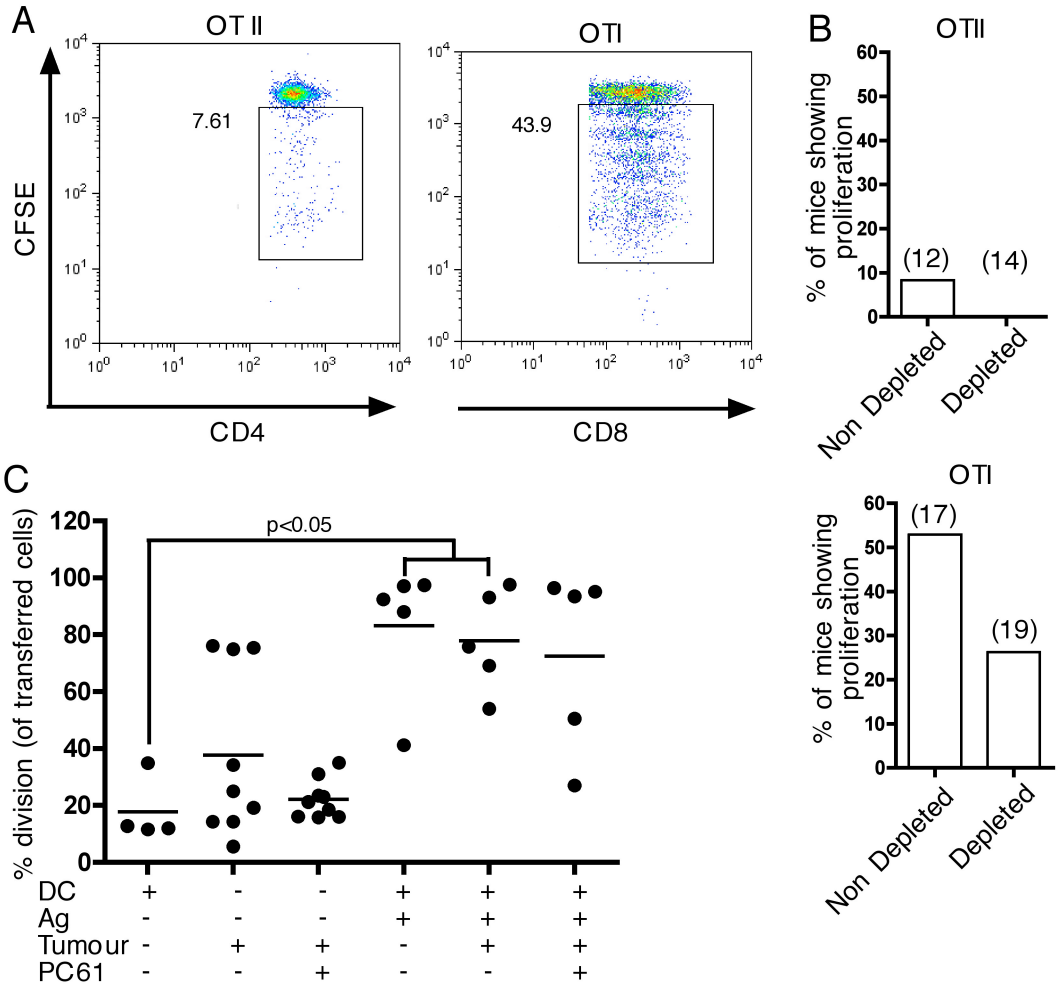
A
OT II
OTI
7.61
43.9
CFSE
CD4
CD8
B
OTII
% of mice showing proliferation
(12)
(14)
Non Depleted
Depleted
C
p<0.05
% division (of transferred cells)
DC
Ag
Tumour
PC61
OTI
(17)
(19)

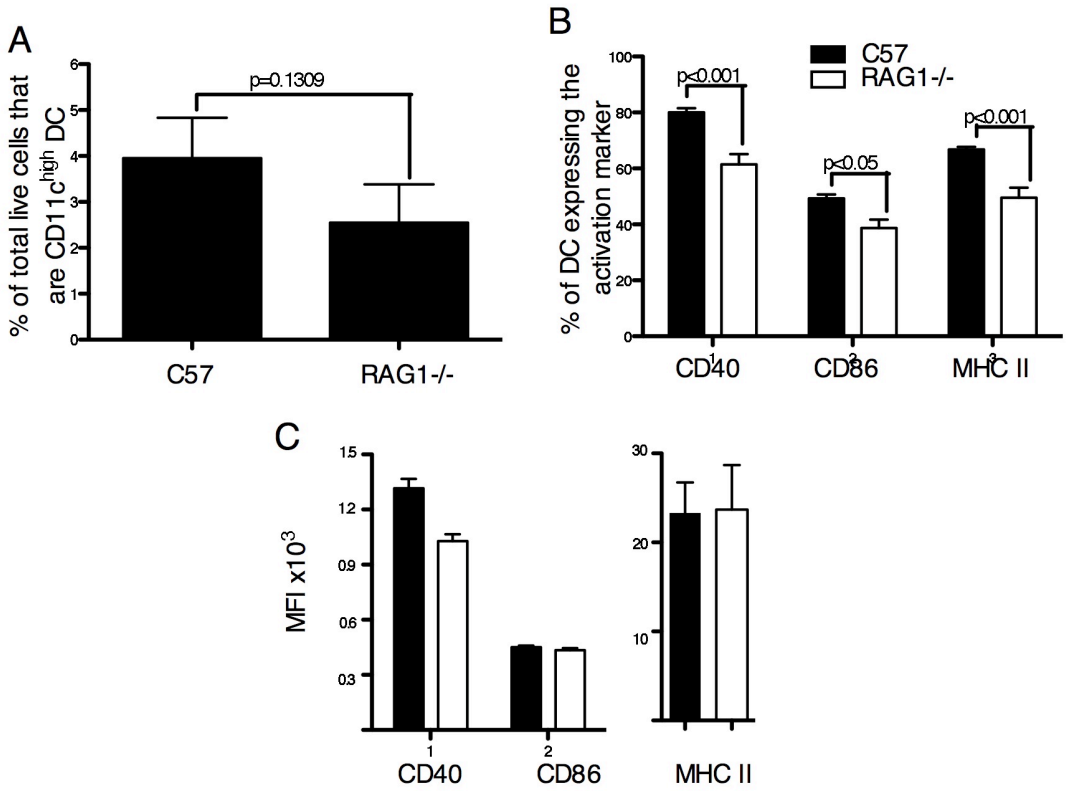

Figure 5.9: TIDC from RAG1-/- mice show slightly impaired maturation.

C57BL/6 and RAG1-/- mice were inoculated with B16.OVA cells. Tumours were excised from mice 17 days after tumour inoculation and analysed by flow cytometry. A) The frequency of $CD11c^{high}$ TIDC in the live cell population was compared and *p* was calculated using an unpaired, one tailed students *t* test. B) The frequency of $CD11b^{+}$ $CD11c^{high}$ DC expressing the activation markers CD40, CD86 and MHC II were compared. Values of *p*, where *=$p<0.05$ and ***=$p<0.001$, were calculated using a two-way ANOVA test with a Bonferroni post-test. C) The MFI values were calculated only for the cells that showed positive staining for the relevant marker as defined in B. Data shown is from one experiment with 9-10 mice per group and bars show the average + SD.

It was of interest to determine whether the presence of T cells or Treg could alter the frequency of mature DC in the tumour or lymph nodes of RAG1-/- mice. RAG1-/- mice were reconstituted with 10^6 purified naive OTI T cells or naïve $CD4^+$ $CD25^+$ Treg from OTII mice one day before tumour inoculation and tumour size (Figure 5.10) and the phenotype of intratumoral and lymph node DC was assessed 17 days later (Figure 5.11). OTI T cells were chosen to reduce the possibility of cells converting into Treg *in vivo*. Reconstituting RAG1-/- mice with naïve OTI T cells significantly delayed tumour growth to the extent that the tumours were not large enough to be reliably weighed. These results suggest the OTI T cells have obtained some effector function, possibly as the result of lymphopenia-induced proliferation (393) or in response to the direct presentation of Ag to these T cells by the tumour cells (394). The presence of OTI T cells also appeared to slightly increase the frequency of $CD40^+$ DC (Figure 5.11A) and decrease the level of MHC II (Figure 5.11A) expressed on TIDC. In the non-draining lymph node, reconstituted mice showed a slightly increased level of MHC II over the naïve non-tumour bearing control, however, this was not significantly different to the level seen in the non-reconstituted mice (Figure 5.11D).

When the effect of Treg on tumour growth was compared, no difference was found in tumour weight (Figure 5.10A), however, a slight reduction in the tumour cell number was seen (Figure 5.10B). A small but significant increase in the amount of MHC II expressed by TIDC was observed in the presence of Treg but without an increase in CD40 or CD86 expression this is unlikely to be of consequence (Figure 5.12A). The lymph node DC appeared to express slightly more MHC II than DC from a naïve RAG1-/- mouse. There was no significant difference between the Treg reconstituted and non-reconstituted, tumour bearing RAG1-/- mice, however, indicating that Treg do not affect MHC II expression by the lymph node DC of RAG1-/- mice (Figure 5.12D). Overall these results show that the

reconstitution of RAG1-/- mice with $CD8^+$ T cells or Treg does not affect the maturation of intratumoral or lymph node DC.

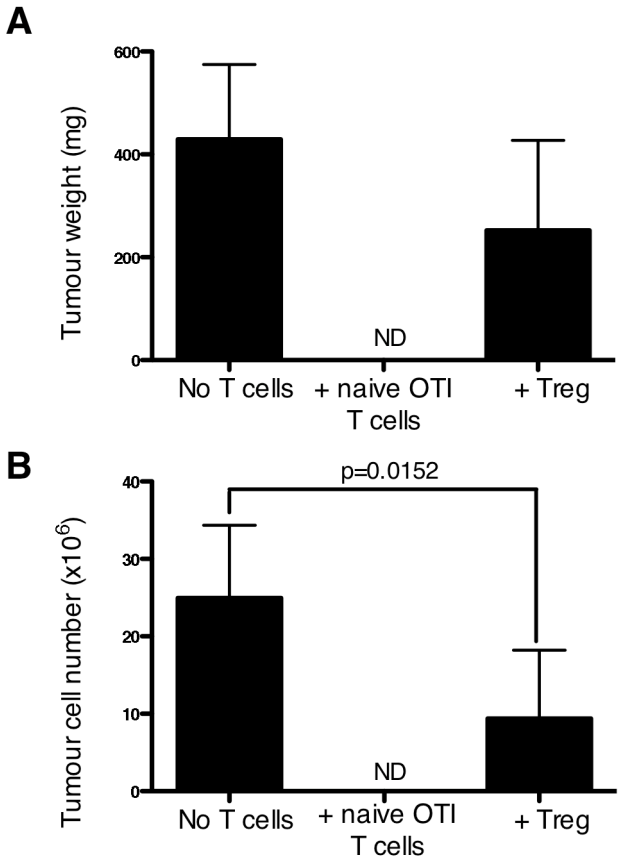

Figure 5.10: The adoptive transfer of $CD8^+$ T cells or Treg into tumour bearing RAG1-/- mice causes a delay in tumour growth.

Purified naïve OTI T cells (10^6) or $CD4^+$ $CD25^+$ Treg from OTII mice (10^5) were adoptively transferred into RAG1-/- mice one day before inoculation with B16.OVA cells. A) Tumours were removed 17 days after inoculation and weighed. B) Tumours were then processed into single cell suspensions and the number of live cells was counted using trypan blue exclusion. In some instances, tumours were not detectable (ND).

Figure 5.11: The adoptive transfer of $CD8^+$ T cells into tumour bearing RAG1-/- mice does not affect the phenotype of intratumoral or lymph node DC.

Purified naïve OTI T cells (10^6) were adoptively transferred into RAG1-/- mice one day before inoculation with B16.OVA cells. Tumours (A) and lymph nodes (B-D) were removed 17 days after inoculation and analysed by flow cytometry for the expression of CD40, CD86 and MHC II on $CD45^+$ $CD11c^{high}$ $CD11b^+$ DC. Lymph nodes from a naïve RAG1-/- mouse were used as the untreated control. Data shown is from one experiment with 5-6 mice per group. Bars show the average + SD and values of *p* were calculated using a two-way ANOVA test with a Bonferroni post-test.

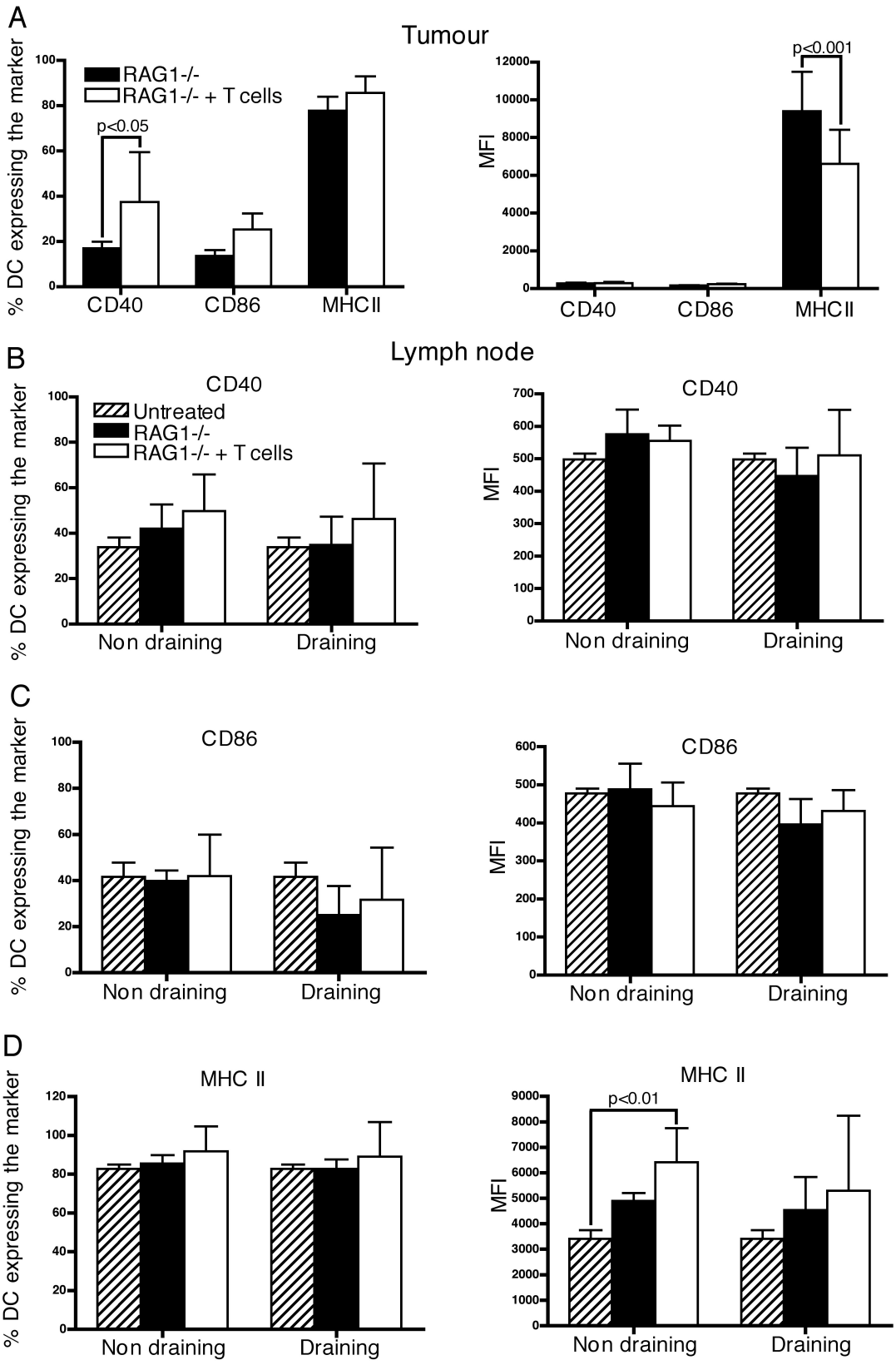
A
Tumour
% DC expressing the marker
RAG1-/-
RAG1-/- + T cells
p<0.05
CD40
CD86
MHCII
MFI
p<0.001
B
Lymph node
CD40
Untreated
RAG1-/-
RAG1-/- + T cells
Non draining
Draining
C
CD86
D
MHC II
p<0.01

Figure 5.12: The adoptive transfer of Treg into tumour bearing RAG1-/- mice does not affect the phenotype of intratumoral or lymph node DC.

$CD4^+$ $CD25^+$ Treg were isolated from the lymph nodes of naïve OTII mice and 10^5 cells were adoptively transferred into RAG1-/- mice one day before inoculation with B16.OVA cells. Tumours (A) and lymph nodes (B-D) were removed 17 days after inoculation and analysed by flow cytometry for the expression of CD40, CD86 and MHC II on $CD45^+$ $CD11c^{high}$ $CD11b^+$ DC. Lymph nodes from a naïve RAG1-/- mouse were used as the untreated control. Data shown is from one experiment with 5-6 mice per group. Bars show the average + SD and values of *p* were calculated using a two-way ANOVA test with a Bonferroni post-test.

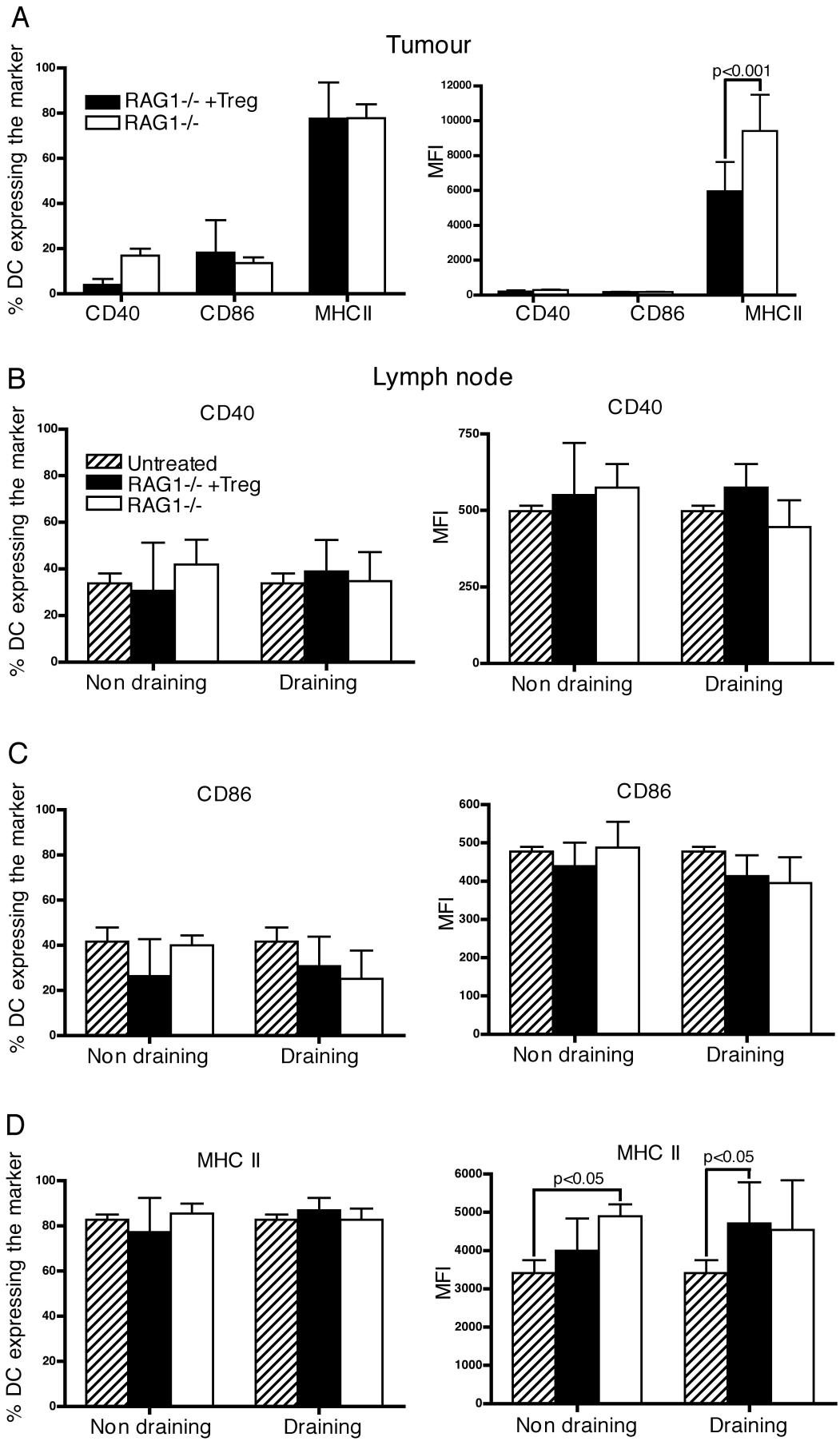
A
Tumour
% DC expressing the marker
RAG1-/- +Treg
RAG1-/-
CD40
CD86
MHCII
MFI
p<0.001
B
Lymph node
CD40
Untreated
RAG1-/- +Treg
RAG1-/-
Non draining
Draining
C
CD86
D
MHC II
p<0.05

For the same reasons described above, it was also important to investigate the function of DC in the presence or complete absence of Treg using a RAG1-/- mouse model. C57BL/6 and RAG1-/- mice were inoculated either with B16.OVA or the parental B16.F1, which does not express the OVA protein. Mice also received naïve CFSE labelled OTI cells and CD25 depleted OTII cells 15 days after tumour inoculation. A further 3 days after adoptive T cell transfer, tumours were measured and the tumour draining and non-draining lymph nodes were removed and processed for analysis by flow cytometry (Figure 5.13). After identifying the transferred cells based on their expression of CD45.1, the level of $CD8^+$ and $CD4^+$ T cell proliferation within the $V\alpha2^+$ $V\beta5.1,5.2^+$ Ag specific population was analysed (Figure 5.13). A large proportion of $CD4^+$ and $CD8^+$ T cells will undergo homeostatic proliferation when transferred into lymphopenic, but not into T cell sufficient hosts (393, 395, 396). It has been shown, however, that only 2-3 rounds of homeostatic proliferation occur in lymphopenic hosts in the absence of Ag (393, 395). In contrast, in the presence of Ag, T cells in lymphopenic hosts will proliferate extensively (395). Consistent with these studies, Figure 5.13 showed that a significant proportion of the transferred cells in both B16.OVA and B16.F1 tumour bearing RAG1-/- mice underwent some proliferation. Only a significant proportion of the transferred cells in C57BL/6 mice bearing B16.OVA, however, but not B16.F1 tumours proliferated more than three times. Based on these observations, the frequency of Ag specific proliferation by the Ag specific T cells was defined as the percentage of cells that had proliferated more than 3 times.

Figure 5.13: Flow cytometric analysis of the antigen specific T cell proliferation in response to tumours *in vivo.*

C57BL/6 and RAG1-/- mice were inoculated with either 10^5 B16.OVA cells or 10^5 of the parental B16.F1 tumour cell line. Fifteen days later mice were then given purified naïve, CFSE labelled OTI T cells (2 x10^6) and CD25 depleted, CFSE labelled OTII T cells (1.5 x10^6) by i.v. injection. A further 3 days after the adoptive T cell transfer, the tumour draining and non-draining lymph nodes were removed, processed into single cell suspensions and analysed by flow cytometry. Transferred cells were identified using the congenic CD45.1 marker while co-expression of the Vα2 and Vβ5.1,5.2 chains of the TCR was used to identify Ag specific T cells. Ag specific proliferation was defined as cells that had undergone more than 3 divisions. Numbers shown in the graphs represent the percentage of cells expressing the relevant markers.

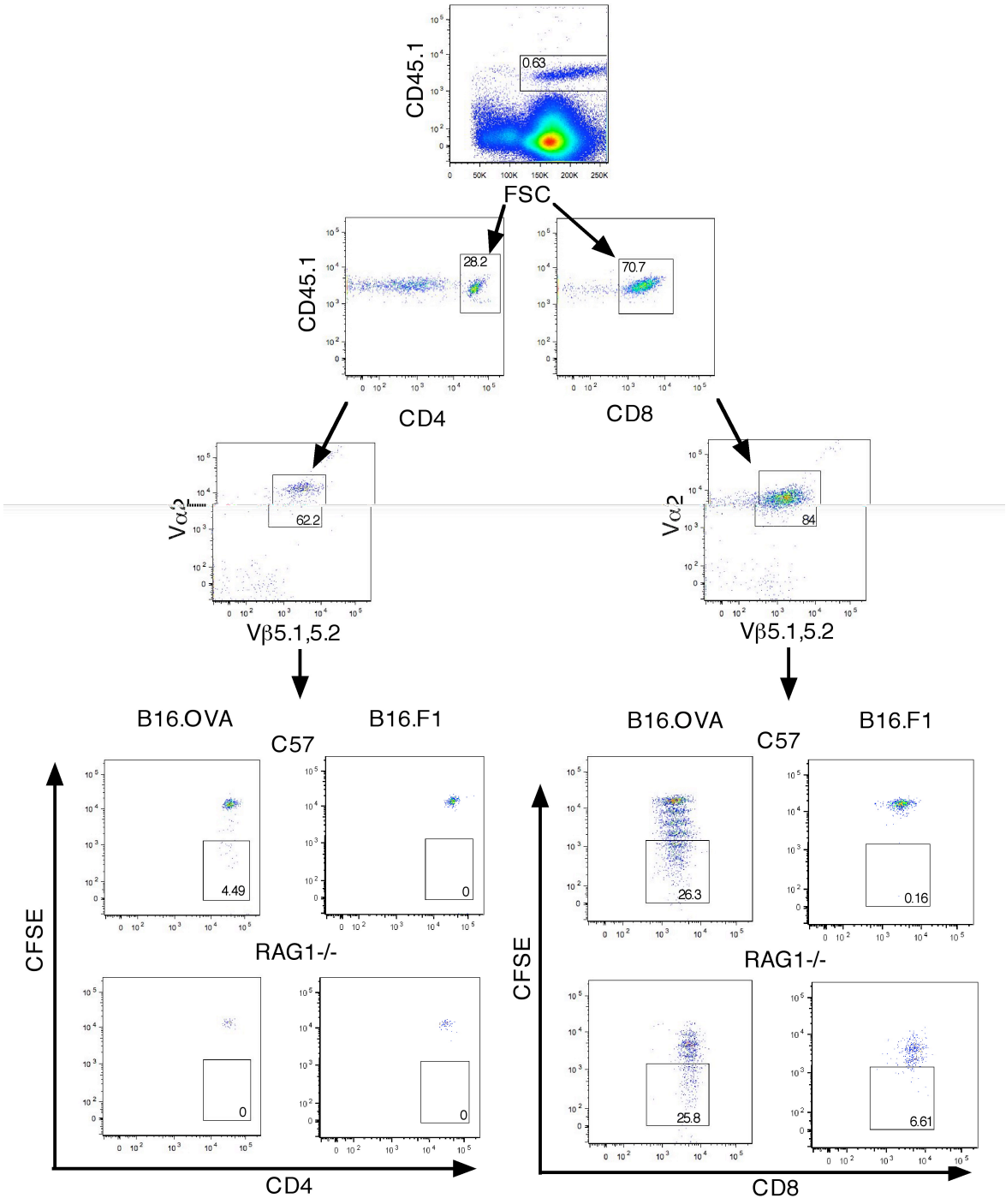
CD45.1
0.63
FSC
CD45.1
28.2
70.7
CD4
CD8
Vα2
62.2
Vβ5.1,5.2
Vα2
84
Vβ5.1,5.2
B16.OVA
B16.F1
C57
CFSE
4.49
0
RAG1-/-
0
0
CD4
B16.OVA
B16.F1
C57
CFSE
26.3
0.16
RAG1-/-
25.8
6.61
CD8

No difference in tumour size was found between any of the groups 18 days after tumour inoculation (Figure 5.14A). These results indicate that the B16.OVA and B16.F1 tumours grow at a similar rate and that the anti-tumour response is similarly poor in both C57 and RAG1-/- mice.

A significant increase in the proliferation of OTI T cells was observed in the draining lymph nodes in comparison to the non-draining lymph node of C57BL/6 mice inoculated with B16.OVA (Figure 5.14B). A similar trend was observed in the RAG1-/- mice but this was not found to be statistically significant (Figure 5.14B). C57BL/6 and RAG1-/- mice inoculated with B16.F1 showed negligible levels of Ag specific T cell proliferation because the tumour cells do not express OVA. Although similar results were observed for the proliferation of OT II cells, the very low levels of proliferation observed were probably background (Figure 5.14C). These data show that the level of Ag specific proliferation in the draining lymph node of Treg deficient (RAG1-/-) mice is not improved in comparison to Treg sufficient (C57BL/6) mice. Both the RAG1-/- mouse model and the PC61 treatment model have therefore shown that Treg do not affect DC frequency, phenotype or function in response to the B16.OVA tumour.

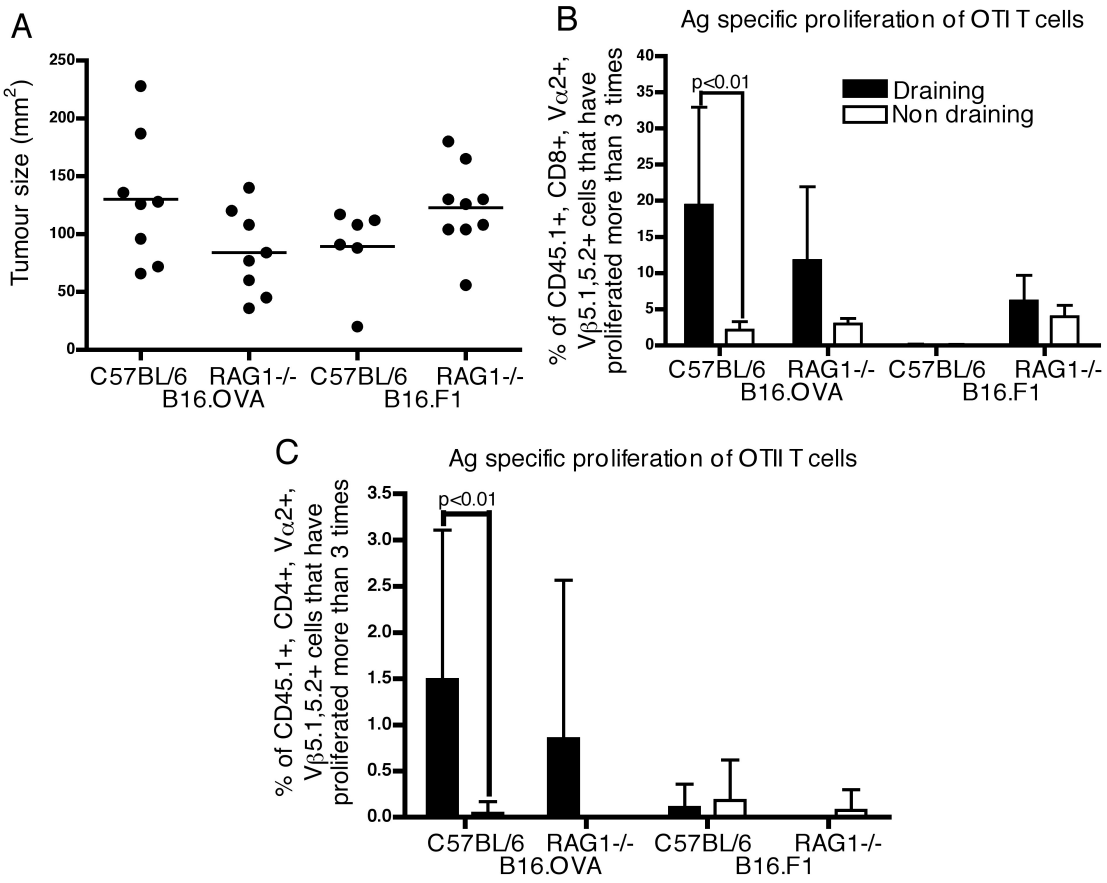

Figure 5.14: Proliferation of tumour specific T cells in C57BL/6 and RAG1-/- mice.

Mice were treated as in Figure 5.12. A) Tumour size was compared at the experimental endpoint. Each dot represents a single mouse. Statistical analysis was performed using a non-parametric one-way ANOVA test. The frequency of Ag specific proliferation of the OTI (B) and CD25 depleted OTII (C) T cells was compared between the draining and non-draining lymph nodes of mice. Bars show the average + SD. Statistical analysis was performed using an unmatched two-way ANOVA test with a Bonferroni post-test. Data shown is from one experiment with 6-9 mice per group.

5.3.7 Treg do not suppress activated T cells

In the experiments presented so far, Treg were found to have no effect on DC frequency, phenotype or function. It was then hypothesised, that the delayed tumour growth in response to PC61 treatment seen in Figure 4.7 may be the result of the absence of direct Treg mediated suppression on the T cells. To test this possibility, activated OTI T cells were transferred into Treg-depleted or non-depleted mice 17 days after tumour inoculation, and mice were monitored for tumour size (Figure 5.15A) and survival (Figure 5.15B). PC61 treated and untreated mice showed a similar delay in tumour growth and survival indicating that Treg do not affect activated T cells. It is possible that these results were observed because the OTI T cells were transferred 17 days after PC61 treatment at which time some of the Treg had become functional again as indicated by the re-expression of CD25 (Figure 4.12). Based on the results shown in Figure 5.15, it was therefore not possible to determine whether PC61 treatment failed to show a delay in tumour growth in mice that received *in vitro* activated OTI T cells because the Treg population had partially recovered, or because Treg were unable to suppress the activated T cells. To address these issues, tumour size and survival were monitored in RAG1-/- and C57BL/6 mice that received activated OTI T cells 11 days after tumour inoculation. C57BL/6 and RAG1-/- mice showed a similar delay in tumour growth (Figure 5.16A) and survival (Figure 5.16B). The results found using the RAG1-/- model, therefore, were similar to the findings using the PC61 treatment model and were consistent with the hypothesis that Treg were unable to suppress the anti-tumour activity of activated T cells.

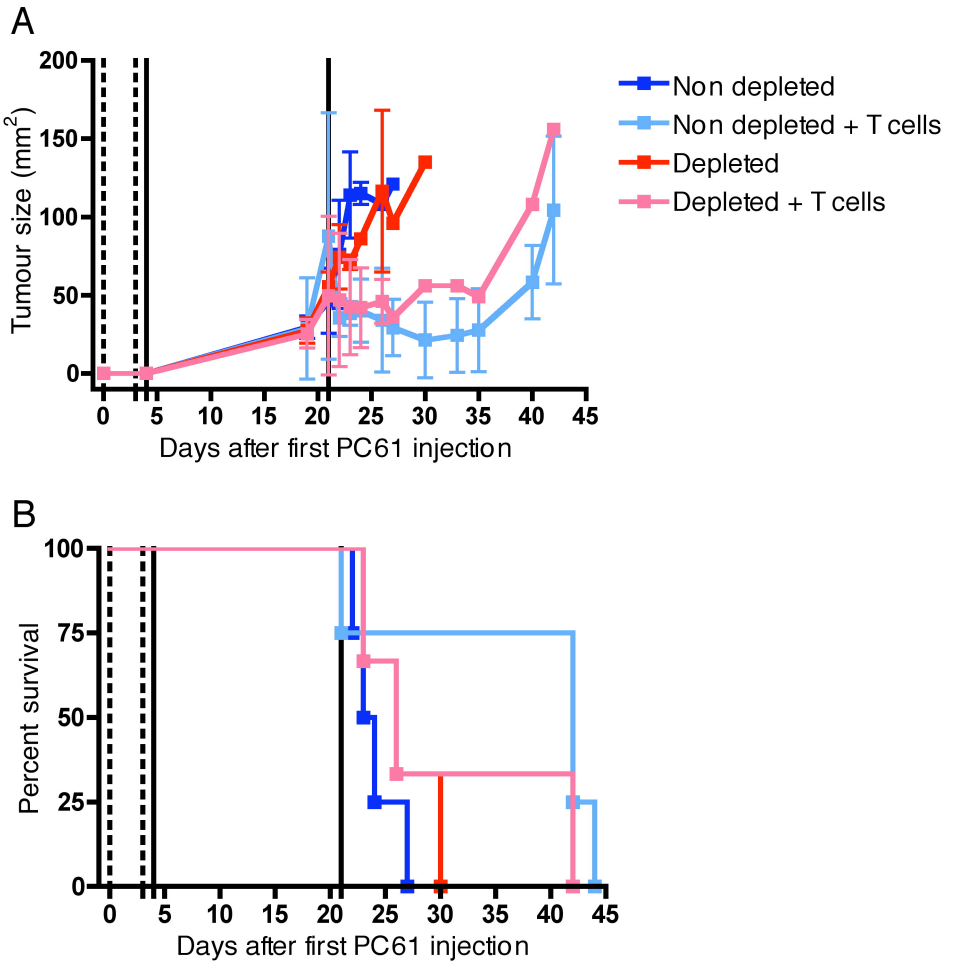

Figure 5.15: PC61 treatment does not affect the anti-tumour activity of adoptively transferred, activated OT I T cells.

C57BL/6 mice were treated with two 100 μg doses of PC61 (dotted black lines) or left untreated, and inoculated with B16.OVA cells (first solid black line). Mice received 10^7 SIINFEKL activated OTI T cells 17 days after tumour inoculation (second solid black line). A) Tumour growth was monitored over time and average tumour size ± SD is shown. B) Survival was also monitored over time. Data is from 1 of 3 experiments that showed similar results and each experiment had 3-6 mice per group.

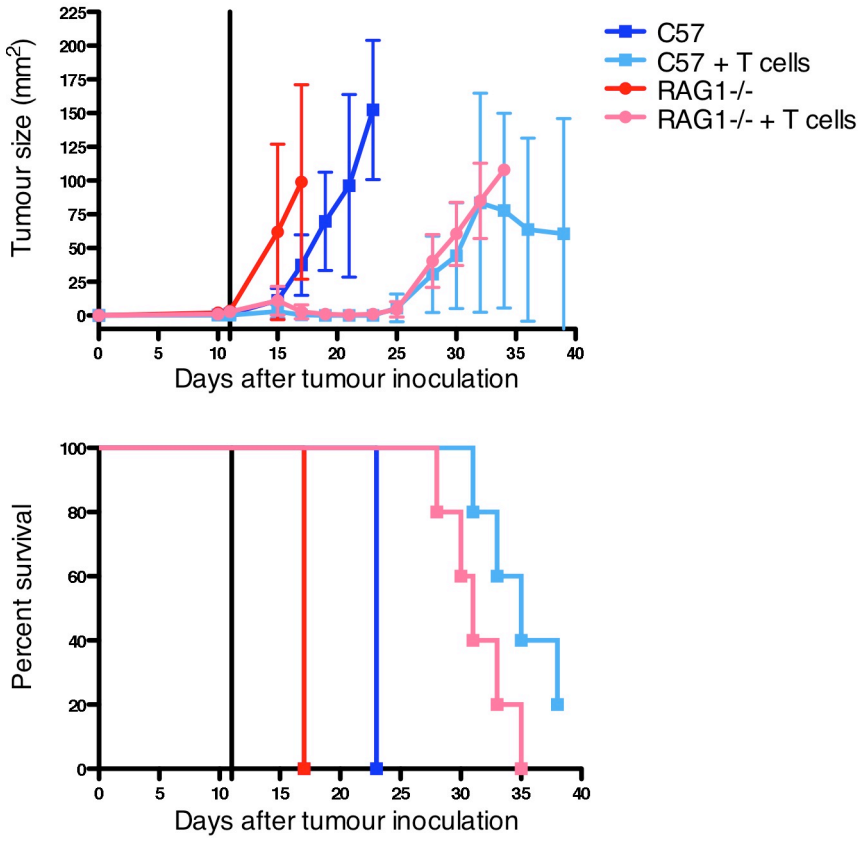

Figure 5.16: Treg do not affect the anti-tumour activity of adoptively transferred, activated OTI T cells.

C57BL/6 and RAG1-/- mice were inoculated with B16.OVA cells on day 0 and given activated OTI T cells on day 11 (solid black line). A) Tumour growth was monitored over time and average tumour size ± SD is shown. B) Survival was also monitored over time. Data is from one experiment with 2-5 mice in the tumour only groups and 5 mice in the groups that received T cells.

5.4 Discussion

The purpose of the experiments described in this chapter was to investigate the effects of Treg on DC in the murine B16.OVA melanoma model. As described in the general introduction, PC61 mAb treatment is not the only method of depleting Treg, however, it has shown success in improving anti-tumour responses in a number of tumour models.

No increase in DC migration from the tumour to the draining lymph node was observed in Treg depleted mice despite the fact that PC61 treatment was found to cause a prolonged reduction in Treg frequency and a delay in tumour growth. Consistent with the observation that DC migrate to the lymph node upon expressing the lymph node homing chemokine receptor CCR7 (391), $CCR7^+$ DC could only be found in the lymph nodes and not the tumour. Surprisingly, PC61 treatment appeared to decrease CCR7 expression on lymph node DC, however, this was not sufficient to result in a reduced frequency of DC in the draining lymph node. The ability of B16.OVA tumour cells to become established and grow in immune sufficient mice indicates that, without further treatment, the mice are unable to mount an efficient anti-tumour immune response in time to control the tumour. This possibility is supported by studies that show that treatments that improve DC maturation status and migration to the lymph node are effective anti-tumour immunotherapies (156, 378). These results collectively imply that while the inefficient anti-tumour response seen in the B16.OVA model may be partly due to the inefficient migration of Ag loaded DC to the draining lymph node, this is not due to Treg mediated suppression.

The results presented in this chapter are consistent with a previous study showing that OX86 (anti-OX40) mAb treatment but not PC61 treatment resulted in an increase in the

frequency of DC in the tumour draining lymph node (156). As discussed in the general introduction, OX40 is expressed constitutively on Treg but is also upregulated on activated T cells (300). Piconese *et al* showed that inactivation of Treg using the OX86 mAb caused an increase in the migration of DC from the tumour to the draining lymph node. These DC were then able to stimulate an efficient anti-tumour immune response resulting in complete tumour regression. In comparison the study also showed that PC61 treatment did not cause a significant increase in DC frequency in the tumour draining lymph node and caused only incomplete tumour regression (156). The failure to see a difference in DC migration after PC61 treatment in the B16.OVA model may be because a small sub-population of $CD25^+$ Treg is present in the PC61 treated group by the end of the experiment, and this population may be sufficient to suppress DC migration. It is also possible that unlike the CT26 colon carcinoma model used by Piconese *et al*, treatment of B16.OVA melanoma bearing mice may not result in an increase in the number of DC migrating from the tumour to the draining lymph node and therefore PC61 treatment could also not be expected to result in a similar increase.

PC61 treatment was not found to improve the activation status of tumour infiltrating or lymph node DC. The TIDC appeared to be semi-mature according to the MFI values but the lack of an appropriate tissue control again makes it difficult to comment on the maturation status. It is obvious however that the TIDC did not show increased activation in response to PC61 treatment. The lymph node DC showed an increase in the amount of CD86 and MHC II expressed in comparison to lymph node DC taken from a naïve mouse indicating some maturation had occurred in response to the presence of tumour. A failure to increase the amount of CD40 expressed by these DC may help explain why tumour-bearing mice fail to mount an efficient immune response. Activated DC are able to activate $CD4^+$ T helper cells, which then transiently upregulate CD40L expression (397, 398).

CD40-CD40L ligation can then feed back on the DC causing further up regulation of the activation markers ICAM-1, CD80 and CD86. CD40 ligation further results in the production of cytokines such as IL-12 by the DC leading to $CD8^+$ T cell proliferation and production of IFN-γ (23). The failure of DC to upregulate CD40 expression due to the absence of an inflammatory signal or the presence of suppressive factors such as Treg would then prevent the DC from becoming "licensed" to adequately stimulate a T cell response (399-401).

Despite the fact that no change in DC frequency or phenotype was observed, a wealth of *in vitro* (272-275, 295) and non-tumour *in vivo* data (402) suggests that Treg have some effect on DC function. Consistent with previous work (366), experiments performed in this thesis showed that TIDC were unable to stimulate tumour Ag specific CD4 or CD8 T cell proliferation *ex vivo* unless the DC were first pulsed with the cognate peptide. Depletion of Treg failed to improve this response. It was decided to investigate if these TIDC were defective in their ability to take up or process proteins because the TIDC were able to present peptide that was pre-incubated with the DC but were unable to present Ag from the tumour. TIDC were able to stimulate a low level of antigen specific CD4 and CD8 T cell proliferation in response to pre-incubation with OVA protein (Figure 5.7). It is important to note that these cultures contained only 3 $x10^3$ DC per well and yet still achieved a level of T cell proliferation similar to or greater than that seen using 20 fold more DC (60 $x10^3$) in the absence of further Ag or protein (Figure 5.6). This indicates that despite the low level of proliferation in response to protein pulsed DC in comparison to Ag pulsed DC, this proliferation is real and not background. These findings suggest that the TIDC are able to take up and process proteins *ex vivo*, however, removing the DC from the tumours may also reverse the suppressive effect of the Treg making it important to study the effect of Treg on DC function *in vivo*. Similar to the *ex vivo* data, PC61 treatment did not improve

the ability of the DC to stimulate either $CD4^+$ or $CD8^+$ T cell proliferation *in vivo*. If the lack of an anti-tumour immune response was caused by tolerisation of the DC, it could be expected that the T cells would undergo an abortive program of proliferation. Since proliferation was observed in only a few mice, it is likely, instead, that the DC have defective Ag presenting function.

DC phenotype and function was analysed at least 18 days after mice were treated with PC61. At this time point, PC61 treated mice had significantly less Treg in the tumour, lymph nodes and blood than untreated mice, however, they still had significant levels of Treg present. It was therefore important to confirm these findings in a model where more profound depletion could be achieved. The administration of diphtheria toxin to Foxp3-DTR mice results in the complete depletion of Treg (249). The advantage of using these mice is that unlike PC61, the toxin can be administered multiple times to maintain Treg depletion without the possibility of affecting other cell groups such as activated T cells. The distinct disadvantage is that these mice have been shown to develop severe autoimmunity leading to death after 10-20 days of continuous treatment (249). Since the tumour experiments in this thesis routinely last 17-22 days after tumour inoculation, the Foxp3-DTR mice are likely to die during the tumour assays. Treatment could be delayed until the later stages of tumour growth however the resulting autoimmunity is still likely to cause some complications when assaying the anti-tumour response. For this reason, it was instead decided to investigate DC phenotype and function using RAG1-/- mice, which lack Treg but do not develop autoimmunity because they also lack mature T and B cells (328).

Only a small difference in DC phenotype was found between the RAG1-/- and C57 mice and no difference in DC function was observed, which is consistent with the results found using PC61 to deplete Treg from C57BL/6 mice. Shreedhar et al have shown that DC

maturation, migration and function may be impaired in T cell deficient mouse strains such as RAG2-/- and SCID mice (403). The Authors used a hapten-sensitised skin model and were probably investigating the responses of skin resident DC populations in contrast to the experiments performed in this thesis, which examine the non-dermal DC population. Experiments were performed in this chapter to determine if, similar to the work of Shreedhar et al, the addition of T cells to the RAG1-/- mice would affect DC maturation. Mice were re-constituted with $CD8^+$ T cells or Treg, however, they were not reconstituted with $CD4^+$ T cells to avoid confounding results due to the possibility of conversion of the $CD4^+$ $CD25^-$ T cells to Treg in mice during the course of a tumour experiment. Despite the lack of CD4 T cell help, the experiments performed in this chapter found no difference in the frequency of TIDC and only a small decrease in the ability of the DC to mature in RAG1-/- mice. These results would suggest that the absence of T cell help has a minimal effect on DC maturation in B16.OVA bearing RAG1-/- mice. During the *in vivo* proliferation assays, naïve OT II T cells were also transferred into the tumour bearing RAG1-/- and C57BL/6 mice for the last 3 days of the experiment. During this time it is unlikely that these T cells would be able to convert to Treg, however, these cells would be able to provide some CD4 T cell help to the DC. The lack of CD4 T cell help in this model therefore cannot fully explain why RAG1-/- mice do not show improved T cell proliferation over the C57BL/6 mice. It is more likely that RAG1-/- mice do not show an improvement in T cell proliferation because, as the results using the PC61 model suggested, Treg do not significantly affect DC frequency, phenotype or function in an *in vivo* mouse tumour model.

Previous experiments in this thesis have shown that PC61 treatment causes a delay in tumour growth, which was not found to be the result of improved DC function. PC61 treated and untreated mice showed a similar delay in tumour growth in response to the

transfer of *in vitro* activated tumour specific T cells, which suggests that Treg do not directly suppress activated T cells either. It has been shown that despite the fact that CD25 is expressed by both Treg and activated T cells, PC61 treatment selectively depletes the Treg population without affecting the $CD4^+$ or $CD8^+$ populations (138). The failure of PC61 treatment to further delay tumour growth after the transfer of *in vitro* activated tumour specific $CD8^+$ T cells was, therefore, not likely to be due to a negative effect of PC61 on the T cells. It is unlikely that PC61 treatment failed to improve the anti-tumour activity of the transferred, activated OTI T cells due to the transient nature of PC61 treatment because similar results were obtained when comparing the anti-tumour activity of the activated T cells in C57BL/6 and RAG1-/- mice. These results suggest that Treg are unable to suppress T cells that have already been activated, however, the possibility that the number of transferred, activated OTI T cells may have been too great for the Treg to suppress must also be considered.

5.5 Conclusions

Experiments performed in this chapter showed that delayed tumour growth in Treg depleted mice was not the result of an improvement in DC migration, activation status or ability to stimulate proliferation of tumour specific T cells both *ex vivo* and *in vivo* in the absence of Treg. Experiments investigating the anti-tumour effect of activated tumour specific CTL also showed that Treg did not suppress these cells. These results would lead to the conclusion that the main mechanism of immunosuppression by which Treg promote tumour growth is their ability to suppress initial T cell activation and/or induction of effector function. The interaction of Treg and TIDC may, therefore, be the result of the Treg being "armed" in the tissue before migrating to the lymph node and suppressing T cell expansion and function, rather than the suppression of TIDC function by Treg.

CHAPTER SIX

PERFORIN DEFICIENT TREG INHIBIT $CD8^+$ T CELL RESPONSES *IN VIVO*

6.1 Introduction

As discussed in detail in the general introduction, the perforin-granzyme pathway is one of two lytic pathways used by $CD8^+$ T cells to cause Ag specific target cell apoptosis and has been shown to be the main pathway responsible for the clearance of most viruses and cancers (91, 92). As expected, perforin knockout (PKO) mice are unable to clear infections by cytopathic viruses and some cancers, which are controlled in immune sufficient mice (92, 93). In addition, PKO mice show increased $CD8^+$ T cell responses after some types of immunizations such as with the superantigen Staphylococcal Enterotoxin B or viral infections such as Lymphocytic Choriomeningitis virus and Cytomegalovirus (97, 98). These findings suggest that perforin may be a critical component of immunoregulatory mechanisms that limit the expansion of $CD8^+$ T cells *in vivo* (98).

In brief, the perforin-granzyme pathway is activated by recognition of the target cell through interaction of the TCR-MHC/peptide complexes, and involves the release of lytic granules containing perforin and granzymes from the CTL (404). The contents of the lytic granules are taken up by the target cell into vesicles by mechanisms that probably include receptor dependent and independent endocytosis (96, 99, 104). Perforin is then thought to allow the granzymes to exit the vesicle and enter the cytoplasm (96) to activate various caspases and trigger apoptosis of the target cell (405-408).

Recently, a number of *in vitro* studies have shown that both murine (306) and human (307, 308) Treg show increased expression of granzymes after polyclonal stimulation. The addition of Treg to the *in vitro* culture of $CD4^+$ $CD25^-$ effector T cells caused a significant increase in the level of effector T cell apoptosis (306-308). *In vitro* studies of Treg

function, however, are of limited relevance to *in vivo* immune responses. One *in vivo* study has shown that the frequency of apoptotic NK and T cells within the tumour ascites increased in wild type mice in comparison to either Treg depleted (by treatment with PC61), granzyme B deficient (GzmB-/-) or PKO mice (305). This study showed that in GzmB-/- mice, where growth of the TAP deficient subline of the Rauscher leukaemia virus-induced lymphoma (RMAS) is controlled significantly better than in wild type mice, only the transfer of wild type but not GzmB-/- or PKO Treg could partially restore the growth of tumours. In contrast, RMAS tumours in PKO mice grew slightly faster than in wild type mice. These results led the authors to conclude that one of the mechanisms by which Treg suppress immune responses is to directly kill target cells using the perforin-granzyme pathway (305). These results suggest that the perforin-granzyme pathway is important for both Treg and T cell function, however, it is unclear if the survival of adoptively transferred wild type, GzmB-/- and PKO Treg was similar. This assay was performed in GzmB-/- mice where the T cells have impaired effector function, which may also make these results difficult to interpret. Furthermore, the authors did not directly test the mechanism by which the T cells died. In addition, it is known that while murine Treg are able to up-regulate granzyme B in response to *in vitro* anti-CD3 stimulation (72, 306, 409), they do not up-regulate perforin (306). It is clear that a more comprehensive study using an *in vivo* assay with less confounding interactions is required to investigate the possibility of direct target cell killing by Treg.

6.2 Aims

The experiments described in this chapter were designed to investigate if the previously reported increased $CD8^+$ T cell response seen in PKO mice might be due to Treg function being affected by the lack of perforin. Immune responses in C57BL/6 and PKO mice were examined with and without PC61 treatment to deplete the perforin sufficient and deficient Treg. T cell responses to OVA were studied because the OVA specific OTI mice were available. It was hypothesised that Treg could suppress T cell function in a perforin-independent manner.

The specific aims were:

- To determine if perforin deficient Treg can suppress the expansion, effector phenotype or effector function of *in vivo* activated T cells
- To determine if perforin deficient Treg can suppress the anti-tumour response

6.3 Results

6.3.1 Treg mediated suppression of CD8$^+$ T cell clonal expansion in vivo is not perforin dependent

Studies have shown that in order for cells to be killed by granzyme, perforin must also be present (96, 407). Perforin deficient cells are, therefore, unable to utilise the perforin-granzyme pathway of target cell lysis, which makes them a powerful tool for analysing the role of perforin in various cell types. To determine the role of perforin in Treg mediated suppression of T cell responses, the response of transferred, perforin sufficient OTI T cells (CD45.1$^+$) was therefore examined with and without PC61 treatment in C57BL/6 (CD45.2$^+$) and PKO (CD45.2$^+$) mice. This model was designed so that the transferred (CD45.1$^+$) T cells were perforin sufficient in all host mice, whereas the Treg were perforin sufficient or deficient depending on the host mouse used. Mice were depleted of Treg using PC61 to show that the T cell response could be suppressed by functional Treg and to assess whether Treg require the expression of perforin to suppress the response.

C57BL/6 and PKO mice were treated with a single 100 μg i.p. injection of PC61 on day -3 or left untreated. All groups received naïve congenic lymph node cells i.v. on day -1 followed by *in vitro* generated, bone marrow derived DC (BMDC) i.v. on day 0. In initial experiments, PC61 untreated and treated groups received BMDC that had been incubated with OVA and the NKT cell specific glycolipid α–Galactosylceramide (α–Gal) for the final 24 hours of culture. α-Gal is a powerful adjuvant known to boost T cell responses via its effect on NKT cells (410). In later experiments, PC61 untreated and treated groups received BMDC that had been incubated with OVA and LPS for the final 24 and 16 hours of culture, respectively, to avoid any confounding factors resulting from the α-Gal dependent activation of NKT cells (Figure 6.1).

Figure 6.1 shows the scheme of the experimental model used to assess the ability of perforin sufficient and deficient Treg to suppress T cell clonal expansion and effector function. This assay has several benefits over other models used to assess the role of perforin in Treg mediated suppression of the T cell response. This model is an *in vivo* assay and a number of different T cell responses can be easily monitored in the blood (or spleens for cytokine production). In addition, the assay has minimal interference from other cell types because the response of a single, specific population is directly measured.

Treg are known to suppress clonal T cell expansion (260). For this reason, the response of normal cells in the presence of perforin sufficient or deficient Treg was compared. C57BL/6 and PKO mice were treated as in Figure 6.1 and expansion of the $CD45.1^+$ T cell population was assessed 7 days after DC treatment. After gating on the live lymphocytes the frequency of transferred T cells was calculated as a percentage of the total $CD8^+$ population (Figure 6.2A). Mice that received OVA-loaded DC showed a trend towards increased $CD8^+$ T cell expansion in comparison to mice that received untreated DC (negative control), however, this difference was not found to be significant. Treatment of mice with PC61 before the transfer of OVA-loaded DC showed a trend towards increased expansion of the $CD8^+$ T cell population in comparison to both the negative control group and the group that received OVA-loaded DC but no PC61 treatment. In PKO mice, the level of expansion of the $CD8^+$ T cell population in mice that received PC61 treatment and OVA-loaded DC was significantly increased over the negative control (Figure 6.2B). These results show that Treg suppress expansion of the T cell population and suggest that PKO Treg are still functional.

Figure 6.1: Diagram of the experimental set up used to test the function of PKO Treg.
C57 and PKO mice (both $CD45.2^+$) received a single 100 μg i.p. injection of PC61 followed 2 days later by the i.v. injection of 7.5 $x10^4$ naïve, unsorted OTIxB6 congenic ($CD45.1^+$) lymph node cells. A further 24 hours later, mice received either 5 $x10^5$ untreated BMDC or OVA-loaded BMDC. Expansion, survival and phenotype of the transferred T cell population were investigated by tail bleeding mice 7 and 15 days after the transfer of BMDC. Production of effector cytokines by the transferred T cells was determined 7 days after the transfer of DC. A killing assay was also performed to determine the effector function of the transferred T cells 7 days after the transfer of BMDC.

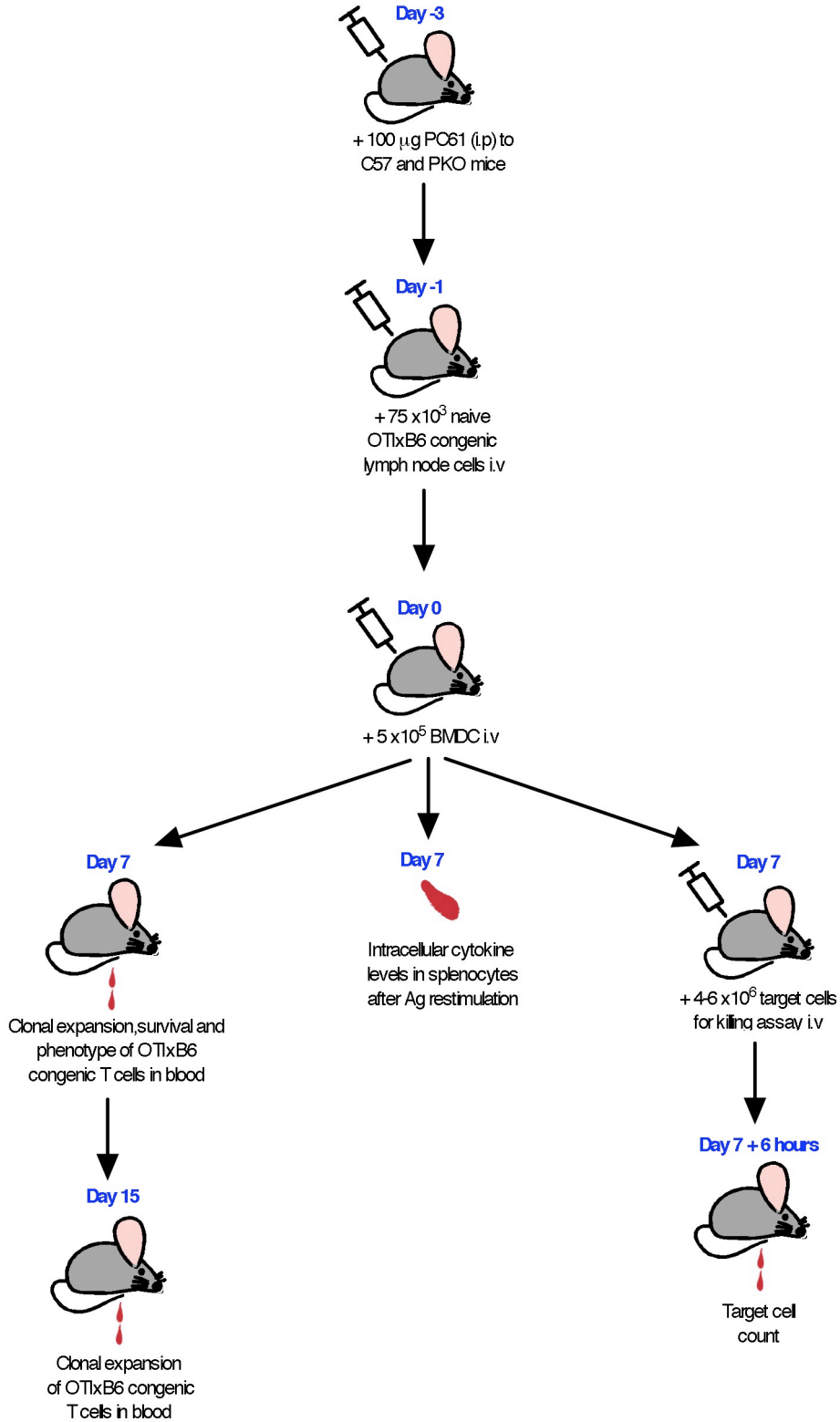
Day -3
+ 100 μg PC61 (i.p) to C57 and PKO mice
Day -1
+ 75 x10^3 naive OTIxB6 congenic lymph node cells i.v
Day 0
+ 5 x10^5 BMDC i.v
Day 7
Clonal expansion,survival and phenotype of OTIxB6 congenic T cells in blood
Day 15
Clonal expansion of OTIxB6 congenic T cells in blood
Day 7
Intracellular cytokine levels in splenocytes after Ag restimulation
Day 7
+ 4-6 x10^6 target cells for killing assay i.v
Day 7 + 6 hours
Target cell count

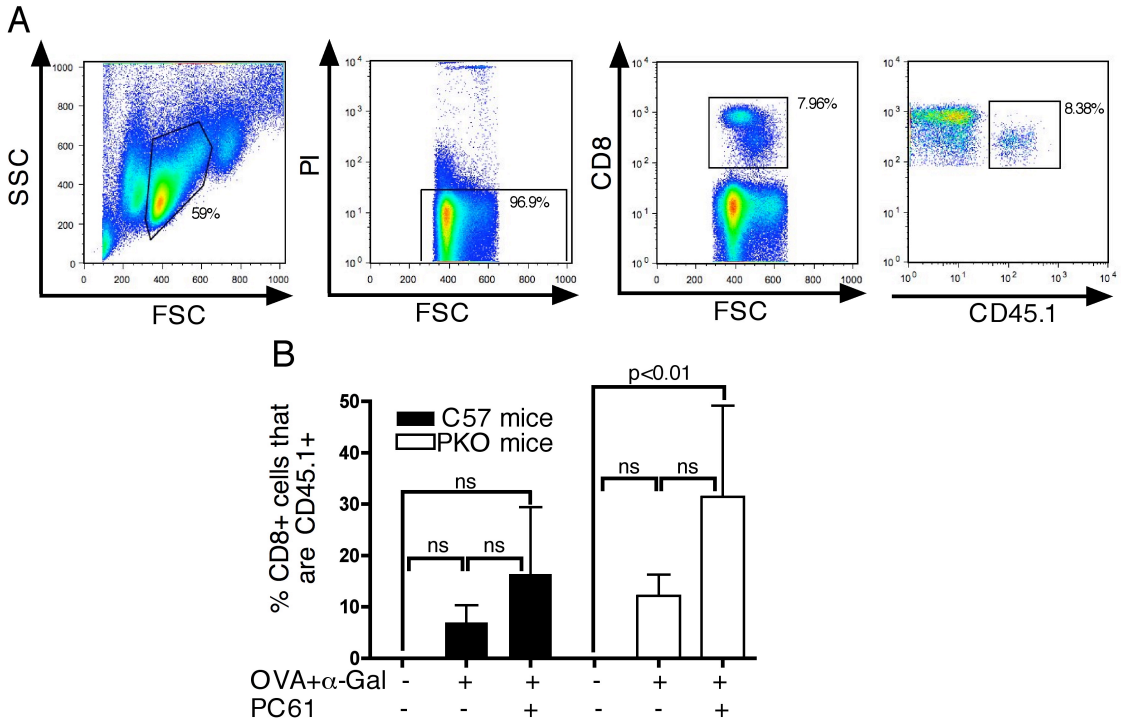

Figure 6.2: Perforin deficient Treg can suppress clonal T cell expansion *in vivo*.
C57 and PKO mice were treated as shown in Figure 6.1. A) Mice were tail bled 7 days after receiving DC and samples were analysed by flow cytometry. Live lymphocytes were identified based on PI exclusion and FSC vs. SSC properties. Expansion of the transferred T cell population was then determined by comparing the frequency of CD45.1$^+$ cells within the total CD8$^+$ population. B) Blood samples were analysed 7 days after immunisation with α–Gal treated or untreated DC. Data is from one experiment with 4-5 mice per group and bars show the mean + SD. *p* was calculated using a non-parametric one-way ANOVA and ns stands for not significant.

Treating mice with OVA and α–Gal loaded BMDC triggers expansion of the T cell population by first activating NKT cells. These NKT cells can then activate and mature the DC leading to expansion of the T cells (410). It has been shown, however, that NKT cells have a role in stimulating Treg (411, 412) and in humans, Treg are known to be able to suppress NKT cell activation and function (413). This makes it more difficult to draw accurate conclusions about the role of perforin in Treg mediated suppression. It was decided, therefore, to examine whether treating DC with LPS instead of α–Gal would still

induce clonal expansion of the transferred $CD8^+$ T cells in a manner that would again be susceptible to Treg mediated suppression. A pilot study using C57BL/6 mice showed that expansion of the $CD8^+$ T cell population 7 days after BMDC treatment was significantly increased only in PC61 treated mice compared to the negative control (Figure 6.3A). When this experiment was repeated using C57BL/6 and PKO mice, PC61 treatment was found to increase expansion of the $CD8^+$ T cell population after the transfer of OVA-loaded DC in comparison to the negative control in both C57BL/6 and PKO mice (Figure 6.3B). Similar results were seen 15 days after the transfer of OVA-loaded BMDC, although the size of the transferred T cell population had decreased in comparison to day 7 indicating the response had already peaked and begun to decline by day 15 (Figure 6.3C). These data show that Treg do not require perforin to suppress clonal expansion of the transferred T cells.

Expansion of a T cell population is the overall result of both proliferation and death of the cells during a response. It was, therefore, important to also look at the cell death in response to the different treatments. In the presence of Treg, there was more death of the transferred $CD8^+$ T cells in both C57BL/6 and PKO mice compared to Treg depleted mice (Figure 6.4A). Analysis of the $CD45.1^-$ (host) $CD8^+$ T cell population showed that the overall level of cell death was similar in all groups (Figure 6.4B) indicating that the increased death found in Figure 6.4A was not due to bias introduced during sample preparation. These results suggest that death of the transferred $CD8^+$ T cells does not involve direct killing by the Treg using the perforin-granzyme pathway.

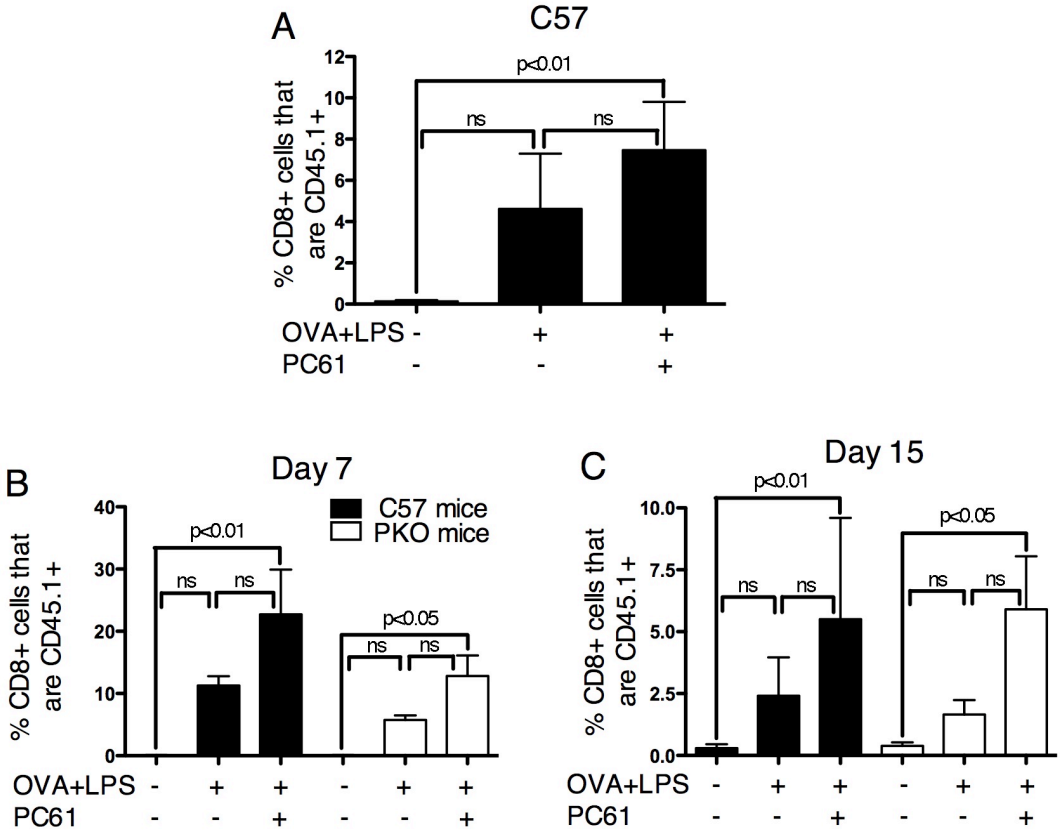

Figure 6.3: Clonal expansion of the transferred CD8$^+$ T cells in response to OVA loaded DC is increased at day 7.

C57BL/6 and PKO mice were treated as shown in Figure 6.1 and the frequency of live CD8$^+$ T cells that were CD45.1$^+$ T cells was determined as shown in Figure 6.2. A) Blood samples were analysed 7 days after C57BL/6 mice received LPS treated or untreated BMDC. Data is from one experiment with 5 mice per group. B) Blood samples were analysed 7 days after C57BL/6 and PKO mice received LPS treated or untreated BMDC. Data is from one of 11 experiments, each showing similar results, with 4-7 mice per group. C) Blood samples from the same mice shown in B were collected and analysed 15 days after mice received LPS treated or untreated BMDC. Data is from 1 of 5 experiments each of which contained 4-7 mice per group and which showed similar results. All bars show the mean + SD. Values of *p* were calculated using a non-parametric one-way ANOVA test with a Dunn's multiple comparison post-test and ns stands for not significant.

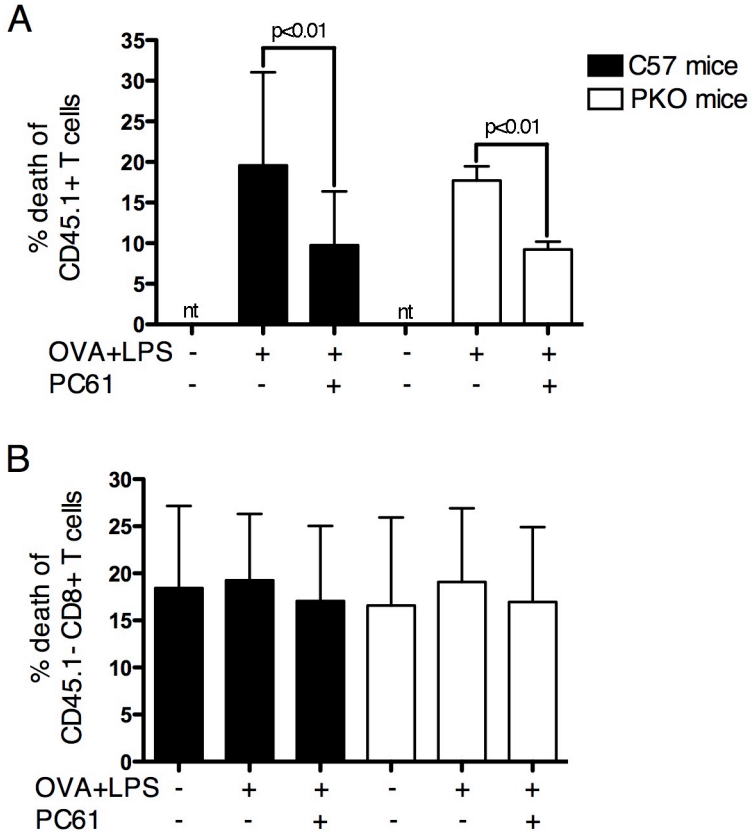

Figure 6.4: Increased death of the transferred CD8$^+$ T cells in the presence of Treg does not require perforin.

C57BL/6 and PKO mice were treated as shown in Figure 6.1. Blood samples were analysed 7 days after C57BL/6 and PKO mice received LPS treated or untreated BMDC. Lymphocytes were identified based on FSC vs. SSC properties. The frequency of dying cells within the A) transferred CD45.1$^+$ and B) host CD45.1$^-$ populations was determined by uptake of the viability dyes PI or DAPI. Death of the transferred T cells in the groups that received untreated DC was not tested (nt) because this population was too small for analysis. Bars show mean + SD and values of *p* were calculated using a non-parametric one-way ANOVA test with a Dunn's multiple comparisons post-test. Data was compiled from 4 experiments each with 4-7 mice per group and which showed similar results.

It was also of interest to determine if perforin deficient Treg were able to affect the expression of an activated phenotype by T cells. KLRG1 is an ubiquitously expressed NK cell receptor, which, when expressed at high levels ($KLRG1^{high}$) is an indicator of T cell activation (71). To determine whether Treg impair the ability of $CD8^+$ T cells to become activated, the frequency of $KLRG1^{high}$ cells was compared in C57BL/6 and PKO mice with or without PC61 treatment. The frequency of $KLRG1^{high}$ cells was similar in PC61 treated and untreated mice indicating that PC61 treatment does not affect the ability of transferred, naïve T cells to become activated (Figure 6.5A and B). To account for differences in the level of expansion of the $CD45.1^+$ population (Figures 6.2 and 6.3), the frequency of $CD45.1^+$ $KLRG1^{high}$ effector T cells was calculated as a percentage of the total $CD8^+$ population and compared in C57BL/6 and PKO mice with or without PC61 treatment. PC61 treated C57BL/6 and PKO mice both showed an increase in the frequency of $KLRG1^{high}$ cells. (Figure 6.5C and D). These data show that perforin-deficient Treg are able to inhibit the ability of the $CD8^+$ T cell population to expand but there was no effect of Treg on the ability of $CD8^+$ T cells to express an effector phenotype.

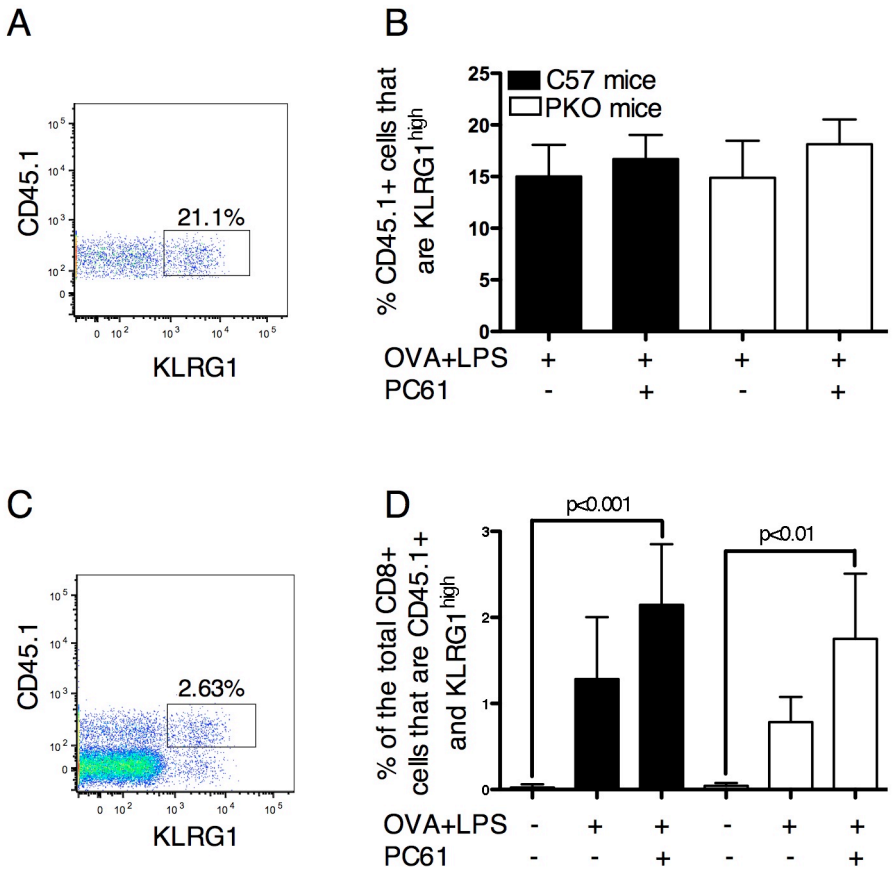

Figure 6.5: PC61 treatment does not affect the ability of transferred T cells to become activated.

C57BL/6 and PKO mice were treated as shown in Figure 6.1. Blood samples were taken 7 days after BMDC transfer and analysed by flow cytometry. A) Representative dot plot showing the frequency of KLRG1^{high} effector T cells within the transferred CD45.1^{+} T cell population. B) The frequency of KLRG1^{high} effector T cells within the transferred CD45.1^{+} T cell population was compared between groups that received treated BMDC. C) Representative dot plot showing the frequency of CD45.1^{+} KLRG1^{high} effector T cells within the total CD8^{+} T cell population. D) The frequency of CD45.1^{+} KLRG1^{high} effector T cells within the total CD8^{+} T cell population was compared between groups that received treated BMDC. Bars show mean and SD and values of *p* were calculated using a non-parametric one-way ANOVA test with a Dunn's multiple comparison post-test. Data is from one of two experiments each with 4-7 mice per group and which showed similar results.

6.3.2 Treg mediated suppression of effector cytokine production by T cells is not perforin dependent

The experiments in 6.3.1 found no role for perforin expressed by Treg in the Treg mediated suppression of T cell expansion, however, it is known that proliferation and effector function can be uncoupled during a response (414). As discussed in the general introduction, T cells can kill target cells using the contact dependent perforin-granzyme and FAS-FASL pathways, however T cells can also kill target cells by producing TNF-α and IFN-γ (85, 86, 415). It was, therefore, of interest to investigate the possibility that Treg may require perforin to suppress the production of effector cytokines by T cells.

Analysis of intracellular TNF-α in unstimulated and stimulated splenocyte samples in comparison to appropriately matched isotype controls showed that cells required Ag re-stimulation to produce TNF-α (Figure 6.6A). When the CD45.1$^+$ population was compared between the treatment groups and mouse strains, a trend towards an increased number of cells expressing TNF-α was observed in the absence of Treg, however, this did not reach statistical significance (Figure 6.6B). A similar trend was also observed for the level of TNF-α produced per cell (Figure 6.6C). TNF-α production was not tested in the groups that did not receive OVA-loaded DC because Figure 6.3 shows that the population did not expand.

To account for differences in the level of expansion of the CD45.1$^+$ population (Figure 6.3), the level of TNF-α production within the total CD8$^+$ population was also analysed. TNF-α was produced by the transferred CD45.1$^+$ CD8$^+$ T cells but not the host CD45.1$^-$ CD8$^+$ T cells (Figure 6.6D). Both the C57BL/6 and PKO mice that received OVA loaded BMDC and PC61 treatment showed an increase in the frequency of TNF-α producing cells

indicating that the expression of perforin by Treg is not required to suppress the production of TNF-α. Intracellular IFN-γ production was also analysed and the results were found to be similar to those described for TNF-α (Figure 6.7).

6.3.3 Suppression of the in vivo killing of target cells does not require the expression of perforin by Treg

The experiments performed in Figures 6.2 to 6.7 found that increased death of Ag specific CD8$^+$ T cells in the presence of Treg and suppression of clonal T cell expansion, effector phenotype and effector cytokine production did not require the expression of perforin by Treg. To assess the role of perforin expression by Treg on the overall response of the transferred T cells, an *in vivo* killing assay was performed.

To evaluate the cytotoxic function of the transferred T cells *in vivo* in each of the groups 7 days after DC treatment, mice were given an equal number of non-Ag pulsed, CTO labelled control splenocytes, and low and high dose Ag pulsed target splenocytes labelled with low and high concentrations of CFSE, respectively. Blood samples were collected 4 hours after the transfer of splenocytes and analysed by flow cytometry (Figure 6.8A). The percentage of target cell killing was determined by comparing the number of high dose Ag pulsed target splenocytes to control splenocytes in each mouse. The groups that received treated BMDC showed a trend towards an increase in Ag specific target cell killing, however, this was only found to be significant in the groups that also received PC61 treatment (Figure 6.8B). Results were similar in both C57BL/6 and PKO mice indicating that perforin deficient Treg are capable of suppressing the cytotoxic function of *in vivo* activated OTI T cells.

Figure 6.6: Increased production of TNF-α by transferred T cells does not require the expression of perforin by Treg.

C57BL/6 and PKO mice were treated as shown in Figure 6.1. Spleens were removed 7 days after BMDC transfer, processed into single cell suspensions, restimulated with SIINFEKL for 4 hours in the presence of Golgi stop and analysed by flow cytometry. A) Representative histograms showing the percent of CD45.1$^+$ T cells expressing TNF-α (solid green line) in comparison to the appropriately matched isotype control (grey filled histogram). The percentage of CD45.1$^+$ expressing TNF-α (B) and the MFI of CD45.1$^+$ cells expressing TNF-α (C) was compared between the treatments and mouse strains, respectively. D) A representative dot plot of the expression of TNF-α within the total CD8$^+$ population. E) The percentage of total CD8$^+$ cells that were TNF-α expressing CD45.1$^+$ T cells was determined as shown in panel D and compared between the treatments and mouse strains, respectively. Bars show the mean + SD and values of *p* were calculated using a non-parametric one-way ANOVA test with a Dunn's multiple comparisons post-test. Data is from one of two experiments each with 4-7 mice per group and which show similar results. TNF-α expression by the CD45.1$^+$ T cells was not tested (nt) in panels B and C.

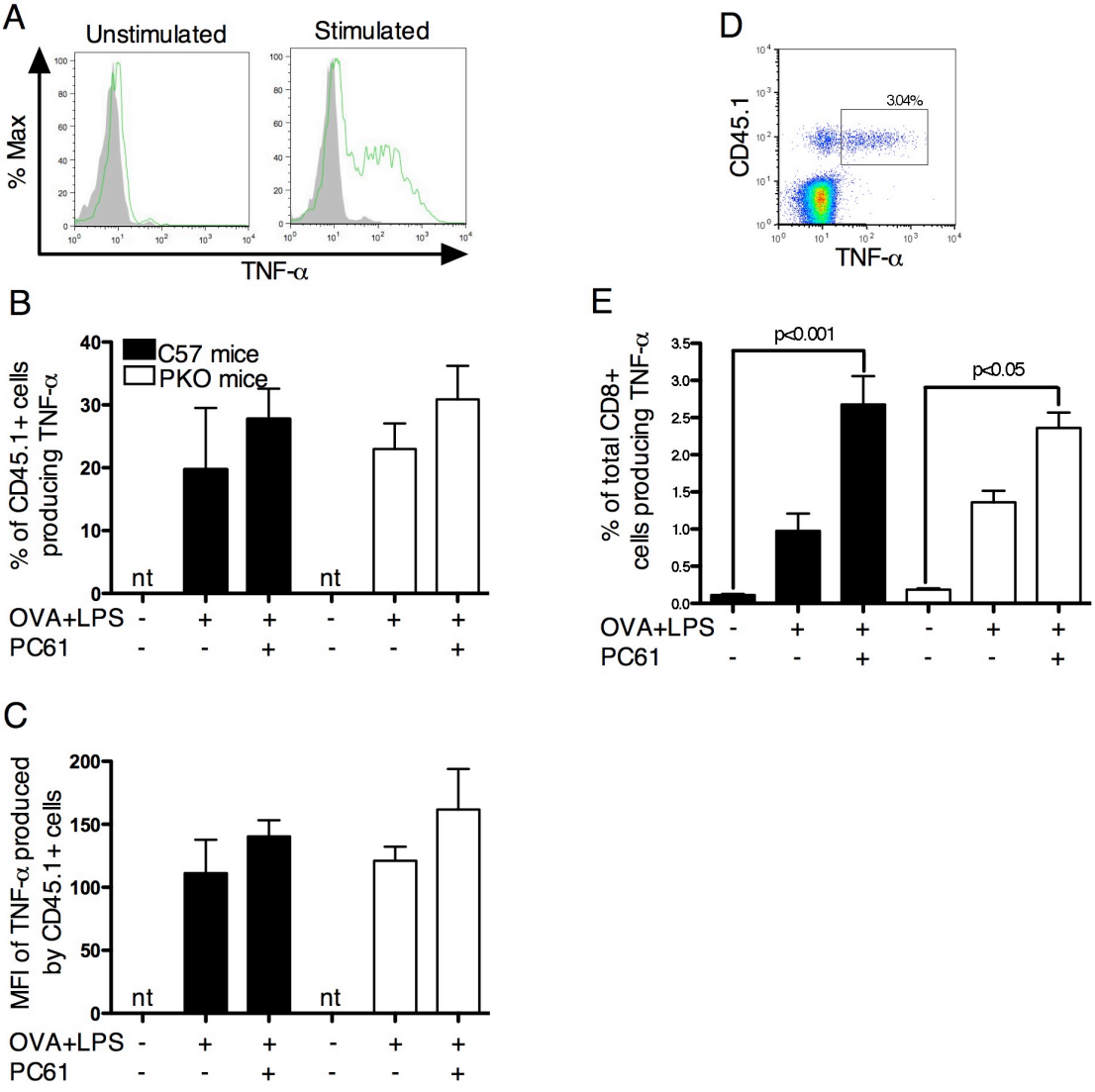
A
Unstimulated
Stimulated
% Max
TNF-α
B
% of CD45.1+ cells producing TNF-α
C57 mice
PKO mice
nt
nt
OVA+LPS
PC61
C
MFI of TNF-α produced by CD45.1+ cells
D
CD45.1
3.04%
TNF-α
E
% of total CD8+ cells producing TNF-α
p<0.001
p<0.05

Figure 6.7: Increased production of IFN-γ by transferred T cells does not require the expression of perforin by Treg.

C57BL/6 and PKO mice were treated as shown in Figure 6.1. Spleens were removed 7 days after BMDC transfer, processed into single cell suspensions, restimulated with SIINFEKL for 4 hours in the presence of Golgi stop and analysed by flow cytometry. A) Representative histograms showing the percent of $CD45.1^+$ T cells expressing IFN-γ (solid green line) in comparison to the appropriately matched isotype control (grey filled histogram). The percentage of $CD45.1^+$ expressing IFN-γ (B) and the MFI of $CD45.1^+$ cells expressing IFN-γ (C) was compared between the treatments and mouse strains respectively. D) A representative dot plot of the expression of IFN-γ within the total $CD8^+$ population. E) The percentage of total $CD8^+$ cells that were IFN-γ expressing $CD45.1^+$ T cells was determined as in panel D and compared between the treatments and mouse strains respectively. Bars show the mean + SD and values of *p* were calculated using a non-parametric one-way ANOVA test with a Dunn's multiple comparisons post-test. Data is from one of two experiments each with 4-7 mice per group and which show similar results. IFN-γ expression by the $CD45.1^+$ T cells was not tested (nt) in panels B and C.

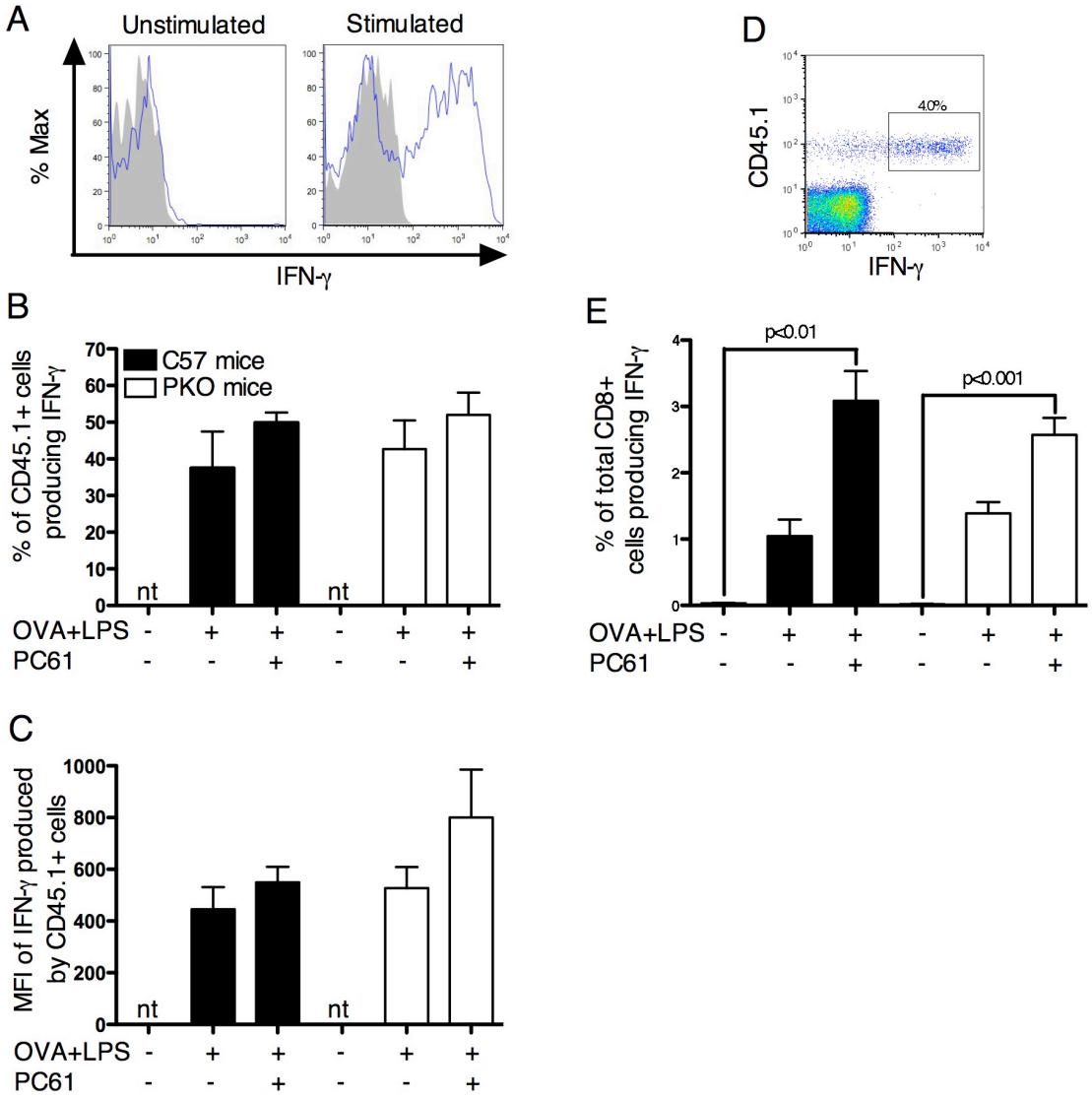
A
Unstimulated
Stimulated
% Max
IFN-γ
D
CD45.1
4.0%
IFN-γ
B
% of CD45.1+ cells producing IFN-γ
C57 mice
PKO mice
nt
nt
OVA+LPS - + + - + +
PC61 - - + - - +
E
% of total CD8+ cells producing IFN-γ
p<0.01
p<0.001
OVA+LPS - + + - + +
PC61 - - + - - +
C
MFI of IFN-γ produced by CD45.1+ cells
nt
nt
OVA+LPS - + + - + +
PC61 - - + - - +

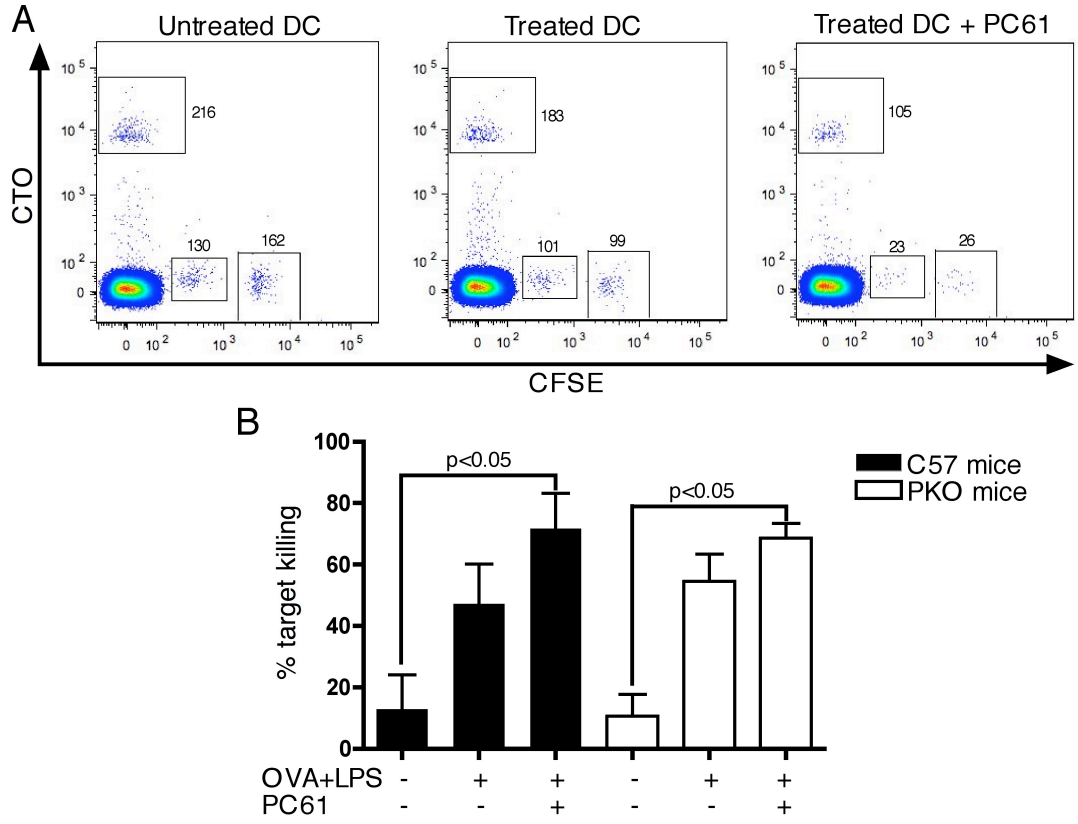

Figure 6.8: Perforin deficient Treg can suppress the killing of target cells *in vivo.*

C57BL/6 and PKO mice were treated as shown in Figure 6.1. Seven days after BMDC treatment, mice received an equal ratio (4-6 x10^6 of each) of non-Ag pulsed, CTO (10 μM) labelled control splenocytes and target splenocytes that had been pulsed with 10 or 100 nM SIINFEKL and labelled with 0.2 μM or 2 μM CFSE, respectively. Mice were tail bled 4 hours later and samples were analysed by flow cytometry. A) Representative dot plots showing the number of control and target splenocytes recovered from mice from each treatment group within the live cell population. B) To determine the percentage of target killing, the number of 100 nM Ag-pulsed, 2 μM CFSE labelled splenocytes was compared to the number of control, CTO labelled splenocytes from each mouse. Bars show the mean + SD and values of *p* were calculated using a non-parametric one-way ANOVA test with a Dunn's multiple comparisons post-test. Data is from one of two experiments each with 4-7 mice per group and which show similar results.

6.3.4 Increased expansion of the T cell population in response to PC61 treatment does not lead to an improved anti-tumour response

Figures 6.2 to 6.8 showed that perforin deficient Treg are capable of suppressing T cell proliferation, effector phenotype and effector function in response to OVA-loaded BMDC. It was of interest to determine whether perforin deficient Treg mediated suppression of the T cell response would be sufficient to affect tumour growth. To address this question, the model established in Figure 6.1 was adapted so that the expansion and function of the transferred lymphocyte population could be assessed in tumour bearing mice. This assay was set up in parallel with the experiment shown in Figure 6.3B using the same donor lymphocytes and BMDC to immunise the mice. Mice were treated with PC61 followed a day later by inoculation with B16.OVA. Mice were given naïve lymphocytes 9 days after receiving the tumour inoculation and a further 24 hours later when tumours were barely palpable, mice received untreated or OVA and LPS treated BMDC (Figure 6.9A). Expansion of the transferred T cell population was assessed 7 days after BMDC treatment and was significantly increased in the absence of Treg in both the C57BL/6 and PKO mice (Figure 6.9B). Expansion of the transferred lymphocytes in tumour bearing mice (Figure 6.9B) was found to be approximately half that seen in non-tumour bearing mice (Figure 6.3B). The experiments performed in Figures 6.3 and 6.9 were set up side by side using the same donor DC and T cells, however, the tumour bearing mice were treated with PC61 9 days before the non-tumour bearing mice. Mice in Figure 6.9 received a 150 μg dose of PC61 instead of the 100 μg used in Figures 6.2-6.8 because in the tumour bearing mice the T cell assay was performed 8 days later than in the non-tumour bearing mice. This data suggests that while in tumour bearing mice this assay still results in increased expansion of the T cell population in the absence of Treg, the tumour may be able to suppress the response of the transferred T cells in a Treg-independent manner. Treatment with OVA

and LPS loaded BMDC succeeded in delaying tumour growth in both C57BL/6 and PKO mice, however, pre-treatment of mice with PC61 to remove Treg did not further improve the anti-tumour response observed in either C57BL/6 or PKO mice. This assay, therefore, could not be used to determine if Treg mediated suppression of the anti-tumour response is perforin-dependent.

Figure 6.9: PC61 treatment does not improve the anti-tumour activity of *in vivo* activated T cells.

A) Schematic diagram of the experimental set up used to test the anti-tumour activity of *in vivo* activated T cells and the effect of perforin sufficient and deficient Treg thereon. B) Expansion of the transferred T cells 7 days after BMDC treatment was analysed and gated as shown in Figure 6.2. Bars show the mean + SD and values of *p* were calculated using a non-parametric one-way ANOVA test with a Dunn's multiple comparisons post-test. Mice were monitored for C) tumour growth and D) survival over time. Arrows indicate when mice received each of the following treatments: PC61 (black arrow), B16.OVA (orange arrow), OTIxB6 congenic lymphocytes (green arrow), untreated or treated DC (blue arrow). In addition, the grey arrow indicates when expansion of the transferred T cells was analysed. C) Bars show the mean and SD. D) Statistical significance was calculated using a Logrank test and shows a significant delay in tumour growth in all groups that received treated DC but no difference between the groups that received treated DC. *** = $p<0.0001$. Data is from one of two experiments each with 2-5 mice in the control groups that received untreated DC and 3-7 mice per group that received the treated DC. Both experiments showed similar results.

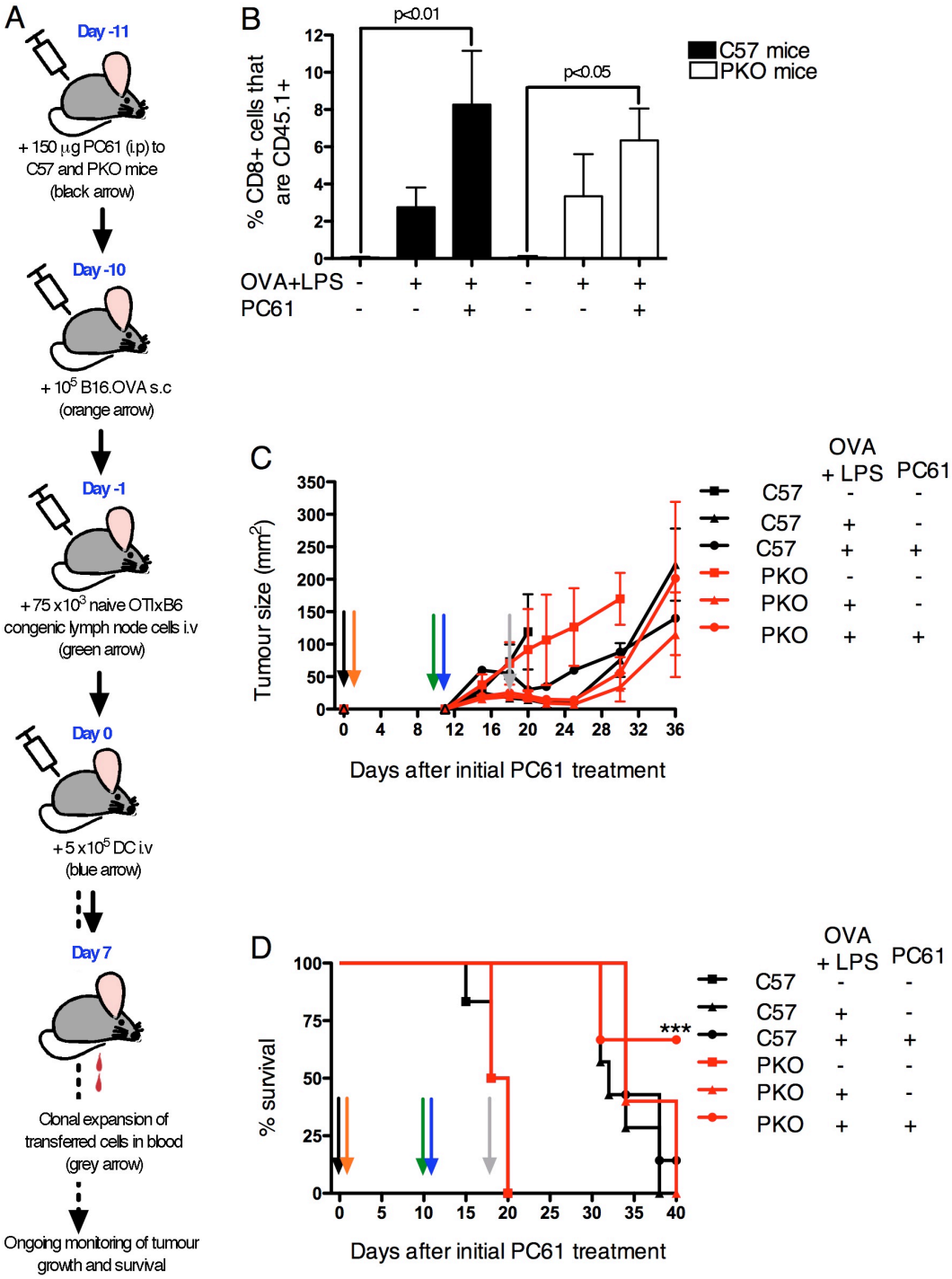
A
Day -11
+ 150 μg PC61 (i.p) to C57 and PKO mice (black arrow)
Day -10
+ 10^5 B16.OVA s.c (orange arrow)
Day -1
+ 75 x10^3 naive OTIxB6 congenic lymph node cells i.v (green arrow)
Day 0
+ 5 x10^5 DC i.v (blue arrow)
Day 7
Clonal expansion of transferred cells in blood (grey arrow)
Ongoing monitoring of tumour growth and survival
B
p<0.01
p<0.05
C57 mice
PKO mice
% CD8+ cells that are CD45.1+
OVA+LPS
PC61
C
Tumour size (mm2)
Days after initial PC61 treatment
OVA + LPS
PC61
C57
PKO
D
% survival
***
Days after initial PC61 treatment

6.4 Discussion

The experiments described in this chapter were designed to determine whether Treg utilize the perforin-granzyme pathway to suppress immune responses.

In contrast to some studies using viral models (97, 98), in this study, PKO mice did not exhibit an increased T cell response over that seen in C57BL/6 mice. This is probably because in the viral models, the PKO mice were unable to clear the infection as efficiently as the C67BL/6 mice. The model used in this study was based on the transfer of Ag-loaded DC and as such, the Ag source is similar in both the C67BL/6 and PKO mice, meaning the size of the T cell response is also similar in these mice.

Similar to previous studies (261, 303), experiments described in this chapter found the presence of Treg led to suppression of T cell proliferation and inhibition of effector cytokine production and cytotoxic function. All results observed, however, were similar in C57BL/6 and PKO mice indicating Treg do not require perforin to mediate these effects in the *in vivo* model used.

The results of this chapter contrast with a number of *in vitro* and *in vivo* studies. Firstly, Gondek *et al* (306) found that murine Treg show increased expression of GzmB mRNA and protein after *in vitro* polyclonal stimulation. In addition, that study found that while GzmB-/- Treg were less capable of suppressing $CD4^+$ $CD25^-$ effector T cell proliferation *in vitro* than wt Treg, PKO Treg did not show impaired suppressive ability. When the effector T cells from the co-culture of T cells and wt Treg were analysed, the rate of apoptosis was found to increase as the number of Treg in the culture increased, which suggests that Treg may directly kill the effector T cells. The study did not, however,

compare the rate of effector T cell apoptosis from the co-culture of T cells and GzmB-/- Treg to show that in the presence of GzmB-/- Treg the rate of effector T cell apoptosis did not increase. The study also failed to rule out the possibility that the wt, PKO and GzmB-/- Treg differ in their capacity to survive. Without these controls it is difficult to conclude that the Treg were killing the effector T cells in a Gzm-dependent manner. Furthermore, the findings of Gondek *et al* are inconsistent with a number of studies that show that although granzyme is responsible for the majority of the target cell death, without perforin, granzyme cannot mediate its cytotoxic effect (92, 96, 104, 415). Two studies by Grossman *et al* have found that polyclonally activated natural (307) and adaptive (308) human Treg express granzymes. The addition of Treg to the *in vitro* culture of $CD4^+$ $CD25^-$ effector T cells caused a significant increase in the level of effector T cell apoptosis (307, 308). Apoptosis of effector T cells in the presence of Treg was prevented by the addition of EGTA to the culture to block the calcium-dependent perforin polymerisation (307, 308). Based on these findings it was concluded that Treg were directly killing the effector T cells using the perforin-granzyme pathway (307, 308). These studies by Gondek *et al* and Grossman *et al* rely on polyclonal activation of the cells in *in vitro* cultures. As discussed in the general introduction, Treg are known to have different requirements for suppression in *in vitro* and *in vivo* models, which makes the physiological relevance of these *in vitro* studies limited.

A recent study by Cao *et al* (305) using an *in vivo* tumour model has found that wild type mice showed an increase in the frequency of apoptotic NK and T cells within the tumour ascites in comparison to either Treg depleted (by treatment with PC61), GzmB-/- or PKO mice (305). These results suggest Treg require the perforin-granzyme pathway to cause apoptosis of NK and T cell populations. While the results themselves are indisputable, the interpretation of these results, as discussed below, may have broader implications than

those initially suggested. Using tumour clearance as the readout for an *in vivo* assay in perforin or granzyme knock out mice, which have had wild type or knock out Treg transferred back in only reflects the end result of a number of complex *in vivo* interactions. The lack of either granzyme or perforin in the host mice may confuse the issue of whether or not Treg require granzyme and perforin to mediate suppression because the host T cells will also lack granzyme or perforin. Furthermore, there are also a number of factors that complicate these findings: The treatment of GzmB-/- or PKO mice with PC61 further reduced the frequency of NK and T cell apoptosis indicating that these Treg are still capable of causing target cell apoptosis independent of the perforin-granzyme pathway. The possibility that NK and T cell apoptosis was caused by Treg utilizing the Fas-FasL pathway cannot be ruled out because this has not been tested in mice. One study has shown, however, using human cells that the Fas-FasL pathway was not found to have a role in the Treg mediated increase in target cell apoptosis (307). It is possible, instead, that the NK and T cells receive better survival signals because the DC are more highly activated in the absence of Treg. Experiments in Chapter 5 of this thesis showed that DC did not up-regulate the activation markers CD40, CD86 and MHC II *in vivo* in the absence of Treg. However, it is possible that the T cell-DC interaction is still improved in the absence of Treg leading to an improved T cell response. The study by Cao *et al* (305) also did not assess the total number of live or dead NK and T cells. Figures 6.2 and 6.3 of this chapter showed that in the absence of Treg, the $CD8^+$ T cell population expanded more. Therefore the decreased frequency of apoptosis seen in Treg depleted mice might actually be due to an increase in the total population size with little or no increase in apoptosis.

The assay used in this thesis circumvents the issues encountered in previous studies providing a more direct readout of *in vivo* immune responses, and would lead to the conclusion that Treg mediated suppression of the T cell response does not require perforin.

The role of granzyme was not directly examined in this thesis, however, perforin is required for the majority of granzyme-mediated killing (82), suggesting that if GzmB is involved in Treg mediated suppression of the T cell response, it is by a mechanism other than direct killing of the T cells.

Attempts to investigate the use of perforin by Treg in a tumour model were unsuccessful because treating mice with PC61 before tumour inoculation did not result in an improved anti-tumour response of the *in vivo* activated T cells. This was unlikely to be the result of an adverse effect of PC61 on the T cells because a previous study has shown PC61 does not deplete T cell populations other than Treg (138). It is possible that the anti-tumour response did not improve in Treg depleted mice over the non depleted mice because of the long delay between PC61 treatment and the re-establishment of tumour growth. The *in vivo* activation of tumour specific T cells caused the partial regression of the tumour to a similar degree in both the Treg depleted and non depleted mice and this probably negated any initial delay in tumour growth caused by the PC61 treatment. Mice received DC treatment 11 days after PC61 treatment, and although serum levels of PC61 were likely reduced by this stage (416), they were still sufficient to significantly suppress T cell expansion. According to Figure 6.3, at day 26 after PC61 treatment, which is also 15 days after DC treatment, the transferred T cell population may be expected to have contracted approximately 4 fold. At this stage, there would be a small population of functional Treg in the PC61 treated mice and the re-establishment of tumour growth indicated that the transferred T cell population was no longer capable of controlling tumour growth in both the Treg depleted and non depleted groups.

6.5 Conclusions

An *in vivo* immunisation model was successfully adapted and used to show that Treg do not require perforin to mediate suppression of clonal T cell expansion or effector function. Increased cell death was observed in the presence of perforin sufficient and deficient Treg, indicating that it is unlikely that the Treg are directly killing T cells using the perforin-granzyme pathway as a mechanism of suppression. The model was found to be unsuitable to assess the perforin dependence of Treg mediated suppression of an anti-tumour response.

CHAPTER SEVEN

GENERAL DISCUSSION

The purpose of this thesis was to investigate and design strategies to improve the T cell mediated anti-tumour response. In particular, it was of interest to determine if the anti-tumour activity of activated $CD8^+$ T cells could be improved by inhibiting adenosine signalling. This thesis showed that both activated tumour specific T cells and tumour cells were inhibited *in vitro* by adenosine, an immunosuppressive molecule found in high amounts in the tumour microenvironment. Attempts to silence the A2a adenosine receptor gene in activated tumour specific $CD8^+$ T cells or treating mice with the adenosine receptor antagonist caffeine, however, did not result in an improved anti-tumour response when using the B16.OVA model.

The possibility that Treg are able to directly suppress the Ag presenting function of DC was also examined. TIDC and Treg were found to co-localise, suggesting that these cells might interact in the tumour environment. TIDC were also found to be defective in their ability to stimulate an anti-tumour immune response, however, this was not the result of Treg mediated suppression.

Lastly, this thesis investigated the hypothesis that Treg mediated suppression of the $CD8^+$ T cell response is perforin-dependent. The presence of Treg was associated with an increased rate of T cell death and Treg were found to suppress the proliferation of, the production of effector cytokines by and the cytotoxic function of $CD8^+$ T cells. These suppressive mechanisms of Treg, however, were not found to involve the perforin-granzyme pathway.

These findings further the understanding of how tumours evade the anti-tumour immune response and provide insight into designing new strategies or successfully combining existing strategies for the treatment of cancer using immunotherapy.

7.1 Implications of the findings of this thesis

As discussed in the general introduction, tumours contain a number of immunosuppressive factors, which lead to defective Ag presenting function of DC and impaired anti-tumour T cell responses. A wealth of *in vitro* and non-tumour *in vivo* data has suggested that DC function is inhibited by Treg, however, the results of this thesis suggest the defective TIDC function observed was not the result of Treg mediated suppression.

Tumours contain high numbers of Treg, which are associated with a poor survival outcome. It is currently unclear whether Treg accumulate in the tumour mostly as the result of CCL22 mediated recruitment of natural Treg, which are produced by the thymus, or if $CD4^+$ $Foxp3^-$ T cells are converted to Treg as the result of high levels of TGF-β, which is produced by malignant cells, Treg and MDSC. Treg are known to suppress the anti-tumour response but the target cell of Treg *in vivo* is unclear. The results of this thesis suggest that the phenotype and function of DC is unaffected by the presence of Treg. This is probably because the main mechanism of Treg mediated suppression of T cell responses is thought to be through the production of TGF-β and IL-10, which are also known to suppress DC function. Tumours typically have elevated levels of TGF-β and IL-10 but malignant cells and MDSC also produce these cytokines. Treg may, therefore, be capable of suppressing DC in tumours by producing TGF-β and IL-10, however this mechanism may be redundant in the tumour model because of the TGF-β and IL-10 produced by other cells. Experiments described in this thesis showed that Treg are able to suppress the anti-tumour immune response and this would suggest that in a tumour model, in addition to suppression by TGF-β and IL-10 production, Treg must also use TGF-β and IL-10 independent suppressive mechanisms. If this possibility were true, combining anti-TGF-β or anti-IL-10 therapies with therapies designed to inhibit or deplete Treg and MDSC may,

therefore, result in an anti-cancer immunotherapy of improved efficacy over the individual treatments.

Preliminary results from this thesis also indicated that the anti-tumour activity of *in vitro* activated $CD8^+$ T cells may be unaffected by the presence of Treg. These results suggest that Treg may mediate anti-tumour immune suppression *in vivo* by inhibiting early activation of the T cells. These findings suggest that the anti-tumour efficacy of *in vitro* activated T cells would not be improved by Treg depletion, however, the efficacy of *in vivo* activated T cells would be. This point is particularly important in human clinical trials where Treg are depleted using ONTAK, which consists of recombinant human IL-2 fused to fragments of diphtheria toxin. Unlike PC61, ONTAK is known to deplete $Foxp3^-$ $CD25^+$ T cells in addition to depleting $Foxp3^+$ $CD25^+$ Treg (138), which may confound the effects of Treg depletion using ONTAK. According to the points discussed below, both *in vitro* and *in vivo* activated T cell therapies are likely to show improved efficacy when given in combination with anti-MDSC treatments.

This thesis has shown that the defective Ag presenting function of TIDC is not the result of Treg mediated suppression of the DC instead, it may be because of the high levels of adenosine typically observed by other Authors in tumours. A number of *in vitro* studies have shown that adenosine is able to inhibit DC function in mice and humans (202-205). It is also possible that IL-10 producing MDSC are responsible for causing the defective Ag presenting function of TIDC (193, 417).

Studies have shown that many tumours contain high numbers of MDSC, which are negatively correlated with disease outcome. MDSC are known to directly suppress $CD8^+$ T cell proliferation and effector function, mostly through the production of TGF-β and IL-10

(222, 351, 359, 362). Interestingly, experiments described in this thesis that involved the adoptive transfer of activated OTI T cells into tumour bearing mice resulted in a significant increase in the frequency of $CD45^+$ $CD11b^+$ $Gr1^+$ cells, a phenotype consistent with MDSC. Activated T cells produce IFN-γ and GM-CSF (357, 418), both of which are known to cause the conversion of myeloid cells to MDSC (358-361). These findings suggest that the efficacy of adoptive T cell therapy in treating tumour-bearing individuals would be improved by concomitant treatments to block MDSC recruitment to the tumour or function. Treatments designed to inhibit MDSC function or prevent adenosine signalling may also improve the efficacy of cancer immunotherapies by improving the ability of DC to stimulate a T cell response and by restoring effector function to T cells.

It is evident from the findings of this thesis that there is considerable redundancy in the immunosuppressive mechanisms used by tumours, which means that these mechanisms may be able to compensate when one or more suppressive factors are reduced in response to immunotherapy. This possibility emphasises the need to understand the similarities and differences in the suppressive mechanisms utilised by tumours in order to design more effective tumour immunotherapies. Given the number of immunosuppressive mechanisms used by tumours and the level of redundancy of these mechanisms, the most reasonable strategy to treat cancer may involve combining active and passive forms of immunotherapy, rather than concentrating solely on treatments designed to relieve immunosuppression. For example, the adoptive transfer of activated $CD8^+$ T cells or tumour Ag loaded DC with mAb specific for TGF-β, to relieve immunosuppression and OX86 or CTLA-4, which can simultaneously inhibit Treg function and directly stimulate activated $CD8^+$ T cells is likely to be a promising approach to cancer immunotherapy in the future.

7.2 Summary and Conclusions

The main findings of this thesis can be summarised with the following points:

- Adenosine inhibits the proliferation of both activated $CD8^+$ T cells and tumour cells.
- The adoptive transfer of activated tumour specific $CD8^+$ T cells may result in an increase in the frequency of tumour infiltrating MDSC.
- The depletion of Treg causes a delay in tumour growth.
- Treg and DC have the potential to interact within tumours.
- The Ag presenting function of TIDC is defective, however, this is not due to suppression of the TIDC by Treg.
- Treg do not affect the ability of activated tumour specific $CD8^+$ T cells to reject tumours.
- In the presence of Treg there was more $CD8^+$ T cell apoptosis and the proliferation, production of effector cytokines and cytotoxic function of $CD8^+$ T cells was suppressed using a mechanism that does not include the perforin-granzyme pathway.

In conclusion, this thesis shows that high levels of adenosine and the presence of Treg are two mechanisms by which tumours evade the immune response. These mechanisms are distinct and yet they have some similarities in that one of the outcomes of both mechanisms may be the increased level of TGF-β and IL-10 in the tumour. These findings provide insight into future strategies for improving cancer immunotherapy such as improving the function or survival of DC. Understanding how immune suppression occurs

will help determine which treatments are most likely to combine favourably to further improve cancer immunotherapy techniques.

7.3 Future directions

The following is a list of suggestions for future work based on the findings of this thesis and indications for how these questions may be investigated:

- The development of a method to silence the A2a adenosine receptor of activated T cells that is reliable and yields a high percentage of successfully silenced, long-lived cells is necessary to make this therapy feasible in large scale clinical trials.
- Further work is necessary to establish whether adenosine affects the growth of B16.OVA (and other) tumours *in vivo* and to determine if the expression profile of the adenosine receptor subtypes on tumours affects their growth in the presence of adenosine.
    - The effect of adenosine on tumour cell proliferation *in vivo* could be investigated by comparing the growth of B16.OVA tumours to B16.OVA tumours in which the A2a receptors gene has been knocked out.
- It is important to determine if the naïve, OTI T cells that were able to proliferate in the *in vivo* proliferation assay after being transferred into tumour bearing hosts in the late stages of tumour growth were able to become effector T cells or if these cells became anergic.
    - OTI T cells could be isolated from the lymph nodes and spleens of mice 3 days after T cell transfer (~17 days after tumour inoculation) and transferred into tumour bearing hosts to determine if the cells have acquired effector function.

- It is of interest to determine whether Treg must traffic through the tumour tissue to fully acquire the ability to suppress anti-tumour immune responses in the lymph node.
    - The trafficking of Treg to lymph nodes and tumours requires expression of the Chemokine Receptors CCR7 (419) and CCR4 respectively (372, 375, 420). Therefore comparing the immune responses in RAG1-/- mice that have received CCR7 KO, CCR4 KO, CCR7 and CCR4 KO or wild type Treg should address this issue.
- There are a number of possibilities which need to be investigated to determine how Treg mediate suppression of the anti-tumour response:
    - Treg may prevent $CD8^+$ T cells from becoming fully activated which may result in T cell death
    - Treg may restrict access of the T cells to the DC resulting in fewer T cells becoming activated
    - TIDC do not stimulate a $CD4^+$ T cell response, regardless of the presence of Treg, however, DC vaccines are capable of eliciting a $CD4^+$ T cell response in the absence of Treg (139). These $CD4^+$ T cells may provide survival signals to the DC resulting in a prolonged and expanded $CD8^+$ T cell response in the absence of Treg. Therefore it is of interest to investigate the expression of pro-survival molecules such as bcl-2 and bcl-xl and anti-survival molecules such as bax and bad in DC and T cells in the presence and absence of Treg.

The findings of this thesis demonstrate that the tumour microenvironment is characterised by a number of different immunosuppressive factors. Often, eliminating one known suppressive factor fails to significantly improve the anti-tumour response because other

mechanisms are able to compensate for this loss. These observations emphasise the need to understand how the immunosuppressive mechanisms in tumours interact and overlap in addition to understanding the individual components.

REFERENCES

1. Steinman, R. M. 1991. The dendritic cell system and its role in immunogenicity. *Annu Rev Immunol* 9:271-296.
2. Mellman, I., S. J. Turley, and R. M. Steinman. 1998. Antigen processing for amateurs and professionals. *Trends Cell Biol* 8:231-237.
3. Inaba, K., and R. M. Steinman. 1984. Resting and sensitized T lymphocytes exhibit distinct stimulatory (antigen-presenting cell) requirements for growth and lymphokine release. *J Exp Med* 160:1717-1735.
4. Anjuere, F., P. Martin, I. Ferrero, M. L. Fraga, G. M. del Hoyo, N. Wright, and C. Ardavin. 1999. Definition of dendritic cell subpopulations present in the spleen, Peyer's patches, lymph nodes, and skin of the mouse. *Blood* 93:590-598.
5. Vremec, D., J. Pooley, H. Hochrein, L. Wu, and K. Shortman. 2000. CD4 and CD8 expression by dendritic cell subtypes in mouse thymus and spleen. *J Immunol* 164:2978-2986.
6. Henri, S., D. Vremec, A. Kamath, J. Waithman, S. Williams, C. Benoist, K. Burnham, S. Saeland, E. Handman, and K. Shortman. 2001. The dendritic cell populations of mouse lymph nodes. *J Immunol* 167:741-748.
7. d'Ostiani, C. F., G. Del Sero, A. Bacci, C. Montagnoli, A. Spreca, A. Mencacci, P. Ricciardi-Castagnoli, and L. Romani. 2000. Dendritic cells discriminate between yeasts and hyphae of the fungus Candida albicans. Implications for initiation of T helper cell immunity in vitro and in vivo. *J Exp Med* 191:1661-1674.
8. Langenkamp, A., M. Messi, A. Lanzavecchia, and F. Sallusto. 2000. Kinetics of dendritic cell activation: impact on priming of TH1, TH2 and nonpolarized T cells. *Nat Immunol* 1:311-316.
9. Anjuere, F., G. Martinez del Hoyo, P. Martin, and C. Ardavin. 2000. Langerhans cells acquire a CD8+ dendritic cell phenotype on maturation by CD40 ligation. *J Leukoc Biol* 67:206-209.
10. Merad, M., L. Fong, J. Bogenberger, and E. G. Engleman. 2000. Differentiation of myeloid dendritic cells into CD8alpha-positive dendritic cells in vivo. *Blood* 96:1865-1872.
11. Belz, G. T., C. M. Smith, L. Kleinert, P. Reading, A. Brooks, K. Shortman, F. R. Carbone, and W. R. Heath. 2004. Distinct migrating and nonmigrating dendritic cell populations are involved in MHC class I-restricted antigen presentation after lung infection with virus. *Proc Natl Acad Sci U S A* 101:8670-8675.
12. Allan, R. S., C. M. Smith, G. T. Belz, A. L. van Lint, L. M. Wakim, W. R. Heath, and F. R. Carbone. 2003. Epidermal viral immunity induced by CD8alpha+ dendritic cells but not by Langerhans cells. *Science* 301:1925-1928.
13. Allan, R. S., J. Waithman, S. Bedoui, C. M. Jones, J. A. Villadangos, Y. Zhan, A. M. Lew, K. Shortman, W. R. Heath, and F. R. Carbone. 2006. Migratory dendritic cells transfer antigen to a lymph node-resident dendritic cell population for efficient CTL priming. *Immunity* 25:153-162.
14. den Haan, J. M., S. M. Lehar, and M. J. Bevan. 2000. CD8(+) but not CD8(-) dendritic cells cross-prime cytotoxic T cells in vivo. *J Exp Med* 192:1685-1696.
15. Pooley, J. L., W. R. Heath, and K. Shortman. 2001. Cutting edge: intravenous soluble antigen is presented to CD4 T cells by CD8- dendritic cells, but cross-presented to CD8 T cells by CD8+ dendritic cells. *J Immunol* 166:5327-5330.

16. Sallusto, F., P. Schaerli, P. Loetscher, C. Schaniel, D. Lenig, C. R. Mackay, S. Qin, and A. Lanzavecchia. 1998. Rapid and coordinated switch in chemokine receptor expression during dendritic cell maturation. *Eur J Immunol* 28:2760-2769.
17. Albert, M. L., M. Jegathesan, and R. B. Darnell. 2001. Dendritic cell maturation is required for the cross-tolerization of CD8+ T cells. *Nat Immunol* 2:1010-1017.
18. Kamath, A. T., J. Pooley, M. A. O'Keeffe, D. Vremec, Y. Zhan, A. M. Lew, A. D'Amico, L. Wu, D. F. Tough, and K. Shortman. 2000. The development, maturation, and turnover rate of mouse spleen dendritic cell populations. *J Immunol* 165:6762-6770.
19. Jiang, A., O. Bloom, S. Ono, W. Cui, J. Unternaehrer, S. Jiang, J. A. Whitney, J. Connolly, J. Banchereau, and I. Mellman. 2007. Disruption of E-cadherin-mediated adhesion induces a functionally distinct pathway of dendritic cell maturation. *Immunity* 27:610-624.
20. Adler, A. J., D. W. Marsh, G. S. Yochum, J. L. Guzzo, A. Nigam, W. G. Nelson, and D. M. Pardoll. 1998. CD4+ T cell tolerance to parenchymal self-antigens requires presentation by bone marrow-derived antigen-presenting cells. *J Exp Med* 187:1555-1564.
21. Anderson, M. J., K. Shafer-Weaver, N. M. Greenberg, and A. A. Hurwitz. 2007. Tolerization of tumor-specific T cells despite efficient initial priming in a primary murine model of prostate cancer. *J Immunol* 178:1268-1276.
22. Kurts, C., H. Kosaka, F. R. Carbone, J. F. Miller, and W. R. Heath. 1997. Class I-restricted cross-presentation of exogenous self-antigens leads to deletion of autoreactive CD8(+) T cells. *J Exp Med* 186:239-245.
23. Cella, M., D. Scheidegger, K. Palmer-Lehmann, P. Lane, A. Lanzavecchia, and G. Alber. 1996. Ligation of CD40 on dendritic cells triggers production of high levels of interleukin-12 and enhances T cell stimulatory capacity: T-T help via APC activation. *J Exp Med* 184:747-752.
24. Koch, F., U. Stanzl, P. Jennewein, K. Janke, C. Heufler, E. Kampgen, N. Romani, and G. Schuler. 1996. High level IL-12 production by murine dendritic cells: upregulation via MHC class II and CD40 molecules and downregulation by IL-4 and IL-10. *J Exp Med* 184:741-746.
25. Heath, W. R., and F. R. Carbone. 2001. Cross-presentation in viral immunity and self-tolerance. *Nat Rev Immunol* 1:126-134.
26. Kaisho, T., and S. Akira. 2001. Dendritic-cell function in Toll-like receptor- and MyD88-knockout mice. *Trends Immunol* 22:78-83.
27. Akira, S., K. Takeda, and T. Kaisho. 2001. Toll-like receptors: critical proteins linking innate and acquired immunity. *Nat Immunol* 2:675-680.
28. Cumberbatch, M., and I. Kimber. 1995. Tumour necrosis factor-alpha is required for accumulation of dendritic cells in draining lymph nodes and for optimal contact sensitization. *Immunology* 84:31-35.
29. Roake, J. A., A. S. Rao, P. J. Morris, C. P. Larsen, D. F. Hankins, and J. M. Austyn. 1995. Dendritic cell loss from nonlymphoid tissues after systemic administration of lipopolysaccharide, tumor necrosis factor, and interleukin 1. *J Exp Med* 181:2237-2247.
30. Farkas, A. M., T. M. Kilgore, and M. T. Lotze. 2007. Detecting DNA: getting and begetting cancer. *Curr Opin Investig Drugs* 8:981-986.
31. Nylandsted, J., M. Gyrd-Hansen, A. Danielewicz, N. Fehrenbacher, U. Lademann, M. Hoyer-Hansen, E. Weber, G. Multhoff, M. Rohde, and M. Jaattela. 2004. Heat shock protein 70 promotes cell survival by inhibiting lysosomal membrane permeabilization. *J Exp Med* 200:425-435.

32. Lu, W. J., N. P. Lee, S. Fatima, and J. M. Luk. 2009. Heat shock proteins in cancer: signaling pathways, tumor markers and molecular targets in liver malignancy. *Protein Pept Lett* 16:508-516.
33. Hsieh, C. S., S. E. Macatonia, C. S. Tripp, S. F. Wolf, A. O'Garra, and K. M. Murphy. 1993. Development of TH1 CD4+ T cells through IL-12 produced by Listeria-induced macrophages. *Science* 260:547-549.
34. Macatonia, S. E., N. A. Hosken, M. Litton, P. Vieira, C. S. Hsieh, J. A. Culpepper, M. Wysocka, G. Trinchieri, K. M. Murphy, and A. O'Garra. 1995. Dendritic cells produce IL-12 and direct the development of Th1 cells from naive CD4+ T cells. *J Immunol* 154:5071-5079.
35. Stoll, S., H. Jonuleit, E. Schmitt, G. Muller, H. Yamauchi, M. Kurimoto, J. Knop, and A. H. Enk. 1998. Production of functional IL-18 by different subtypes of murine and human dendritic cells (DC): DC-derived IL-18 enhances IL-12-dependent Th1 development. *Eur J Immunol* 28:3231-3239.
36. Siegemund, S., N. Schutze, M. A. Freudenberg, M. B. Lutz, R. K. Straubinger, and G. Alber. 2007. Production of IL-12, IL-23 and IL-27p28 by bone marrow-derived conventional dendritic cells rather than macrophages after LPS/TLR4-dependent induction by Salmonella Enteritidis. *Immunobiology* 212:739-750.
37. Yasuda, K., C. Richez, J. W. Maciaszek, N. Agrawal, S. Akira, A. Marshak-Rothstein, and I. R. Rifkin. 2007. Murine dendritic cell type I IFN production induced by human IgG-RNA immune complexes is IFN regulatory factor (IRF)5 and IRF7 dependent and is required for IL-6 production. *J Immunol* 178:6876-6885.
38. Sparwasser, T., E. S. Koch, R. M. Vabulas, K. Heeg, G. B. Lipford, J. W. Ellwart, and H. Wagner. 1998. Bacterial DNA and immunostimulatory CpG oligonucleotides trigger maturation and activation of murine dendritic cells. *Eur J Immunol* 28:2045-2054.
39. Rigby, R. J., S. C. Knight, M. A. Kamm, and A. J. Stagg. 2005. Production of interleukin (IL)-10 and IL-12 by murine colonic dendritic cells in response to microbial stimuli. *Clin Exp Immunol* 139:245-256.
40. Zhu, J., and W. E. Paul. 2008. CD4 T cells: fates, functions, and faults. *Blood* 112:1557-1569.
41. Sad, S., R. Marcotte, and T. R. Mosmann. 1995. Cytokine-induced differentiation of precursor mouse CD8+ T cells into cytotoxic CD8+ T cells secreting Th1 or Th2 cytokines. *Immunity* 2:271-279.
42. Croft, M., L. Carter, S. L. Swain, and R. W. Dutton. 1994. Generation of polarized antigen-specific CD8 effector populations: reciprocal action of interleukin (IL)-4 and IL-12 in promoting type 2 versus type 1 cytokine profiles. *J Exp Med* 180:1715-1728.
43. Moore, M. W., F. R. Carbone, and M. J. Bevan. 1988. Introduction of soluble protein into the class I pathway of antigen processing and presentation. *Cell* 54:777-785.
44. Probst, H. C., and M. van den Broek. 2005. Priming of CTLs by lymphocytic choriomeningitis virus depends on dendritic cells. *J Immunol* 174:3920-3924.
45. Uebel, S., and R. Tampe. 1999. Specificity of the proteasome and the TAP transporter. *Curr Opin Immunol* 11:203-208.
46. York, I. A., and K. L. Rock. 1996. Antigen processing and presentation by the class I major histocompatibility complex. *Annu Rev Immunol* 14:369-396.
47. Khalil, H., A. Brunet, I. Saba, R. Terra, R. P. Sekaly, and J. Thibodeau. 2003. The MHC class II beta chain cytoplasmic tail overcomes the invariant chain p35-encoded endoplasmic reticulum retention signal. *Int Immunol* 15:1249-1263.

48. Lamb, C. A., and P. Cresswell. 1992. Assembly and transport properties of invariant chain trimers and HLA-DR-invariant chain complexes. *J Immunol* 148:3478-3482.
49. Trombetta, E. S., M. Ebersold, W. Garrett, M. Pypaert, and I. Mellman. 2003. Activation of lysosomal function during dendritic cell maturation. *Science* 299:1400-1403.
50. Burgdorf, S., A. Kautz, V. Bohnert, P. A. Knolle, and C. Kurts. 2007. Distinct pathways of antigen uptake and intracellular routing in CD4 and CD8 T cell activation. *Science* 316:612-616.
51. Bevan, M. J. 1987. Antigen recognition. Class discrimination in the world of immunology. *Nature* 325:192-194.
52. Huang, A. Y., P. Golumbek, M. Ahmadzadeh, E. Jaffee, D. Pardoll, and H. Levitsky. 1994. Role of bone marrow-derived cells in presenting MHC class I-restricted tumor antigens. *Science* 264:961-965.
53. Kurts, C., J. F. Miller, R. M. Subramaniam, F. R. Carbone, and W. R. Heath. 1998. Major histocompatibility complex class I-restricted cross-presentation is biased towards high dose antigens and those released during cellular destruction. *J Exp Med* 188:409-414.
54. Pfeifer, J. D., M. J. Wick, R. L. Roberts, K. Findlay, S. J. Normark, and C. V. Harding. 1993. Phagocytic processing of bacterial antigens for class I MHC presentation to T cells. *Nature* 361:359-362.
55. Kovacsovics-Bankowski, M., and K. L. Rock. 1995. A phagosome-to-cytosol pathway for exogenous antigens presented on MHC class I molecules. *Science* 267:243-246.
56. Ramirez, M. C., and L. J. Sigal. 2002. Macrophages and dendritic cells use the cytosolic pathway to rapidly cross-present antigen from live, vaccinia-infected cells. *J Immunol* 169:6733-6742.
57. Shen, Z., G. Reznikoff, G. Dranoff, and K. L. Rock. 1997. Cloned dendritic cells can present exogenous antigens on both MHC class I and class II molecules. *J Immunol* 158:2723-2730.
58. Ackerman, A. L., C. Kyritsis, R. Tampe, and P. Cresswell. 2003. Early phagosomes in dendritic cells form a cellular compartment sufficient for cross presentation of exogenous antigens. *Proc Natl Acad Sci U S A* 100:12889-12894.
59. Guermonprez, P., L. Saveanu, M. Kleijmeer, J. Davoust, P. Van Endert, and S. Amigorena. 2003. ER-phagosome fusion defines an MHC class I cross-presentation compartment in dendritic cells. *Nature* 425:397-402.
60. Houde, M., S. Bertholet, E. Gagnon, S. Brunet, G. Goyette, A. Laplante, M. F. Princiotta, P. Thibault, D. Sacks, and M. Desjardins. 2003. Phagosomes are competent organelles for antigen cross-presentation. *Nature* 425:402-406.
61. Inaba, K., M. Inaba, M. Naito, and R. M. Steinman. 1993. Dendritic cell progenitors phagocytose particulates, including bacillus Calmette-Guerin organisms, and sensitize mice to mycobacterial antigens in vivo. *J Exp Med* 178:479-488.
62. Sallusto, F., M. Cella, C. Danieli, and A. Lanzavecchia. 1995. Dendritic cells use macropinocytosis and the mannose receptor to concentrate macromolecules in the major histocompatibility complex class II compartment: downregulation by cytokines and bacterial products. *J Exp Med* 182:389-400.
63. Jiang, W., W. J. Swiggard, C. Heufler, M. Peng, A. Mirza, R. M. Steinman, and M. C. Nussenzweig. 1995. The receptor DEC-205 expressed by dendritic cells and thymic epithelial cells is involved in antigen processing. *Nature* 375:151-155.

64. Curtsinger, J. M., D. C. Lins, and M. F. Mescher. 2003. Signal 3 determines tolerance versus full activation of naive CD8 T cells: dissociating proliferation and development of effector function. *J Exp Med* 197:1141-1151.
65. Shortman, K., and Y. J. Liu. 2002. Mouse and human dendritic cell subtypes. *Nat Rev Immunol* 2:151-161.
66. Testi, R., J. H. Phillips, and L. L. Lanier. 1989. T cell activation via Leu-23 (CD69). *J Immunol* 143:1123-1128.
67. D'Souza, W. N., and L. Lefrancois. 2003. IL-2 is not required for the initiation of CD8 T cell cycling but sustains expansion. *J Immunol* 171:5727-5735.
68. Pihlgren, M., C. Arpin, T. Walzer, M. Tomkowiak, A. Thomas, J. Marvel, and P. M. Dubois. 1999. Memory CD44(int) CD8 T cells show increased proliferative responses and IFN-gamma production following antigenic challenge in vitro. *Int Immunol* 11:699-706.
69. Venturi, G. M., L. Tu, T. Kadono, A. I. Khan, Y. Fujimoto, P. Oshel, C. B. Bock, A. S. Miller, R. M. Albrecht, P. Kubes, D. A. Steeber, and T. F. Tedder. 2003. Leukocyte migration is regulated by L-selectin endoproteolytic release. *Immunity* 19:713-724.
70. Schluns, K. S., and L. Lefrancois. 2003. Cytokine control of memory T-cell development and survival. *Nat Rev Immunol* 3:269-279.
71. Voehringer, D., M. Koschella, and H. Pircher. 2002. Lack of proliferative capacity of human effector and memory T cells expressing killer cell lectinlike receptor G1 (KLRG1). *Blood* 100:3698-3702.
72. McHugh, R. S., M. J. Whitters, C. A. Piccirillo, D. A. Young, E. M. Shevach, M. Collins, and M. C. Byrne. 2002. CD4(+)CD25(+) immunoregulatory T cells: gene expression analysis reveals a functional role for the glucocorticoid-induced TNF receptor. *Immunity* 16:311-323.
73. Gelfanova, V., Y. Lai, V. Gelfanov, S. Tzou, Y. Tu, and N. Liao. 1999. Modulation of cytokine responses of murine CD8+ alphabeta intestinal intraepithelial lymphocytes by IL-4 and IL-12. *J Biomed Sci* 6:269-276.
74. Auphan-Anezin, N., G. Verdeil, and A. M. Schmitt-Verhulst. 2003. Distinct thresholds for CD8 T cell activation lead to functional heterogeneity: CD8 T cell priming can occur independently of cell division. *J Immunol* 170:2442-2448.
75. Masopust, D., and R. Ahmed. 2004. Reflections on CD8 T-cell activation and memory. *Immunol Res* 29:151-160.
76. Sallusto, F., D. Lenig, R. Forster, M. Lipp, and A. Lanzavecchia. 1999. Two subsets of memory T lymphocytes with distinct homing potentials and effector functions. *Nature* 401:708-712.
77. Barry, M., and R. C. Bleackley. 2002. Cytotoxic T lymphocytes: all roads lead to death. *Nat Rev Immunol* 2:401-409.
78. Lavrik, I., A. Golks, and P. H. Krammer. 2005. Death receptor signaling. *J Cell Sci* 118:265-267.
79. Dighe, A. S., E. Richards, L. J. Old, and R. D. Schreiber. 1994. Enhanced in vivo growth and resistance to rejection of tumor cells expressing dominant negative IFN gamma receptors. *Immunity* 1:447-456.
80. Kaplan, D. H., V. Shankaran, A. S. Dighe, E. Stockert, M. Aguet, L. J. Old, and R. D. Schreiber. 1998. Demonstration of an interferon gamma-dependent tumor surveillance system in immunocompetent mice. *Proc Natl Acad Sci U S A* 95:7556-7561.
81. Street, S. E., E. Cretney, and M. J. Smyth. 2001. Perforin and interferon-gamma activities independently control tumor initiation, growth, and metastasis. *Blood* 97:192-197.

82. Street, S. E., J. A. Trapani, D. MacGregor, and M. J. Smyth. 2002. Suppression of lymphoma and epithelial malignancies effected by interferon gamma. *J Exp Med* 196:129-134.
83. Schreiber, R. D., L. J. Hicks, A. Celada, N. A. Buchmeier, and P. W. Gray. 1985. Monoclonal antibodies to murine gamma-interferon which differentially modulate macrophage activation and antiviral activity. *J Immunol* 134:1609-1618.
84. Spiotto, M. T., D. A. Rowley, and H. Schreiber. 2004. Bystander elimination of antigen loss variants in established tumors. *Nat Med* 10:294-298.
85. Beatty, G., and Y. Paterson. 2001. IFN-gamma-dependent inhibition of tumor angiogenesis by tumor-infiltrating CD4+ T cells requires tumor responsiveness to IFN-gamma. *J Immunol* 166:2276-2282.
86. Ratner, A., and W. R. Clark. 1993. Role of TNF-alpha in CD8+ cytotoxic T lymphocyte-mediated lysis. *J Immunol* 150:4303-4314.
87. Wen, L. P., K. Madani, J. A. Fahrni, S. R. Duncan, and G. D. Rosen. 1997. Dexamethasone inhibits lung epithelial cell apoptosis induced by IFN-gamma and Fas. *Am J Physiol* 273:L921-929.
88. Deiss, L. P., H. Galinka, H. Berissi, O. Cohen, and A. Kimchi. 1996. Cathepsin D protease mediates programmed cell death induced by interferon-gamma, Fas/APO-1 and TNF-alpha. *EMBO J* 15:3861-3870.
89. Shustov, A., P. Nguyen, F. Finkelman, K. B. Elkon, and C. S. Via. 1998. Differential expression of Fas and Fas ligand in acute and chronic graft-versus-host disease: up-regulation of Fas and Fas ligand requires CD8+ T cell activation and IFN-gamma production. *J Immunol* 161:2848-2855.
90. Nagata, S., and P. Golstein. 1995. The Fas death factor. *Science* 267:1449-1456.
91. Ebnet, K., M. Hausmann, F. Lehmann-Grube, A. Mullbacher, M. Kopf, M. Lamers, and M. M. Simon. 1995. Granzyme A-deficient mice retain potent cell-mediated cytotoxicity. *EMBO J* 14:4230-4239.
92. Kagi, D., B. Ledermann, K. Burki, P. Seiler, B. Odermatt, K. J. Olsen, E. R. Podack, R. M. Zinkernagel, and H. Hengartner. 1994. Cytotoxicity mediated by T cells and natural killer cells is greatly impaired in perforin-deficient mice. *Nature* 369:31-37.
93. van den Broek, M. E., D. Kagi, F. Ossendorp, R. Toes, S. Vamvakas, W. K. Lutz, C. J. Melief, R. M. Zinkernagel, and H. Hengartner. 1996. Decreased tumor surveillance in perforin-deficient mice. *J Exp Med* 184:1781-1790.
94. Blott, E. J., and G. M. Griffiths. 2002. Secretory lysosomes. *Nat Rev Mol Cell Biol* 3:122-131.
95. Browne, K. A., E. Blink, V. R. Sutton, C. J. Froelich, D. A. Jans, and J. A. Trapani. 1999. Cytosolic delivery of granzyme B by bacterial toxins: evidence that endosomal disruption, in addition to transmembrane pore formation, is an important function of perforin. *Mol Cell Biol* 19:8604-8615.
96. Pinkoski, M. J., M. Hobman, J. A. Heibein, K. Tomaselli, F. Li, P. Seth, C. J. Froelich, and R. C. Bleackley. 1998. Entry and trafficking of granzyme B in target cells during granzyme B-perforin-mediated apoptosis. *Blood* 92:1044-1054.
97. Andrews, D. M., C. E. Andoniou, P. Fleming, M. J. Smyth, and M. A. Degli-Esposti. 2008. The early kinetics of cytomegalovirus-specific CD8+ T-cell responses are not affected by antigen load or the absence of perforin or gamma interferon. *J Virol* 82:4931-4937.
98. Kagi, D., B. Odermatt, and T. W. Mak. 1999. Homeostatic regulation of CD8+ T cells by perforin. *Eur J Immunol* 29:3262-3272.
99. Trapani, J. A., V. R. Sutton, K. Y. Thia, Y. Q. Li, C. J. Froelich, D. A. Jans, M. S. Sandrin, and K. A. Browne. 2003. A clathrin/dynamin- and mannose-6-phosphate

receptor-independent pathway for granzyme B-induced cell death. *J Cell Biol* 160:223-233.

100. Shi, L., R. P. Kraut, R. Aebersold, and A. H. Greenberg. 1992. A natural killer cell granule protein that induces DNA fragmentation and apoptosis. *J Exp Med* 175:553-566.
101. Dennert, G., and E. R. Podack. 1983. Cytolysis by H-2-specific T killer cells. Assembly of tubular complexes on target membranes. *J Exp Med* 157:1483-1495.
102. Dourmashkin, R. R., P. Deteix, C. B. Simone, and P. Henkart. 1980. Electron microscopic demonstration of lesions in target cell membranes associated with antibody-dependent cellular cytotoxicity. *Clin Exp Immunol* 42:554-560.
103. Podack, E. R., and G. Dennert. 1983. Assembly of two types of tubules with putative cytolytic function by cloned natural killer cells. *Nature* 302:442-445.
104. Shi, L., S. Mai, S. Israels, K. Browne, J. A. Trapani, and A. H. Greenberg. 1997. Granzyme B (GraB) autonomously crosses the cell membrane and perforin initiates apoptosis and GraB nuclear localization. *J Exp Med* 185:855-866.
105. Odake, S., C. M. Kam, L. Narasimhan, M. Poe, J. T. Blake, O. Krahenbuhl, J. Tschopp, and J. C. Powers. 1991. Human and murine cytotoxic T lymphocyte serine proteases: subsite mapping with peptide thioester substrates and inhibition of enzyme activity and cytolysis by isocoumarins. *Biochemistry* 30:2217-2227.
106. Barry, M., J. A. Heibein, M. J. Pinkoski, S. F. Lee, R. W. Moyer, D. R. Green, and R. C. Bleackley. 2000. Granzyme B short-circuits the need for caspase 8 activity during granule-mediated cytotoxic T-lymphocyte killing by directly cleaving Bid. *Mol Cell Biol* 20:3781-3794.
107. Heibein, J. A., I. S. Goping, M. Barry, M. J. Pinkoski, G. C. Shore, D. R. Green, and R. C. Bleackley. 2000. Granzyme B-mediated cytochrome c release is regulated by the Bcl-2 family members bid and Bax. *J Exp Med* 192:1391-1402.
108. Sutton, V. R., J. E. Davis, M. Cancilla, R. W. Johnstone, A. A. Ruefli, K. Sedelies, K. A. Browne, and J. A. Trapani. 2000. Initiation of apoptosis by granzyme B requires direct cleavage of bid, but not direct granzyme B-mediated caspase activation. *J Exp Med* 192:1403-1414.
109. Tafani, M., T. G. Schneider, J. G. Pastorino, and J. L. Farber. 2000. Cytochrome c-dependent activation of caspase-3 by tumor necrosis factor requires induction of the mitochondrial permeability transition. *Am J Pathol* 156:2111-2121.
110. Slee, E. A., M. T. Harte, R. M. Kluck, B. B. Wolf, C. A. Casiano, D. D. Newmeyer, H. G. Wang, J. C. Reed, D. W. Nicholson, E. S. Alnemri, D. R. Green, and S. J. Martin. 1999. Ordering the cytochrome c-initiated caspase cascade: hierarchical activation of caspases-2, -3, -6, -7, -8, and -10 in a caspase-9-dependent manner. *J Cell Biol* 144:281-292.
111. Medema, J. P., R. E. Toes, C. Scaffidi, T. S. Zheng, R. A. Flavell, C. J. Melief, M. E. Peter, R. Offringa, and P. H. Krammer. 1997. Cleavage of FLICE (caspase-8) by granzyme B during cytotoxic T lymphocyte-induced apoptosis. *Eur J Immunol* 27:3492-3498.
112. Yang, X., H. R. Stennicke, B. Wang, D. R. Green, R. U. Janicke, A. Srinivasan, P. Seth, G. S. Salvesen, and C. J. Froelich. 1998. Granzyme B mimics apical caspases. Description of a unified pathway for trans-activation of executioner caspase-3 and -7. *J Biol Chem* 273:34278-34283.
113. Hoption Cann, S. A., J. P. van Netten, and C. van Netten. 2003. Dr William Coley and tumour regression: a place in history or in the future. *Postgrad Med J* 79:672-680.
114. Ehrlich, P. 1909. Ueber den jetzigen Stand der Karzinomforschung. *Net. Tijdschr. Geneeskd.* 5:273-290.

115. Burnet, M. 1957. Cancer; a biological approach. I. The processes of control. *Br Med J* 1:779-786.
116. Burnet, M. 1964. Immunological Factors in the Process of Carcinogenesis. *Br Med Bull* 20:154-158.
117. Dunn, G. P., L. J. Old, and R. D. Schreiber. 2004. The immunobiology of cancer immunosurveillance and immunoediting. *Immunity* 21:137-148.
118. Smyth, M. J., K. Y. Thia, S. E. Street, E. Cretney, J. A. Trapani, M. Taniguchi, T. Kawano, S. B. Pelikan, N. Y. Crowe, and D. I. Godfrey. 2000. Differential tumor surveillance by natural killer (NK) and NKT cells. *J Exp Med* 191:661-668.
119. Smyth, M. J., K. Y. Thia, S. E. Street, D. MacGregor, D. I. Godfrey, and J. A. Trapani. 2000. Perforin-mediated cytotoxicity is critical for surveillance of spontaneous lymphoma. *J Exp Med* 192:755-760.
120. Shankaran, V., H. Ikeda, A. T. Bruce, J. M. White, P. E. Swanson, L. J. Old, and R. D. Schreiber. 2001. IFNgamma and lymphocytes prevent primary tumour development and shape tumour immunogenicity. *Nature* 410:1107-1111.
121. Gatti, R. A., and R. A. Good. 1971. Occurrence of malignancy in immunodeficiency diseases. A literature review. *Cancer* 28:89-98.
122. Penn, I. 1999. Posttransplant malignancies. *Transplant Proc* 31:1260-1262.
123. Birkeland, S. A., H. H. Storm, L. U. Lamm, L. Barlow, I. Blohme, B. Forsberg, B. Eklund, O. Fjeldborg, M. Friedberg, L. Frodin, and et al. 1995. Cancer risk after renal transplantation in the Nordic countries, 1964-1986. *Int J Cancer* 60:183-189.
124. Boshoff, C., and R. Weiss. 2002. AIDS-related malignancies. *Nat Rev Cancer* 2:373-382.
125. van der Bruggen, P., C. Traversari, P. Chomez, C. Lurquin, E. De Plaen, B. Van den Eynde, A. Knuth, and T. Boon. 1991. A gene encoding an antigen recognized by cytolytic T lymphocytes on a human melanoma. *Science* 254:1643-1647.
126. Maraskovsky, E., S. Sjolander, D. P. Drane, M. Schnurr, T. T. Le, L. Mateo, T. Luft, K. A. Masterman, T. Y. Tai, Q. Chen, S. Green, A. Sjolander, M. J. Pearse, F. A. Lemonnier, W. Chen, J. Cebon, and A. Suhrbier. 2004. NY-ESO-1 protein formulated in ISCOMATRIX adjuvant is a potent anticancer vaccine inducing both humoral and CD8+ t-cell-mediated immunity and protection against NY-ESO-1+ tumors. *Clin Cancer Res* 10:2879-2890.
127. Kawakami, Y., S. Eliyahu, C. H. Delgado, P. F. Robbins, K. Sakaguchi, E. Appella, J. R. Yannelli, G. J. Adema, T. Miki, and S. A. Rosenberg. 1994. Identification of a human melanoma antigen recognized by tumor-infiltrating lymphocytes associated with in vivo tumor rejection. *Proc Natl Acad Sci U S A* 91:6458-6462.
128. Kawakami, Y., S. Eliyahu, K. Sakaguchi, P. F. Robbins, L. Rivoltini, J. R. Yannelli, E. Appella, and S. A. Rosenberg. 1994. Identification of the immunodominant peptides of the MART-1 human melanoma antigen recognized by the majority of HLA-A2-restricted tumor infiltrating lymphocytes. *J Exp Med* 180:347-352.
129. Kawakami, Y., X. Wang, T. Shofuda, H. Sumimoto, J. Tupesis, E. Fitzgerald, and S. Rosenberg. 2001. Isolation of a new melanoma antigen, MART-2, containing a mutated epitope recognized by autologous tumor-infiltrating T lymphocytes. *J Immunol* 166:2871-2877.
130. Yotnda, P., H. Firat, F. Garcia-Pons, Z. Garcia, G. Gourru, J. P. Vernant, F. A. Lemonnier, V. Leblond, and P. Langlade-Demoyen. 1998. Cytotoxic T cell response against the chimeric p210 BCR-ABL protein in patients with chronic myelogenous leukemia. *J Clin Invest* 101:2290-2296.

131. MacKie, R. M., R. Reid, and B. Junor. 2003. Fatal melanoma transferred in a donated kidney 16 years after melanoma surgery. *N Engl J Med* 348:567-568.
132. Wilson, L. J., R. T. Horvat, L. Tilzer, A. M. Meis, L. Montag, and M. Huntrakoon. 1992. Identification of donor melanoma in a renal transplant recipient. *Diagn Mol Pathol* 1:266-271.
133. Koebel, C. M., W. Vermi, J. B. Swann, N. Zerafa, S. J. Rodig, L. J. Old, M. J. Smyth, and R. D. Schreiber. 2007. Adaptive immunity maintains occult cancer in an equilibrium state. *Nature* 450:903-907.
134. Engel, A. M., I. M. Svane, J. Rygaard, and O. Werdelin. 1997. MCA sarcomas induced in scid mice are more immunogenic than MCA sarcomas induced in congenic, immunocompetent mice. *Scand J Immunol* 45:463-470.
135. Svane, I. M., A. M. Engel, M. B. Nielsen, H. G. Ljunggren, J. Rygaard, and O. Werdelin. 1996. Chemically induced sarcomas from nude mice are more immunogenic than similar sarcomas from congenic normal mice. *Eur J Immunol* 26:1844-1850.
136. Takahashi, H., F. Feuerhake, J. L. Kutok, S. Monti, P. Dal Cin, D. Neuberg, J. C. Aster, and M. A. Shipp. 2006. FAS death domain deletions and cellular FADD-like interleukin 1beta converting enzyme inhibitory protein (long) overexpression: alternative mechanisms for deregulating the extrinsic apoptotic pathway in diffuse large B-cell lymphoma subtypes. *Clin Cancer Res* 12:3265-3271.
137. Shin, M. S., H. S. Kim, S. H. Lee, W. S. Park, S. Y. Kim, J. Y. Park, J. H. Lee, S. K. Lee, S. N. Lee, S. S. Jung, J. Y. Han, H. Kim, J. Y. Lee, and N. J. Yoo. 2001. Mutations of tumor necrosis factor-related apoptosis-inducing ligand receptor 1 (TRAIL-R1) and receptor 2 (TRAIL-R2) genes in metastatic breast cancers. *Cancer Res* 61:4942-4946.
138. Matsushita, N., S. A. Pilon-Thomas, L. M. Martin, and A. I. Riker. 2008. Comparative methodologies of regulatory T cell depletion in a murine melanoma model. *J Immunol Methods* 333:167-179.
139. Prasad, S. J., K. J. Farrand, S. A. Matthews, J. H. Chang, R. S. McHugh, and F. Ronchese. 2005. Dendritic cells loaded with stressed tumor cells elicit long-lasting protective tumor immunity in mice depleted of CD4+CD25+ regulatory T cells. *J Immunol* 174:90-98.
140. Hermans, I. F., A. Daish, P. Moroni-Rawson, and F. Ronchese. 1997. Tumor-peptide-pulsed dendritic cells isolated from spleen or cultured in vitro from bone marrow precursors can provide protection against tumor challenge. *Cancer Immunol Immunother* 44:341-347.
141. Rawson, P., I. F. Hermans, S. P. Huck, J. M. Roberts, H. Pircher, and F. Ronchese. 2000. Immunotherapy with dendritic cells and tumor major histocompatibility complex class I-derived peptides requires a high density of antigen on tumor cells. *Cancer Res* 60:4493-4498.
142. Mayordomo, J. I., T. Zorina, W. J. Storkus, L. Zitvogel, C. Celluzzi, L. D. Falo, C. J. Melief, S. T. Ildstad, W. M. Kast, A. B. Deleo, and et al. 1995. Bone marrow-derived dendritic cells pulsed with synthetic tumour peptides elicit protective and therapeutic antitumour immunity. *Nat Med* 1:1297-1302.
143. Zitvogel, L., J. I. Mayordomo, T. Tjandrawan, A. B. DeLeo, M. R. Clarke, M. T. Lotze, and W. J. Storkus. 1996. Therapy of murine tumors with tumor peptide-pulsed dendritic cells: dependence on T cells, B7 costimulation, and T helper cell 1-associated cytokines. *J Exp Med* 183:87-97.
144. Fields, R. C., K. Shimizu, and J. J. Mule. 1998. Murine dendritic cells pulsed with whole tumor lysates mediate potent antitumor immune responses in vitro and in vivo. *Proc Natl Acad Sci U S A* 95:9482-9487.

145. Merad, M., T. Sugie, E. G. Engleman, and L. Fong. 2002. In vivo manipulation of dendritic cells to induce therapeutic immunity. *Blood* 99:1676-1682.
146. Celluzzi, C. M., J. I. Mayordomo, W. J. Storkus, M. T. Lotze, and L. D. Falo, Jr. 1996. Peptide-pulsed dendritic cells induce antigen-specific CTL-mediated protective tumor immunity. *J Exp Med* 183:283-287.
147. Peng, L., J. C. Krauss, G. E. Plautz, S. Mukai, S. Shu, and P. A. Cohen. 2000. T cell-mediated tumor rejection displays diverse dependence upon perforin and IFN-gamma mechanisms that cannot be predicted from in vitro T cell characteristics. *J Immunol* 165:7116-7124.
148. Macgregor, J. N., Q. Li, A. E. Chang, T. M. Braun, D. P. Hughes, and K. T. McDonagh. 2006. Ex vivo culture with interleukin (IL)-12 improves CD8(+) T-cell adoptive immunotherapy for murine leukemia independent of IL-18 or IFN-gamma but requires perforin. *Cancer Res* 66:4913-4921.
149. Boissonnas, A., L. Fetler, I. S. Zeelenberg, S. Hugues, and S. Amigorena. 2007. In vivo imaging of cytotoxic T cell infiltration and elimination of a solid tumor. *J Exp Med* 204:345-356.
150. Mumberg, D., P. A. Monach, S. Wanderling, M. Philip, A. Y. Toledano, R. D. Schreiber, and H. Schreiber. 1999. CD4(+) T cells eliminate MHC class II-negative cancer cells in vivo by indirect effects of IFN-gamma. *Proc Natl Acad Sci U S A* 96:8633-8638.
151. Goldenberg, M. M. 1999. Trastuzumab, a recombinant DNA-derived humanized monoclonal antibody, a novel agent for the treatment of metastatic breast cancer. *Clin Ther* 21:309-318.
152. Shan, D., J. A. Ledbetter, and O. W. Press. 1998. Apoptosis of malignant human B cells by ligation of CD20 with monoclonal antibodies. *Blood* 91:1644-1652.
153. Minard-Colin, V., Y. Xiu, J. C. Poe, M. Horikawa, C. M. Magro, Y. Hamaguchi, K. M. Haas, and T. F. Tedder. 2008. Lymphoma depletion during CD20 immunotherapy in mice is mediated by macrophage FcgammaRI, FcgammaRIII, and FcgammaRIV. *Blood* 112:1205-1213.
154. Onizuka, S., I. Tawara, J. Shimizu, S. Sakaguchi, T. Fujita, and E. Nakayama. 1999. Tumor rejection by in vivo administration of anti-CD25 (interleukin-2 receptor alpha) monoclonal antibody. *Cancer Res* 59:3128-3133.
155. Llopiz, D., J. Dotor, A. Zabaleta, J. J. Lasarte, J. Prieto, F. Borras-Cuesta, and P. Sarobe. 2008. Combined immunization with adjuvant molecules poly(I:C) and anti-CD40 plus a tumor antigen has potent prophylactic and therapeutic antitumor effects. *Cancer Immunol Immunother* 57:19-29.
156. Piconese, S., B. Valzasina, and M. P. Colombo. 2008. OX40 triggering blocks suppression by regulatory T cells and facilitates tumor rejection. *J Exp Med* 205:825-839.
157. Quezada, S. A., K. S. Peggs, M. A. Curran, and J. P. Allison. 2006. CTLA4 blockade and GM-CSF combination immunotherapy alters the intratumor balance of effector and regulatory T cells. *J Clin Invest* 116:1935-1945.
158. Dannull, J., Z. Su, D. Rizzieri, B. K. Yang, D. Coleman, D. Yancey, A. Zhang, P. Dahm, N. Chao, E. Gilboa, and J. Vieweg. 2005. Enhancement of vaccine-mediated antitumor immunity in cancer patients after depletion of regulatory T cells. *J Clin Invest* 115:3623-3633.
159. Jonuleit, H., A. Giesecke-Tuettenberg, T. Tuting, B. Thurner-Schuler, T. B. Stuge, L. Paragnik, A. Kandemir, P. P. Lee, G. Schuler, J. Knop, and A. H. Enk. 2001. A comparison of two types of dendritic cell as adjuvants for the induction of melanoma-specific T-cell responses in humans following intranodal injection. *Int J Cancer* 93:243-251.

160. Thurner, B., I. Haendle, C. Roder, D. Dieckmann, P. Keikavoussi, H. Jonuleit, A. Bender, C. Maczek, D. Schreiner, P. von den Driesch, E. B. Brocker, R. M. Steinman, A. Enk, E. Kampgen, and G. Schuler. 1999. Vaccination with mage-3A1 peptide-pulsed mature, monocyte-derived dendritic cells expands specific cytotoxic T cells and induces regression of some metastases in advanced stage IV melanoma. *J Exp Med* 190:1669-1678.
161. Banchereau, J., A. K. Palucka, M. Dhodapkar, S. Burkeholder, N. Taquet, A. Rolland, S. Taquet, S. Coquery, K. M. Wittkowski, N. Bhardwaj, L. Pineiro, R. Steinman, and J. Fay. 2001. Immune and clinical responses in patients with metastatic melanoma to CD34(+) progenitor-derived dendritic cell vaccine. *Cancer Res* 61:6451-6458.
162. Rosenberg, S. A., R. M. Sherry, K. E. Morton, W. J. Scharfman, J. C. Yang, S. L. Topalian, R. E. Royal, U. Kammula, N. P. Restifo, M. S. Hughes, D. Schwartzentruber, D. M. Berman, S. L. Schwarz, L. T. Ngo, S. A. Mavroukakis, D. E. White, and S. M. Steinberg. 2005. Tumor progression can occur despite the induction of very high levels of self/tumor antigen-specific CD8+ T cells in patients with melanoma. *J Immunol* 175:6169-6176.
163. Schuler-Thurner, B., E. S. Schultz, T. G. Berger, G. Weinlich, S. Ebner, P. Woerl, A. Bender, B. Feuerstein, P. O. Fritsch, N. Romani, and G. Schuler. 2002. Rapid induction of tumor-specific type 1 T helper cells in metastatic melanoma patients by vaccination with mature, cryopreserved, peptide-loaded monocyte-derived dendritic cells. *J Exp Med* 195:1279-1288.
164. Mackensen, A., B. Herbst, J. L. Chen, G. Kohler, C. Noppen, W. Herr, G. C. Spagnoli, V. Cerundolo, and A. Lindemann. 2000. Phase I study in melanoma patients of a vaccine with peptide-pulsed dendritic cells generated in vitro from CD34(+) hematopoietic progenitor cells. *Int J Cancer* 86:385-392.
165. Rosenberg, S. A., J. C. Yang, and N. P. Restifo. 2004. Cancer immunotherapy: moving beyond current vaccines. *Nat Med* 10:909-915.
166. Richardson, M. A., T. Ramirez, N. C. Russell, and L. A. Moye. 1999. Coley toxins immunotherapy: a retrospective review. *Altern Ther Health Med* 5:42-47.
167. Ryschich, E., J. Schmidt, G. J. Hammerling, E. Klar, and R. Ganss. 2002. Transformation of the microvascular system during multistage tumorigenesis. *Int J Cancer* 97:719-725.
168. Nagy, J. A., S. H. Chang, A. M. Dvorak, and H. F. Dvorak. 2009. Why are tumour blood vessels abnormal and why is it important to know? *Br J Cancer* 100:865-869.
169. Helmlinger, G., F. Yuan, M. Dellian, and R. K. Jain. 1997. Interstitial pH and pO2 gradients in solid tumors in vivo: high-resolution measurements reveal a lack of correlation. *Nat Med* 3:177-182.
170. Blohm, U., D. Potthoff, A. J. van der Kogel, and H. Pircher. 2006. Solid tumors "melt" from the inside after successful CD8 T cell attack. *Eur J Immunol* 36:468-477.
171. Milne, K., R. O. Barnes, A. Girardin, M. A. Mawer, N. J. Nesslinger, A. Ng, J. S. Nielsen, R. Sahota, E. Tran, J. R. Webb, M. Q. Wong, D. A. Wick, A. Wray, E. McMurtrie, M. Kobel, S. E. Kalloger, C. B. Gilks, P. H. Watson, and B. H. Nelson. 2008. Tumor-infiltrating T cells correlate with NY-ESO-1-specific autoantibodies in ovarian cancer. *PLoS One* 3:e3409.
172. Karpati, R. M., S. M. Banks, B. Malissen, S. A. Rosenberg, M. A. Sheard, J. S. Weber, and R. J. Hodes. 1991. Phenotypic characterization of murine tumor-infiltrating T lymphocytes. *J Immunol* 146:2043-2051.

173. Chaput, N., G. Darrasse-Jeze, A. S. Bergot, C. Cordier, S. Ngo-Abdalla, D. Klatzmann, and O. Azogui. 2007. Regulatory T cells prevent CD8 T cell maturation by inhibiting CD4 Th cells at tumor sites. *J Immunol* 179:4969-4978.
174. Gerner, M. Y., K. A. Casey, and M. F. Mescher. 2008. Defective MHC class II presentation by dendritic cells limits CD4 T cell help for antitumor CD8 T cell responses. *J Immunol* 181:155-164.
175. Radoja, S., M. Saio, D. Schaer, M. Koneru, S. Vukmanovic, and A. B. Frey. 2001. CD8(+) tumor-infiltrating T cells are deficient in perforin-mediated cytolytic activity due to defective microtubule-organizing center mobilization and lytic granule exocytosis. *J Immunol* 167:5042-5051.
176. Chen, M. L., M. J. Pittet, L. Gorelik, R. A. Flavell, R. Weissleder, H. von Boehmer, and K. Khazaie. 2005. Regulatory T cells suppress tumor-specific CD8 T cell cytotoxicity through TGF-beta signals in vivo. *Proc Natl Acad Sci U S A* 102:419-424.
177. Derre, L., M. Corvaisier, B. Charreau, A. Moreau, E. Godefroy, A. Moreau-Aubry, F. Jotereau, and N. Gervois. 2006. Expression and release of HLA-E by melanoma cells and melanocytes: potential impact on the response of cytotoxic effector cells. *J Immunol* 177:3100-3107.
178. Tripathi, P., and S. Agrawal. 2006. Non-classical HLA-G antigen and its role in the cancer progression. *Cancer Invest* 24:178-186.
179. Curti, A., S. Trabanelli, V. Salvestrini, M. Baccarani, and R. M. Lemoli. 2009. The role of indoleamine 2,3-dioxygenase in the induction of immune tolerance: focus on hematology. *Blood* 113:2394-2401.
180. Gajewski, T. F., Y. Meng, C. Blank, I. Brown, A. Kacha, J. Kline, and H. Harlin. 2006. Immune resistance orchestrated by the tumor microenvironment. *Immunol Rev* 213:131-145.
181. Dummer, W., B. C. Bastian, N. Ernst, C. Schanzle, A. Schwaaf, and E. B. Brocker. 1996. Interleukin-10 production in malignant melanoma: preferential detection of IL-10-secreting tumor cells in metastatic lesions. *Int J Cancer* 66:607-610.
182. Kong, F. M., M. S. Anscher, T. Murase, B. D. Abbott, J. D. Iglehart, and R. L. Jirtle. 1995. Elevated plasma transforming growth factor-beta 1 levels in breast cancer patients decrease after surgical removal of the tumor. *Ann Surg* 222:155-162.
183. Blay, J., T. D. White, and D. W. Hoskin. 1997. The extracellular fluid of solid carcinomas contains immunosuppressive concentrations of adenosine. *Cancer Res* 57:2602-2605.
184. Apasov, S., J. F. Chen, P. Smith, and M. Sitkovsky. 2000. A(2A) receptor dependent and A(2A) receptor independent effects of extracellular adenosine on murine thymocytes in conditions of adenosine deaminase deficiency. *Blood* 95:3859-3867.
185. Huang, S., S. Apasov, M. Koshiba, and M. Sitkovsky. 1997. Role of A2a extracellular adenosine receptor-mediated signaling in adenosine-mediated inhibition of T-cell activation and expansion. *Blood* 90:1600-1610.
186. Koshiba, M., H. Kojima, S. Huang, S. Apasov, and M. V. Sitkovsky. 1997. Memory of extracellular adenosine A2A purinergic receptor-mediated signaling in murine T cells. *J Biol Chem* 272:25881-25889.
187. Lappas, C. M., J. M. Rieger, and J. Linden. 2005. A2A adenosine receptor induction inhibits IFN-gamma production in murine CD4+ T cells. *J Immunol* 174:1073-1080.
188. Dong, H., S. E. Strome, D. R. Salomao, H. Tamura, F. Hirano, D. B. Flies, P. C. Roche, J. Lu, G. Zhu, K. Tamada, V. A. Lennon, E. Celis, and L. Chen. 2002.

Tumor-associated B7-H1 promotes T-cell apoptosis: a potential mechanism of immune evasion. *Nat Med* 8:793-800.

189. Blank, C., I. Brown, A. C. Peterson, M. Spiotto, Y. Iwai, T. Honjo, and T. F. Gajewski. 2004. PD-L1/B7H-1 inhibits the effector phase of tumor rejection by T cell receptor (TCR) transgenic CD8+ T cells. *Cancer Res* 64:1140-1145.
190. Iwai, Y., M. Ishida, Y. Tanaka, T. Okazaki, T. Honjo, and N. Minato. 2002. Involvement of PD-L1 on tumor cells in the escape from host immune system and tumor immunotherapy by PD-L1 blockade. *Proc Natl Acad Sci U S A* 99:12293-12297.
191. Grauer, O. M., S. Nierkens, E. Bennink, L. W. Toonen, L. Boon, P. Wesseling, R. P. Sutmuller, and G. J. Adema. 2007. CD4+FoxP3+ regulatory T cells gradually accumulate in gliomas during tumor growth and efficiently suppress antiglioma immune responses in vivo. *Int J Cancer* 121:95-105.
192. Almand, B., J. R. Resser, B. Lindman, S. Nadaf, J. I. Clark, E. D. Kwon, D. P. Carbone, and D. I. Gabrilovich. 2000. Clinical significance of defective dendritic cell differentiation in cancer. *Clin Cancer Res* 6:1755-1766.
193. Bunt, S. K., L. Yang, P. Sinha, V. K. Clements, J. Leips, and S. Ostrand-Rosenberg. 2007. Reduced inflammation in the tumor microenvironment delays the accumulation of myeloid-derived suppressor cells and limits tumor progression. *Cancer Res* 67:10019-10026.
194. Sica, A., T. Schioppa, A. Mantovani, and P. Allavena. 2006. Tumour-associated macrophages are a distinct M2 polarised population promoting tumour progression: potential targets of anti-cancer therapy. *Eur J Cancer* 42:717-727.
195. Hamzah, J., M. Jugold, F. Kiessling, P. Rigby, M. Manzur, H. H. Marti, T. Rabie, S. Kaden, H. J. Grone, G. J. Hammerling, B. Arnold, and R. Ganss. 2008. Vascular normalization in Rgs5-deficient tumours promotes immune destruction. *Nature* 453:410-414.
196. Brown, J. M., and W. R. Wilson. 2004. Exploiting tumour hypoxia in cancer treatment. *Nat Rev Cancer* 4:437-447.
197. Cronstein, B. N. 1994. Adenosine, an endogenous anti-inflammatory agent. *J Appl Physiol* 76:5-13.
198. Bontemps, F., G. Van den Berghe, and H. G. Hers. 1983. Evidence for a substrate cycle between AMP and adenosine in isolated hepatocytes. *Proc Natl Acad Sci U S A* 80:2829-2833.
199. Bontemps, F., G. Van den Berghe, and H. G. Hers. 1986. Pathways of adenine nucleotide catabolism in erythrocytes. *J Clin Invest* 77:824-830.
200. Decking, U. K., G. Schlieper, K. Kroll, and J. Schrader. 1997. Hypoxia-induced inhibition of adenosine kinase potentiates cardiac adenosine release. *Circ Res* 81:154-164.
201. Fredholm, B. B., I. J. AP, K. A. Jacobson, K. N. Klotz, and J. Linden. 2001. International Union of Pharmacology. XXV. Nomenclature and classification of adenosine receptors. *Pharmacol Rev* 53:527-552.
202. Wilson, J. M., W. G. Ross, O. N. Agbai, R. Frazier, R. A. Figler, J. Rieger, J. Linden, and P. B. Ernst. 2009. The A2B adenosine receptor impairs the maturation and immunogenicity of dendritic cells. *J Immunol* 182:4616-4623.
203. Panther, E., S. Corinti, M. Idzko, Y. Herouy, M. Napp, A. la Sala, G. Girolomoni, and J. Norgauer. 2003. Adenosine affects expression of membrane molecules, cytokine and chemokine release, and the T-cell stimulatory capacity of human dendritic cells. *Blood* 101:3985-3990.
204. Novitskiy, S. V., S. Ryzhov, R. Zaynagetdinov, A. E. Goldstein, Y. Huang, O. Y. Tikhomirov, M. R. Blackburn, I. Biaggioni, D. P. Carbone, I. Feoktistov, and M.

M. Dikov. 2008. Adenosine receptors in regulation of dendritic cell differentiation and function. *Blood* 112:1822-1831.

205. Panther, E., M. Idzko, Y. Herouy, H. Rheinen, P. J. Gebicke-Haerter, U. Mrowietz, S. Dichmann, and J. Norgauer. 2001. Expression and function of adenosine receptors in human dendritic cells. *FASEB J* 15:1963-1970.
206. Williams, B. A., A. Manzer, J. Blay, and D. W. Hoskin. 1997. Adenosine acts through a novel extracellular receptor to inhibit granule exocytosis by natural killer cells. *Biochem Biophys Res Commun* 231:264-269.
207. Hourani, S. M. 1996. Purinoceptors and platelet aggregation. *J Auton Pharmacol* 16:349-352.
208. Raskovalova, T., X. Huang, M. Sitkovsky, L. C. Zacharia, E. K. Jackson, and E. Gorelik. 2005. Gs protein-coupled adenosine receptor signaling and lytic function of activated NK cells. *J Immunol* 175:4383-4391.
209. Link, A. A., T. Kino, J. A. Worth, J. L. McGuire, M. L. Crane, G. P. Chrousos, R. L. Wilder, and I. J. Elenkov. 2000. Ligand-activation of the adenosine A2a receptors inhibits IL-12 production by human monocytes. *J Immunol* 164:436-442.
210. Hasko, G., D. G. Kuhel, J. F. Chen, M. A. Schwarzschild, E. A. Deitch, J. G. Mabley, A. Marton, and C. Szabo. 2000. Adenosine inhibits IL-12 and TNF-[alpha] production via adenosine A2a receptor-dependent and independent mechanisms. *FASEB J* 14:2065-2074.
211. Parmely, M. J., W. W. Zhou, C. K. Edwards, 3rd, D. R. Borcherding, R. Silverstein, and D. C. Morrison. 1993. Adenosine and a related carbocyclic nucleoside analogue selectively inhibit tumor necrosis factor-alpha production and protect mice against endotoxin challenge. *J Immunol* 151:389-396.
212. Fredholm, B. B., Y. Zhang, and I. van der Ploeg. 1996. Adenosine A2A receptors mediate the inhibitory effect of adenosine on formyl-Met-Leu-Phe-stimulated respiratory burst in neutrophil leucocytes. *Naunyn Schmiedebergs Arch Pharmacol* 354:262-267.
213. Revan, S., M. C. Montesinos, D. Naime, S. Landau, and B. N. Cronstein. 1996. Adenosine A2 receptor occupancy regulates stimulated neutrophil function via activation of a serine/threonine protein phosphatase. *J Biol Chem* 271:17114-17118.
214. van der Hoeven, D., T. C. Wan, and J. A. Auchampach. 2008. Activation of the A(3) adenosine receptor suppresses superoxide production and chemotaxis of mouse bone marrow neutrophils. *Mol Pharmacol* 74:685-696.
215. Raskovalova, T., A. Lokshin, X. Huang, Y. Su, M. Mandic, H. M. Zarour, E. K. Jackson, and E. Gorelik. 2007. Inhibition of cytokine production and cytotoxic activity of human antimelanoma specific CD8+ and CD4+ T lymphocytes by adenosine-protein kinase A type I signaling. *Cancer Res* 67:5949-5956.
216. Sakaguchi, S., N. Sakaguchi, M. Asano, M. Itoh, and M. Toda. 1995. Immunologic self-tolerance maintained by activated T cells expressing IL-2 receptor alpha-chains (CD25). Breakdown of a single mechanism of self-tolerance causes various autoimmune diseases. *J Immunol* 155:1151-1164.
217. Chen, Y., V. K. Kuchroo, J. Inobe, D. A. Hafler, and H. L. Weiner. 1994. Regulatory T cell clones induced by oral tolerance: suppression of autoimmune encephalomyelitis. *Science* 265:1237-1240.
218. Groux, H., A. O'Garra, M. Bigler, M. Rouleau, S. Antonenko, J. E. de Vries, and M. G. Roncarolo. 1997. A CD4+ T-cell subset inhibits antigen-specific T-cell responses and prevents colitis. *Nature* 389:737-742.
219. Brunkow, M. E., E. W. Jeffery, K. A. Hjerrild, B. Paeper, L. B. Clark, S. A. Yasayko, J. E. Wilkinson, D. Galas, S. F. Ziegler, and F. Ramsdell. 2001.

Disruption of a new forkhead/winged-helix protein, scurfin, results in the fatal lymphoproliferative disorder of the scurfy mouse. *Nat Genet* 27:68-73.

220. Noble, A., A. Giorgini, and J. A. Leggat. 2006. Cytokine-induced IL-10-secreting CD8 T cells represent a phenotypically distinct suppressor T-cell lineage. *Blood* 107:4475-4483.
221. Takahashi, T., T. Tagami, S. Yamazaki, T. Uede, J. Shimizu, N. Sakaguchi, T. W. Mak, and S. Sakaguchi. 2000. Immunologic self-tolerance maintained by CD25(+)CD4(+) regulatory T cells constitutively expressing cytotoxic T lymphocyte-associated antigen 4. *J Exp Med* 192:303-310.
222. Wing, K., Y. Onishi, P. Prieto-Martin, T. Yamaguchi, M. Miyara, Z. Fehervari, T. Nomura, and S. Sakaguchi. 2008. CTLA-4 control over Foxp3+ regulatory T cell function. *Science* 322:271-275.
223. Fontenot, J. D., J. P. Rasmussen, M. A. Gavin, and A. Y. Rudensky. 2005. A function for interleukin 2 in Foxp3-expressing regulatory T cells. *Nat Immunol* 6:1142-1151.
224. Hori, S., T. Nomura, and S. Sakaguchi. 2003. Control of regulatory T cell development by the transcription factor Foxp3. *Science* 299:1057-1061.
225. Takeda, I., S. Ine, N. Killeen, L. C. Ndhlovu, K. Murata, S. Satomi, K. Sugamura, and N. Ishii. 2004. Distinct roles for the OX40-OX40 ligand interaction in regulatory and nonregulatory T cells. *J Immunol* 172:3580-3589.
226. Deaglio, S., K. M. Dwyer, W. Gao, D. Friedman, A. Usheva, A. Erat, J. F. Chen, K. Enjyoji, J. Linden, M. Oukka, V. K. Kuchroo, T. B. Strom, and S. C. Robson. 2007. Adenosine generation catalyzed by CD39 and CD73 expressed on regulatory T cells mediates immune suppression. *J Exp Med* 204:1257-1265.
227. Borsellino, G., M. Kleinewietfeld, D. Di Mitri, A. Sternjak, A. Diamantini, R. Giometto, S. Hopner, D. Centonze, G. Bernardi, M. L. Dell'Acqua, P. M. Rossini, L. Battistini, O. Rotzschke, and K. Falk. 2007. Expression of ectonucleotidase CD39 by Foxp3+ Treg cells: hydrolysis of extracellular ATP and immune suppression. *Blood* 110:1225-1232.
228. Liu, W., A. L. Putnam, Z. Xu-Yu, G. L. Szot, M. R. Lee, S. Zhu, P. A. Gottlieb, P. Kapranov, T. R. Gingeras, B. Fazekas de St Groth, C. Clayberger, D. M. Soper, S. F. Ziegler, and J. A. Bluestone. 2006. CD127 expression inversely correlates with FoxP3 and suppressive function of human CD4+ T reg cells. *J Exp Med* 203:1701-1711.
229. Wang, J., A. Ioan-Facsinay, E. I. van der Voort, T. W. Huizinga, and R. E. Toes. 2007. Transient expression of FOXP3 in human activated nonregulatory CD4+ T cells. *Eur J Immunol* 37:129-138.
230. Zheng, Y., S. Z. Josefowicz, A. Kas, T. T. Chu, M. A. Gavin, and A. Y. Rudensky. 2007. Genome-wide analysis of Foxp3 target genes in developing and mature regulatory T cells. *Nature* 445:936-940.
231. Sharon, M., R. D. Klausner, B. R. Cullen, R. Chizzonite, and W. J. Leonard. 1986. Novel interleukin-2 receptor subunit detected by cross-linking under high-affinity conditions. *Science* 234:859-863.
232. Sadlack, B., H. Merz, H. Schorle, A. Schimpl, A. C. Feller, and I. Horak. 1993. Ulcerative colitis-like disease in mice with a disrupted interleukin-2 gene. *Cell* 75:253-261.
233. Suzuki, H., T. M. Kundig, C. Furlonger, A. Wakeham, E. Timms, T. Matsuyama, R. Schmits, J. J. Simard, P. S. Ohashi, H. Griesser, and et al. 1995. Deregulated T cell activation and autoimmunity in mice lacking interleukin-2 receptor beta. *Science* 268:1472-1476.

234. Liu, Y., P. Zhang, J. Li, A. B. Kulkarni, S. Perruche, and W. Chen. 2008. A critical function for TGF-beta signaling in the development of natural CD4+CD25+Foxp3+ regulatory T cells. *Nat Immunol* 9:632-640.
235. Huehn, J., J. K. Polansky, and A. Hamann. 2009. Epigenetic control of FOXP3 expression: the key to a stable regulatory T-cell lineage? *Nat Rev Immunol* 9:83-89.
236. Tran, D. Q., D. D. Glass, G. Uzel, D. A. Darnell, C. Spalding, S. M. Holland, and E. M. Shevach. 2009. Analysis of adhesion molecules, target cells, and role of IL-2 in human FOXP3+ regulatory T cell suppressor function. *J Immunol* 182:2929-2938.
237. Asano, M., M. Toda, N. Sakaguchi, and S. Sakaguchi. 1996. Autoimmune disease as a consequence of developmental abnormality of a T cell subpopulation. *J Exp Med* 184:387-396.
238. Fontenot, J. D., M. A. Gavin, and A. Y. Rudensky. 2003. Foxp3 programs the development and function of CD4+CD25+ regulatory T cells. *Nat Immunol* 4:330-336.
239. Fantini, M. C., C. Becker, G. Monteleone, F. Pallone, P. R. Galle, and M. F. Neurath. 2004. Cutting edge: TGF-beta induces a regulatory phenotype in CD4+CD25- T cells through Foxp3 induction and down-regulation of Smad7. *J Immunol* 172:5149-5153.
240. Valzasina, B., S. Piconese, C. Guiducci, and M. P. Colombo. 2006. Tumor-induced expansion of regulatory T cells by conversion of CD4+CD25- lymphocytes is thymus and proliferation independent. *Cancer Res* 66:4488-4495.
241. Williams, L. M., and A. Y. Rudensky. 2007. Maintenance of the Foxp3-dependent developmental program in mature regulatory T cells requires continued expression of Foxp3. *Nat Immunol* 8:277-284.
242. Walker, M. R., D. J. Kasprowicz, V. H. Gersuk, A. Benard, M. Van Landeghen, J. H. Buckner, and S. F. Ziegler. 2003. Induction of FoxP3 and acquisition of T regulatory activity by stimulated human CD4+CD25- T cells. *J Clin Invest* 112:1437-1443.
243. Allan, S. E., L. Passerini, R. Bacchetta, N. Crellin, M. Dai, P. C. Orban, S. F. Ziegler, M. G. Roncarolo, and M. K. Levings. 2005. The role of 2 FOXP3 isoforms in the generation of human CD4+ Tregs. *J Clin Invest* 115:3276-3284.
244. Gavin, M. A., T. R. Torgerson, E. Houston, P. DeRoos, W. Y. Ho, A. Stray-Pedersen, E. L. Ocheltree, P. D. Greenberg, H. D. Ochs, and A. Y. Rudensky. 2006. Single-cell analysis of normal and FOXP3-mutant human T cells: FOXP3 expression without regulatory T cell development. *Proc Natl Acad Sci U S A* 103:6659-6664.
245. Allan, S. E., S. Q. Crome, N. K. Crellin, L. Passerini, T. S. Steiner, R. Bacchetta, M. G. Roncarolo, and M. K. Levings. 2007. Activation-induced FOXP3 in human T effector cells does not suppress proliferation or cytokine production. *Int Immunol* 19:345-354.
246. Earle, K. E., Q. Tang, X. Zhou, W. Liu, S. Zhu, M. L. Bonyhadi, and J. A. Bluestone. 2005. In vitro expanded human CD4+CD25+ regulatory T cells suppress effector T cell proliferation. *Clin Immunol* 115:3-9.
247. Samy, E. T., K. M. Wheeler, R. J. Roper, C. Teuscher, and K. S. Tung. 2008. Cutting edge: Autoimmune disease in day 3 thymectomized mice is actively controlled by endogenous disease-specific regulatory T cells. *J Immunol* 180:4366-4370.
248. Dujardin, H. C., O. Burlen-Defranoux, L. Boucontet, P. Vieira, A. Cumano, and A. Bandeira. 2004. Regulatory potential and control of Foxp3 expression in newborn CD4+ T cells. *Proc Natl Acad Sci U S A* 101:14473-14478.

249. Kim, J. M., J. P. Rasmussen, and A. Y. Rudensky. 2007. Regulatory T cells prevent catastrophic autoimmunity throughout the lifespan of mice. *Nat Immunol* 8:191-197.
250. Gambineri, E., T. R. Torgerson, and H. D. Ochs. 2003. Immune dysregulation, polyendocrinopathy, enteropathy, and X-linked inheritance (IPEX), a syndrome of systemic autoimmunity caused by mutations of FOXP3, a critical regulator of T-cell homeostasis. *Curr Opin Rheumatol* 15:430-435.
251. Wildin, R. S., and A. Freitas. 2005. IPEX and FOXP3: clinical and research perspectives. *J Autoimmun* 25 Suppl:56-62.
252. Maloy, K. J., L. Salaun, R. Cahill, G. Dougan, N. J. Saunders, and F. Powrie. 2003. CD4+CD25+ T(R) cells suppress innate immune pathology through cytokine-dependent mechanisms. *J Exp Med* 197:111-119.
253. Hori, S., T. L. Carvalho, and J. Demengeot. 2002. CD25+CD4+ regulatory T cells suppress CD4+ T cell-mediated pulmonary hyperinflammation driven by Pneumocystis carinii in immunodeficient mice. *Eur J Immunol* 32:1282-1291.
254. Suvas, S., A. K. Azkur, B. S. Kim, U. Kumaraguru, and B. T. Rouse. 2004. CD4+CD25+ regulatory T cells control the severity of viral immunoinflammatory lesions. *J Immunol* 172:4123-4132.
255. Kingsley, C. I., M. Karim, A. R. Bushell, and K. J. Wood. 2002. CD25+CD4+ regulatory T cells prevent graft rejection: CTLA-4- and IL-10-dependent immunoregulation of alloresponses. *J Immunol* 168:1080-1086.
256. Gregori, S., M. Casorati, S. Amuchastegui, S. Smiroldo, A. M. Davalli, and L. Adorini. 2001. Regulatory T cells induced by 1 alpha,25-dihydroxyvitamin D3 and mycophenolate mofetil treatment mediate transplantation tolerance. *J Immunol* 167:1945-1953.
257. Rouse, B. T., and S. Suvas. 2004. Regulatory cells and infectious agents: detentes cordiale and contraire. *J Immunol* 173:2211-2215.
258. Antony, P. A., C. A. Piccirillo, A. Akpinarli, S. E. Finkelstein, P. J. Speiss, D. R. Surman, D. C. Palmer, C. C. Chan, C. A. Klebanoff, W. W. Overwijk, S. A. Rosenberg, and N. P. Restifo. 2005. CD8+ T cell immunity against a tumor/self-antigen is augmented by CD4+ T helper cells and hindered by naturally occurring T regulatory cells. *J Immunol* 174:2591-2601.
259. Golgher, D., E. Jones, F. Powrie, T. Elliott, and A. Gallimore. 2002. Depletion of CD25+ regulatory cells uncovers immune responses to shared murine tumor rejection antigens. *Eur J Immunol* 32:3267-3275.
260. Thornton, A. M., and E. M. Shevach. 1998. CD4+CD25+ immunoregulatory T cells suppress polyclonal T cell activation in vitro by inhibiting interleukin 2 production. *J Exp Med* 188:287-296.
261. Piccirillo, C. A., and E. M. Shevach. 2001. Cutting edge: control of CD8+ T cell activation by CD4+CD25+ immunoregulatory cells. *J Immunol* 167:1137-1140.
262. Takahashi, T., Y. Kuniyasu, M. Toda, N. Sakaguchi, M. Itoh, M. Iwata, J. Shimizu, and S. Sakaguchi. 1998. Immunologic self-tolerance maintained by CD25+CD4+ naturally anergic and suppressive T cells: induction of autoimmune disease by breaking their anergic/suppressive state. *Int Immunol* 10:1969-1980.
263. Thornton, A. M., and E. M. Shevach. 2000. Suppressor effector function of CD4+CD25+ immunoregulatory T cells is antigen nonspecific. *J Immunol* 164:183-190.
264. Collison, L. W., M. R. Pillai, V. Chaturvedi, and D. A. Vignali. 2009. Regulatory T cell suppression is potentiated by target T cells in a cell contact, IL-35- and IL-10-dependent manner. *J Immunol* 182:6121-6128.

265. Nakamura, K., A. Kitani, and W. Strober. 2001. Cell contact-dependent immunosuppression by CD4(+)CD25(+) regulatory T cells is mediated by cell surface-bound transforming growth factor beta. *J Exp Med* 194:629-644.
266. Collison, L. W., C. J. Workman, T. T. Kuo, K. Boyd, Y. Wang, K. M. Vignali, R. Cross, D. Sehy, R. S. Blumberg, and D. A. Vignali. 2007. The inhibitory cytokine IL-35 contributes to regulatory T-cell function. *Nature* 450:566-569.
267. Floess, S., J. Freyer, C. Siewert, U. Baron, S. Olek, J. Polansky, K. Schlawe, H. D. Chang, T. Bopp, E. Schmitt, S. Klein-Hessling, E. Serfling, A. Hamann, and J. Huehn. 2007. Epigenetic control of the foxp3 locus in regulatory T cells. *PLoS Biol* 5:e38.
268. Lewkowicz, P., N. Lewkowicz, A. Sasiak, and H. Tchorzewski. 2006. Lipopolysaccharide-activated CD4+CD25+ T regulatory cells inhibit neutrophil function and promote their apoptosis and death. *J Immunol* 177:7155-7163.
269. Mahajan, D., Y. Wang, X. Qin, G. Zheng, Y. M. Wang, S. I. Alexander, and D. C. Harris. 2006. CD4+CD25+ regulatory T cells protect against injury in an innate murine model of chronic kidney disease. *J Am Soc Nephrol* 17:2731-2741.
270. Zhao, D. M., A. M. Thornton, R. J. DiPaolo, and E. M. Shevach. 2006. Activated CD4+CD25+ T cells selectively kill B lymphocytes. *Blood* 107:3925-3932.
271. Ghiringhelli, F., C. Menard, M. Terme, C. Flament, J. Taieb, N. Chaput, P. E. Puig, S. Novault, B. Escudier, E. Vivier, A. Lecesne, C. Robert, J. Y. Blay, J. Bernard, S. Caillat-Zucman, A. Freitas, T. Tursz, O. Wagner-Ballon, C. Capron, W. Vainchencker, F. Martin, and L. Zitvogel. 2005. CD4+CD25+ regulatory T cells inhibit natural killer cell functions in a transforming growth factor-beta-dependent manner. *J Exp Med* 202:1075-1085.
272. Serra, P., A. Amrani, J. Yamanouchi, B. Han, S. Thiessen, T. Utsugi, J. Verdaguer, and P. Santamaria. 2003. CD40 ligation releases immature dendritic cells from the control of regulatory CD4+CD25+ T cells. *Immunity* 19:877-889.
273. Cederbom, L., H. Hall, and F. Ivars. 2000. CD4+CD25+ regulatory T cells down-regulate co-stimulatory molecules on antigen-presenting cells. *Eur J Immunol* 30:1538-1543.
274. Misra, N., J. Bayry, S. Lacroix-Desmazes, M. D. Kazatchkine, and S. V. Kaveri. 2004. Cutting edge: human CD4+CD25+ T cells restrain the maturation and antigen-presenting function of dendritic cells. *J Immunol* 172:4676-4680.
275. Tadokoro, C. E., G. Shakhar, S. Shen, Y. Ding, A. C. Lino, A. Maraver, J. J. Lafaille, and M. L. Dustin. 2006. Regulatory T cells inhibit stable contacts between CD4+ T cells and dendritic cells in vivo. *J Exp Med* 203:505-511.
276. Obst, R., H. M. van Santen, D. Mathis, and C. Benoist. 2005. Antigen persistence is required throughout the expansion phase of a CD4(+) T cell response. *J Exp Med* 201:1555-1565.
277. Schrum, A. G., and L. A. Turka. 2002. The proliferative capacity of individual naive CD4(+) T cells is amplified by prolonged T cell antigen receptor triggering. *J Exp Med* 196:793-803.
278. Bajenoff, M., O. Wurtz, and S. Guerder. 2002. Repeated antigen exposure is necessary for the differentiation, but not the initial proliferation, of naive CD4(+) T cells. *J Immunol* 168:1723-1729.
279. van Stipdonk, M. J., E. E. Lemmens, and S. P. Schoenberger. 2001. Naive CTLs require a single brief period of antigenic stimulation for clonal expansion and differentiation. *Nat Immunol* 2:423-429.
280. Wong, P., and E. G. Pamer. 2004. Disparate in vitro and in vivo requirements for IL-2 during antigen-independent CD8 T cell expansion. *J Immunol* 172:2171-2176.

281. Bennett, S. R., F. R. Carbone, F. Karamalis, J. F. Miller, and W. R. Heath. 1997. Induction of a CD8+ cytotoxic T lymphocyte response by cross-priming requires cognate CD4+ T cell help. *J Exp Med* 186:65-70.
282. Husmann, L. A., and M. J. Bevan. 1988. Cooperation between helper T cells and cytotoxic T lymphocyte precursors. *Ann N Y Acad Sci* 532:158-169.
283. Liu, K., G. D. Victora, T. A. Schwickert, P. Guermonprez, M. M. Meredith, K. Yao, F. F. Chu, G. J. Randolph, A. Y. Rudensky, and M. Nussenzweig. 2009. In vivo analysis of dendritic cell development and homeostasis. *Science* 324:392-397.
284. Darrasse-Jeze, G., S. Deroubaix, H. Mouquet, G. D. Victora, T. Eisenreich, K. H. Yao, R. F. Masilamani, M. L. Dustin, A. Rudensky, K. Liu, and M. C. Nussenzweig. 2009. Feedback control of regulatory T cell homeostasis by dendritic cells in vivo. *J Exp Med*.
285. Kobie, J. J., P. R. Shah, L. Yang, J. A. Rebhahn, D. J. Fowell, and T. R. Mosmann. 2006. T regulatory and primed uncommitted CD4 T cells express CD73, which suppresses effector CD4 T cells by converting 5'-adenosine monophosphate to adenosine. *J Immunol* 177:6780-6786.
286. Uhlig, H. H., J. Coombes, C. Mottet, A. Izcue, C. Thompson, A. Fanger, A. Tannapfel, J. D. Fontenot, F. Ramsdell, and F. Powrie. 2006. Characterization of Foxp3+CD4+CD25+ and IL-10-secreting CD4+CD25+ T cells during cure of colitis. *J Immunol* 177:5852-5860.
287. Klein, L., K. Khazaie, and H. von Boehmer. 2003. In vivo dynamics of antigen-specific regulatory T cells not predicted from behavior in vitro. *Proc Natl Acad Sci U S A* 100:8886-8891.
288. Pandiyan, P., L. Zheng, S. Ishihara, J. Reed, and M. J. Lenardo. 2007. CD4+CD25+Foxp3+ regulatory T cells induce cytokine deprivation-mediated apoptosis of effector CD4+ T cells. *Nat Immunol* 8:1353-1362.
289. Oberle, N., N. Eberhardt, C. S. Falk, P. H. Krammer, and E. Suri-Payer. 2007. Rapid suppression of cytokine transcription in human CD4+CD25 T cells by CD4+Foxp3+ regulatory T cells: independence of IL-2 consumption, TGF-beta, and various inhibitors of TCR signaling. *J Immunol* 179:3578-3587.
290. Krummel, M. F., and J. P. Allison. 1995. CD28 and CTLA-4 have opposing effects on the response of T cells to stimulation. *J Exp Med* 182:459-465.
291. Waterhouse, P., J. M. Penninger, E. Timms, A. Wakeham, A. Shahinian, K. P. Lee, C. B. Thompson, H. Griesser, and T. W. Mak. 1995. Lymphoproliferative disorders with early lethality in mice deficient in Ctla-4. *Science* 270:985-988.
292. Paust, S., L. Lu, N. McCarty, and H. Cantor. 2004. Engagement of B7 on effector T cells by regulatory T cells prevents autoimmune disease. *Proc Natl Acad Sci U S A* 101:10398-10403.
293. Saverino, D., C. Tenca, D. Zarcone, A. Merlo, A. M. Megiovanni, M. T. Valle, F. Manca, C. E. Grossi, and E. Ciccone. 1999. CTLA-4 (CD152) inhibits the specific lysis mediated by human cytolytic T lymphocytes in a clonally distributed fashion. *J Immunol* 162:651-658.
294. Peggs, K. S., S. A. Quezada, C. A. Chambers, A. J. Korman, and J. P. Allison. 2009. Blockade of CTLA-4 on both effector and regulatory T cell compartments contributes to the antitumor activity of anti-CTLA-4 antibodies. *J Exp Med* 206:1717-1725.
295. Tang, Q., E. K. Boden, K. J. Henriksen, H. Bour-Jordan, M. Bi, and J. A. Bluestone. 2004. Distinct roles of CTLA-4 and TGF-beta in CD4+CD25+ regulatory T cell function. *Eur J Immunol* 34:2996-3005.
296. Nocentini, G., L. Giunchi, S. Ronchetti, L. T. Krausz, A. Bartoli, R. Moraca, G. Migliorati, and C. Riccardi. 1997. A new member of the tumor necrosis

factor/nerve growth factor receptor family inhibits T cell receptor-induced apoptosis. *Proc Natl Acad Sci U S A* 94:6216-6221.

297. Shimizu, J., S. Yamazaki, T. Takahashi, Y. Ishida, and S. Sakaguchi. 2002. Stimulation of CD25(+)CD4(+) regulatory T cells through GITR breaks immunological self-tolerance. *Nat Immunol* 3:135-142.
298. Stephens, G. L., R. S. McHugh, M. J. Whitters, D. A. Young, D. Luxenberg, B. M. Carreno, M. Collins, and E. M. Shevach. 2004. Engagement of glucocorticoid-induced TNFR family-related receptor on effector T cells by its ligand mediates resistance to suppression by CD4+CD25+ T cells. *J Immunol* 173:5008-5020.
299. Ronchetti, S., O. Zollo, S. Bruscoli, M. Agostini, R. Bianchini, G. Nocentini, E. Ayroldi, and C. Riccardi. 2004. GITR, a member of the TNF receptor superfamily, is costimulatory to mouse T lymphocyte subpopulations. *Eur J Immunol* 34:613-622.
300. Valzasina, B., C. Guiducci, H. Dislich, N. Killeen, A. D. Weinberg, and M. P. Colombo. 2005. Triggering of OX40 (CD134) on CD4(+)CD25+ T cells blocks their inhibitory activity: a novel regulatory role for OX40 and its comparison with GITR. *Blood* 105:2845-2851.
301. Vu, M. D., X. Xiao, W. Gao, N. Degauque, M. Chen, A. Kroemer, N. Killeen, N. Ishii, and X. Chang Li. 2007. OX40 costimulation turns off Foxp3+ Tregs. *Blood* 110:2501-2510.
302. So, T., and M. Croft. 2007. Cutting edge: OX40 inhibits TGF-beta- and antigen-driven conversion of naive CD4 T cells into CD25+Foxp3+ T cells. *J Immunol* 179:1427-1430.
303. Mempel, T. R., M. J. Pittet, K. Khazaie, W. Weninger, R. Weissleder, H. von Boehmer, and U. H. von Andrian. 2006. Regulatory T cells reversibly suppress cytotoxic T cell function independent of effector differentiation. *Immunity* 25:129-141.
304. Green, E. A., L. Gorelik, C. M. McGregor, E. H. Tran, and R. A. Flavell. 2003. CD4+CD25+ T regulatory cells control anti-islet CD8+ T cells through TGF-beta-TGF-beta receptor interactions in type 1 diabetes. *Proc Natl Acad Sci U S A* 100:10878-10883.
305. Cao, X., S. F. Cai, T. A. Fehniger, J. Song, L. I. Collins, D. R. Piwnica-Worms, and T. J. Ley. 2007. Granzyme B and perforin are important for regulatory T cell-mediated suppression of tumor clearance. *Immunity* 27:635-646.
306. Gondek, D. C., L. F. Lu, S. A. Quezada, S. Sakaguchi, and R. J. Noelle. 2005. Cutting edge: contact-mediated suppression by CD4+CD25+ regulatory cells involves a granzyme B-dependent, perforin-independent mechanism. *J Immunol* 174:1783-1786.
307. Grossman, W. J., J. W. Verbsky, W. Barchet, M. Colonna, J. P. Atkinson, and T. J. Ley. 2004. Human T regulatory cells can use the perforin pathway to cause autologous target cell death. *Immunity* 21:589-601.
308. Grossman, W. J., J. W. Verbsky, B. L. Tollefsen, C. Kemper, J. P. Atkinson, and T. J. Ley. 2004. Differential expression of granzymes A and B in human cytotoxic lymphocyte subsets and T regulatory cells. *Blood* 104:2840-2848.
309. Kohm, A. P., J. S. McMahon, J. R. Podojil, W. S. Begolka, M. DeGutes, D. J. Kasprowicz, S. F. Ziegler, and S. D. Miller. 2006. Cutting Edge: Anti-CD25 monoclonal antibody injection results in the functional inactivation, not depletion, of CD4+CD25+ T regulatory cells. *J Immunol* 176:3301-3305.
310. Zelenay, S., and J. Demengeot. 2006. Comment on "Cutting edge: anti-CD25 monoclonal antibody injection results in the functional inactivation, not depletion,

of CD4+CD25+ T regulatory cells". *J Immunol* 177:2036-2037; author reply 2037-2038.

311. McNeill, A., E. Spittle, and B. T. Backstrom. 2007. Partial depletion of CD69low-expressing natural regulatory T cells with the anti-CD25 monoclonal antibody PC61. *Scand J Immunol* 65:63-69.
312. Zhang, P., A. L. Cote, V. C. de Vries, E. J. Usherwood, and M. J. Turk. 2007. Induction of postsurgical tumor immunity and T-cell memory by a poorly immunogenic tumor. *Cancer Res* 67:6468-6476.
313. Jackaman, C., A. M. Lew, Y. Zhan, J. E. Allan, B. Koloska, P. T. Graham, B. W. Robinson, and D. J. Nelson. 2008. Deliberately provoking local inflammation drives tumors to become their own protective vaccine site. *Int Immunol* 20:1467-1479.
314. Mahnke, K., K. Schonfeld, S. Fondel, S. Ring, S. Karakhanova, K. Wiedemeyer, T. Bedke, T. S. Johnson, V. Storn, S. Schallenberg, and A. H. Enk. 2007. Depletion of CD4+CD25+ human regulatory T cells in vivo: kinetics of Treg depletion and alterations in immune functions in vivo and in vitro. *Int J Cancer* 120:2723-2733.
315. Yamaguchi, T., K. Hirota, K. Nagahama, K. Ohkawa, T. Takahashi, T. Nomura, and S. Sakaguchi. 2007. Control of immune responses by antigen-specific regulatory T cells expressing the folate receptor. *Immunity* 27:145-159.
316. Leach, D. R., M. F. Krummel, and J. P. Allison. 1996. Enhancement of antitumor immunity by CTLA-4 blockade. *Science* 271:1734-1736.
317. Weinberg, A. D., M. M. Rivera, R. Prell, A. Morris, T. Ramstad, J. T. Vetto, W. J. Urba, G. Alvord, C. Bunce, and J. Shields. 2000. Engagement of the OX-40 receptor in vivo enhances antitumor immunity. *J Immunol* 164:2160-2169.
318. Ko, K., S. Yamazaki, K. Nakamura, T. Nishioka, K. Hirota, T. Yamaguchi, J. Shimizu, T. Nomura, T. Chiba, and S. Sakaguchi. 2005. Treatment of advanced tumors with agonistic anti-GITR mAb and its effects on tumor-infiltrating Foxp3+CD25+CD4+ regulatory T cells. *J Exp Med* 202:885-891.
319. Lee, A., K. J. Farrand, N. Dickgreber, C. M. Hayman, S. Jurs, I. F. Hermans, and G. F. Painter. 2006. Novel synthesis of alpha-galactosyl-ceramides and confirmation of their powerful NKT cell agonist activity. *Carbohydr Res* 341:2785-2798.
320. Chen, Y., S. Epperson, L. Makhsudova, B. Ito, J. Suarez, W. Dillmann, and F. Villarreal. 2004. Functional effects of enhancing or silencing adenosine A2b receptors in cardiac fibroblasts. *Am J Physiol Heart Circ Physiol* 287:H2478-2486.
321. Platzer, C., G. Richter, K. Uberla, H. Hock, T. Diamantstein, and T. Blankenstein. 1992. Interleukin-4-mediated tumor suppression in nude mice involves interferon-gamma. *Eur J Immunol* 22:1729-1733.
322. Traunecker, A., F. Oliveri, and K. Karjalainen. 1991. Myeloma based expression system for production of large mammalian proteins. *Trends Biotechnol* 9:109-113.
323. Lugade, A. A., J. P. Moran, S. A. Gerber, R. C. Rose, J. G. Frelinger, and E. M. Lord. 2005. Local radiation therapy of B16 melanoma tumors increases the generation of tumor antigen-specific effector cells that traffic to the tumor. *J Immunol* 174:7516-7523.
324. Stockert, E., E. A. Boyse, Y. Obata, H. Ikeda, N. H. Sarkar, and H. A. Hoffman. 1975. New mutant and congenic mouse stocks expressing the murine leukemia virus-associated thymocyte surface antigen GIX. *J Exp Med* 142:512-517.
325. Fontenot, J. D., J. P. Rasmussen, L. M. Williams, J. L. Dooley, A. G. Farr, and A. Y. Rudensky. 2005. Regulatory T cell lineage specification by the forkhead transcription factor foxp3. *Immunity* 22:329-341.

326. Barnden, M. J., J. Allison, W. R. Heath, and F. R. Carbone. 1998. Defective TCR expression in transgenic mice constructed using cDNA-based alpha- and beta-chain genes under the control of heterologous regulatory elements. *Immunol Cell Biol* 76:34-40.
327. Hogquist, K. A., S. C. Jameson, W. R. Heath, J. L. Howard, M. J. Bevan, and F. R. Carbone. 1994. T cell receptor antagonist peptides induce positive selection. *Cell* 76:17-27.
328. Mombaerts, P., J. Iacomini, R. S. Johnson, K. Herrup, S. Tonegawa, and V. E. Papaioannou. 1992. RAG-1-deficient mice have no mature B and T lymphocytes. *Cell* 68:869-877.
329. Garrigan, K., P. Moroni-Rawson, C. McMurray, I. Hermans, N. Abernethy, J. Watson, and F. Ronchese. 1996. Functional comparison of spleen dendritic cells and dendritic cells cultured in vitro from bone marrow precursors. *Blood* 88:3508-3512.
330. Hermans, I. F., J. D. Silk, J. Yang, M. J. Palmowski, U. Gileadi, C. McCarthy, M. Salio, F. Ronchese, and V. Cerundolo. 2004. The VITAL assay: a versatile fluorometric technique for assessing CTL- and NKT-mediated cytotoxicity against multiple targets in vitro and in vivo. *J Immunol Methods* 285:25-40.
331. Tijsterman, M., R. F. Ketting, K. L. Okihara, T. Sijen, and R. H. Plasterk. 2002. RNA helicase MUT-14-dependent gene silencing triggered in C. elegans by short antisense RNAs. *Science* 295:694-697.
332. Fire, A., S. Xu, M. K. Montgomery, S. A. Kostas, S. E. Driver, and C. C. Mello. 1998. Potent and specific genetic interference by double-stranded RNA in Caenorhabditis elegans. *Nature* 391:806-811.
333. Agrawal, N., P. V. Dasaradhi, A. Mohmmed, P. Malhotra, R. K. Bhatnagar, and S. K. Mukherjee. 2003. RNA interference: biology, mechanism, and applications. *Microbiol Mol Biol Rev* 67:657-685.
334. Popescu, F. D. 2005. Antisense- and RNA interference-based therapeutic strategies in allergy. *J Cell Mol Med* 9:840-853.
335. Plasterk, R. H. 2002. RNA silencing: the genome's immune system. *Science* 296:1263-1265.
336. McManus, M. T., B. B. Haines, C. P. Dillon, C. E. Whitehurst, L. van Parijs, J. Chen, and P. A. Sharp. 2002. Small interfering RNA-mediated gene silencing in T lymphocytes. *J Immunol* 169:5754-5760.
337. Ohta, A., E. Gorelik, S. J. Prasad, F. Ronchese, D. Lukashev, M. K. Wong, X. Huang, S. Caldwell, K. Liu, P. Smith, J. F. Chen, E. K. Jackson, S. Apasov, S. Abrams, and M. Sitkovsky. 2006. A2A adenosine receptor protects tumors from antitumor T cells. *Proc Natl Acad Sci U S A* 103:13132-13137.
338. Apasov, S. G., and M. V. Sitkovsky. 1999. The extracellular versus intracellular mechanisms of inhibition of TCR-triggered activation in thymocytes by adenosine under conditions of inhibited adenosine deaminase. *Int Immunol* 11:179-189.
339. Zhao, Y., Z. Zheng, C. J. Cohen, L. Gattinoni, D. C. Palmer, N. P. Restifo, S. A. Rosenberg, and R. A. Morgan. 2006. High-efficiency transfection of primary human and mouse T lymphocytes using RNA electroporation. *Mol Ther* 13:151-159.
340. Gessi, S., K. Varani, S. Merighi, A. Morelli, D. Ferrari, E. Leung, P. G. Baraldi, G. Spalluto, and P. A. Borea. 2001. Pharmacological and biochemical characterization of A3 adenosine receptors in Jurkat T cells. *Br J Pharmacol* 134:116-126.
341. Merighi, S., K. Varani, S. Gessi, E. Cattabriga, V. Iannotta, C. Ulouglu, E. Leung, and P. A. Borea. 2001. Pharmacological and biochemical characterization of

adenosine receptors in the human malignant melanoma A375 cell line. *Br J Pharmacol* 134:1215-1226.

342. Suh, B. C., T. D. Kim, J. U. Lee, J. K. Seong, and K. T. Kim. 2001. Pharmacological characterization of adenosine receptors in PGT-beta mouse pineal gland tumour cells. *Br J Pharmacol* 134:132-142.
343. Madi, L., A. Ochaion, L. Rath-Wolfson, S. Bar-Yehuda, A. Erlanger, G. Ohana, A. Harish, O. Merimski, F. Barer, and P. Fishman. 2004. The A3 adenosine receptor is highly expressed in tumor versus normal cells: potential target for tumor growth inhibition. *Clin Cancer Res* 10:4472-4479.
344. Feoktistov, I., S. Ryzhov, H. Zhong, A. E. Goldstein, A. Matafonov, D. Zeng, and I. Biaggioni. 2004. Hypoxia modulates adenosine receptors in human endothelial and smooth muscle cells toward an A2B angiogenic phenotype. *Hypertension* 44:649-654.
345. Fenton, B. M., S. F. Paoni, B. K. Beauchamp, and I. Ding. 2002. Zonal image analysis of tumour vascular perfusion, hypoxia, and necrosis. *Br J Cancer* 86:1831-1836.
346. Fredholm, B. B., K. Battig, J. Holmen, A. Nehlig, and E. E. Zvartau. 1999. Actions of caffeine in the brain with special reference to factors that contribute to its widespread use. *Pharmacol Rev* 51:83-133.
347. Maughan, R. J., J. Griffin. 2003. Caffeine ingestion and fluid balance: a review. *J Hum Nutr Dietet* 16:411-420.
348. Nehlig, A., J. L. Daval, and G. Debry. 1992. Caffeine and the central nervous system: mechanisms of action, biochemical, metabolic and psychostimulant effects. *Brain Res Brain Res Rev* 17:139-170.
349. Feoktistov, I., A. E. Goldstein, S. Ryzhov, D. Zeng, L. Belardinelli, T. Voyno-Yasenetskaya, and I. Biaggioni. 2002. Differential expression of adenosine receptors in human endothelial cells: role of A2B receptors in angiogenic factor regulation. *Circ Res* 90:531-538.
350. Feoktistov, I., S. Ryzhov, A. E. Goldstein, and I. Biaggioni. 2003. Mast cell-mediated stimulation of angiogenesis: cooperative interaction between A2B and A3 adenosine receptors. *Circ Res* 92:485-492.
351. Movahedi, K., M. Guilliams, J. Van den Bossche, R. Van den Bergh, C. Gysemans, A. Beschin, P. De Baetselier, and J. A. Van Ginderachter. 2008. Identification of discrete tumor-induced myeloid-derived suppressor cell subpopulations with distinct T cell-suppressive activity. *Blood* 111:4233-4244.
352. Lagasse, E., and I. L. Weissman. 1996. Flow cytometric identification of murine neutrophils and monocytes. *J Immunol Methods* 197:139-150.
353. McGarry, M. P., and C. C. Stewart. 1991. Murine eosinophil granulocytes bind the murine macrophage-monocyte specific monoclonal antibody F4/80. *J Leukoc Biol* 50:471-478.
354. Murdoch, C., M. Muthana, S. B. Coffelt, and C. E. Lewis. 2008. The role of myeloid cells in the promotion of tumour angiogenesis. *Nat Rev Cancer* 8:618-631.
355. Lozupone, F., F. Luciani, M. Venditti, L. Rivoltini, S. Pupa, G. Parmiani, F. Belardelli, and S. Fais. 2000. Murine granulocytes control human tumor growth in SCID mice. *Int J Cancer* 87:569-573.
356. Cormier, S. A., A. G. Taranova, C. Bedient, T. Nguyen, C. Protheroe, R. Pero, D. Dimina, S. I. Ochkur, K. O'Neill, D. Colbert, T. R. Lombari, S. Constant, M. P. McGarry, J. J. Lee, and N. A. Lee. 2006. Pivotal Advance: eosinophil infiltration of solid tumors is an early and persistent inflammatory host response. *J Leukoc Biol* 79:1131-1139.

357. Shi, Y., C. H. Liu, A. I. Roberts, J. Das, G. Xu, G. Ren, Y. Zhang, L. Zhang, Z. R. Yuan, H. S. Tan, G. Das, and S. Devadas. 2006. Granulocyte-macrophage colony-stimulating factor (GM-CSF) and T-cell responses: what we do and don't know. *Cell Res* 16:126-133.
358. Bronte, V., D. B. Chappell, E. Apolloni, A. Cabrelle, M. Wang, P. Hwu, and N. P. Restifo. 1999. Unopposed production of granulocyte-macrophage colony-stimulating factor by tumors inhibits CD8+ T cell responses by dysregulating antigen-presenting cell maturation. *J Immunol* 162:5728-5737.
359. Gallina, G., L. Dolcetti, P. Serafini, C. De Santo, I. Marigo, M. P. Colombo, G. Basso, F. Brombacher, I. Borrello, P. Zanovello, S. Bicciato, and V. Bronte. 2006. Tumors induce a subset of inflammatory monocytes with immunosuppressive activity on CD8+ T cells. *J Clin Invest* 116:2777-2790.
360. Xiang, X., A. Poliakov, C. Liu, Y. Liu, Z. B. Deng, J. Wang, Z. Cheng, S. V. Shah, G. J. Wang, L. Zhang, W. E. Grizzle, J. Mobley, and H. G. Zhang. 2009. Induction of myeloid-derived suppressor cells by tumor exosomes. *Int J Cancer* 124:2621-2633.
361. Mazzoni, A., V. Bronte, A. Visintin, J. H. Spitzer, E. Apolloni, P. Serafini, P. Zanovello, and D. M. Segal. 2002. Myeloid suppressor lines inhibit T cell responses by an NO-dependent mechanism. *J Immunol* 168:689-695.
362. Dugast, A. S., T. Haudebourg, F. Coulon, M. Heslan, F. Haspot, N. Poirier, R. Vuillefroy de Silly, C. Usal, H. Smit, B. Martinet, P. Thebault, K. Renaudin, and B. Vanhove. 2008. Myeloid-derived suppressor cells accumulate in kidney allograft tolerance and specifically suppress effector T cell expansion. *J Immunol* 180:7898-7906.
363. Huang, B., P. Y. Pan, Q. Li, A. I. Sato, D. E. Levy, J. Bromberg, C. M. Divino, and S. H. Chen. 2006. Gr-1+CD115+ immature myeloid suppressor cells mediate the development of tumor-induced T regulatory cells and T-cell anergy in tumor-bearing host. *Cancer Res* 66:1123-1131.
364. Yang, R., Z. Cai, Y. Zhang, W. H. t. Yutzy, K. F. Roby, and R. B. Roden. 2006. CD80 in immune suppression by mouse ovarian carcinoma-associated Gr-1+CD11b+ myeloid cells. *Cancer Res* 66:6807-6815.
365. Chaux, P., N. Favre, M. Martin, and F. Martin. 1997. Tumor-infiltrating dendritic cells are defective in their antigen-presenting function and inducible B7 expression in rats. *Int J Cancer* 72:619-624.
366. Stoitzner, P., L. K. Green, J. Y. Jung, K. M. Price, H. Ataera, B. Kivell, and F. Ronchese. 2008. Inefficient presentation of tumor-derived antigen by tumor-infiltrating dendritic cells. *Cancer Immunol Immunother* 57:1665-1673.
367. Preynat-Seauve, O., P. Schuler, E. Contassot, F. Beermann, B. Huard, and L. E. French. 2006. Tumor-infiltrating dendritic cells are potent antigen-presenting cells able to activate T cells and mediate tumor rejection. *J Immunol* 176:61-67.
368. Ebert, L. M., B. S. Tan, J. Browning, S. Svobodova, S. E. Russell, N. Kirkpatrick, C. Gedye, D. Moss, S. P. Ng, D. MacGregor, I. D. Davis, J. Cebon, and W. Chen. 2008. The regulatory T cell-associated transcription factor FoxP3 is expressed by tumor cells. *Cancer Res* 68:3001-3009.
369. Hinz, S., L. Pagerols-Raluy, H. H. Oberg, O. Ammerpohl, S. Grussel, B. Sipos, R. Grutzmann, C. Pilarsky, H. Ungefroren, H. D. Saeger, G. Kloppel, D. Kabelitz, and H. Kalthoff. 2007. Foxp3 expression in pancreatic carcinoma cells as a novel mechanism of immune evasion in cancer. *Cancer Res* 67:8344-8350.
370. Karanikas, V., M. Speletas, M. Zamanakou, F. Kalala, G. Loules, T. Kerenidi, A. K. Barda, K. I. Gourgoulianis, and A. E. Germenis. 2008. Foxp3 expression in human cancer cells. *J Transl Med* 6:19.

371. Bates, G. J., S. B. Fox, C. Han, R. D. Leek, J. F. Garcia, A. L. Harris, and A. H. Banham. 2006. Quantification of regulatory T cells enables the identification of high-risk breast cancer patients and those at risk of late relapse. *J Clin Oncol* 24:5373-5380.
372. Curiel, T. J., G. Coukos, L. Zou, X. Alvarez, P. Cheng, P. Mottram, M. Evdemon-Hogan, J. R. Conejo-Garcia, L. Zhang, M. Burow, Y. Zhu, S. Wei, I. Kryczek, B. Daniel, A. Gordon, L. Myers, A. Lackner, M. L. Disis, K. L. Knutson, L. Chen, and W. Zou. 2004. Specific recruitment of regulatory T cells in ovarian carcinoma fosters immune privilege and predicts reduced survival. *Nat Med* 10:942-949.
373. Leffers, N., M. J. Gooden, R. A. de Jong, B. N. Hoogeboom, K. A. ten Hoor, H. Hollema, H. M. Boezen, A. G. van der Zee, T. Daemen, and H. W. Nijman. 2009. Prognostic significance of tumor-infiltrating T-lymphocytes in primary and metastatic lesions of advanced stage ovarian cancer. *Cancer Immunol Immunother* 58:449-459.
374. Stephens, L. A., D. Gray, and S. M. Anderton. 2005. CD4+CD25+ regulatory T cells limit the risk of autoimmune disease arising from T cell receptor crossreactivity. *Proc Natl Acad Sci U S A* 102:17418-17423.
375. Mailloux, A. W., and M. R. Young. 2009. NK-dependent increases in CCL22 secretion selectively recruits regulatory T cells to the tumor microenvironment. *J Immunol* 182:2753-2765.
376. Pulendran, B., J. Lingappa, M. K. Kennedy, J. Smith, M. Teepe, A. Rudensky, C. R. Maliszewski, and E. Maraskovsky. 1997. Developmental pathways of dendritic cells in vivo: distinct function, phenotype, and localization of dendritic cell subsets in FLT3 ligand-treated mice. *J Immunol* 159:2222-2231.
377. Buckanovich, R. J., A. Facciabene, S. Kim, F. Benencia, D. Sasaroli, K. Balint, D. Katsaros, A. O'Brien-Jenkins, P. A. Gimotty, and G. Coukos. 2008. Endothelin B receptor mediates the endothelial barrier to T cell homing to tumors and disables immune therapy. *Nat Med* 14:28-36.
378. Furumoto, K., L. Soares, E. G. Engleman, and M. Merad. 2004. Induction of potent antitumor immunity by in situ targeting of intratumoral DCs. *J Clin Invest* 113:774-783.
379. Isomura, I., K. Tsujimura, and A. Morita. 2006. Antigen-specific peripheral tolerance induced by topical application of NF-kappaB decoy oligodeoxynucleotide. *J Invest Dermatol* 126:97-104.
380. Grabenbauer, G. G., G. Lahmer, L. Distel, and G. Niedobitek. 2006. Tumor-infiltrating cytotoxic T cells but not regulatory T cells predict outcome in anal squamous cell carcinoma. *Clin Cancer Res* 12:3355-3360.
381. Carreras, J., A. Lopez-Guillermo, B. C. Fox, L. Colomo, A. Martinez, G. Roncador, E. Montserrat, E. Campo, and A. H. Banham. 2006. High numbers of tumor-infiltrating FOXP3-positive regulatory T cells are associated with improved overall survival in follicular lymphoma. *Blood* 108:2957-2964.
382. Llopiz, D., J. Dotor, N. Casares, J. Bezunartea, N. Diaz-Valdes, M. Ruiz, F. Aranda, P. Berraondo, J. Prieto, J. J. Lasarte, F. Borras-Cuesta, and P. Sarobe. 2009. Peptide inhibitors of transforming growth factor-beta enhance the efficacy of antitumor immunotherapy. *Int J Cancer*.
383. Ghiringhelli, F., P. E. Puig, S. Roux, A. Parcellier, E. Schmitt, E. Solary, G. Kroemer, F. Martin, B. Chauffert, and L. Zitvogel. 2005. Tumor cells convert immature myeloid dendritic cells into TGF-beta-secreting cells inducing CD4+CD25+ regulatory T cell proliferation. *J Exp Med* 202:919-929.

384. Zheng, S. G., J. Wang, P. Wang, J. D. Gray, and D. A. Horwitz. 2007. IL-2 is essential for TGF-beta to convert naive CD4+CD25- cells to CD25+Foxp3+ regulatory T cells and for expansion of these cells. *J Immunol* 178:2018-2027.
385. Moo-Young, T. A., J. W. Larson, B. A. Belt, M. C. Tan, W. G. Hawkins, T. J. Eberlein, P. S. Goedegebuure, and D. C. Linehan. 2009. Tumor-derived TGF-beta mediates conversion of CD4+Foxp3+ regulatory T cells in a murine model of pancreas cancer. *J Immunother* 32:12-21.
386. Bui, J. D., R. Uppaluri, C. S. Hsieh, and R. D. Schreiber. 2006. Comparative analysis of regulatory and effector T cells in progressively growing versus rejecting tumors of similar origins. *Cancer Res* 66:7301-7309.
387. D'Cruz, L. M., and L. Klein. 2005. Development and function of agonist-induced CD25+Foxp3+ regulatory T cells in the absence of interleukin 2 signaling. *Nat Immunol* 6:1152-1159.
388. Zhang, N., B. Schroppel, G. Lal, C. Jakubzick, X. Mao, D. Chen, N. Yin, R. Jessberger, J. C. Ochando, Y. Ding, and J. S. Bromberg. 2009. Regulatory T cells sequentially migrate from inflamed tissues to draining lymph nodes to suppress the alloimmune response. *Immunity* 30:458-469.
389. Youn, J. I., S. Nagaraj, M. Collazo, and D. I. Gabrilovich. 2008. Subsets of myeloid-derived suppressor cells in tumor-bearing mice. *J Immunol* 181:5791-5802.
390. MartIn-Fontecha, A., S. Sebastiani, U. E. Hopken, M. Uguccioni, M. Lipp, A. Lanzavecchia, and F. Sallusto. 2003. Regulation of dendritic cell migration to the draining lymph node: impact on T lymphocyte traffic and priming. *J Exp Med* 198:615-621.
391. Ohl, L., M. Mohaupt, N. Czeloth, G. Hintzen, Z. Kiafard, J. Zwirner, T. Blankenstein, G. Henning, and R. Forster. 2004. CCR7 governs skin dendritic cell migration under inflammatory and steady-state conditions. *Immunity* 21:279-288.
392. Ardavin, C., and K. Shortman. 1992. Cell surface marker analysis of mouse thymic dendritic cells. *Eur J Immunol* 22:859-862.
393. Cho, B. K., V. P. Rao, Q. Ge, H. N. Eisen, and J. Chen. 2000. Homeostasis-stimulated proliferation drives naive T cells to differentiate directly into memory T cells. *J Exp Med* 192:549-556.
394. Schuler, T., and T. Blankenstein. 2003. Cutting edge: CD8+ effector T cells reject tumors by direct antigen recognition but indirect action on host cells. *J Immunol* 170:4427-4431.
395. Kieper, W. C., and S. C. Jameson. 1999. Homeostatic expansion and phenotypic conversion of naive T cells in response to self peptide/MHC ligands. *Proc Natl Acad Sci U S A* 96:13306-13311.
396. Rocha, B., N. Dautigny, and P. Pereira. 1989. Peripheral T lymphocytes: expansion potential and homeostatic regulation of pool sizes and CD4/CD8 ratios in vivo. *Eur J Immunol* 19:905-911.
397. Castle, B. E., K. Kishimoto, C. Stearns, M. L. Brown, and M. R. Kehry. 1993. Regulation of expression of the ligand for CD40 on T helper lymphocytes. *J Immunol* 151:1777-1788.
398. Roy, M., T. Waldschmidt, A. Aruffo, J. A. Ledbetter, and R. J. Noelle. 1993. The regulation of the expression of gp39, the CD40 ligand, on normal and cloned CD4+ T cells. *J Immunol* 151:2497-2510.
399. Bennett, S. R., F. R. Carbone, F. Karamalis, R. A. Flavell, J. F. Miller, and W. R. Heath. 1998. Help for cytotoxic-T-cell responses is mediated by CD40 signalling. *Nature* 393:478-480.

400. Ridge, J. P., F. Di Rosa, and P. Matzinger. 1998. A conditioned dendritic cell can be a temporal bridge between a CD4+ T-helper and a T-killer cell. *Nature* 393:474-478.
401. Schoenberger, S. P., R. E. Toes, E. I. van der Voort, R. Offringa, and C. J. Melief. 1998. T-cell help for cytotoxic T lymphocytes is mediated by CD40-CD40L interactions. *Nature* 393:480-483.
402. Hanig, J., and M. B. Lutz. 2008. Suppression of mature dendritic cell function by regulatory T cells in vivo is abrogated by CD40 licensing. *J Immunol* 180:1405-1413.
403. Shreedhar, V., A. M. Moodycliffe, S. E. Ullrich, C. Bucana, M. L. Kripke, and L. Flores-Romo. 1999. Dendritic cells require T cells for functional maturation in vivo. *Immunity* 11:625-636.
404. Shen, D. T., J. S. Ma, J. Mather, S. Vukmanovic, and S. Radoja. 2006. Activation of primary T lymphocytes results in lysosome development and polarized granule exocytosis in CD4+ and CD8+ subsets, whereas expression of lytic molecules confers cytotoxicity to CD8+ T cells. *J Leukoc Biol* 80:827-837.
405. Gu, Y., C. Sarnecki, M. A. Fleming, J. A. Lippke, R. C. Bleackley, and M. S. Su. 1996. Processing and activation of CMH-1 by granzyme B. *J Biol Chem* 271:10816-10820.
406. Adrain, C., B. M. Murphy, and S. J. Martin. 2005. Molecular ordering of the caspase activation cascade initiated by the cytotoxic T lymphocyte/natural killer (CTL/NK) protease granzyme B. *J Biol Chem* 280:4663-4673.
407. Trapani, J. A., and M. J. Smyth. 2002. Functional significance of the perforin/granzyme cell death pathway. *Nat Rev Immunol* 2:735-747.
408. Shi, L., G. Chen, G. MacDonald, L. Bergeron, H. Li, M. Miura, R. J. Rotello, D. K. Miller, P. Li, T. Seshadri, J. Yuan, and A. H. Greenberg. 1996. Activation of an interleukin 1 converting enzyme-dependent apoptosis pathway by granzyme B. *Proc Natl Acad Sci U S A* 93:11002-11007.
409. Herman, A. E., G. J. Freeman, D. Mathis, and C. Benoist. 2004. CD4+CD25+ T regulatory cells dependent on ICOS promote regulation of effector cells in the prediabetic lesion. *J Exp Med* 199:1479-1489.
410. Hermans, I. F., J. D. Silk, U. Gileadi, M. Salio, B. Mathew, G. Ritter, R. Schmidt, A. L. Harris, L. Old, and V. Cerundolo. 2003. NKT cells enhance CD4+ and CD8+ T cell responses to soluble antigen in vivo through direct interaction with dendritic cells. *J Immunol* 171:5140-5147.
411. Jiang, S., D. S. Game, D. Davies, G. Lombardi, and R. I. Lechler. 2005. Activated CD1d-restricted natural killer T cells secrete IL-2: innate help for CD4+CD25+ regulatory T cells? *Eur J Immunol* 35:1193-1200.
412. Liu, R., A. La Cava, X. F. Bai, Y. Jee, M. Price, D. I. Campagnolo, P. Christadoss, T. L. Vollmer, L. Van Kaer, and F. D. Shi. 2005. Cooperation of invariant NKT cells and CD4+CD25+ T regulatory cells in the prevention of autoimmune myasthenia. *J Immunol* 175:7898-7904.
413. Azuma, T., T. Takahashi, A. Kunisato, T. Kitamura, and H. Hirai. 2003. Human CD4+ CD25+ regulatory T cells suppress NKT cell functions. *Cancer Res* 63:4516-4520.
414. Hernandez, J., S. Aung, K. Marquardt, and L. A. Sherman. 2002. Uncoupling of proliferative potential and gain of effector function by CD8(+) T cells responding to self-antigens. *J Exp Med* 196:323-333.
415. Lowin, B., F. Beermann, A. Schmidt, and J. Tschopp. 1994. A null mutation in the perforin gene impairs cytolytic T lymphocyte- and natural killer cell-mediated cytotoxicity. *Proc Natl Acad Sci U S A* 91:11571-11575.

416. Eckert, K. B. 2008. Possible helminth-induced immune mechanisms contributing to the decrease in efficacy of bacille Calmette Guerin vaccination. In *Masters thesis*. Copenhagen University, Copenhagen. 45-48.
417. Vicari, A. P., C. Chiodoni, C. Vaure, S. Ait-Yahia, C. Dercamp, F. Matsos, O. Reynard, C. Taverne, P. Merle, M. P. Colombo, A. O'Garra, G. Trinchieri, and C. Caux. 2002. Reversal of tumor-induced dendritic cell paralysis by CpG immunostimulatory oligonucleotide and anti-interleukin 10 receptor antibody. *J Exp Med* 196:541-549.
418. Ernst, D. N., W. O. Weigle, D. J. Noonan, D. N. McQuitty, and M. V. Hobbs. 1993. The age-associated increase in IFN-gamma synthesis by mouse CD8+ T cells correlates with shifts in the frequencies of cell subsets defined by membrane CD44, CD45RB, 3G11, and MEL-14 expression. *J Immunol* 151:575-587.
419. Menning, A., U. E. Hopken, K. Siegmund, M. Lipp, A. Hamann, and J. Huehn. 2007. Distinctive role of CCR7 in migration and functional activity of naive- and effector/memory-like Treg subsets. *Eur J Immunol* 37:1575-1583.
420. Lee, I., L. Wang, A. D. Wells, M. E. Dorf, E. Ozkaynak, and W. W. Hancock. 2005. Recruitment of Foxp3+ T regulatory cells mediating allograft tolerance depends on the CCR4 chemokine receptor. *J Exp Med* 201:1037-1044.

PUBLICATIONS

Publications arising from the work presented in this thesis include:

Stoitzner, P., L. K. Green, J. Y. Jung, K. M. Price, **H. Ataera**, B. Kivell, and F. Ronchese. 2008. Inefficient presentation of tumor-derived antigen by tumor-infiltrating dendritic cells. *Cancer Immunol Immunother* 57:1665-1673.

Manuscripts in preparation:

Ataera, H., E. Spittle, P. Stoitzner, F. Ronchese. 2009. Murine melanoma infiltrating dendritic cells are defective in antigen presenting function regardless of the presence of Treg. To be submitted to *J Immunol*.

Ataera, H., T. Petersen, E. Spittle, F. Ronchese. 2009. Perforin deficient Treg inhibit CD8+ T cell responses *in vivo*.